

Return periods and clustering of potential losses associated with European windstorms in a changing climate

Inaugural-Dissertation

zur

Erlangung des Doktorgrades

der Mathematisch-Naturwissenschaftlichen Fakultät

der Universität zu Köln

vorgelegt von

Melanie Katharina Karremann

aus Schwäbisch Gmünd

Köln 2015

Berichterstatter: Prof. Dr. Michael Kerschgens

Prof. Dr. Roel Neggers

Tag der mündlichen Prüfung: 06. Oktober 2014

Abstract

Windstorms are one of the most damaging natural hazards in Western and Central Europe. A recent example was the windstorm series in winter 2013/2014, which affected primarily Great Britain. This indicates the importance of the estimation of potential losses linked to extreme windstorms as well as their return periods for present and future climate conditions. In particular, the occurrence of groups of windstorms (clustering) is of high interest, as they cause the top year losses. The present thesis consists of three studies. The first study quantifies the intensity of individual storms by potential losses estimated with empirical models. One model considers only impacts due to wind speeds (MI), while another also includes population density information as proxy for insured values within an area (LI). The models are applied to reanalysis data and general circulation model (GCM) data for recent (20C: 1960-2000) and future climate conditions for three Intergovernmental Panel on Climate Change climate scenarios (B1, A1B, A2: 2060-2100). Focus of the investigation is given on Europe. The projected tendencies for LI and MI are generally in accordance, with a correlation of about 99%, e.g. for Germany. However, the relationship between MI and LI is reduced when the evaluated area increases. Based on the identified event set, changes of intensity and return periods of single storm events are quantified. Return periods are estimated using the extreme value distribution with the peak over threshold method. Independent from the future climate scenario, results show shorter return periods and higher intensities for most countries. Nevertheless, changes are not always statistically significant.

In the second study, a reliable method to quantify clustering of losses associated with historical storm series and return periods of clustered events are quantified for Germany. With this aim, the empirical storm loss model used in study 1 is further developed and applied to clearly separate potential losses associated with individual storms. Using reanalysis datasets and observations from German weather stations for 30 winters, event sets exceeding selected return levels (1-, 2- and 5-year) are analysed. The distribution of the chosen events over the winters is used as basis for the Poisson and the negative Binomial distribution. Additionally, about 4000 years of GCM simulations with current climate conditions (20C) are investigated. Results of reanalysis data differ between the methods: in particular, for less frequent series

the Poisson distribution based assessments clearly deviate from empirical data. The negative Binomial distribution provides better estimates, even though a dependency on return levels of single storms and the dataset is identified. The consideration of about 4000 years GCM data provides similar estimates and a strong reduction of uncertainties.

In the third study, the methods of study 2 are applied to quantify possible changes of clustering and return periods of high potential losses associated with multiple extreme storms in Europe. 21 countries and regions are investigated. Additionally, a second critical value for the event identification is used (fixed LI 20C for 1-, 2-, 5-year return level), and thus possible changes in intensity of events can be regarded. Reanalysis data for 40 years as well as simulations for 800 years each of the present (20C) and the future (A1B) scenario are investigated. As for Germany, for present day climate conditions results for other regions obtained with the negative Binomial distribution show better agreements with empirical data than the Poisson distribution. Future changes in return periods and clustering estimated with both empirical and with the negative Binomial distribution depend on the region, the return level, the method and number of events per winter. For fixed return levels (e.g. 1-year), only small changes in return periods of storm series are identified. Shorter return periods of storm clusters under future climate conditions are identified for Europe, except for the Mediterranean area considering a fixed LI of 20C. However, evidence is found that the projected changes may be within the range of natural climate variability.

The detected change in clustering of extreme losses is of high interest for re-insurance companies, especially for the risk assessment. The three studies are an essential extend of the current state of research about future changes of clustering of losses associated with windstorms and may help to develop protection and mitigation measures for the infrastructure.

Zusammenfassung

Winterstürme gehören zu den schadenträchtigsten Naturgefahren in West- und Mitteleuropa. Ein gegenwärtiges Beispiel ist die Sturmserie im Winter 2013/2014, die überwiegend Großbritannien betraf. Aus diesem Grund ist es wichtig die potentielle Schadenträchtigkeit extremer Sturmereignisse und deren Wiederkehrperioden unter gegenwärtigen und künftigen Klimabedingungen abzuschätzen. Besonders das Auftreten von Stürmen in Gruppen (clustering) ist von großem Interesse, da diese die jährlichen Spitzenschäden ausmachen. Die vorliegende Arbeit besteht aus drei Studien. Die erste Studie analysiert die Intensität potentieller Schäden einzelner Sturmereignisse anhand empirischer Modelle. Ein Modell berücksichtigt ausschließlich Schäden, die durch Windgeschwindigkeiten verursacht werden (MI). Ein anderes (LI) beinhaltet zusätzlich die Information der Bevölkerungsdichte, die als Maß versicherter Daten dient. Die Modelle werden auf Reanalysen sowie Klimasimulationen des allgemeinen Zirkulation-Modells ("general circulation model", GCM) für das gegenwärtige Klima (20C, 1960-2000) und für drei Zukunftsszenarien des internationalen Ausschusses zum Klimawandel ("Intergovernmental Panel on Climate Change") (B1, A1B, A2, 2060-2100) angewendet. Der Schwerpunkt der Untersuchungen liegt in Europa. Die projizierte Tendenz von LI und MI stimmen mit einer Korrelation von etwa 99% z.B. für Deutschland überein. Der Zusammenhang zwischen MI und LI wird jedoch geringer, je größer das untersuchte Gebiet ist. Auf Basis der identifizierten Ereignisse werden sowohl Änderungen der Intensität als auch Änderungen der Wiederkehrperioden individueller Stürme geschätzt. Wiederkehrperioden werden mit der Extremwertstatistik oberhalb eines Mindestschadens ("peak over threshold") geschätzt. Unabhängig vom Zukunftsklimaszenario zeigen die meisten Länder kürzere Wiederkehrperioden, die jedoch nicht immer signifikant sind.

In der zweiten Studie wird eine Methode zur Quantifizierung historischer Sturmserien in Deutschland bestimmt. Das Sturmschadenmodell aus Studie 1 wird weiter entwickelt, so dass Schäden besser zu individuellen Stürmen zugeordnet werden können. Für Reanalysen sowie Beobachtungen an Stationen des Deutschen Wetterdienstes werden die stärksten Ereignisse aus 30 Wintern für das 1-, 2- und 5-Jahre Wiederkehrniveau untersucht. Die Verteilung der ausgewählten Ereignisse innerhalb

der Winter dient als Basis für die Poisson-Verteilung und die Negativ-Binomial-Verteilung. Zusätzlich werden etwa 4000 Jahre GCM Simulationen für das gegenwärtige Klima (20C) untersucht. Für die Reanalysedaten unterscheiden sich die Ergebnisse der Methoden. Insbesondere für seltene Sturmserien zeigen die Poisson basierten Ergebnisse eine deutliche Abweichung zu den empirisch geschätzten. Mit Hilfe der Negativ-Binomial-Verteilung werden dagegen gute Ergebnisse erzielt, obwohl eine Abhängigkeit vom Wiederkehrniveau der einzelnen Stürme und der Datensätze erkennbar ist. Die Berücksichtigung von über 4000 Jahren GCM Daten zeigt ähnliche Ergebnisse, verringert jedoch den Fehlerbereich.

In der dritten Studie werden mit den Methoden aus Studie 2 mögliche Änderungen der Schaden basierten Sturmserien und deren Wiederkehrperioden in Europa abgeschätzt. 21 Länder und Regionen werden untersucht. Als zusätzlicher Grenzwert zur Bestimmung der Ereignisse, wird der Schaden aus 20C für das 1-, 2-, 5-jährige Wiederkehrniveau gesetzt und berücksichtigt dabei eine mögliche Intensitäts-Änderung einzelner Stürme. Es werden Reanalysen für 40 Winter und je 800 Jahre GCM Simulationen für die Gegenwart (20C: 1960-2000) und die Zukunft (A1B: 2060-2100) genutzt. Wie für Deutschland zeigt sich für die anderen Regionen für die Gegenwart eine bessere Übereinstimmung der empirisch geschätzten Ergebnisse mit denen der anhand der Negativ-Binomial-Verteilung bestimmten. Mögliche zukünftige Veränderungen von Sturmserien und deren Wiederkehrperioden hängen von der Region, dem Wiederkehrniveau, der Methode und der Anzahl an Ereignissen, die zu der Sturmserie gezählt werden, ab. Ergebnisse, denen ein festes Wiederkehrniveau zugrunde liegen (z.B. 1 Jahr), zeigen nur geringe Änderungen der Wiederkehrperioden. Unter Berücksichtigung eines festen Schadenwerts von 20C LI werden mit Ausnahme des Mittelmeergebietes kürzere Wiederkehrperioden für Sturmserien unter zukünftigen Klimabedingungen erwartet. Trotzdem liegen die projizierten Änderungen möglicherweise innerhalb der natürlichen Klimavariabilität.

Die erwartete Änderung des seriellen Auftretens von extremen Schäden sind von besonders großem Interesse für Rückversicherer, besonders im Bezug auf Schadenabschätzungen. Die drei Studien sind eine wesentliche Erweiterung der gegenwärtigen Forschung über zukünftige Änderungen des seriellen Auftretens von Sturmschäden und können zur Entwicklung von Schutzmaßnahmen für die Infrastruktur beitragen.

Contents

Abstract	i
Zusammenfassung	iii
1 Introduction	1
1.1 Motivation	1
1.2 Meteorological Background	4
1.3 Storm Loss Models	11
2 Storm Severity Indices	14
3 Loss Potentials associated with European Windstorms under Future Climate Conditions	21
4 Climate Change Projections of Cyclones and Losses	42
5 On the Clustering of Winter Storm Loss Events over Germany	45
6 Return Periods of Losses associated with European Windstorm Series in a Changing Climate	67
7 Summary and Discussion	102
7.1 Summary Paper I (Chapter 3)	103
7.2 Summary Paper II (Chapter 5):	104
7.3 Summary Paper III (Chapter 6):	105
7.4 Discussion and Outlook	106
8 References	110
9 List of Abbreviations	122
10 Appendix	123

11 Danksagung	I
12 Beiträge	II
13 Erklärung	IV

1 Introduction

1.1 Motivation

The regular passage of high and low pressure systems dominate the day-to-day weather variability in the mid-latitudes. Cyclones with low core pressure can lead to extreme weather with high wind speeds and heavy precipitation. In fact, windstorms are one of the most costly and dangerous natural hazards in Europe, which typically occur in winter (e.g. Lamb, 1991). Within the last decades, extreme mid-latitude cyclones had a high impact on society and economy. Not only infrastructure, forests and farming may be damaged, but also sea coastal areas as well as off-shore activities and shipping could be affected (Storch and Weisse, 2007). A recent example was windstorm Christian¹ (27./28.10.2013) with a maximum peak wind gust of about 193 km/h (53 m/s) recorded in Kegnaes Fyr (54°N 9°E), which was the strongest wind measured in Denmark's history (Deutsche Rück, 2014). This storm lead to storm surges, electric power outages and interruptions of the public transport and 19 fatalities across Europe. Beside Christian (Hewson et al., 2014) other extreme storms hit Europe within a comparatively short time period in winter 2013/2014: Sylvester (24./25.11.2013), Xaver (05./06.12.2013), Dirk (23./24.12.2013) and Erich (26.12.2013). Anne (03.01.2014), Christina (05.01.2014), Dagmar (09./10.01.2014) and Lilli (26.01.2014) primarily affected the British Isles. In February 2014 Petra (05.02.2014), Quamira (06./07.02.2014), Ruth (08.02.2014), Tini (12.02.2014) and Ulla (14./15.02.2014) caused high losses even on the Iberian Peninsula. Insured costs solely caused by Christian and Xaver are expected to be about 2bn € (Deutsche Rück, 2014). Another prominent example for such storm series is the one in winter

¹Storm names are given by the Freie Universität Berlin as used by the German Weather Service.
Source: <http://www.met.fu-berlin.de/adopt-a-vortex/historie>

1989/1990 including the storms Daria, Herta, Nana, Judith, Ottilie, Polly, Vivian and Wiebke, which reached total costs of circa 5.5bn € indexed to 2012 (AON Benfield, 2013). In fact, insured losses associated with the windstorm series in December 1999 and January 2007 are among the highest in the last decades, reaching 1.5bn € and about 3bn €, respectively (AON Benfield, 2013). Such storm series are examples that storms tend to occur in groups (serial clustering) and further document that windstorms and windstorm series are one of the most crucial and devastating natural hazards affecting Europe.

The above presented facts indicate the importance of a detailed investigation of storm severity of individual windstorms and storm series. This is also relevant with respect to climate change impacts. Furthermore, a reliable method to estimate the clustering of high potential loss events as well as return periods of such storm series under present and future climate conditions is necessary. To accomplish this aim, this thesis focus on the following issues:

- The identification of reliable indices to estimate the storm severity for countries in Europe considering both the cyclone intensity and a proxy for insured values within a certain area. All analysed indices are based on the storm loss model of Klawns and Ulbrich (2003, Chapter 2, 3).
- The investigation of possible changes in frequency and intensity of individual windstorms affecting Europe for future climate conditions using general circulation models (GCM) data (20C: 1960-2000 vs. B1, A1B, A2: 2060-2100). With this aim return periods of individual losses associated with extreme events are estimated by fitting an extreme value distribution using the peak over threshold method to potential storm losses. Additionally, shifts in rankings of storm events are analysed (Chapter 3). An example for the applications of LIs in Germany as well as a study about changes in clustering of cyclones is presented in Chapter 4.
- The quantification of clustering of events with high loss potential and of their return periods for Germany based on three reanalysis datasets (NCEP, ERA40, ERA-Interim), observations from weather stations in Germany and about 4000 years GCM data (20C) using the Poisson and the negative Binomial distributions (Chapter 5).

- The assessment of possible changes of clustering and return periods of high potential losses associated with multiple extreme storms for future climate conditions in Europe. Estimates are performed with GCM data (20C: 1960-2000 and A1B: 2060-2100) empirically and with the Poisson and the negative Binomial distribution (Chapter 6).

The main focus is on Core Europe, defined as the countries: France, Belgium, Ireland, Denmark, Germany, Great Britain and the Netherlands (see Fig. 1.1). The structure of the work is as follows. Section 1.2 and 1.3 give a short overview of the meteorological background, including extra-tropical cyclones and clustering, and common storm loss models. Chapter 2 includes an overview of adaptations and applications of the storm loss model of Klawns and Ulbrich (2003). Chapter 3 presents work about changes in intensity and return periods of single storms and differences between changes only due to changes in cyclone activity as well as on the hit region. Chapter 4 features an application of LI to climate change projections of losses in Germany as well as future projections for cyclone clustering. In the following it is analysed what methods are reliable to estimate clustering of loss events (Chapter 5) and how far the clustering as well as the return periods of multiple events per winter may change under future climate conditions (Chapter 6). A summary and discussion of the presented results as well as an outlook of possible future investigations is given in Chapter 7.

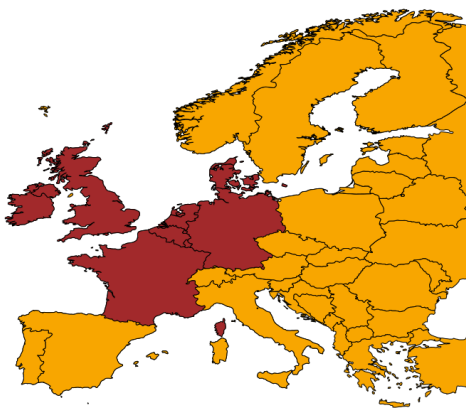


Fig. 1.1: The countries of Europe.
Red: countries defined as Core Europe.

1.2 Meteorological Background

Early descriptions of the mechanisms leading to the development and structure of extra-tropical cyclones are given in the polar front theory (Bjerknes and Solberg, 1922). The polar front is a hyper-baroclinic zone, which separates cold polar air masses and warm subtropical air masses. The development of extra-tropical cyclones typically starts along this baroclinic zone with small perturbations in the western North Atlantic basin, near the warm oceanic surface currents. Embedded in the westerly flow, cyclones typically undergo a strong intensification, while crossing the North Atlantic Ocean towards Europe. Extra-tropical cyclones are three-dimensional features, with divergence at upper levels leading to rising air masses and a decreasing pressure and convergence at the surface. Characteristics are a warm sector bounded by a leading warm and a following cold front, both exhibiting typical cloud distributions (e.g. Browning and Reynolds, 1994). Different stages of the cyclone depend on the occlusion process (e.g. Schultz and Vaughan, 2011): warm air rises together with a shift of the cyclone towards the cold side of the polar front and finally leads to the decay of the cyclone. At this stage the cyclone is characterised by its lowest pressure, leading to strong winds several 100km south of the cyclone centre (e.g. Fink et al., 2009).

Another concept of the three-dimensional air flow through an extra-tropical cyclone is given by the conveyor belts (e.g. Carlson, 1980; Browning and Reynolds, 1994; Semple, 2003), which can be used to describe e.g. the cloud structure associated with extra-tropical cyclones. The main air flows linked to frontal zones are the warm conveyor belt (e.g. Carlson, 1980), the cold conveyor belt (Harrold, 1973) and the dry intrusion (Browning and Reynolds, 1994). The cloud structure and precipitation pattern associated with a warm front can be mainly described by the warm conveyor belt, a flow of warm air crossing the surface warm front, while rising from lower and mid troposphere levels at its southern end towards the upper troposphere at its northern end. If the air contains a lot of humidity, the ascending motion leads to an elongated observed band of clouds along the front. The cold conveyor belt is initially below the warm conveyor belt ahead of the warm front and moves westwards. Due to evaporation of precipitation of the warm conveyor belt falling into the region of the cold conveyor belt, it redistributes moisture within the system. The rising of air

leads to low cloud formation. Dry air originating near the tropopause-level descends on the backside of the cold front towards mid tropospheric levels. This could lead to potential instability as it overruns the cold front, and thus the warm air associated with the warm conveyor belt (Browning and Reynolds, 1994). Dry intrusions are characterised by dry air masses and high values of potential Vorticity. An area without clouds is usually obvious on water vapour imagery. As the temperature gradient near the polar front is steeper in winter, and the westerly flow over the North Atlantic is stronger, cyclones, which have high impacts on Europe typically occur in winter.

The development of extreme cyclones are affected by the combination of several factors (see below). In the past, a large number of studies investigating the cyclone activity and cyclone tracks became available. A first approach estimating manually the climatology of low pressure systems and cyclone tracks is given by Köppen (1881). Nowadays Lagrangian methods like cyclone tracking (e.g. Blender et al., 1997; Hodges et al., 2003; Simmonds et al., 2003) or Eulerian measures like band-pass filtered 500 hPa geopotential height (Blackmon, 1976) are used to analyse the synoptic scale variability. Orlanski (1998) found a high correlation between high-frequency eddies in the major mid-latitude storm track areas and the stationary atmospheric circulation. In reanalysis data, two regions of high cyclone activities are detected: one over the North Atlantic and one over the North Pacific.

Extra-tropical cyclones crossing the jet stream undergo a rapid deepening phase (Baehr et al., 1999). So, a strong upper-tropospheric jet stream (e.g. Fink et al., 2009; Wernli et al., 2002; Ulbrich et al., 2001) and upper-level divergence at the left side of the exit region of the jet stream are important for cyclone development. Furthermore, dry air intrusions at the upper-level, which overrun the frontal structures (e.g. Uccellini, 1990), and the inclusion of anomalously warm and humid air in the warm sector of a cyclone (e.g. Chang, 1993) play a role. Other factors, which are important for the development of extra-tropical cyclones are the condensation of water vapour (Danard, 1964; Uccellini, 1990) or baroclinic instability over the Mid-latitudes (Charney, 1947). Additionally, non-baroclinic mechanisms like large scale strain (e.g. Dritschel et al., 1991; Bishop and Thorpe, 1994; Renfrew et al., 1997; Dacre and Gray, 2006), frontal shear (Chaboureaud and Thorpe, 1999; Joly and Thorpe, 1991), latent heat release (Joly and Thorpe, 1991; Schär and Davies,

1990; Plant et al., 2003) and boundary layer friction (Adamson et al., 2006) may influence their development.

There is a strong relationship between the development of extra-tropical cyclones and major teleconnection patterns of the northern hemisphere. The first is the North Atlantic Oscillation (NAO), which is defined as the pressure gradient between the anticyclone over the Azores and the trough of Icelandic low pressure (e.g. Wanner et al., 2001; Bader et al., 2011; Gómara et al., 2014). The second is the Pacific North America (PNA) pattern, which is defined by pressure anomalies in 700 or 500 hPa in Central Pacific ocean and Western Canada/South-Eastern USA. For example, in years with a positive NAO index a frequent occurrence of winter storms in Europe is identified (Pinto et al., 2009). Nevertheless, the relation between circulation patterns and extreme intensified cyclones differ from region to region. For example, in Northern Europe cyclones are associated to a slightly counter-clockwise rotated NAO-like pattern with focus over South-Western Greenland and Central Europe. On the other hand in Southern Europe a blocking-like pattern extending over Central and Northern Europe is identified (Raible, 2007).

According to Mailier et al. (2006) the most damaging storms belong to one of three types: rapid developers, slow movers or serial storms. Rapid developers are also known as cyclone "bombs" with a deepening rate of at least 24 hPa per day, like Kyrill in 2007 (Fink et al., 2009). Slow movers are able to produce large accumulations of precipitation over small regions (e.g. European summer flood 2013; Grams et al. (2014)). Serial storms are storms affecting the same area within a relative short time period, like in winter of 1989/1990 (Klawns and Ulbrich, 2003). Storm series occur under particular atmospheric conditions. At least two possible physical mechanisms contribute to the clustering process.

The first factor is the intensity and the variability of extra-tropical cyclones linked with large-scale atmospheric conditions (Raible, 2007; Bader et al., 2011). For example, the steering of cyclones over the Eastern North Atlantic towards Western Europe is largely associated with the phase of the NAO (e.g. Hurrell and Deser, 2009) effectively modulating large-scale factors, which are important for the cyclone development (e.g. Pinto et al., 2009). In particular, optimal conditions for cyclone clustering are provided by an intensified, quasi-stationary jet extended toward Europe near 50 °N (Pinto et al., 2014). One prominent example is the large-scale flow

in January 2007. In that case a quasi-stationary zonal upper air and surface flow, stronger than average, with enhanced baroclinicity dominated over the whole North Atlantic/Europe (Fink et al., 2009). These atmospheric conditions supported the development and propagation of a succession of extra-tropical cyclones following a very similar path, including some high impact storms like Franz, Hanno, and Kyrill (11, 14, and 18 January 2007, respectively, see Pinto et al., 2014).

A second factor is the so called secondary cyclogenesis. Here, groups of storms occur when successive unstable waves develop along a trailing front in the wake of a primary low, leading to the occurrence of cyclone families (e.g. Bjerknes and Solberg, 1922; Parker, 1998) (see Fig. 1.2). The new cyclone typically develops south of the parent low (e.g. Parker, 1998; Rivals et al., 1998; Dacre and Gray, 2006).

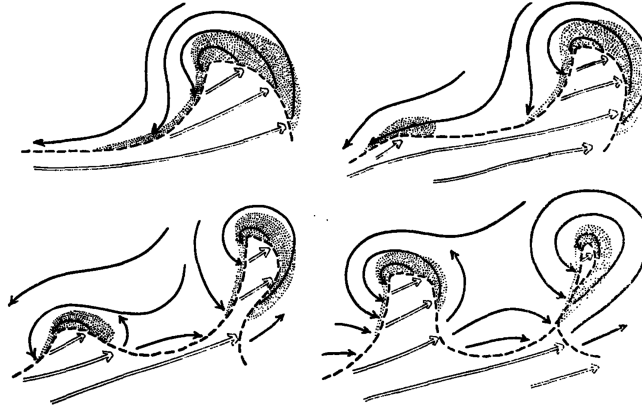


Fig. 1.2: Scheme of secondary cyclogenesis on a waving cold front. Figure 3 from Henry (1922). (©American Meteorological Society. Used with permission.)

Cyclone series can theoretically also be linked to downstream development, with cyclogenesis near the downstream (e.g. eastward) of an existing parent low due to Rossby wave dispersion (e.g. Simmons and Hoskins, 1979; Chang, 1993; Riemer et al., 2008). Indication is found that downstream development may play a role for secondary cyclones of a storm series, but cannot explain for example the cyclone clustering in the seasons analysed in Pinto et al. (2014). They stated also a strong relation between upstream cyclone development (new cyclogenesis on trailing front of parent lows) and clustering of multiple cyclones developing on a single jet streak. Nevertheless, no objective method is able to differentiate secondary cyclones from other types of cyclones (Parker, 1998). Generally, primary frontal cyclones develop

in large-scale baroclinic regions, while secondary frontal cyclones generate in more localised baroclinic regions, like trailing cold fronts of pre-existing frontal cyclones. The life-cycle of a primary cyclone is typically 3-4 days and 1-2 days for secondary cyclones (Pinto et al., 2014). A difference between a primary low and a secondary low can also be found in the horizontal scale with about 2000 km for primary cyclones and about 1000 km for secondary cyclones (Renfrew et al., 1997). The role of non-baroclinic mechanisms are more important for the development of secondary frontal cyclones than for primary frontal cyclones (Pinto et al., 2014). Large-scale conditions for secondary cyclogenesis are supported by multiple Rossby wave breaking occurrences on the poleward/equator-ward flanks of the jet, which lead to a downstream development, with cyclogenesis occurring eastward of the parent cyclone due to Rossby wave dispersion (Simmons and Hoskins, 1979; Chang, 1993). In most cases the clustering of cyclones is caused by a combination of the above described mechanisms (Mailier et al., 2006; Pinto et al., 2014).

In recent years, many studies aimed to identify possible changes of cyclone characteristics in the 2nd half of the 20th century (Feser et al., 2014). Based on observation data as well as on proxy data, like mean sea level pressure, most of the studies found no trend in storm frequency over the British Isles and the North Sea (e.g. Allan et al., 2009; Ciavola et al., 2011; Weisse et al., 2005), while for Central Europe a decrease is identified (e.g. Brönnimann et al., 2012; Matulla et al., 2008). The number of cyclones north of 60°N is detected to increase (e.g. Weisse et al., 2005; Simmonds and Keay, 2002). This trend is also identified for strong cyclones between 1958 and 2001 (e.g. Wang et al., 2006). On the other hand the majority of studies show a decrease in the number of cyclones south of 60°N (e.g. Wang et al., 2006). Nevertheless, Brönnimann et al. (2012); Donat et al. (2011) detected an increase also over the North sea area. Furthermore, a shift of storm tracks is suggested for the last decades towards the pole (Wang et al., 2006; McCabe et al., 2001; Trigo, 2006) and to the east (Gulev et al., 2001). Some studies found a changing trend from an increase to a decrease in severe storm frequency towards the end of the 1990ties (Weisse et al., 2005). A strong decadal variability of intensities is observed by Alexandersson et al. (2000), Barring and von Storch (2004) and Trenberth et al. (2007). These variabilities over Northern and Central Europe are confirmed by Matulla et al. (2008), who found an increase in storminess from 1960s to 1990s, which is comparable to the storminess

at the beginning of the 20th century. Results of Simmonds and Keay (2002) show that the trend to more intense cyclones over the Pacific is statistically significant. As a consequence, despite observed changes in storminess over Europe indication for an anthropogenic contribution to storm trends persists uncertain (Hegerl et al., 2007).

GCM models with present-day forcing conditions are generally able to reproduce the structures of the observed climatological storm-track patterns (e.g. Pinto et al., 2007; Zappa et al., 2013). The representation of the region in the North Atlantic depend on the spatial resolution of the data as well as on the considered model. Nevertheless, GCMs are able to identify reliable cyclone activities (Ulbrich et al., 2009). Hence, GCMs constitute a plausible tool for the assessment of characteristics of single cyclones in a future climate. The global climate change may increase the probability of conditions necessary for the development of cyclones. For example, almost all models assess an increase in water vapour within the atmosphere, which could have an impact in the intensity and frequency of extreme cyclones (e.g. Pinto et al., 2009; Fink et al., 2012; Ludwig et al., 2014). Most GCM models indicate to an increasing number of cyclones for certain regions like the North Atlantic, the British Isles and the North Pacific (e.g. Rockel and Woth, 2007; Della-Marta and Pinto, 2009; Donat et al., 2010a). On the other hand the total number of cyclones on the northern hemisphere will be reduced (e.g. Ulbrich et al., 2009; Bengtsson et al., 2006; Lambert and Fyfe, 2006; Leckebusch et al., 2008). However, differences between these studies are found as the outcomes are sensitive to the methodologies, datasets and scenarios (e.g. Feser et al., 2014; Ulbrich et al., 2009). For example, some older studies identified a northward shift of cyclone tracks (e.g. Bengtsson et al., 2009) for the end of the 21st century. An intensification of cyclones and a southward shift of cyclone activity in the northern hemisphere are expected (Raible, 2007). More intense storms over the North Sea and the North Atlantic are forecasted for example by Zappa et al. (2013) based on CMIP5 data and Bengtsson et al. (2006) considering CMIP3 GCMs (Harvey et al., 2012). Projections of CMIP 3 and 5 are in general agreement in the response of storm tracks to the mean global temperature. Although results for climate projections are not all in agreement, most of them tend towards higher intensity and frequency of extreme cyclones. Nevertheless, projections of the frequencies and intensities of (extreme) cyclones must be interpreted carefully. This

is attributed to the fact, that they are not able to reproduce tracks of single cyclones exact. Furthermore, small scale processes, which are important for small and strong cyclones (e.g. Lothar), are not depicted well enough in climate simulations.

Despite its importance for the European socio-economic aspects only sparse literature on a possible future change of clustering of cyclones is available. Mailier (2007) analysed a small set of three IPCC climate models of the SRES scenario A1B: HadGEM1, BCM and ECHAM. Results show only little change with a possible decrease in serial clustering of extra-tropical cyclones in the North Atlantic and over Europe for the end of the 21st century. Based on a multi-ensemble of ECHAM5 GCM data for present (20C: 1960-2000) and future climate conditions (A1B: 2060-2100), Pinto et al. (2013) analysed the possible change of clustering of cyclones. Results indicate that serial clustering may decrease over the North Atlantic storm track area and parts of Western Europe.

1.3 Storm Loss Models

One of the main impacts of strong cyclones are strong near-surface winds and wind gusts. High losses are caused by the velocity pressure, which is proportional to the second exponent of the wind speed in 10 m. 50% of extreme cyclones between 1970 and 1997 caused 80% of insured losses (e.g. Klawns and Ulbrich, 2003). In particular, large losses are usually produced by storm events affecting large areas. In general, meteorological parameters like the wind speed are only partly responsible for losses associated with windstorms. Therefore, considerations of factors, which could contribute to damages are necessary. Damages can be directly associated with storms or non-directly, like flooding after bursting of a dam or trees falling on houses. Several factors control if the tree falls or not: the frequency of wind gusts, the maximum wind speed, the health of the tree (Amtmann, 1986), if the ground is frozen or rain-drenched, the duration of a storm, or the wind direction (Schraft et al., 1993). Nevertheless, studies found no clear dependency between the duration of a storm and the potential loss (Dorland, 1999; Angermann, 1993). However, this may be attributed to the fact that few data were available and therefore no statistical robust results were found. Another important factor is the density of leaves, as the pressure on the tree is higher with more leaves, so in autumn higher damages are expected than in winter considering the same meteorological conditions. Furthermore, if in an area for a long time no extreme wind speeds were measured, higher losses are expected, as for example old trees or roof tops are more prone to high wind speeds. On the other hand, if a recent storm caused already high damages, it is possible that a second extreme event in the same area may cause comparatively less damages. Or the other way round, trees or building could be only slightly damaged by a first storm, so the second needs less wind speed to cause high damages. Nevertheless, insurance data is also affected by factors like insurance fraud, which increased over the years. The above presented facts show that a storm loss model cannot consider all parameters but can focus on certain factors, like destruction of infrastructure and buildings.

As a general rule, insurance companies in Germany usually pay for storm losses if gusts above 21m/s (8 bft) are measured at a neighbouring station. German flatland constructions take peak wind gusts at a certain return level into account (e.g. Chan-

dler et al., 2001) and therefore buildings are build more robust and get less damaged. In order to quantify expected losses associated with windstorms in Europe, storm loss models have been developed (e.g. MunichRe, 2001; Dorland, 1999; Klawe and Ulbrich, 2003). This is important for both insurance companies and society, as loss mitigation or protection strategies could be developed. Such models are almost all empirical and adjusted to real loss data provided by insurance companies. Storm loss models usually are based on three main assumptions. First, losses are only expected if a critical threshold wind speed is exceeded. Second, the peak wind is primarily responsible for the loss. And third, potential losses are related to the maximum wind speed (v_{max}) during an event with an exponential power function. Other factors (see above) like the duration and the precipitation amount are generally discarded. Munich Re insurance company found a loss - wind relation of $v_{max}^{2.7}$, for the windstorms in winter 1989/1990 and of v^4 or v^5 for the winter 1999/2000 (MunichRe, 1993, 2001). This is similar to suggestions by other studies, which found an exponent of 3 (e.g. Palutikof and Skellern, 1991; Lamb, 1991). Dorland (1999) developed a storm loss model for the Netherlands using an exponential approach ($loss \sim exp(v_{max})$).

In this thesis, modified versions of the storm loss model of Klawe and Ulbrich (2003) are developed and analysed (see Chapter 2). The model is originally performed for yearly accumulated losses for Germany based on the v^3 approach using the maximum wind gust data of 24 stations of Germany. To take local conditions into account the gust wind values are scaled with the 98th percentile of the local climatology permitting a spatial interpolation of the wind signature. The choice of this threshold v_{ij}^{98} is supported by (MunichRe, 1993). Above 22 m/s or 25 m/s the average losses increase exponential (MunichRe, 2001; Schraft et al., 1993). Instead of the 98th percentile other values like the mean, standard deviation, Weibull parameter or the roughness length are possible (Dorland, 1999). The loss index is a combination of the scaled wind speed and the population density, used as proxy for insured values, which could be affected by a windstorm. An example of the considered grid points exceeding the 98th percentile for windstorm "Kyrill" is presented in Fig. 1.3. The annual severity of storms is given by the aggregated storm indices.

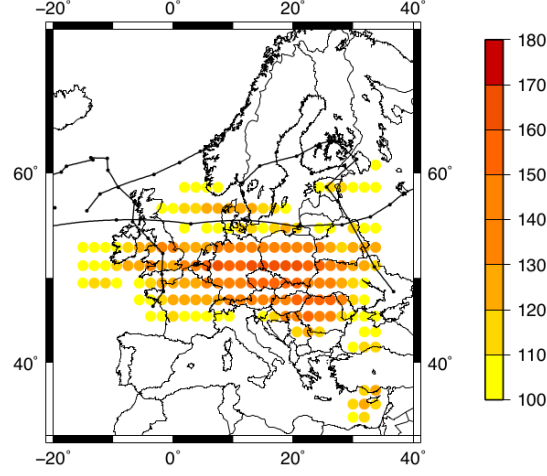


Fig. 1.3: Wind signature of the windstorm Kyrill on 18.01.2007. The colours denote the exceedance of the 98th percentile in [%]. The storm tracks of storms crossing Europe are included in black. Black dots mark the 6-hourly positions of the cyclone.

More details to the used approaches can be found in the following chapters. Physically the cube of wind speed is proportional to the advection of kinetic energy (Businger and Businger, 2001), which supports the identified v^3 relationship of the previous studies. The use of the cube of the exceedance over threshold implies that a small increase in wind speed will have a strong effect on loss. Further studies used similar approaches (e.g. Donat et al., 2010b; Leckebusch et al., 2007; Welker and Martius, 2013). For example, Schwierz et al. (2010) quantified the development of losses in Europe for the end of the 21st century based on HadCM3 and ECHAM5 GCMs. Roberts et al. (2014) composed a storm catalogue based on several indices using downscaled ERA-Interim data. In the following Chapter more approaches developed in this study are presented and compared.

2 Storm Severity Indices

In the present work, different storm severity indices are considered. These indices are based on an approach of Klawns and Ulbrich (2003) and estimate losses from wind data either of station data or gridded data. The indices focus on the meteorological impact of a storm (MI) as well as on socio-economic factors (LI). MI includes the exceedance of the daily maximum wind speed of the 98th percentile for the winter wind climatology (v_{ij}^{98}) to analyse the impact of wind speed. The second index (LI) is also considering the population density, which is a proxy for insured values within a certain area. The comparison of MI and LI helps to quantify if detected changes in losses are primarily due to changes in the severity of events (e.g. larger MI if storms are more intense) or to other factors like a change in the cyclone path (hitting highly populated areas like the Ruhr more often). MI_{ls} is defined as the sum of all grid points (ij) over land and sea, where the daily maximum wind exceeds v_{ij}^{98} of each dataset. MI_l is similar but considers only grid points over land. Both indices are also investigated using a cubistic approach approximating the storm loss models (see section 1.3; MI_{ls}^3 and MI_l^3). Additionally, the two indices over land are weighted with the population density (pop_{ij}) of the nearest grid point (LI , LI^3), used as a proxy for insured values within the area. An overview of all analysed indices is given in Table 2.1. All indices are applied to three reanalysis datasets (NCEP, ERA40 and ERA-Interim) for the period of 1979-2001, which is the time-frame common to all three reanalysis datasets. The focus is on Core Europe, the region of France, Belgium, Great Britain, Denmark, the Netherlands, and Germany. For each storm severity index daily time series with potential losses are derived. These outcomes are ranked and the 115 top events, representing 5 events a year, are further investigated. The comparison of the identified events reveal that all methods are similar, identifying the historical top events, but feature a different ranking of

storms. An agreement of 69% (ERA40) to 73% (NCEP) between MI_{ls} and MI_l is found. MI_{ls} and LI are between 65% (ERA40) and 77% (NCEP) in consent. As expected, the agreement between LI and MI_l for each reanalysis considering only land is higher with about 78% (ERA-Interim) to 85% (ERA40) same identified events. This indicates that LI values are only partly influenced by the meteorological severity of events but also depends on the region, which is affected. Considering that loss in reality is linked to buildings and infrastructure (see section 1.3), it is meaningful to consider the severity only over land weighting potential wind-losses with population density. Nevertheless, MI_l , MI_l^3 , LI , LI^3 show both similar statistical characteristics and rankings.

Tab. 2.1: List of investigated storm severity indices.

Name	Formula
MI_{ls}	$\sum_{i=1}^N \sum_{j=1}^M (\frac{v_{ij}}{v_{98}} - 1)$ for ij over land and sea
MI_{ls}^3	$\sum_{i=1}^N \sum_{j=1}^M (\frac{v_{ij}}{v_{98}} - 1)^3$ for ij over land and sea
MI_l	$\sum_{i=1}^N \sum_{j=1}^M (\frac{v_{ij}}{v_{98}} - 1)$ for ij over land
MI_l^3	$\sum_{i=1}^N \sum_{j=1}^M (\frac{v_{ij}}{v_{98}} - 1)^3$ for ij over land
LI	$\sum_{i=1}^N \sum_{j=1}^M (\frac{v_{ij}}{v_{98}} - 1)pop_{ij}$ for ij over land
LI^3	$\sum_{i=1}^N \sum_{j=1}^M (\frac{v_{ij}}{v_{98}} - 1)^3 pop_{ij}$ for ij over land

In order to analyse if the different resolutions of the reanalysis datasets lead to differences in the top 115 identified events both ECMWF reanalysis data are interpolated by a bilinear interpolation method to the grid of NCEP data. After the interpolation (following indexed with int) new estimates of potential losses are performed with the storm loss model. For MI for ERA40 and ERA-Interim datasets 72 % of identified events are identical when comparing the interpolated and not interpolated data. Results for LI are different, with a bit more shared events (74%) for ERA-Interim and less agreement for ERA40 (64%). This may be explained by the use of an interpolation that allocates the maximum wind speeds sometimes to other population density grid boxes, and therefore other regions of population den-

sity are more weighted. Beside the resolution of wind data, the resolution of the population grid may play a role. Therefore the indices are estimated based on 1° as well as on 0.25° resolution of the population density. Comparing the identified events with both resolutions, an accordance between 70% (ERA-Interim) and 96% (ERA40) is found. This indicates that the resolution of population data is important for ERA-Interim with a high resolution of wind data, but can almost be neglected for NCEP and ERA40. This may be attributed to the fact that for ERA-Interim local information of wind speed are assigned differently when connecting to the 1° population density grid boxes.

Another important factor which leads to different identified event sets are the re-analysis data themselves. Independent from the resolution of wind or population density, less than 50% of events are identified in all three datasets for MI_1^3 (see Fig. 2.1). For LI^3 , agreements are slightly better with around 57% events found in all datasets (see Fig. 2.2). Nevertheless, differences in the identified events are primarily attributed to the analysed dataset, and not to the resolution of the data. This is at least partly traced back to the method assessing the data, e.g. by different assimilation methods. A prominent example is winter storm Lothar, which is known to be under-represented in NCEP data (Ulbrich et al., 2001; Donat et al., 2010a).

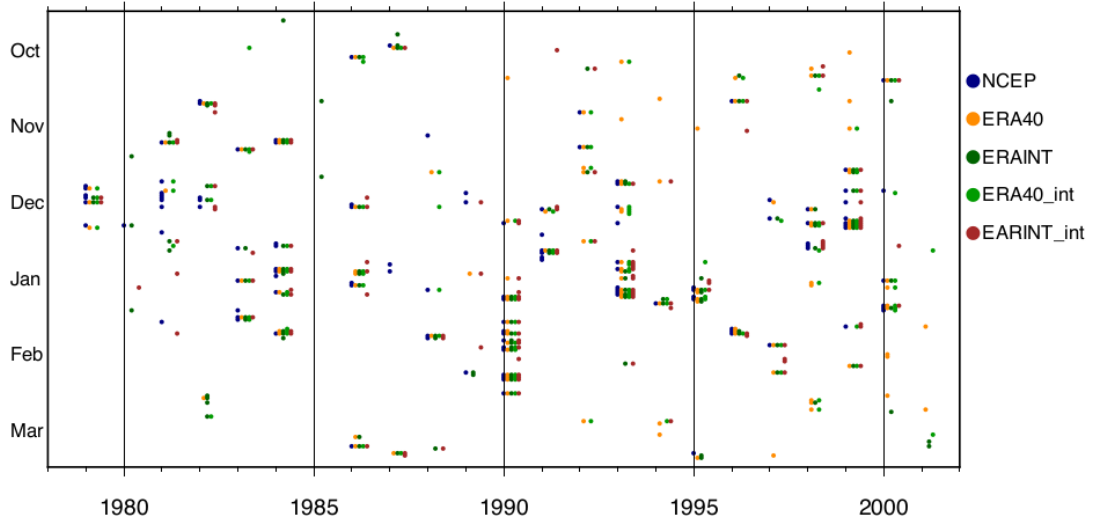


Fig. 2.1: Identified 115 events for NCEP (blue), ERA40 (yellow), ERA-Interim (dark green), ERA40_{int} (green) and ERA-Interim_{int} data (red) based on MI_1^3 .

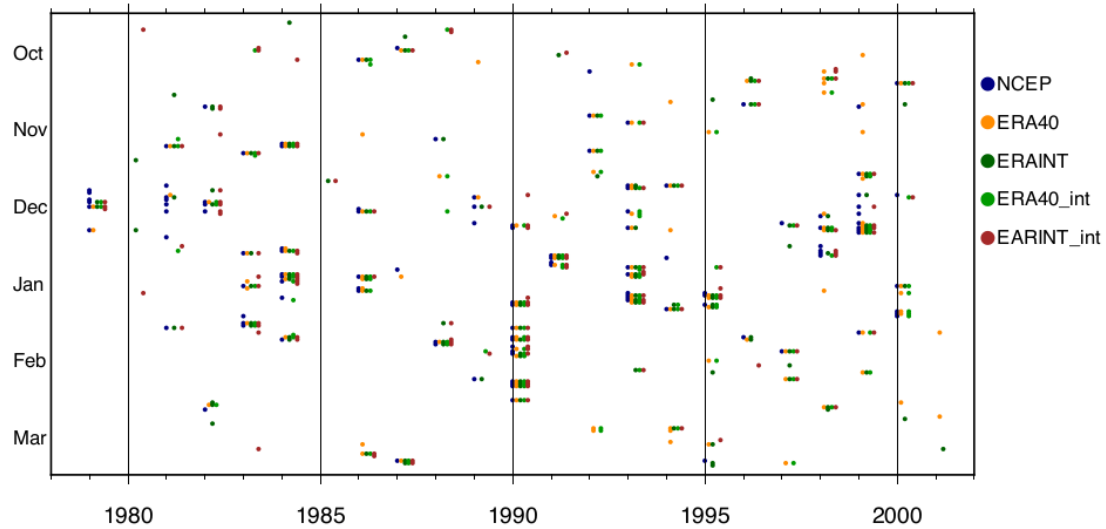


Fig. 2.2: Identified 115 events for NCEP (blue), ERA40 (yellow), ERA-Interim (dark green), ERA40_{int} (green) and ERA-Interim_{int} data (red) based on LI^3 with 1° population density.

In addition, the ranking of five events included in the top 10 loss events ordered by insured losses provided by MunichRe NatCatSERVICE (2014) between 1980 and 2013 are analysed. Only five of the top ten events are considered, because only events between 1980 and 2001 can be taken into account (common period 1979-2001). Nevertheless, five of the top 10 events are within this period. All storms except Lothar and Martin (see above; Ulbrich et al., 2001) are within the top 115 for each dataset (see Tab. 2.2), which suggest the robustness of the methods. So all indices and datasets are useful for the identification of historical extreme storm events in Core Europe. However, the most severe windstorms could be identified in all three reanalysis datasets with all resolutions. Therefore, all indices are able to identify the most severe storms in history. These results are similar to the conclusions of Deroche et al. (2014), who also analysed different severity indices to identify high potential loss events (based on wind, mean sea level pressure and anomalies of mean sea level pressure). The choice of the index should depend on the aim, which should be investigated. For studies, estimating losses associated to the cyclone activity MI or MI_1^3 is useful. If focus is given on (insured) losses associated with windstorms, the best index is LI and LI^3 , where the restriction to land areas and the weighting with population density is suitable.

Tab. 2.2: Rankings of the five events included in the top 10 loss events ordered by insured losses provided by MunichRe NatCatSERVICE (2014) between 1980 and 2013. The number in brackets is according to the rang of the MunichRe list. The presented storm severity indices are: MI_{ls} , MI_1 , MI and LI considering a population density of 1° (index 1) and 0.25° (index 0.25) respectively (indexed with 1 or 0.25). The ranks are based on NCEP, ERA40, ERA-Interim, ERA40_{int} and ERA-Interim_{int}.

NCEP	MI_{ls}	MI_1	$MI_{0.25}$	LI_1	$LI_{0.25}$
Lothar - 26.12.1999 (1)	34	11	19	56	78
Daria - 25.01.1990 (3)	1	3	1	1	1
87J - 15.10.1987 (4)	105	79	71	102	90
Martin - 27.12.1999 (8)	58	54	99	-	-
Anatol - 03.12.1999 (9)	45	30	37	14	21
Vivian - 26.02.1990 (10)	3	2	3	2	2
ERA40 _{int}	MI_{ls}	MI_1	$MI_{0.25}$	LI_1	$LI_{0.25}$
Lothar - 26.12.1999 (1)	-	-	-	-	-
Daria - 25.01.1990 (3)	24	16	12	10	6
87J - 15.10.1987 (4)	100	-	114	80	87
Martin - 27.12.1999 (8)	-	-	-	-	-
Anatol - 03.12.1999 (9)	72	34	3	19	16
Vivian - 26.02.1990 (10)	2	2	2	2	1
ERA-Interim _{int}	MI_{ls}	MI_1	$MI_{0.25}$	LI_1	$LI_{0.25}$
Lothar - 26.12.1999 (1)	14	26	49	114	-
Daria - 25.01.1990 (3)	4	5	4	5	3
87J - 15.10.1987 (4)	44	55	67	55	76
Martin - 27.12.1999 (8)	29	-	-	-	-
Anatol - 03.12.1999 (9)	16	59	44	11	11
Vivian - 26.02.1990 (10)	2	2	1	1	1
ERA40	MI_{ls}	MI_1	$MI_{0.25}$	LI_1	$LI_{0.25}$
Lothar - 26.12.1999 (1)	65	58	58	-	-
Daria - 25.01.1990 (3)	8	6	6	3	2
87J - 15.10.1987 (4)	38	56	61	51	51
Martin - 27.12.1999 (8)	92	110	-	-	-
Anatol - 03.12.1999 (9)	31	61	40	48	29
Vivian - 26.02.1990 (10)	2	1	1	1	1
ERA-Interim	MI_{ls}	MI_1	$MI_{0.25}$	LI_1	$LI_{0.25}$
Lothar - 26.12.1999 (1)	18	18	24	153	-
Daria - 25.01.1990 (3)	4	3	3	3	3
87J - 15.10.1987 (4)	28	41	15	43	11
Martin - 27.12.1999 (8)	47	94	75	-	-
Anatol - 03.12.1999 (9)	15	24	63	16	26
Vivian - 26.02.1990 (10)	2	2	2	1	1

Due to different wind climatologies, the 98th percentile used as threshold for Central Europe may be too low to produce any loss in some regions of Europe. Hence, further investigations concerning the critical wind speed, which needs to be exceeded to cause damages, are performed. Gust speeds of about 21m/s (8bft) (see section 1.3) are expected to produce damages on buildings and infrastructure. This value corresponds to a wind speed between 8m/s and 11m/s depending on the gust factor (e.g. Wieringa, 1973; Born et al., 2012). Therefore the values 8m/s, 9m/s, 10m/s and 11m/s are investigated as possible threshold alternative. This analysis is done for the three reanalysis datasets and the present day climate conditions of GCM data (as used in Chapter 3, 5 and 6). Fig. 2.3 exemplarily shows regions in Europe where the 98th percentile of the winter wind climatology is below 9m/s (red shading) and above 9m/s (blue areas). The distribution shows slight differences for the three reanalysis datasets. Nevertheless, the pattern based on GCM data is similar to the three datasets (Fig. 2.3).

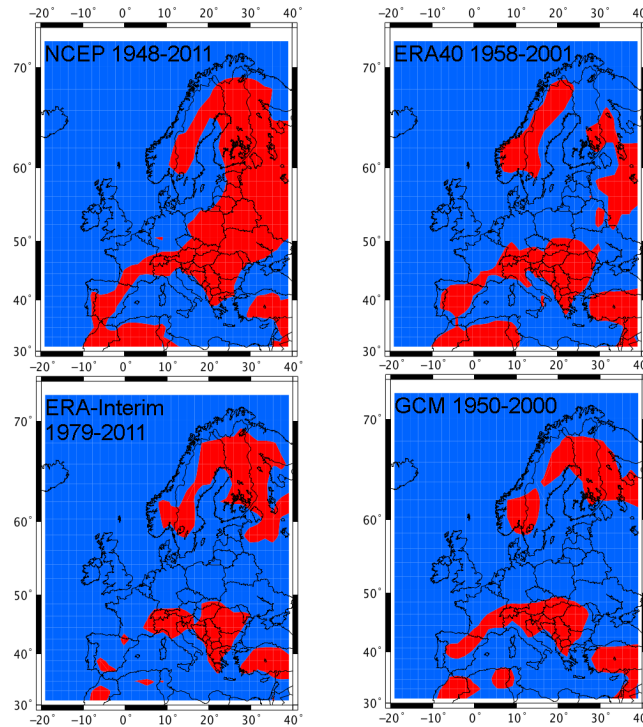


Fig. 2.3: 98th percentile for NCEP (upper left), ERA40 (upper right), ERA-Interim (lower left) and GCM (lower right). Blue: 98th percentile > 9ms red: 98th percentile < 9ms.

For all four datasets, 9m/s seems to be the best compromise threshold. This is given by the fact that the threshold should not be changed in Central Europe, where the 98th percentile is a realistic value for the estimation of losses (Klawa and Ulbrich, 2003). However, in regions like in Southern Europe this value is too low to produce losses. For 8m/s almost no regions fall below this threshold, while for 10m/s and 11m/s wide areas of Central Europe are below this value (Appendix). For NCEP data, the region with an exceedance of 9m/s is largest, also containing Eastern Europe. For ERA40 and ERA-Interim data, the areas where the 98th percentile do not exceed 9m/s are primarily in the Mediterranean area and Scandinavia. Based on these results 9m/s is used in Chapter 6 as threshold for Austria, Switzerland, Finland, Hungary, Slovakia, Italy, Norway, Spain and Sweden instead of the 98th percentile. An example of grid point, where the threshold is changed within the 115 analysed events is presented in Fig. 2.4. Over Central and western Europe more than 90% of wind speeds within the 115 events are higher than 9m/s, while for the Mediterranean area, Eastern Europe and Scandinavia less than 50% are exceeding this threshold (Fig. 2.4, blue/white regions). This indicates that in these regions a threshold of 9m/s may change the event identification towards more events causing high potential losses, which is the desired effect. The differences between the cubistic approach and the not cubistic approach of LI and MI are similar. Therefore the three studies are based only on some of the presented indices: in Chapter 3 LI^3 , MI_1^3 and MI_{ls}^3 , in Chapter 5 LI^3 and MI_1^3 , and in Chapter 6 LI^3 are analysed.

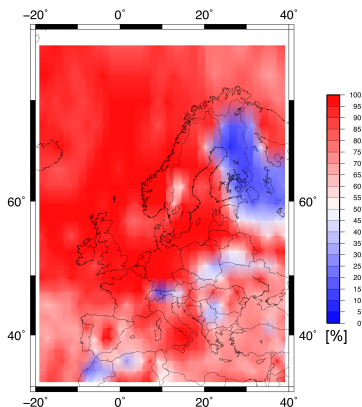


Fig. 2.4: Percentage of the 115 events exceeding a wind speed of 9m/s.

3 Loss Potentials associated with European Windstorms under Future Climate Conditions

Reference:

Pinto J.G., Karremann M.K., Born K., Della-Marta P.M. and Klawe M. (2012): Loss potentials associated with European windstorms under future climate conditions, *Clim Res*, **54**: 1-20, doi:10.3354/cr01111

©Inter-Research 2012

Permission to reprint:

The licence to reprint the above-named article within this PhD thesis was granted by Ian Steward, permissions manager of Inter-Research, on 31.07.2014 via email.

Page numbers are as published in Climate Research.



Loss potentials associated with European windstorms under future climate conditions

Joaquim G. Pinto^{1,*}, Melanie K. Karremann¹, Kai Born¹, Paul M. Della-Marta²,
Matthias Klawa³

¹Institute for Geophysics and Meteorology, University of Cologne, Kerpener Str. 13, 50937 Cologne, Germany

²Partner Reinsurance Europe Limited, Bellerivestrasse 36, 8034 Zurich, Switzerland

³DeutscheRück AG, Hansaallee 177, 40549 Düsseldorf, Germany

ABSTRACT: Possible changes in the frequency and intensity of windstorms under future climate conditions during the 21st century are investigated based on an ECHAM5 GCM multi-scenario ensemble. The intensity of a storm is quantified by the associated estimated loss derived with using an empirical model. The geographical focus is 'Core Europe', which comprises countries of Western Europe. Possible changes of losses are analysed by comparing ECHAM5 GCM data for recent (20C, 1960 to 2000) and future climate conditions (B1, A1B, A2; 2060 to 2100), each with 3 ensemble members. Changes are quantified using both rank statistics and return periods (RP) estimated by fitting an extreme value distribution using the peak over threshold method to potential storm losses. The estimated losses for ECHAM5 20C and reanalysis events show similar statistical features in terms of return periods. Under future climate conditions, all climate scenarios show an increase in both frequency and magnitude of potential losses caused by windstorms for Core Europe. Future losses that are double the highest ECHAM5 20C loss are identified for some countries. While positive changes of ranking are significant for many countries and multiple scenarios, significantly shorter RPs are mostly found under the A2 scenario for return levels correspondent to 20 yr losses or less. The emergence time of the statistically significant changes in loss varies from 2027 to 2100. These results imply an increased risk of occurrence of windstorm-associated losses, which can be largely attributed to changes in the meteorological severity of the events. Additionally, factors such as changes in the cyclone paths and in the location of the wind signatures relative to highly populated areas are also important to explain the changes in estimated losses.

KEY WORDS: Windstorm · Storm damage · Property losses · Risk · Extreme value analysis · Future climate change · Insurance · Uncertainty

— Resale or republication not permitted without written consent of the publisher —

1. INTRODUCTION

Extra-tropical cyclones belong to the most destructive natural hazards affecting Europe. For example, the storms 'Kyrill'¹ (18.01.2007, dd.mm.yyyy; Fink et al. 2009) and 'Klaus' (24.01.2009; Liberato et al. 2011) have recently caused insured losses of €~3 to

3.5 billion and over €1.5 billion, respectively. Economic losses from these events are estimated to be at least twice as much as insured losses (MunichRe 2008; SwissRe 2008; Aon-Benfield 2010). The storm series of 1990 (McCallum & Norris 1990) and 1999 (Ulbrich et al. 2001) caused economic losses of €~10 billion each (MunichRe 2001). Such events have caused considerable disruption to social services, public transportation and energy supply, as well as leading to a large number of fatalities. The analysis of windstorms and their effects are thus highly relevant, both from a scientific and an economic point of

¹Since 1954, the Institute of Meteorology of the Freie Universität Berlin has named all vortices in Central Europe. This list of names is used here. Source: www.met.fu-berlin.de/adopt-a-vortex/historie/

view. This is documented by several recent studies (e.g. Della-Marta et al. 2010, Pinto et al. 2010, Schwierz et al. 2010, Haylock 2011).

Within this context, an important question is the extent that storm activity in general, and for Europe in particular, is influenced by climate change. This can be addressed through the analysis of simulated cyclone activity (e.g. Bengtsson et al. 2006, Löptien et al. 2008). Currently, most general circulation models (GCMs) estimate a decrease in the total number of winter cyclones (e.g. Lambert & Fyfe 2006, Pinto et al. 2007b). However, for some regions, e.g. the British Isles region, an increased number of intense cyclones is identified in transient GCM simulations, such as the ECHAM5/MPI-OM1 GCM (e.g. Bengtsson et al. 2006, 2009, Della-Marta & Pinto 2009). These changes in cyclone activity are connected with an increase in wind extremes over Western and Central Europe (e.g. Leckebusch et al. 2006, Pinto et al. 2007b, Rockel & Woth 2007). While the spatial patterns of the abovementioned signals over Western Europe are largely coherent among GCMs and regional climate models (RCMs), the magnitude of the signal clearly depends on the choice of GCMs and RCMs. Typically, changes are smaller for RCMs than for GCMs (e.g. Pryor et al. 2006, 2010, Beniston et al. 2007, Donat et al. 2010a, Goyette 2011). As a consequence, loss potential (and notably its inter-annual variability) is estimated to increase over Western Europe under future climate conditions (e.g. Leckebusch et al. 2007, Pinto et al. 2007a, Donat et al. 2011).

An important aspect within the context of extreme events, climate change and impacts is an adequate estimation of uncertainties, particularly in terms of the choice of GCMs, pre-defined forcing scenarios and initial conditions. For example, Schwierz et al. (2010) analysed an ensemble of coupled climate scenarios for 2 different GCMs (ECHAM5/MPI-OM1 and HadAM3), and identified an increase in intensity of extreme storms and associated losses over Central Europe. This effect is more pronounced for stronger (and rarer) events. In fact, extreme storms typically show the largest climate change sensitivity, but assessments have large uncertainties. Extreme value statistics (e.g. Coles 2001) have been widely used to calculate the return period (RP) of windstorms (e.g. Brodin & Rootzen 2009, Della-Marta et al. 2009, Hofherr & Kunz 2010, Kunz et al. 2010). In particular, Della-Marta & Pinto (2009) quantified the changes in the intensity of storms over Western and Central Europe, identifying a statistically significant shortening of the RP of storms over this area when consider-

ing the Laplacian of mean sea level pressure as a measure of cyclone intensity. Based on this evidence, it is now important to quantify possible changes of the associated event based storm losses, extending the work of the aforementioned studies (this paragraph). With this aim, the main objectives are (1) to estimate the magnitude of the projected changes in storm losses under future climate conditions, (2) to sample the uncertainty of these changes by using a multi-scenario multi-member GCM ensemble, (3) to quantify possible changes in the intensity and frequency of potential losses using different evaluation techniques and (4) to distinguish between systematic changes in potential loss associated with alterations in the severity of events and other changes associated with sampling (e.g. intense storms may by chance hit a highly populated area more frequently).

With this aim, a modified version of the empirical storm loss model by Klawns & Ulbrich (2003), originally developed for station data, was applied. Since this first publication, the original storm loss model has been adapted for use in gridded model data and applied in a number of studies dealing with climate change impacts (e.g. Leckebusch et al. 2007, Pinto et al. 2007a, Donat et al. 2010b). Unlike those studies, our analysis focuses on event-based losses (single windstorms), not on annual aggregated losses. Further, it is not restricted to individual countries in Western Europe, and considers most of Europe. This choice is motivated by the occurrence of storms like 'Klaus', and 'Xynthia', which affected the Iberian Peninsula and the Western Mediterranean, and 'Kyrill', which also hit Eastern Europe. Eastern European countries have currently lower insured values than in Western European countries, but their economies grew much faster during the last 10 yr², so that in the future storm losses in these countries resulting from pan European events are likely to make up a greater proportion of Europe-wide losses than in the past.

2. DATA

2.1. ERA-40 and NCEP/NCAR-reanalysis

Reanalysis data from the ERA-40-project (ERA-40) of the European Centre for Medium Range Weather Forecasts (ECMWF) and the National Center for Environmental Prediction/National Center for Atmo-

²<http://epp.eurostat.ec.europa.eu/portal/page/portal/eurostat/home>

spheric Research (NCEP/NCAR; hereafter NCEP) are used for model calibration and validation. ERA-40 is available 6-hourly from September 1957 to August 2002 (Uppala et al. 2005). Its spatial resolution is N80 (Gaussian grid), which is equivalent to $\sim 1.125^\circ \times 1.125^\circ$ (~ 110 km over Central Europe). NCEP is available from 1948 to present (Kalnay et al. 1996, Kistler et al. 2001), with a spatial resolution of T62 ($\sim 1.875^\circ \times 1.875^\circ$; 180 km over Central Europe), and a time resolution of 6 h. NCEP data encompasses the larger time window and is, unlike ERA-40, constantly updated. Further, its spatial resolution is similar to the considered GCM (see Section 2.2). For both datasets, 6-hourly instantaneous 10 m wind values are used as input for the storm loss model. This analysis is performed for the winter half year (October to March), corresponding to the period when most windstorms occur over Central Europe (Lamb 1991, Klawns & Ulbrich 2003). For comparison with the GCM data, the 40 winters 1960/1961 to 1999/2000 are used as a reference. This period is referred to as 1960 to 2000; the same nomenclature is used for other periods.

2.2. Climate simulations of ECHAM5/MPI-OM1

Multi-scenario ensemble climate change experiments performed with the atmosphere-ocean coupled GCM ECHAM5/MPI-OM1 (European Centre Hamburg Model version 5/Max-Planck-Institut ocean model version 1; Jungclaus et al. 2006) are used in this study. The spectral atmospheric model ECHAM5 has 31 vertical levels and a spatial resolution of T63 (Roeckner et al. 2006), which corresponds to a spatial resolution of $1.875^\circ \times 1.875^\circ$ (~ 180 km over Central Europe). The 23-level ocean model MPI-OM1 includes a dynamic ocean sea-ice model (Marsland et al. 2003). Surface conditions and fluxes are exchanged between both components. The coupled model is hereafter referred to as ECHAM5. The ensemble of climate simulations produced for the 4th Intergovernmental Panel on Climate Change (IPCC) Assessment Report is considered. The 3 ensemble simulations for recent climate conditions (20C, 1960–2000) are computed with radiative forcing according to the historical greenhouse gas concentration (GHG) and aerosol concentrations for 1860 until 2000. The initial conditions for the 3 ensemble runs are different states of the 505 yr pre-industrial control simulation computed with constant 1860 GHG concentration. Further, 3 groups of experiments following the SRES (Special Report on Emission Scenarios; Nakićenović et al. 2000) B1, A1B and A2 up to 2100

are considered (3 ensemble simulations each). CO_2 concentration increases from 367 ppm in 2000 to 550 (B1), 703 (A1B) and 836 ppm (A2) in the year 2100. Wind maxima (wimax) every 6 h from the GCM are used as input to our loss model. This dataset corresponds to the largest value during a 6 h integration period derived from instantaneous values of wind speed at the internal time step of the GCM (~ 15 min). A comparison between wimax and 6-hourly instantaneous values is presented in Pinto et al. (2007a).

2.3. Insurance data and population density

The calibration of the novel event-based storm loss model (cf. Section 3.2) is performed using data from the German Insurance Association (GDV). This dataset provides daily loss ratios for private buildings in Germany for the period 1997–2007, which were aggregated in districts. As the data is collected from most of the German insurance companies, this dataset is a good index for the insured market loss in Germany. Due to the usage of loss ratios, defined as the ratio loss:insured values, inflation effects can be neglected. Other socio-economic factors that may have changed slightly during this period are also neglected.

Since insurance portfolio data are not available on a European scale, the insured values are approximated for purposes of the storm loss model by the population density. The population density for the year 1990 with $1^\circ \times 1^\circ$ resolution is used (Fig. 1a), as provided by CIESIN & CIAT (2005). The area defined as Core Europe consists of the countries Belgium, Denmark, France, Germany, Great Britain, Ireland and The Netherlands, and is depicted in yellow/orange colours. Additional countries considered in this evaluation are illustrated in pink/red colours. Areas not considered are shown in green.

3. METHODS

3.1. Storm loss model

The original storm loss model by Klawns & Ulbrich (2003) was first modified to consider reanalysis and GCM data (Leckebusch et al. 2007, Pinto et al. 2007a). Here, the method is further developed to estimate event-based potential losses from gridded wind data. The short description below focuses on the main assumptions of the storm loss model. Novel aspects introduced in the present study are given in Steps 3, 6 and 7.

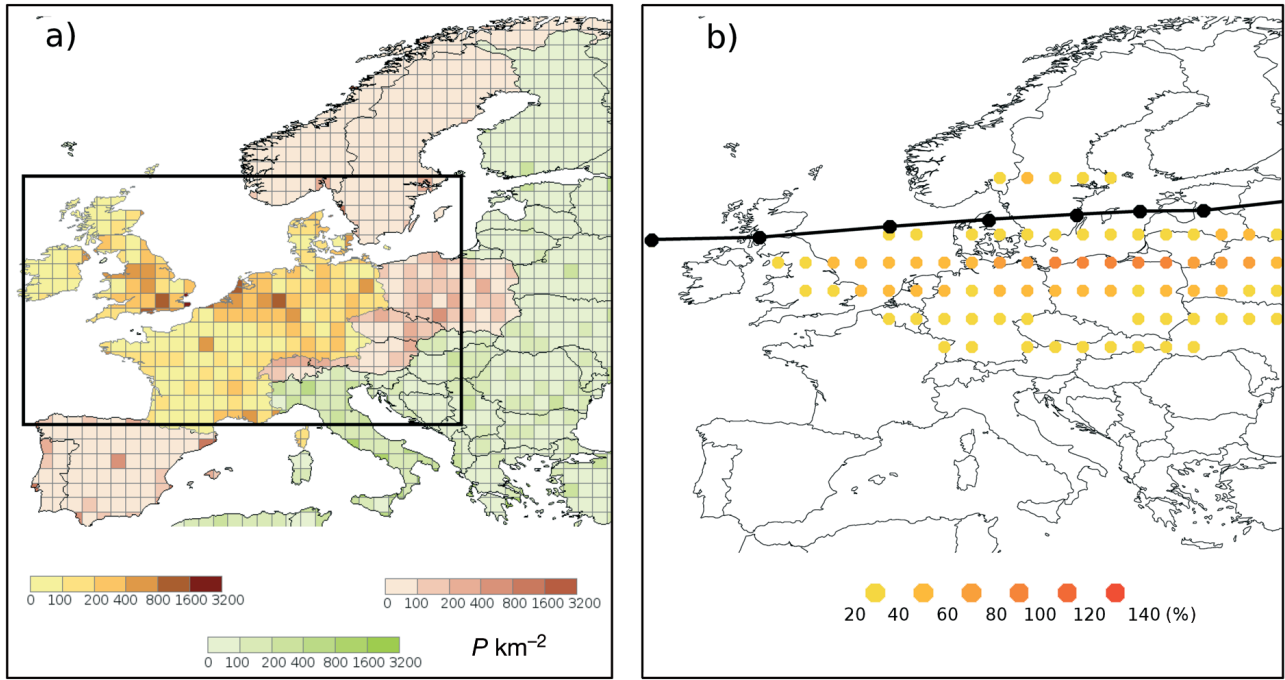


Fig. 1. (a) Population density in Europe ($P \text{ km}^{-2}$). Yellow/orange: Core Europe. Red: additional analysed countries. Green: Mediterranean and Eastern Europe. Black box: area considering a solely meteorological loss index (MI). (b) Wind signature of storm Anatol (3 December 1999). Yellow/red: points with wind values exceeding the 98th percentile in %. Black: cyclone track of storm Anatol in 6-hourly resolution

1. The statistical model assumes that storm damages occur only at 2% of all days (Palutikof & Skellern 1991, Klawa & Ulbrich 2003). This definition implies that the minimum wind speed expected to produce any loss is the regional 98th percentile (v_{98}) of the daily maximum wind speed. Several sensitivity studies have shown the usefulness of this assumption (e.g. Pinto et al. 2007a, Donat et al. 2010a).

2. The vulnerability of buildings to high wind speeds is dependent on local wind climate. The degree of damage increases with growing wind speeds in excess of a threshold, which indicates the minimum wind speed above which losses occur. Therefore, losses depend on both absolute wind speed and a local threshold (v_{98}). The local conditions are taken into account by scaling the wind values with the local v_{98} .

3. A 24 h period is used to sample local maxima of wind speeds for a given area or country. This is performed consecutively by shifting the time window by 6 h each time step.

4. The cube of wind speed is proportional to the kinetic energy flux or flux density. Thus, the potential loss is estimated to increase with the cube of the maximum wind speed. This introduces a (realistic) strong non-linearity in the wind–loss relation. These values are indicated as ‘raw losses’.

5. Insured losses resulting from a single windstorm depend on the values of insurance policies in the affected area. As insurance data is not available, the total value of insured property is assumed to be proportional to the local population density (P ; Section 2.3). Since the resolution of each atmospheric dataset is slightly different, the exact assignment between gridded wind data and P boxes (done with the nearest neighbour approach) is also slightly different. This means that a single wind value for NCEP is used for more P boxes than a single wind value for ERA-40.

6. The total estimated loss for a 24 h window is obtained by adding the potential losses for all grid points that exceed v_{98} . Considering these assumptions, a moving loss index ($LI \text{ raw}$) is calculated:

$$LI \text{ raw}(\text{area}, 24 \text{ h}) = \sum_{i=1}^N \sum_{j=1}^M \left(\frac{v_{ij}}{v_{98ij}} \right)^3 \cdot I(v_{ij}, v_{98ij}) \cdot P_{i,j} \cdot L_{i,j} \quad (1)$$

$$L_{i,j} = \begin{cases} 0 & \text{for seas} \\ 1 & \text{for land} \end{cases}$$

$$I(a,b) = \begin{cases} 0 & a < b \\ 1 & a > b \end{cases}$$

and $P_{i,j}$ = population density per grid box (i,j)

with v_{ij} being the maximum wind speed within 24 h for each grid point, M and N being the number of grid points in the area, $L_{i,j}$ being an indicator if land or sea,

$I(a,b)$ being an indicator of whether the wind speed exceeds the 98th percentile or not, and $v_{98_{ij}}$ the 98th percentile of daily maximum wind speed during the reference period (in this case the whole NCEP period, or 1960 to 2000 for the GCM). The resulting loss model (loss index, LI) is calibrated with historical loss values for Germany (cf. Section 3.2) via a linear regression considering historical event based losses. To reduce the data skewness, a local adjustment in log-log space was additionally performed. A final storm loss model is found with the obtained regression coefficient (A) and the constant (B):

$$LI(\text{area}, 24 \text{ h}) = A \cdot \sum_{i=1}^N \sum_{j=1}^M \left(\frac{v_{ij}}{v_{98_{ij}}} \right)^3 \cdot I(v_{ij}, v_{98_{ij}}) \cdot P_{i,j} \cdot L_{i,j} + B \quad (2)$$

7. In addition to the LI , which includes information of P and which is only defined over continental areas, a meteorological index (MI) is defined for a box covering most of Western Europe (cf. Fig. 1a), but considering all grid points over both land and sea, and without weighting with P . The definition of MI is as follows:

$$MI(\text{area}, 24 \text{ h}) = \sum_{i=1}^N \sum_{j=1}^M \left(\frac{v_{ij}}{v_{98_{ij}}} \right)^3 \cdot I(v_{ij}, v_{98_{ij}}) \quad (3)$$

Comparison of results using this index and the LI of Core Europe allow us to quantify the relative proportion of the changes primarily due to a change in the severity of the events (e.g. larger MI if storms are more intense) or to other factors (changed cyclone paths, highly populated areas like London or Paris are hit more often by chance).

3.2. Model fitting, identification of single storm events and validation

Following the method described in the previous sub-section, 6-hourly reanalysis 10 m wind data are used as input for the storm loss model. The first step is to identify the 24 h local wind maxima for each grid point. These values are compared to the local v_{98} . An example of such a wind signature for the storm Anatol (03.12.1999) can be found in Fig. 1b (similar to that presented in Fink et al. 2009, Schwierz et al. 2010). The colours indicate the magnitude of the exceedance over v_{98} . Next, the exceedances above v_{98} for each grid point are cubed. This information indicates the meteorological characteristics of the storm, and is aggregated over the affected area, summarised as the storm index MI , which does not include loss data. Due to the 24-hourly sampling, the peaks included in such wind signatures have been gathered over an effective

time window of ~ 2 calendar days over the whole area, which is approximately the time a typical windstorm needs to cross the western North Atlantic and Europe. This gives the wind signature a spatially smoothed appearance (see Fig. 1b). Another important aspect is the clustering of events (e.g. storms Lothar and Martin in France, December 1999—Ulbrich et al. 2001; or storms Vivian and Wiebke in Germany, February 1990—Lamb 1991). Our method only differentiates 2 events if they are >24 h apart; otherwise they are counted as one. This time frame is just enough to separate Lothar from Martin in France. MI is considered for the area defined in Fig. 1a (black box), which includes countries typically affected by windstorms and large sea areas, including the Bay of Biscay and the North Sea. The choice of a 24 h window is also motivated by market considerations, as it is a good compromise between the ‘named perturbation’ definition and the ‘free hours’ clause used in the insurance industry. On the other hand, a 24 h window is enough to capture the relevant footprint of a major windstorm, as such a storm moves rather fast, typically crossing an area the size of the MI Box (cf. Fig. 1a) in much less than 24 h.

The loss at each grid point of a single storm event is defined as the local maximum of the LI raw time series (Eq. 1). For calculating the event-based LI , this information is summed over the affected (continental) area. In order to obtain realistic loss values, the estimated losses have to be calibrated with real data. The LI values are fitted using a linear regression with the loss ratio data of the GDV for Germany. An example for indexed event losses for Germany can be seen in Fig. 2 for using NCEP data. Since the calibration is performed using only German loss data, loss estimations for other countries may be biased. However, our simple indices MI and LI may be regarded as independent from any particular vulnerability definition or calibration. Therefore, the relative signals may serve as a measure of the expected climate-related changes, assuming the characteristics of private houses for Germany are representative for Western and Central Europe. Further, the climate change signal of losses is estimated solely from GCM data. The loss calibration is only important for validation purposes, and thus has no influence on the findings with respect to climate change impact.

3.3. Ranking and extreme value statistics

A simple and robust way to quantify changes in extreme events between 2 samples of data (e.g.

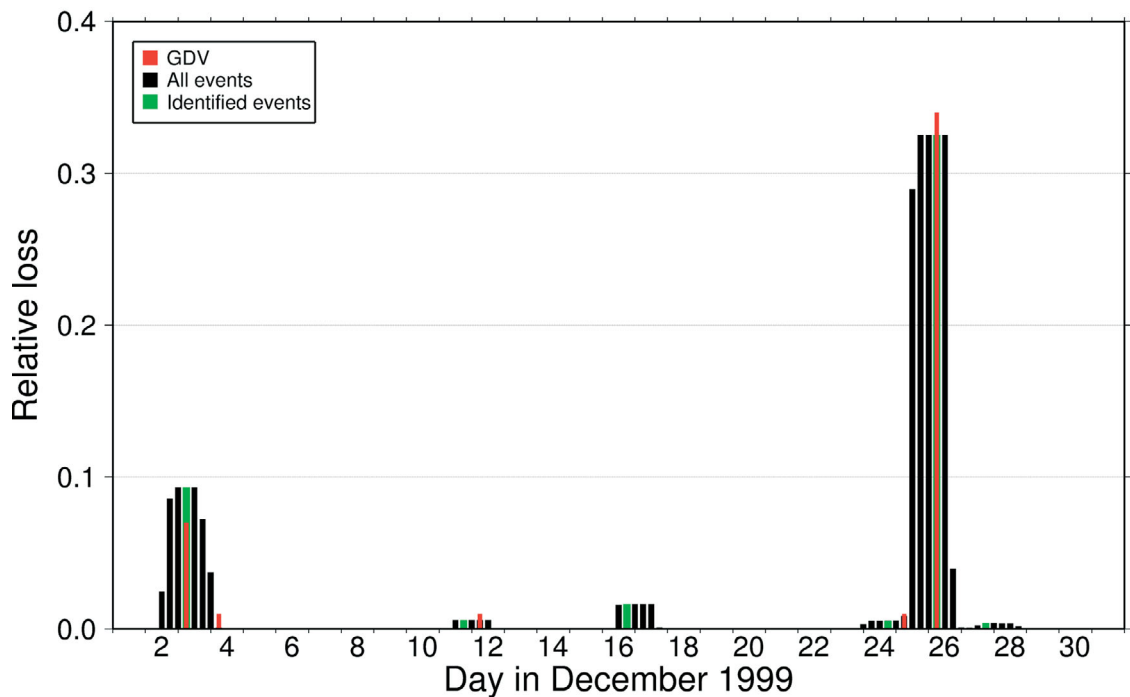


Fig. 2. Black: 24 h moving aggregated losses for Germany in December 1999. Red: historical loss data (German Insurance Association, GDV); green: identified event losses derived by NCEP. Data are relative losses to maximum loss included in the corresponding dataset

recent and future climate, or 2 reanalysis datasets) is using a statistical rank approach. This method compares the relative ranking of events (i.e. position in terms of magnitude) between datasets. Using rank statistics, no assumptions regarding statistical distributions of data are necessary to detect changes in the frequency/intensity relation over time. The Wilcoxon rank sum test (Wilcoxon 1945) allows the assessment of the significance of possible rank changes. This rank sum test is similar to the *U*-test (Mann & Whitney 1947). The significance was tested at the 5% level (two-sided) following Table 7.29 in Sachs & Hedderich (2009). Considered here are independent samples of the same size and with at least 5 values.

Additionally, the RPs of identified events are estimated from a generalised Pareto distribution (GPD) fitted to identified event values (green bars in Fig. 2) of the *LI* and *MI* indices that are above certain thresholds (the so called ‘peak over threshold’ method, see Appendix 1 for details of the method and selected thresholds). Following Della-Marta & Pinto (2009), the GPD is fitted using the maximum-likelihood-method. Uncertainty is calculated using the delta-method (cf. Coles 2001, Della-Marta et al. 2009). RP distributions are significantly different at the 5% level if the 83.4% confidence interval of each RP distribution does not overlap (Julious 2004, their

Table 2). In the description of the results, changes of RPs are always considered for a given return level (e.g. the loss value for 1 yr RP for ECHAM5 20C).

4. EVALUATION FOR RECENT CLIMATE CONDITIONS

In this section the loss model is evaluated on historical storm events. (1) The capability of the storm loss model to identify individual events is discussed. (2) Top loss events extracted from reanalysis data are compared to an independent ranking from MunichRe (2010). (3) Results derived from reanalysis and GCM are compared in order to identify the GCM bias.

4.1. Identification of historical events

The ability of the model to detect the occurrence of loss events is proved. For this purpose, the storm loss model is run with reanalysis data and the events obtained are compared to existing loss information for Germany. In general, the model is able to identify the occurrence of such events in the correct time frame, but the magnitude of the events is represented less well. This can be seen in an example for

December 1999 based on NCEP data (Fig. 2). While the timing is correctly assessed, the magnitude of storm Lothar (26.12.1999) is underestimated, and the magnitude of storm Anatol (3.12.1999) is overestimated. Thus, the loss model generally has difficulty in capturing the lower losses (overestimation), while larger losses are typically slightly underestimated. In particular, the performance for the ERA-40 model is limited for larger losses (not shown). This can largely be attributed to the fact that the validation can only be made for 5 winters (1997/1998 to 2001/2002), and has some implications for the ranking (see Section 4.2). Such difficulties were not unexpected: severe storms typically have above average losses than what could be expected from wind gusts alone, due to market reasons (e.g. claim regulation, awareness of clients). Further, the collection of losses is more exhaustive and detailed than for minor events. For lower losses, overestimations may be largely associated with the fact that the v_{98} threshold is only a rough approximation for the threshold above which losses can occur.

Thus, and given the highly non-linear response of damage to wind speed, these results are viewed as satisfactory. The authors' experience using different assumptions in distributions, vulnerability of insured values and calibrations of the loss functions for Germany and Europe suggests that a higher accuracy in loss determination will not improve the results at this spatial scale. In fact, other current state-of-the-art windstorm loss models use high resolution wind fields (~7 km horizontal resolution) combined with accurate information on the distribution of buildings and their insured values as well as detailed differentiation of the vulnerability of certain building types to obtain a better agreement between modelled and

actual loss (Haylock 2011). Further, the practical experience shows that the uncertainty associated with loss data is often larger than the uncertainty associated with wind data. Given the large uncertainties in any results from future climate projections, combined with uncertainties in the value, distribution and vulnerability of insured values in the future, we see the performance of the present loss model to be sufficient to explore the possible interactions between meteorological changes and the changes in loss.

4.2. Ranking of windstorm losses for the historical period

In a second step, losses derived from reanalysis data were ranked according to their magnitude, and compared to an independent top 10 event list from MunichRe (2010) for the period 1980–2010. The top 10 ranking events of each data source (MunichRe, NCEP, ERA-40) are shown in Table 1. The reanalysis datasets identify the larger events correctly, even though the coherence in terms of ranking is not tight. The NCEP based top 10 contain only 5 of the top 10 losses from MunichRe (2010), while all but one of the other 5 events are ordered within the first 50 events. As ERA-40 does not cover the same time period as NCEP, especially not the last 8 yr (missing storms like Kyrill, Klaus and Xynthia), ERA-40 only has 3 events in the top 10. The strongest historical storm with respect to losses in the last 30 yr was 'Lothar' (26.12.1999; MunichRe 2010). While this storm was on rank 7 based on the NCEP statistics, it is clearly underestimated in the ERA-40 dataset. The weak core pressure of Lothar in ERA-40 has been dis-

Table 1. Top 10 storm losses taken from MunichRe (MR; 2010) for Europe (1980–2010), and based on NCEP (1980–2010) and ERA-40 (1980–2002). Rank: storm rank based on calculated losses for NCEP; ERA-40 reanalysis. **Bold**: events identified by the storm loss model derived with reanalysis. N.N.: no specific name was attributed to this storm. Dates: dd.mm.yyyy. (–) Event outside the ERA-40 reanalysis period

	MR			NCEP		ERA-40	
	Date	Event	Rank	Date	Event	Date	Event
1	26.12.1999	Lothar	7; 231	18.01.2007	Kyrill	25.01.1990	Daria
2	18.01.2007	Kyrill	1; –	25.01.1990	Daria	26.02.1990	Vivian
3	25.01.1990	Daria	2; 1	31.12.2006	Lotte	23.01.1993	Agnes
4	28.02.2010	Xynthia	49; –	26.02.1990	Vivian	08.12.1993	Quena
5	15.10.1987	87J	179; 28	13.01.1984	N.N.	28.02.1990	Wiebke
6	23.01.2009	Klaus	47; –	27.12.1999	Martin	27.03.1987	N.N.
7	07.01.2005	Gudrun	17; –	26.12.1999	Lothar	26.12.1998	N.N.
8	27.12.1999	Martin	6; 104	22.01.1995	Urania	03.12.1999	Anatol
9	04.12.1999	Anatol	18; 12	31.01.1983	N.N.	13.01.1993	Verena
10	26.02.1990	Vivian	4; 2	23.01.1993	Agnes	07.02.1990	Judith

cussed in detail in Ulbrich et al. (2001). The ranking is more coherent with regard to storm 'Daria' (25.01.1990), a storm which affected a much larger area, and which ranks 3 in the MunichRe (2010) list, ranks 2 according to the NCEP results and ranks 1 for the ERA-40 output. Included in the ERA-40 top 10 are 2 Great Britain storms (27.03.1987 and 26.12.1998) with no name but which have been identified as high ranking storms by Hewston & Dorling (2011).

An unambiguous comparison of different reanalysis datasets with respect to extreme storm events is always expected to be difficult. For example, the discrepancy of ranks of both reanalysis datasets may partly be attributed to the different numbers of grid points with wind values $>v_{98}$, and to the different assignment of population data due to the dissimilar grids. Also, the MunichRe list is not independent from economic factors such as inflation: an increase in insured values as well as changes in their geographical distribution have occurred over time. Nevertheless, the loss model identifies the most severe storm events from both reanalysis datasets, and assesses the potential loss similarly if the spatial extent of the event is large enough.

4.3. Comparison of GCM with reanalysis results

The magnitude of the GCM bias is estimated from reanalysis data with respect to storm loss events. First the wind climatology is discussed. Pinto et al. (2007a) investigated the spatial distribution of v_{98} for both

ERA-40 and the ECHAM5 20C simulations for the period 1960–2000, representing 40 winters. Differences between the pattern of ERA-40 and 20C climate simulations are small (their Fig. 3). Over sea, and especially over the North Atlantic, the GCM overestimates wind speeds, while over the continents the values are typically underestimated, but with no strong spatial heterogeneity. This is also the case for NCEP (cf. Pinto et al. 2007b). Thus, the resulting loss based on GCM and reanalysis data may be expected to have similar statistical characteristics.

A comparison of RPs of storms obtained from the GCM and ERA-40 (using data 1960–2000) for *LICore* Europe results are shown in Fig. 3, where the GPD fit to ERA-40 (red) and the ECHAM5 20C ensemble mean (blue) are depicted. The GPD fit for ERA-40 uses 40 yr of data. The fit for ECHAM5 20C considers 120 yr, as it pools together the data from 3 data samples. While the RPs obtained for GCM losses largely agree with those obtained from the reanalysis data, small differences are observed in detail. For example, significant differences exist for frequent events (<1.7 yr), as the CIs do not overlap. Further (non-significant) deviations are also found around 5 yr RPs. These differences may be partially attributed to the different sample size; in fact, they are only statistically significant for 20C runs nos. 2 and 3 (not shown). But overall, we conclude that the GCM derived losses have similar RPs to those obtained from the reanalysis data.

5. CHANGES UNDER FUTURE CLIMATE CONDITIONS

In this section, the impact of increasing GHG forcing on loss estimates is investigated. With this aim, changes in ranking and RPs are analysed, particularly between the end of the 21st century (2060–2100) and the end of the 20th century (1960–2000), both periods containing 40 full winters. Additionally, continuous changes over the whole 21st century are analysed, in order to compare the magnitude of the climate signal against natural variability. All calculations are performed considering v_{98} values for recent climate conditions (no adaptation of constructions to climate change impact, cf. Pinto et al. 2007a).

5.1. Ranking changes for Core Europe

MI and *LI* for Core Europe are derived from the transient ECHAM5 ensemble runs following the 3

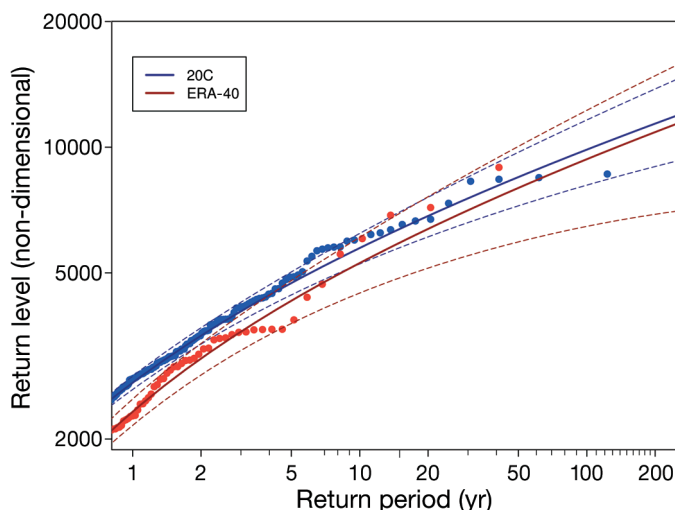


Fig. 3. Return periods (RP) of modelled losses for ERA-40 reanalysis (red) and ECHAM5 20C ensemble mean (blue). Dashed colour lines: generalized Pareto distribution fit 83.4% CI. Non-overlapping CIs for a given return level indicates differences at 5% significance level

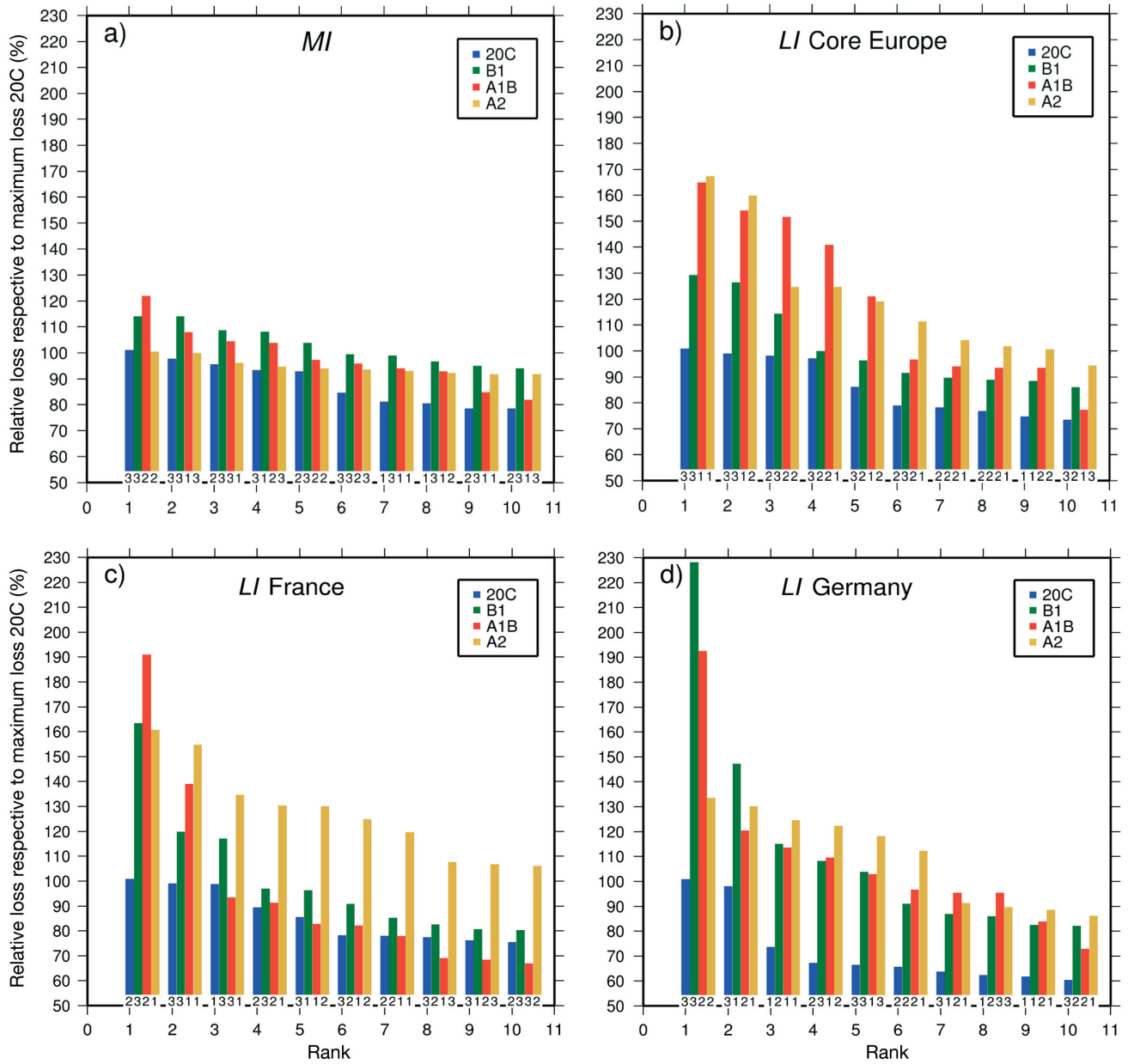


Fig. 4. Percent of loss relative to maximum loss in 20C (1960–2000) of the top 10 estimated losses for different climate scenarios (B1, A1B and A2; 2060–2100) and the present (20C) for (a) meteorological index (*MI* Box), (b) loss index (*LI*) Core Europe (see Fig. 1a), (c) *LI* France and (d) *LI* Germany. Numbers below bars: number of ensemble run

scenarios (B1, A1B and A2). In a first step, the ranking of the estimated losses is compared between the periods 2060–2100 and 1960–2000. For each scenario, data from the 3 ensemble simulation runs were pooled. The ensemble members are assumed as equally probable, and contribute to a total of 120 yr of data. The estimated changes of severity for the top 10 events for *MI* and *LI* Core Europe are presented in Fig. 4a,b. To evaluate the role of single ensemble runs, each bar (representing a single loss) has a sub-script number identifying the ensemble member. *MI*

and *LI* values are shown in percent relative to the strongest event for recent climate conditions (100%, correspondent to the left blue bar). For *MI*, the strongest 20C value is exceeded quite often under future climate conditions, the largest value being identified for the A1B scenario with 121% (Fig. 4a). In order to quantify these changes, rank sum statistics were computed (see Section 3.3). Results show that particularly for B1 and A1B scenarios, significant changes are found from rank 5 onwards (Table 2, upper block). For the A2 scenario a shift to more

Table 2. Significance of the change in rankings for meteorological index (*MI* Box; Fig. 1a), loss index (*LI*) Core Europe (Fig. 1a), *LI* France and *LI* Germany. Results for each scenario B1, A1B and A2 are compared to 20C using the rank sum test, tested at the 5 % significance level. Ensembles: E = pooled ensembles between 2060–2100 and 1960–2000, 1–3 = results for the individual ensemble members. Data are the minimum number of rankings with a significant change, with a minimum of 5, and are the same as presented in Fig. 4

Region (ensemble)	B1	A1B	A2
<i>MI</i> Box			
(E)	5	5	15
(1)	5	5	5
(2)	5	5	14
(3)	5	18	14
<i>LI</i> Core Europe			
(E)	5	5	5
(1)	5	5	5
(2)	5	6	5
(3)	11	11	20
<i>LI</i> France			
(E)	5	5	5
(1)	5	10	5
(2)	10	5	5
(3)	10	-	10
<i>LI</i> Germany			
(E)	5	5	5
(1)	5	5	5
(2)	5	5	5
(3)	10	-	10

severe events is less apparent, with significant differences only from rank 15 onwards (Table 2, upper block). Interestingly, the strongest value of 20C is actually not exceeded for A2 (Fig. 4a). Significant changes in ranking are also found for individual runs, in most cases from rank 5 onwards, in other cases only from rank 14 (A2 runs nos. 2 and 3) or rank 18 (A1B run no. 3; Table 2). The less significant results for run no. 3 for both A1B and A2 scenarios are in line with the weaker changes of extreme surface winds found for these runs compared to runs nos. 1 and 2 (cf. Pinto et al. 2007a, their Fig. 5). A distinctive feature is that the top 10 for the B1 scenario is clearly dominated by run no. 3, contributing to a total of 9 out of 10 events (Fig. 4a). This demonstrates that the results show sensitivity to the choice of data, even if the 3 ensemble runs for a scenario are equally probable.

The changes for *LI* Core Europe are shown in Table 2 and Fig. 4b. The changes of ranking on the pooled ensemble are significant for all 3 scenarios from rank 5 onwards (Table 2). Interestingly, changes in magnitude are quite large, reaching for example a maximum loss of 166 % for the A2 scenario compared

to the strongest 20C event. An exception is ensemble no. 3 for all 3 scenarios, for which changes of ranks are only significant from rank 11 (B1, A1B) or 20 (A2) onwards (Table 2). The results clearly indicate that under future climate conditions, storm events are projected to cause larger losses than in recent decades. When comparing in detail the changes in *MI* and *LI*, 2 main differences are apparent. (1) Changes of *LI* Core Europe are systematically comparatively larger than for *MI* (e.g. 164 versus 121 % for A1B). (2) While the tendencies between *MI* and *LI* Core Europe are similar, some differences are obvious, particularly for the A2 scenario, where results may appear contradictory at first sight. However, this dissimilarity is rather an indication that changes in *LI* are not totally controlled by meteorological severity of the events (*MI*). The correlation coefficient between *LI* and *MI* is in fact only 0.784 (explained variance of 61.47 %). This means that other effects are important. A large part of the difference results from the choice of the spatial domain, particularly whether only land points are considered or not. In fact, if *MI* is quantified only for the land areas associated with *LI* Core Europe, the correlation raises to 0.963 (explained variance of 92.74 %). To use such an *MI*-land-only index would be, however, very inconvenient due to its spatially fragmented nature. Further, even over the continental areas, highly populated regions may be hit more or less frequently simply by chance. These results imply that while the *LI* changes can be largely attributed to changes in *MI*, other factors like the exact cyclone tracks and the location of the wind signature relative to highly populated areas are also important.

In order to show how the magnitude of changes at regional scales differs from the changes for Core Europe, results for France and Germany are presented (Fig. 4c,d). In France, the magnitude of changes is larger than for Core Europe, with top events reaching 165, 193 and 162 % for the 3 climate future scenarios compared to the strongest 20C event (Fig. 4c). The shifts of rankings are significant for all scenarios from rank 5 onwards (Table 2; *LI* France). Run no. 1 dominates the changes for the A2 scenario and run no. 3 for the B1 scenario. For Germany (Fig. 4d) changes of the magnitude are even larger, with the strongest loss for B1 scenario exceeding the 20C maximum loss by 227 %, thus more than doubling the 20C maximum loss. The magnitude changes are similar for all 3 scenarios, all significant from rank 5 onwards (Table 2; lower block). Compared to France, the strongest events are more equally distributed among the 3 runs, even though runs nos. 1 and 2 dominate for A1B and A2. The

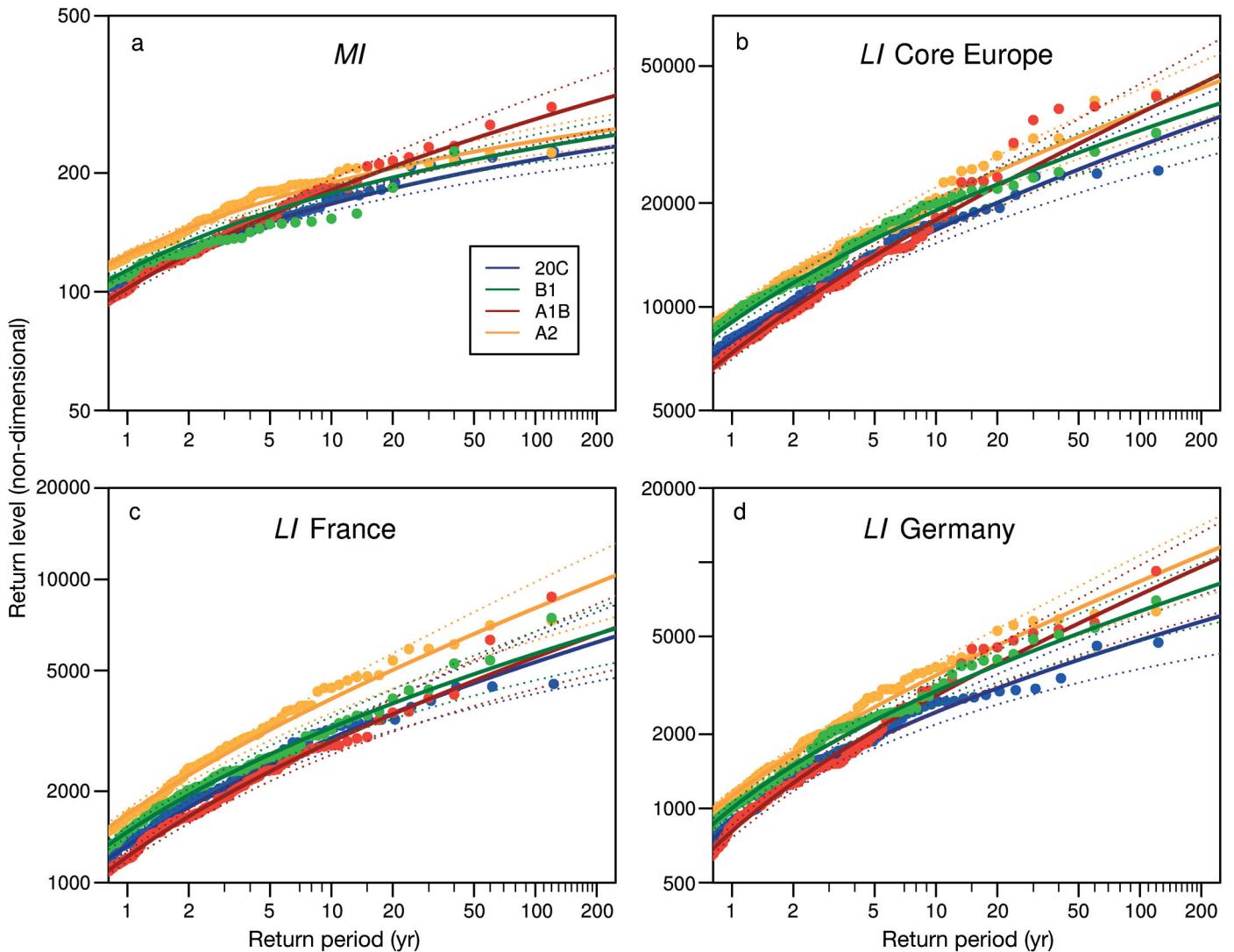


Fig. 5. As for Fig. 3, but for RP of modelled losses for 20C (1960–2000, blue), as well as climate simulations B1 (2060–2100, green), A1B (red) and A2 (yellow) for (a) *MI*, (b) *LI* Core Europe, (c) *LI* France and (d) *LI* Germany. Dashed lines: GPD fit 83.4 % CI. Non-overlapping CIs for a given return level = differences at the 5 % significance level

observed changes in *LI* for Germany and France can directly be attributed to changes in the severity of events. If *MI* is computed for France and Germany, the correlations with *LI* is in both cases ~ 0.992 (explained variance of 98.5 %). This means that the tightness of the relationship between *MI* and *LI* increases strongly for individual countries.

For other countries within Core Europe, changes are similar as for Germany and France. For countries like Denmark, The Netherlands and Belgium the changes of ranking are significant from the rank 5 to 10 onwards, independent of the scenario. An exception is Great Britain and Ireland, which show a shift to lower rankings for the A1B (Great Britain only) and A2 scenarios.

5.2. Return period changes for Core Europe

We analysed *MI* and *LI* values using extreme value statistics. In comparison to the ranking method, this approach aims to reduce the role of the sampling error and allows extrapolation of changes in RPs that are greater than the length of the data.

For *MI*, a shortening of RPs is estimated for all scenarios, except for A1B and short RPs (Fig. 5a; Table 3a). Changes towards more frequent extreme events are only significant for ECHAM5 A2 and for losses correspondent to RPs up to 35 yr for ECHAM5 20C (marked red for 1 to 20 yr in Table 3). For example, a loss value corresponding to a 20 yr RP under current climate conditions is projected to occur for

Table 3. Return period (RP) and CI (Lower and Upper) for given return levels of estimated losses (non-dimensional) for 20C (1960–2000) and estimated RP for the same return levels under different climate scenarios (B1, A1B and A2; 2060–2100) over meteorological index (*MI* Box in Fig. 1a) and loss index (*LI*) for Core Europe (see red countries in Fig. 1a). Non-overlapping CIs for a given return level indicate differences at the 5 % significance level. Significant shortening (**bold**) and lengthening (**bold italics**) of RP

Return level	ECHAM5 20C			ECHAM5 B1			ECHAM5 A1B			ECHAM5 A2		
	Lower	RP	Upper	Lower	RP	Upper	Lower	RP	Upper	Lower	RP	Upper
(a) <i>MI</i>												
109.19	0.86	1	1.07	0.79	0.90	0.98	1.11	1.28	1.43	0.58	0.64	0.70
127.56	1.68	2	2.24	1.42	1.65	1.87	1.91	2.25	2.64	1.01	1.15	1.28
150.52	4.04	5	6.36	3.10	3.71	4.62	3.64	4.40	5.75	2.14	2.49	2.97
166.95	7.75	10	15.01	5.54	6.83	9.68	5.64	6.98	10.2	3.77	4.48	5.93
182.61	14.7	20	38.1	9.76	12.6	21.5	8.39	10.7	17.8	6.59	8.10	12.5
202.18	33.1	50	149	20.2	28.2	68.6	13.4	17.9	36.5	13.6	17.8	37.1
216.18	60.1	100	250+	34.3	51.8	182.2	18.5	25.7	61.5	23.3	32.6	93.1
(b) <i>LI</i> Core Europe												
7901.3	0.87	1	1.08	0.68	0.75	0.82	1.06	1.20	1.35	0.58	0.64	0.70
10237	1.71	5	2.31	1.25	1.41	1.61	1.92	2.22	2.65	1.08	1.20	1.36
13735	4.14	5	6.81	2.85	3.30	4.25	4.03	4.81	6.56	2.42	2.74	3.45
16730	7.95	10	16.4	5.35	6.39	9.53	6.86	8.43	13.2	4.40	5.11	7.22
20062	15.0	20	41.5	10.1	12.5	22.9	11.4	14.5	26.6	7.92	9.50	15.5
25052	34.0	50	152	23.0	31.2	80.4	21.5	29.2	68.0	17.0	21.5	44.3
29325	62.0	100	250+	42.8	63.1	224	34.0	49.0	138	29.9	39.9	100

ECHAM5 A2 about every 8 yr RP. Even though changes are not statistically significant, the results suggest that for long RPs (50 and 100 yr) loss frequency could increase by a factor of 1.8 to 3.9 depending on the scenario.

Regarding *LI* Core Europe, results are more diverse (Fig. 5b, Table 3b). For climate scenarios B1 and A2, shorter RPs are found in all intensities. The changes are significant for 1–4 yr losses for B1 and for 1–16 yr losses for A2. Concerning the A1B scenario, slightly higher (but non-significant) RPs are estimated <5 yr RPs, and shorter RPs >5 yr. Considering changes for RPs ≥50 yr, loss frequency is estimated to increase by a factor of 1.6 to 2.5 depending on the scenario. Although the present results are in line with those obtained for the ranking changes, they do present some interesting additional information about uncertainty and thus, the statistical significance of the change signal.

Regional changes within the 7 countries of Core Europe are analysed in Table 4. Results for the A2 scenario show significant shortening of RPs relative to the ECHAM5 20C return levels for losses with RPs ≤5 yr for Great Britain, 8 yr for Denmark, 20 yr for The Netherlands, 26 yr for Belgium, 73 yr for France and at least 100 yr for Germany (cf. also Figs. 5c,d & 7f). No substantial changes are found for the B1 and A1B scenarios, even though lower RPs are generally predicted for RPs >20 yr. For some countries (Great Britain, Germany and France) and the A1B scenario, longer (shorter) RPs are estimated for RPs below

(above) 2 to 5 yr RPs. For the B1 scenario, shorter RPs are estimated for these 3 countries for all RPs, except for Great Britain for very long RPs.

The results in Table 4 partially depend on the ensemble run, and are in line with the results obtained for the rankings (Fig. 4). For example, the first run for A1B for *LI* Core Europe shows a strong shortening of RPs, the second one slightly shorter RPs, and the third one actually longer RPs (not shown). The sensitivity of results to the ensemble run clearly indicates that climate change assessments should consider larger ensembles to explore better associated uncertainties.

5.3. Return period changes compared to natural variability

To estimate the emergence time at which a possible anthropogenic induced change in *MI* and *LI* may occur, and with the intention to separate the GHG signal from natural variability as much as possible, continuous changes over the period 1960–2100 (winter half year only) are assessed for a few selected cases. With this aim, and following Della-Marta & Pinto (2009), a GPD is fitted to each 40 yr period between 1960 and 2100 in which the respective year corresponds to the ending year of the period (i.e. year 2060 indicates the period 2020–2060).

We focus on the comparison of the *MI* versus *LI* results for Core Europe, where partially dissimilar re-

Table 4. As in Table 3, but for France, Germany, Great Britain, Denmark, The Netherlands, Ireland and Belgium

Return level	ECHAM5 20C			ECHAM5 B1			ECHAM5 A1B			ECHAM5 A2		
	Lower	RP	Upper	Lower	RP	Upper	Lower	RP	Upper	Lower	RP	Upper
France												
1326.10	0.85	1	1.07	0.73	0.82	0.89	1.05	1.23	1.36	0.57	0.63	0.68
1771.67	1.64	2	2.24	1.37	1.60	1.81	2.00	2.43	2.83	1.01	1.15	1.28
2433.94	3.96	5	6.54	3.23	3.92	4.98	4.62	5.86	7.91	2.11	2.47	2.98
2996.88	7.58	10	16.3	6.17	7.75	11.6	8.45	11.2	18.2	3.61	4.30	5.73
3619.45	14.1	20	44.6	11.6	15.4	28.8	15.0	21.1	43.7	6.04	7.39	11.2
4544.80	30.4	50	195	26.0	38.2	108	30.4	47.9	149	11.5	14.9	27.9
5331.36	52.0	100	250+	46.8	76.5	250+	50.0	88.2	250+	18.4	24.9	56.2
Germany												
873.360	0.85	1	1.07	0.74	0.84	0.91	0.99	1.14	1.26	0.62	0.70	0.76
1286.98	1.64	2	2.24	1.32	1.55	1.75	1.75	2.09	2.43	1.12	1.28	1.45
1915.33	3.96	5	6.56	2.84	3.42	4.28	3.55	4.37	5.70	2.33	2.72	3.36
2461.08	7.59	10	16.1	5.00	6.18	8.78	5.79	7.32	10.9	3.89	4.62	6.33
3076.04	14.1	20	43.5	8.61	11.1	18.7	9.10	12.0	20.7	6.28	7.68	11.9
4010.25	30.7	50	182	17.1	23.7	53.6	15.8	22.2	48.5	11.4	14.6	27.4
4821.66	52.9	100	250+	28.1	42.0	123	23.2	34.7	92.0	17.3	23.3	51.3
Great Britain												
2782.57	0.85	1	1.07	0.70	0.79	0.85	1.02	1.18	1.31	0.59	0.65	0.71
3671.73	1.64	2	2.24	1.30	1.53	1.72	1.83	2.21	2.55	1.11	1.27	1.42
5001.65	3.95	5	6.49	3.16	3.83	4.84	3.90	4.88	6.41	2.68	3.20	3.93
6139.14	7.57	10	16.0	6.28	7.91	12.0	6.74	8.73	13.4	5.35	6.60	9.33
7403.91	14.1	20	42.7	12.5	16.8	33.5	11.3	15.4	29.3	10.7	13.9	24.3
9295.63	30.8	50	178	30.5	46.9	161	21.3	32.0	86.3	26.8	38.4	100
10913.6	53.4	100	250+	58.9	105	250+	33.3	55.1	202	53.3	84.8	250+
Denmark												
260.08	0.85	1	1.07	0.73	0.83	0.90	1.02	1.18	1.30	0.57	0.63	0.68
369.05	1.64	2	2.25	1.50	1.77	2.01	1.89	2.28	2.66	1.05	1.20	1.34
539.57	3.97	5	6.56	4.46	5.53	7.48	4.22	5.27	7.05	2.45	2.87	3.56
692.05	7.60	10	16.2	11.0	14.7	27.2	7.50	9.74	15.3	4.64	5.58	7.98
868.28	14.2	20	43.1	28.2	42.9	140	12.9	17.8	34.2	8.67	10.9	19.1
1144.03	30.8	50	175	100	209	250+	25.5	38.5	103	19.4	26.7	66.2
1390.62	53.3	100	250+	250+	250+	250+	41.2	68.5	241	35.1	52.9	180
The Netherlands												
2339.77	0.85	1	1.07	0.71	0.81	0.88	0.88	1.01	1.11	0.57	0.63	0.68
3016.52	1.64	2	2.24	1.27	1.49	1.67	1.54	1.84	2.10	1.01	1.16	1.28
4027.76	3.96	5	6.52	2.88	3.48	4.35	3.26	4.01	5.08	2.21	2.60	3.12
4891.87	7.58	10	16.1	5.43	6.78	10.0	5.64	7.15	10.4	4.01	4.85	6.45
5851.90	14.1	20	43.5	10.2	13.5	26.1	9.55	12.7	22.3	7.25	9.09	14.0
7286.44	30.6	50	185	23.0	34.5	113	18.5	26.7	65.1	15.7	21.0	42.3
8512.27	53.8	100	250+	41.4	71.8	250+	29.6	46.7	153	27.8	40.0	103
Ireland												
753.34	0.85	1	1.07	0.83	0.94	1.03	1.06	1.24	1.37	0.70	0.79	0.86
966.31	1.63	2	2.22	1.46	1.73	1.97	2.08	2.54	2.96	1.38	1.62	1.83
1256.75	3.90	5	6.27	2.96	3.59	4.50	4.95	6.33	8.62	3.40	4.09	5.34
1483.41	7.47	10	14.9	4.80	5.96	8.37	9.16	12.3	20.5	6.53	8.17	13.0
1716.22	14.0	20	38.9	7.49	9.58	15.5	16.3	23.3	51.3	12.1	16.1	33.9
2033.73	31.1	50	161	12.7	17.2	34.9	32.7	52.9	187	26.0	39.0	136
2281.51	54.9	100	250+	18.4	26.1	63.8	53.1	96.3	250+	44.5	75.1	250+
Belgium												
1038.25	0.85	1	1.07	0.68	0.77	0.83	0.84	0.96	1.05	0.55	0.60	0.65
1366.59	1.64	2	2.24	1.20	1.40	1.56	1.47	1.74	1.99	0.97	1.10	1.22
1858.15	3.96	5	6.50	2.73	3.32	4.06	3.03	3.68	4.64	2.10	2.47	2.95
2278.97	7.58	10	16.0	5.34	6.71	9.54	5.05	6.30	8.95	3.80	4.56	6.05
2747.26	14.1	20	42.8	10.7	14.2	26.1	8.20	10.6	17.6	6.82	8.46	13.0
3448.33	30.8	50	178	26.8	40.8	131	14.9	20.6	43.6	14.6	19.3	38.6
4048.51	53.4	100	250+	53.8	95.7	250+	22.8	33.5	87.7	25.5	36.0	92.3

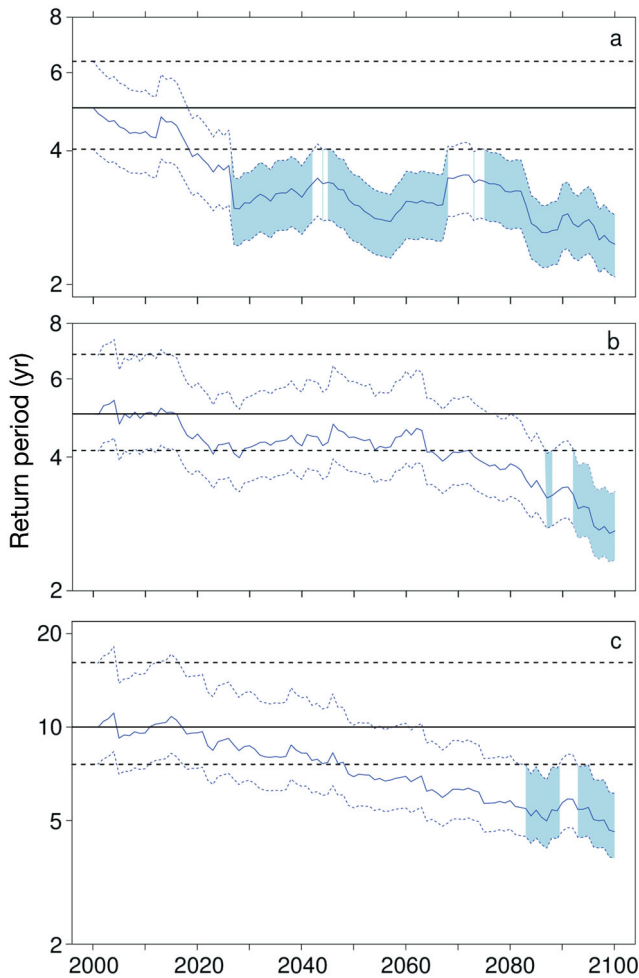


Fig. 6. Change of return period (RP; 20C and A2) over time given a certain return level corresponding to a 5 yr RP for (a) 20C and *MI*, or (b) 20C and *LI* Core Europe; and (c) for a 10-yr RP for 20C and *LI* Germany. Shown are generalised Pareto distribution fits based on moving 40 yr climatologies. The year corresponds to the previous time period (e.g. value for the year 2000 represents time period 1960–2000). Black: 20C RP with 83.4 % CIs. Blue: Estimated RP from the transient run (A2) and 83.4 % CIs. Shaded: non-overlapping CIs for the given return level, indicating differences at the 5 % significance level

sults were identified in the previous sections, and discuss representative examples. Fig. 6a shows the RP change (A2 scenario) for a return level corresponding to a 5 yr loss under recent climate conditions. The change of RP shows strong decadal variability superimposed on a long term trend to shorter RPs. Significantly shorter RPs for *MI* are identified by 2027 (corresponding to the period 1987–2027). While the changes do not always remain significant after 2027, a 20C 5 yr event becomes an event with a RP between 2.5 and 3.5 yr, reaching its lowest value by 2100. These results are in line with Fig. 2 from Della-Marta & Pinto (2009),

which identify significant shorter RPs for cyclone intensity over this area from 2040 onwards. A more detailed analysis of the individual loss events indicates that even though *MI* for 2060–2100 does not exceed the strongest 20C storm, larger events (with a magnitude of 140 % relative to the strongest 20C event) are found in 2027 and 2049, thus explaining the shorter RPs around this time frame. Regarding the *LI* for Core Europe (Fig. 6b), the changes for a loss correspondent to an ECHAM5 20C 5 yr RP occur in a slower but steadier manner than for *MI*. A shortening of RPs is apparent from 2015 onwards, stronger after 2063, but changes are first statistically significant by 2087 (corresponding to 2047–2087), reaching a RP of 2.74 yr by 2100. Finally, the time evolution of losses for Germany is analysed for a loss value correspondent to a 10 yr RP (Fig. 6c). A slow decrease in estimated RPs is found along the whole time series after 2015, reaching 4.62 yr RP by 2100. The signal is first statistically significant by 2083, then continuously from 2093 (2053–2093) onwards. The evaluation of these and further examples documents that the emergence time of the statistically significant changes may occur in some cases as early as 2027, in other cases only by the end of the 21st century.

5.4. Return period changes versus ranking changes for Europe

Here we summarise the results obtained from the 2 different methods for all countries (see Fig. 1a; yellow and red areas). The upper row of Fig. 7 shows changes of rank statistics, whereas the lower row shows changes of RPs. Different colours correspond to different levels of change, with red tones indicating higher losses and shorter RPs, and blue tones lower losses and longer RPs. In Figs. 7a–c, dark (light) tones indicate significant (non-significant) changes to stronger events. The numbers denote the lowest number of considered ranks with significant changes (e.g. 10 events). For RPs, dark tones mark significant changes relative to a given return level for current climate conditions (cf. Tables 3 & 4), and light tones indicate non-significant changes (Fig. 7d–f). The numbers present the RP below which the changes are statistically significant (e.g. an 8 indicates that changes are significant for return levels corresponding to events between 1 and 8 yr RPs under recent climate conditions).

Consistent ranking changes towards higher losses are found for France, Germany, Denmark, Belgium, Netherlands, Austria, Switzerland, Sweden, Czech

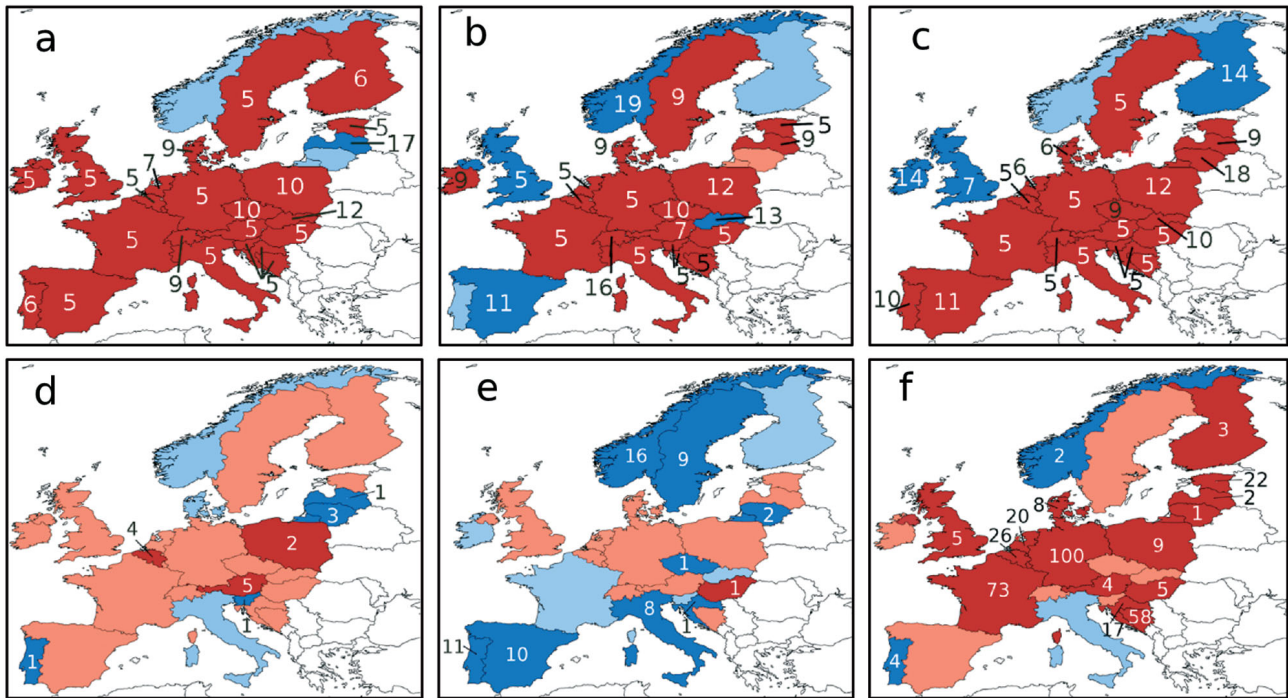


Fig. 7. (a–c) Change of ranking of the maximum loss relative to the present climate scenario (20C) for (a) B1 (b) A1B (c) A2. Dark red: significant increase in intensity of losses in relation to the present climate is estimated for future climate conditions using the rank sum test. Number: minimum number of rankings with a significant change, with a minimum of 5. Light red: more intense events but non-significant changes. Dark blue: significant decreases in the intensity of losses for future climate conditions. Light blue: weaker events but non-significant changes. (d–f) Estimated changes of return periods (RP; yr) for given return levels under current climate conditions for (d) B1 (e) A1B (f) A2. Dark red: significant shortening of RP is found. Light red: non-significant shorter RP. Dark blue: significant longer RP. Light blue: non-significant longer RP is estimated. Numbers: RP up to which changes are significant. In all cases, pooled ensembles for 2060–2100 and 1960–2000 are compared

Republic, Croatia, Estonia, Slovenia and Bosnia, Hungary, Italy and Poland across all 3 scenarios. However, most of the above named countries do not feature significant shorter RPs, except for A2 scenario. In fact, some countries, e.g. Italy and Sweden, actually show a tendency to longer RPs (A1B scenario). On the other hand, changes for Germany are very coherent: All 3 scenarios show significant shifts rank 5 onwards, and shorter RPs are also identified in all cases (cf. Table 4), though only significant for the A2 scenario for RPs. Changes for higher RPs are often not significant due to the large uncertainties, even though the best estimate RP may change by a factor of 3 (e.g. Belgium and Germany for A1B scenario and a 100 yr RP, cf. Table 4). The apparent lack of significant results could be partially associated with the method used for CI estimation (see Appendix 1). However, the present results are largely insensitive to the choice of method due to the high number of threshold exceedances used to fit the GPD. Norway is the only country with a clear indication for lower storm risk under future climate conditions. It shows

a consistent decrease of severe losses, and RPs are longer for all 3 scenarios, being largest for ECHAM5 A1B.

For Finland, Lithuania, Latvia, Slovakia, Portugal, Spain, Great Britain and Ireland, results are more sensitive to the considered scenario. For example, results for Spain show shifts of different sign for the A1B versus B1/A2 scenario. On the other hand, significant lengthening of shorter RPs are estimated for Portugal, while for Spain only the A1B scenario shows this behaviour. For Great Britain, a substantial change to a stronger magnitude is only obtained for the B1 scenario. On the other hand, a tendency to shorter RPs is found for Great Britain only for the A2 scenario, with statistically significant changes up to 5 yr RP.

Interestingly, the magnitude of changes depends only partially on the intensity of the GHG forcing. This means that changes in expected losses are not necessarily the strongest for the A2 scenario and the weakest for the B1 scenario on ensemble average. Such a result is not unexpected, as e.g. Della-Marta

& Pinto (2009) showed that the changes on the intensity of cyclones over Great Britain and the North Sea are statistically undistinguishable for A1B and A2 scenario. This indicates that the relationships between GHG forcing, cyclone activity over Western Europe and losses are far from being a simple linear relationship.

In summary, results obtained with both ranking and extreme value statistics reveal a general and consistent tendency towards an increased frequency of windstorm-related losses over most of Western, Central and Eastern Europe for B1 and A2, and slightly inconsistent findings for A1B. Further, it is clear that the detected changes in rank statistics are more sensitive to the changes in the most extreme events, while RP changes for a given return level are less sensitive to these outliers, as the GPD model is fitted on many more extremes. Finally, losses are expected to reach unseen magnitudes, which for some countries (e.g. Germany) may exceed 200 % of the strongest event in present day climate simulations.

6. SUMMARY AND CONCLUSIONS

The main objectives of this paper was to estimate possible changes in storm losses associated with the activity of winter storm events over Europe, and identify how far these changes are statistically significant. With this aim, a methodology has been developed to estimate event-based losses. Rank statistics and extreme value analysis have been applied to a multi-scenario ECHAM5 GCM ensemble for present day and future climate conditions using the empirically calibrated loss index *LI*, which describes loss estimates based on both meteorological factors and density of insured values. In addition, an index describing purely meteorological forcing (*MI*) of the severity function indicated to what extent such changes are primarily due to changes in cyclone activity. The main conclusions are:

- (1) The simple loss model based on reanalysis data identifies storm events and is calibrated with daily loss estimations from GDV. The selection of the maximum loss value during a time window of 24 h declusters most observed storms.
- (2) The list of storms making up the top 10 ranking estimated losses agrees with independent (not inflation-corrected) statistics (e.g. MunichRe 2010), although the ranking positions for single storms differ. The results derived from NCEP data were in better agreement with insurance industry loss estimations than those from ERA-40.
- (3) Loss estimations derived from ECHAM5 GCM simulations for recent climate conditions (20C, 1960–2000) reveal a similar intensity and frequency of events as the reanalysis. The performance of the loss model is found to be sufficient to explore the possible interactions between meteorological changes and the changes in loss.
- (4) Based on an ensemble of GCM simulations (2060–2100: B1, A1B and A2, 3 ensemble members each) the maximum storm losses of both *LI* and *MI* for current climate conditions are exceeded in the future climate, particularly for countries of Core Europe. Maximum losses could increase by ~65 % by the end of the 21st century, according to the A1B and A2 scenarios. The significance of changes in ranking and therefore of magnitude of storms strongly depend on country and scenario. For many countries, findings point towards higher loss events, significant for at least one scenario. An exception is Norway, for which weaker losses are found.
- (5) *LI* RPs derived from fitted GPDs show a shortening in most countries in Core Europe for a given return level, even though these changes are not always statistically significant at the end of the 21st century. Only the A2 scenario for Core Europe shows a significant shortening of RPs. In contrast to these results, the *MI* shows significant shorter RPs as early as in the third decade of the 21st century for the same scenario.
- (6) In most cases, changes in *LI* and *MI* are in accordance. This could be expected, as the explained variance of *MI* in *LI* is about 98.5 % for a country like Germany or France. For the *MI* Box and *LI* Core Europe, the explained variance drops to 61.5 %. This means that the tightness of the relationship between *MI* and *LI* is reduced when the evaluated area increases, particularly if non-continental areas are considered in *MI*. Therefore, we conclude that while events severity (expressed as *MI*) is a dominant driving force for the detected changes, other factors like the exact cyclone tracks and the location of the wind signatures relative to the highly populated areas become more and more important with increasing area comparatively to the *MI* itself. From this viewpoint, factors which may partially be related with chance also represent a part of the signal in *LI*.
- (7) Considering the *LI* results of both rank statistics and extreme value analysis, 3 different tendencies can be identified: (1) Countries with shorter RPs and higher losses for all 3 climate scenarios: Germany, Belgium, Netherlands, Poland, Estland,

Austria, Croatia, Bosnia and Hungary; (2) Norway with longer RPs and lower losses for all 3 climate scenarios; (3) All other countries have typically higher losses under future climate conditions and in some cases shorter RPs.

- (8) The emergence time of statistically significant changes varies from case to case. This may occur as early as 2027 (correspondent to 1987–2027), in other cases only by the end of the current century.
- (9) Although results differ between scenarios and between ensemble members, in some regions (e.g. Germany) climate change impact signals are coherent for all ensemble members of the 3 scenarios using both analysis methods. The changes in rank statistics are more sensitive to changes in possible outliers, while RP statistics are less sensitive due to the consideration of much more data to fit the GPD model.

The findings of this study are in agreement with those of Schwierz et al. (2010) who postulated increasing losses in Central Europe based on a similar approach, but using regional climate model simulations, and also with previous studies analysing windstorm associated losses on annual basis for some European countries (e.g. Leckebusch et al. 2007, Pinto et al. 2007a, Donat et al. 2011). The main advance of the present study is that it extends previous analysis of storm losses by quantifying the changes of RPs of loss events (instead of annual losses) using extreme value analysis methods. In addition, we evaluated how far the detected changes can be attributed to changes in the meteorological severity of the events (*MI*), and which part of the changes may be caused by the effect that storms hit densely populated areas more frequently. This means that care must be used when relating and interpreting changes of RPs in cyclone activity (e.g. Della-Marta & Pinto 2009) or event severity (*MI*) versus changes in RPs of potential losses (*LI*) on regional, national and continental scale.

Within this context, it is also important to compare regional changes of cyclone intensity, extreme surface winds, *MI* and *LI*. In general terms, the changes in extreme surface winds, *MI* and *LI* are expected to be in the same place. However, the strongest winds associated with a windstorm are typically found several 100s of km south/southwest of the cyclone centre (e.g. Fink et al. 2009). This is also seen in climatological terms (e.g. Bengtsson et al. 2009). Therefore, it is expected that the changes in extreme surface winds to be located on average several 100s of km south/southwest of the main changes in cyclone activity (e.g. Pinto et al. 2007a,b). This means that increased

cyclone intensities over Great Britain induce strong winds over Northern France, Belgium and The Netherlands and only partially over Great Britain itself. In turn this explains why losses over Great Britain only show comparatively weak changes in spite of the shorter RPs of extreme cyclones crossing over the area (e.g. Della-Marta & Pinto 2009). In fact, the *LI* results are largely driven by the large-scale changes in extreme wind speeds (e.g. Pinto et al. 2007b, their Fig. 9) that occur mostly over highly populated areas (e.g. London, Paris, Ruhr), while areas that experience little changes in wind speeds are comparatively sparsely populated. For this reason, the changes in *LI* could be expected to be proportionally greater than *MI*, as found here.

Compared to other IPCC GCMs, ECHAM5 is near the average of the super-ensemble in terms of the climate signal for synoptic activity (Ulbrich et al. 2008) and thus the present results are expected to be near the ensemble mean behaviour of the IPCC GCM simulations.

The expected increase of maximum windstorm losses over Europe and, thus, shorter RPs of winter storms for certain areas during the 21st century might have a large impact on insurance companies (e.g. Changnon et al. 1997). In particular, they must assure that loss claims can be paid out without risking the solvency of the company. Financial authorities, such as the Committee of European Insurance and Occupational Pensions Supervisors, have proposed technical standards to measure the financial strength of insurance companies, which have to meet the requirements of Solvency II (Solvency Capital Requirements, QIS5³). They developed a method to estimate the loss associated with a windstorm that occurs roughly every 200 yr for national and Pan European insurers. According to insurance brokers or providers for insurance market portfolios using the QIS5 method, such a Pan-European windstorm event could cause losses around €36.1 billion⁴. A 200 yr RP loss for Germany could be around €9.8 billion, and for France up to €14.5 billion⁵. Under future climate conditions, the RPs of such a loss could be substantially shorter than 200 yr. Catastrophe models in insurance industry are usually based on historic loss and climatological hazard experience. Therefore, they do not

³<https://eiopa.europa.eu/consultations/qis/quantitative-impact-study-5/index.html>

⁴www.perils.org

⁵www.gccapitalideas.com/2010/12/02/solvency-ii-update-qis5-windstorm-scenarios-are-within-range-of-industry-models/

incorporate possible future climate estimates and trends, which might alter the risk continuously in future years. For Core Europe, the RP for large losses might change considerably already in the first half of the 21st century. Such a change is in line with results by Della-Marta & Pinto (2009), which identified shorter RPs for intense cyclones over the study area already by 2040. Further, and by the year 2100, a 200 yr RP loss for Germany could double its value relative to recent climate conditions (inflation and changes of insurance conditions are not considered). In order to meet the additional capital requirements in a changing climate, it will be necessary to continuously adapt the technical approaches to measuring windstorm risk. As it is not reasonable to calculate the risk of loss for the following year taking possible century long trends into account, it might be reasonable to base loss calculations on storm catalogues, which reflect close-future climate conditions using appropriate GCM simulations.

With this aim, future work will focus on the use of GCM data, e.g. within the new IPCC AR5 scenarios. Additional GCM ensembles could bring more information about variability of long RPs (e.g. 200 yr) and a larger number GCMs could help sample the uncertainty derived from using a single model. At the same time sensitivity analyses must combine the climate variability results with a range of simple and more complex loss models considering other possible factors affecting long term windstorm risk.

Acknowledgements. We acknowledge the provision of loss data by the German Association of Insurers ('Gesamtverband der Deutschen Versicherungswirtschaft', GDV) within a project dealing with the impacts of climate change for the insurance industry in Germany ('Auswirkungen des Klimawandels auf die Schadensituation in der deutschen Versicherungswirtschaft'). The reanalysis data was obtained from the European Centre for Medium Range Weather Forecast (ECMWF) and the National Centers for Environmental Prediction (NCEP). We thank the MPI for Meteorology (Hamburg, Germany) for support and ECHAM5 data, and the DKRZ/WDCC (Hamburg, Germany) and the ZAIK/RRZK (Cologne, Germany) for computing resources. We thank N. Gerresheim (DeutscheRück), A. Reiner (Aon-Benfield) and M. Stowasser (Allianz) for discussions. The comments of the anonymous reviewers are gratefully acknowledged.

LITERATURE CITED

- Aon-Benfield (2010) Annual global climate and catastrophe report IF 2009. Publication of Aon-Benfield. Available at www.aon.com
- Bengtsson L, Hodges KI, Roeckner E (2006) Storm tracks and climate change. *J Clim* 19:3518–3543
- Bengtsson L, Hodges KI, Keenlyside N (2009) Will extra-tropical storms intensify in a warmer climate? *J Clim* 22: 2276–2301
- Beniston M, Stephenson DB, Christensen OB, Ferro CAT, and others (2007) Future extreme events in European climate: an exploration of regional climate model. *Clim Change* 81:71–95
- Brodin E, Rootzen H (2009) Univariate and bivariate GPD methods for predicting extreme wind storm losses. *Insur Math Econ* 44:345–356
- Changnon SA, Changnon D, Fosse ER, Hoganson DC, Roth RJ, Totsch JM (1997) Effects of recent weather extremes on the insurance industry: major implications for the atmospheric sciences. *Bull Am Meteorol Soc* 78: 425–435
- Coles S (2001) An introduction to statistical modeling of extreme values. Springer, London
- CIESIN & CIAT (Center for International Earth Science Information Network Columbia University; and Centro Internacional de Agricultura Tropical) (2005) Gridded population of the world, Version 3 (GPWv3): population density grids. Socioeconomic Data and Applications Center (SEDAC), Columbia University, Palisades, NY. Available at <http://sedac.ciesin.columbia.edu/gpw>
- Della-Marta PM, Pinto JG (2009) The statistical uncertainty of changes in winter storms over the North Atlantic and Europe in an ensemble of transient climate simulations. *Geophys Res Lett* 36:L14703 doi:10.1029/2009GL038557
- Della-Marta PM, Mathis H, Frei C, Liniger MA, Kleinn J, Appenzeller C (2009) The return period of wind storms over Europe. *Int J Climatol* 29:437–459
- Della-Marta PM, Liniger MA, Appenzeller C, Bresch DN, Köllner-Heck P, Muccione V (2010) Improved estimates of the European winter windstorm climate and the risk of reinsurance loss using climate model data. *J Appl Meteorol Climatol* 49:2092–2120
- Donat MG, Leckebusch GC, Pinto JG, Ulbrich U (2010a) European storminess and associated circulation weather types: future changes deduced from a multi-model ensemble of GCM simulations. *Clim Res* 42:27–43
- Donat MG, Leckebusch GC, Wild S, Ulbrich U (2010b) Benefits and limitations of regional multi-model ensembles for storm loss estimations. *Clim Res* 44:211–225
- Donat MG, Leckebusch GC, Wild S, Ulbrich U (2011) Future changes of European winter storm losses and extreme wind speeds in multi-model GCM and RCM simulations. *Nat Hazards Earth Syst Sci* 11:1351–1370
- Fink AH, Brücher T, Ermert V, Krüger A, Pinto JG (2009) The European storm Kyrill in January 2007: synoptic evolution and considerations with respect to climate change. *Nat Hazards Earth Syst Sci* 9:405–423
- Goyette S (2011) Synoptic conditions of extreme windstorms over Switzerland in a changing climate. *Clim Dyn* 36: 845–866
- Haylock MR (2011) European extra-tropical storm damage risk from a multimodel ensemble of dynamically-downscaled global climate models. *Nat Hazards Earth Syst Sci* 11:2847–2857
- Hewston R, Dorling SR (2011) An analysis of observed daily maximum wind gusts in the UK. *J Wind Eng Ind Aerodyn* 99:845–856
- Hofherr T, Kunz M (2010) Extreme wind climatology of winter storms in Germany. *Clim Res* 41:105–123
- Julious SA (2004) Using confidence intervals around individual means to assess statistical significance between two means. *Pharm Stat* 3:217–222
- Jungclaus JH, Keenlyside N, Botzet M, Haak H and others (2006) Ocean circulation and tropical variability in the coupled model ECHAM5/MPI-OM. *J Clim* 19:3952–3972

- Kalnay E, Kanamitsu M, Kistler R, Collins W and others (1996) The NCEP-NCAR 40-year reanalysis project. *Bull Am Meteorol Soc* 77:437–472
- Kistler R, Collins W, Saha S, White G and others (2001) The NCEP/NCAR 50-year reanalysis: monthly-means CD-ROM and documentation. *Bull Am Meteorol Soc* 82: 247–267
- Klawa M, Ulbrich U (2003) A model for the estimation of storm losses and the identification of severe winter storms in Germany. *Nat Hazards Earth Syst Sci* 3:725–732
- Kunz M, Mohr S, Rauthe M, Lux R, Kottmeier C (2010) Assessment of extreme wind speeds from regional climate model. 1. Estimation of return values and their evaluation. *Nat Hazards Earth Syst Sci* 10:907–922
- Lamb HH (1991) Historic storms of the North Sea, British Isles, and Northwest Europe. Cambridge University Press, Cambridge
- Lambert SJ, Fyfe JC (2006) Changes in winter cyclone frequencies and strengths simulated in enhanced greenhouse warming experiments: results from the models participating in the IPCC diagnostic exercise. *Clim Dyn* 26:713–728
- Leckebusch GC, Koffi B, Ulbrich U, Pinto JG, Spangehl T, Zacharias S (2006) Analysis of frequency and intensity of European winter storm events from a multi-model perspective, at synoptic and regional scales. *Clim Res* 31: 59–74
- Leckebusch GC, Ulbrich U, Fröhlich EL, Pinto JG (2007) Property loss potentials for European mid-latitude storms in a changing climate. *Geophys Res Lett* 34:L05703. doi: 10.1029/2006GL027663
- Liberato MRL, Pinto JG, Trigo IF, Trigo RM (2011) Klaus: an exceptional winter storm over Northern Iberia and Southern France. *Weather* 66:330–334
- Löptien U, Zolina O, Gulev SK, Latif M, Soloviev V (2008) Cyclone life cycle characteristics over the northern hemisphere in coupled GCMs. *Clim Dyn* 31:507–532
- Mann HB, Whitney DR (1947) On a test of whether one of two random variables is stochastically larger than the other. *Ann Math Stat* 18:50–60
- Marsland SJ, Haak H, Jungclaus JH, Latif M, Röske F (2003) The Max-Planck-Institute global ocean-sea ice model with orthogonal curvilinear coordinates. *Ocean Model* 5: 91–127
- McCallum E, Norris WJT (1990) The storms of January and February 1990. *Meteorol Mag* 119:201–210
- MunichRe (2001) Winter storms in Europe. II. Analysis of 1999 losses and loss potentials. Publication of Munich Re. Available at www.munichre.com
- MunichRe (2008) Die 10 teuersten Naturkatastrophen 2007. Publication of Munich Re. Available at www.munichre.com
- MunichRe (2010) Significant European winter storms 1980–June 2010. Overall losses. Available at www.munichre.com/app_pages/www/@res/pdf/natcatservice/significant_natural_catastrophes/significant_winter_storms_europe_overall_losses_july2010_de.pdf (in German)
- Nakićenović N, Alcamo J, Davis G, de Vries B and others (2000) IPCC Special Report on Emissions Scenarios. Cambridge University Press, Cambridge
- Palutikof JP, Skellern AR (1991) Storm severity over Britain: a report to Commercial Union. Climatic Research Unit, University of East Anglia, Norwich
- Pinto JG, Fröhlich EL, Leckebusch GC, Ulbrich U (2007a) Changes in storm loss potentials over Europe under modified climate conditions in an ensemble of simulations of ECHAM5/MPI-OM1. *Nat Hazards Earth Syst Sci* 7:165–175
- Pinto JG, Ulbrich U, Leckebusch GC, Spangehl T, Meyers M, Zacharias S (2007b) Changes in storm track and cyclone activity in three SRES ensemble experiments with the ECHAM5/MPI-OM1 GCM. *Clim Dyn* 29:195–210
- Pinto JG, Neuhaus CP, Leckebusch GC, Meyers M, Kerschgens M (2010) Estimation of wind storm impacts over West Germany under future climate conditions using a statistical-dynamical downscaling approach. *Tellus, Ser A, Dyn Meteorol Oceanogr* 62:188–201
- Pryor SC, Schoof JT, Barthelmie RJ (2006) Winds of change? Projections of near-surface winds under climate change scenarios. *Geophys Res Lett* 33:L11702. doi:10.1029/2006GL026000
- Pryor SC, Barthelmie RJ, Clausen NE, Drews M, MacKellar N, Kjellström E (2010) Analyses of possible changes in intense and extreme wind speeds over northern Europe under climate change scenarios. *Clim Dyn* 38:189–208
- Rockel B, Woth K (2007) Future changes in near surface wind speed extremes over Europe from an ensemble of RCM simulations. *Clim Change* 81:267–280
- Roeckner E, Brokopf R, Esch M, Giorgetta M and others (2006) Sensitivity of simulated climate to horizontal and vertical resolution in the ECHAM5 atmosphere model. *J Clim* 19:3771–3791
- Sachs L, Hedderich J (2009) *Angewandte Statistik: Methodensammlung mit R*. Springer-Verlag, Berlin
- Schwierz C, Köllner-Heck P, Zenklusen Mutter E, Bresch DN, Vidale PL, Wild M, Schär C (2010) Modelling European winter wind storm losses in current and future climate. *Clim Change* 101:485–514
- SwissRe (2008) Natural catastrophes and man-made disasters in 2007: high losses in Europe. *Sigma*, Nr. 1/2008. Swiss Re publishing. Available at www.swissre.com/sigma/?year=2008#
- Ulbrich U, Fink AH, Klawa M, Pinto JG (2001) Three extreme storms over Europe in December 1999. *Weather* 56:70–80
- Ulbrich U, Pinto JG, Kupfer H, Leckebusch GC, Spangehl T, Meyers M (2008) Changing Northern Hemisphere storm tracks in an ensemble of IPCC climate change simulations. *J Clim* 21:1669–1679
- Uppala SM, Kallberg P, Hernandez A, Saarinen S and others (2005) The ERA-40 reanalysis. *Q J R Meteorol Soc* 131: 2961–3012
- Wilcoxon F (1945) Individual comparisons by ranking methods. *Biom Bull* 1:80–83

APPENDIX 1. Details of GPD fitting and selected thresholds

The procedure is described in detail in Coles (2001). Only a short summary is given below:

(1) Let all losses X_1, X_2, \dots, X_i of a time series be a sequence of independent and identically distributed variables, having a marginal distribution function F . Extreme events are those of the X_i which exceed a threshold u .

(2) u is set in a simple way by considering the highest 600 events of the time series for meteorological index (MI) and loss index (LI) Core Europe, or rather 300 events for LI of each country, which equates to a return period (RP) of 0.2 or 0.4 yr. This choice is motivated by the fact that the estimated shape and scale parameters are stable above the chosen threshold after allowance for the sampling errors. This threshold is defined once per region or country for the recent climate ($3 \times 20^\circ\text{C}$, 1960–2000).

(3) Having defined u , the parameters for the generalized Pareto distribution (GPD) are estimated via the maximum-likelihood-method. Accepted $y_1 \dots y_k$ are k events exceeding u ($y_k = x_k - u$). For shape parameters $\xi \neq 0$ the same method is also used. The parameters are obtained using numerical techniques.

(4) For a GPD with scale parameter $\sigma > 0$ and shape parameter $\xi > 0$, a suitable model for exceedance of u by a variable X is:

$$\Pr\{X > u\} = \zeta_u \left[1 + \xi \left(\frac{x - u}{\sigma} \right) \right]^{-\frac{1}{\xi}}, \quad \zeta_u = \Pr\{X > u\} \quad (\text{A1})$$

The estimation of ζ_u , the probability of a loss to exceed

u , is estimated via $\hat{\zeta}_u$ which is the sample proportion of points exceeding u :

$$\hat{\zeta}_u = \frac{k}{n} \quad (\text{A2})$$

where n is the number of all events of the time series.

The N -year return level is the level expected once every N year and is defined for $\xi \neq 0$ by:

$$z_N = u + \frac{\sigma}{\xi} \left[(N n_y \zeta_u)^\xi - 1 \right] \quad (\text{A3})$$

where n_y is the number of observations yr^{-1} .

(5) The criteria for significance of RP changes at the 5 % significance level are based on non-overlapping GPD 83.4 % CIs (Julious 2004, their Table 2) calculated using the delta-method. Our sensitivity analysis revealed that the delta-method typically produces slightly wider CIs in comparison to the profile-likelihood-method (details in Coles 2001, Della-Marta et al. 2009), particularly for its lower bound (not shown). This may lead in some cases to slightly less frequent significant results. Nevertheless, due to the large number of samples considered here to fit the GPD (e.g. ~200 events for LI Core Europe), the differences in CIs for the 2 methods are actually quite small (not shown). Thus, the choice of method to derive the CIs only marginally influences the results due to the large number of threshold exceedances used to fit the GPD. The delta-method has the advantage of being easier to implement than the profile-likelihood-method.

4 Climate Change Projections of Cyclones and Losses

In Chapter 3, possible changes in intensity and frequency of losses associated with individual extreme events under future climate conditions (A1B: 2060-2100) compared to the present day climate conditions (20C: 1960-2000) are identified and discussed. Based on the results of Chapter 2 and 3, the methodology is used for event selection in a project (GDV) to estimate projected impacts on winter storm losses in Germany (Held et al., 2013). This study considers three different downscaling methods and applies them to a 3-member ensemble of the ECHAM5/MPI-OM1 A1B scenario. All three methods found also a statistical relationship between single meteorological events and insured losses. Furthermore, for a loss corresponding to a 10 year event for recent climate conditions, changes in the return level (Fig. 4.1; left) and the return period (Fig. 4.1; right) for the end of the 21st century are found. Shorter return periods of up to 40-55% are estimated. These results based on higher resolution data are in line with the outcomes of Chapter 3. Still, it is the occurrence of multiple extreme events per winter, that leads to high socio-economic impacts and accumulated losses.

As a primary step for the analysis presented in Chapter 5 and 6, Pinto et al. (2013) analysed a possible change in the clustering of extra-tropical cyclones for the North Atlantic/Western Europe under future climate conditions. Additionally, the dependence of seriality on cyclone intensity is analysed. The investigation is done for three reanalysis data sets (NCEP, ERA40, ERA-Interim) and a multi-ensemble of 20 runs of ECHAM5 data for present (20C) and future (A1B) climate conditions (same database as in Chapter 6). The clustering is quantified by the dispersion, defined as the ratio of variance and mean of cyclone passages over a certain area (Mailier

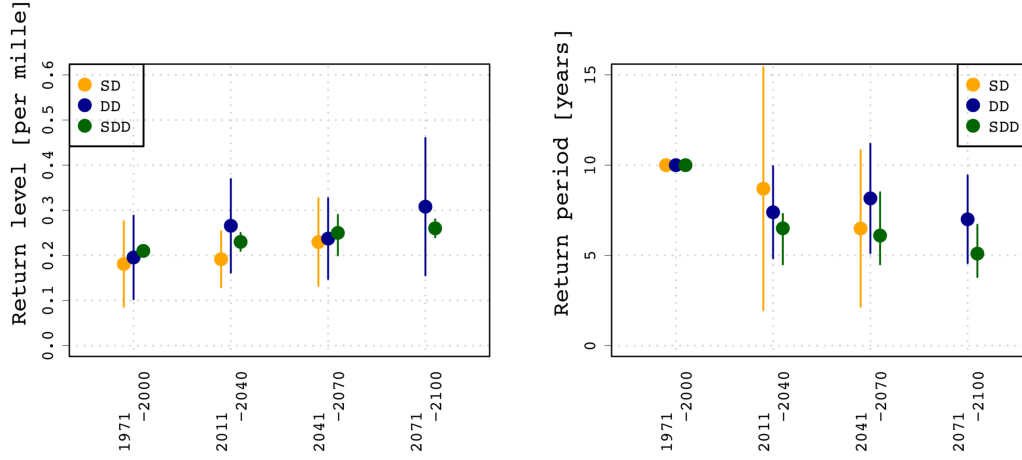


Fig. 4.1: Left: Projected return level of a once-in-10-years loss for three methods (yellow, green, blue) with 95% confidence intervals. Right: Return periods of a 10 years loss of the present period for future climate conditions estimated with three methods (yellow, green, blue) with 95% confidence intervals. Adapted Fig. 1 from Held et al. (2013) (©2013 The Authors, distributed under the Creative Commons Attribution License).

et al., 2006). For the reanalysis data sets serial clustering is identified primarily on both flanks and downstream regions of the North Atlantic storm track (Pinto et al., 2013). For the whole area, extreme cyclones cluster more than non-extreme cyclones. Beside some biases, the GCM data is able to reproduce the spatial patterns of clustering under recent climate conditions (20C: 1960-2000). For example, areas of serial clustering are more zonal than in the reanalysis data. This may be linked to a more zonal polar jet in GCM data (e.g. Pinto et al., 2007; Delcambre et al., 2013; Zappa et al., 2013) related to biases in blocking (Anstey et al., 2013). The climate change signal for cyclone track density shows less cyclones under future climate conditions over the North Atlantic and Europe (Fig. 4.2).

A possible change in clustering of cyclones at the end of the 21st century (A1B: 2060-2100) is suggested. Results show a possible decrease of serial clustering over the North Atlantic storm track area and parts of Western Europe, also for extreme cyclones (Fig. 4.3). Nevertheless, results are not always significant. The decrease is probably linked to an extension of the polar jet towards Europe, implying a tendency to more regular occurrences of cyclones over parts of the North Atlantic Basin poleward of 50°N and Western Europe. The coherence between the 20 ensemble runs is high, which demonstrates the robustness of the results.

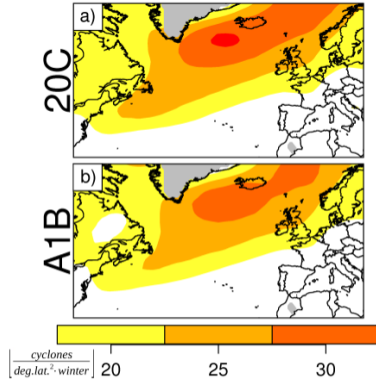


Fig. 4.2: (a) Cyclone track density for GCM ensemble average for winter season (December–February) for the period 1960–2000 (20C, 20 simulations). Values given in cyclone days per winter per (degree latitude). (b) Same as a but for the period 2060–2100 (A1B, 20 simulations). Fig. 4a,b from Pinto et al. (2013) (©2013 American Geophysical Union. Used with permission: license number 3543720432811).

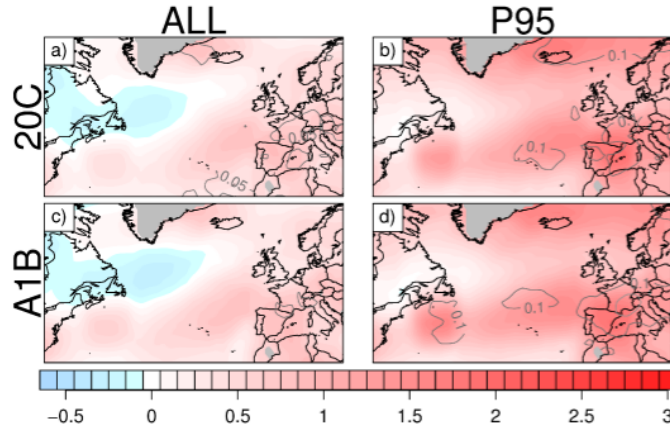


Fig. 4.3: (a) Dispersion statistic of cyclone transits between December–February for GCM ensemble average for 20 runs 20C: 1960–2000. (b) Same as a) but for cyclones with minimum core pressure exceeding the 95th percentile. (c) Same as a) but for 20 runs A1B: 2060–2100. (d) Same as c) but for cyclones with minimum core pressure exceeding the 95th percentile. Blue: regular, white: random process, and red: clustering. Fig. 5a,b,c,d from Pinto et al. (2013)(©2013 American Geophysical Union. Used with permission: license number 3543720432811).

Given that changes in cyclones found in Pinto et al. (2013) are different from changes in MI and especially LI (Chapter 3), it is of high interest to analyse in what kind changes in clustering of losses are linked to changes in clustering of cyclones. Therefore, Chapter 5 aims to quantify a reliable method to estimate historical clustering of losses associated with cyclones for Germany. The analysis is based on reanalysis data and a multi-ensemble of about 4000 years of present day GCM data. In Chapter 6 the methods found in Chapter 5 are applied to 800 years GCM data for present (20C) and future climate conditions (A1B) to identify possible changes in clustering of losses in Europe. Finally, the results of a possible change in clustering of losses are compared to the suggested changes in clustering of cyclones.

5 On the Clustering of Winter Storm Loss Events over Germany

Reference:

Karremann M.K., Pinto J.G., von Bomhard P.J. and Klawe M. (2014): On the clustering of winter storm loss events over Germany, *Nat Hazards Earth Sys* **14**: 2041-2052, doi:10.5194/nhess-14-2041-2014

©Author(s) 2014

Permission to reprint:

This work is distributed under the Creative Commons Attribution 3.0 License. Copyright on this article is retained by the authors. Page numbers are as published in Natural Hazards Earth System Science.



On the clustering of winter storm loss events over Germany

M. K. Karremann¹, J. G. Pinto^{1,2}, P. J. von Bomhard¹, and M. Klawe³

¹Institute for Geophysics and Meteorology, University of Cologne, Cologne, Germany

²Department of Meteorology, University of Reading, Reading, UK

³DeutscheRück AG, Düsseldorf, Germany

Correspondence to: M. K. Karremann (mkarre@meteo.uni-koeln.de)

Received: 5 February 2014 – Published in Nat. Hazards Earth Syst. Sci. Discuss.: 4 March 2014

Revised: 24 June 2014 – Accepted: 2 July 2014 – Published: 8 August 2014

Abstract. During the last decades, several windstorm series hit Europe leading to large aggregated losses. Such storm series are examples of serial clustering of extreme cyclones, presenting a considerable risk for the insurance industry. Clustering of events and return periods of storm series for Germany are quantified based on potential losses using empirical models. Two reanalysis data sets and observations from German weather stations are considered for 30 winters. Histograms of events exceeding selected return levels (1-, 2- and 5-year) are derived. Return periods of historical storm series are estimated based on the Poisson and the negative binomial distributions. Over 4000 years of general circulation model (GCM) simulations forced with current climate conditions are analysed to provide a better assessment of historical return periods. Estimations differ between distributions, for example 40 to 65 years for the 1990 series. For such less frequent series, estimates obtained with the Poisson distribution clearly deviate from empirical data. The negative binomial distribution provides better estimates, even though a sensitivity to return level and data set is identified. The consideration of GCM data permits a strong reduction of uncertainties. The present results support the importance of considering explicitly clustering of losses for an adequate risk assessment for economical applications.

1 Introduction

Intense extratropical storms are the major weather hazard affecting western and central Europe (Klawe and Ulbrich, 2003; Schwierz et al., 2010; Pinto et al., 2012). Such storms typically hit western Europe when the upper tropospheric jet stream is intensified and extended towards Europe (e.g.

Hanley and Caballero, 2012; Gómara et al., 2014). If these large-scale conditions remain over several days, multiple windstorms may affect Europe in a comparatively short time period (Fink et al., 2009). The occurrence of such “cyclone families” (e.g. Bjerknes and Solberg, 1922) can lead to large socio-economic impacts, cumulative losses (sum of losses caused by a particular series of events or aggregated over a defined time period) and fatalities. In statistical terms, this effect is known as serial clustering of events, for example of cyclones (Mailier et al., 2006). A recent study showed that clustering of extratropical cyclones over the eastern North Atlantic and western Europe is a robust feature in reanalysis data (Pinto et al., 2013). Furthermore, there is evidence that clustering increases for extreme cyclones, particularly over the North Atlantic storm track area and western Europe (Vitolo et al., 2009; Pinto et al., 2013). In terms of windstorm-associated losses, a general result is that large annual losses can be traced back to multiple storms within a calendar year (MunichRe, 2001). One of the most severe storm series regarding insured losses for the German market occurred in early 1990, which includes the storms “Daria¹”, “Herta”, “Nana”, “Judith”, “Ottilie”, “Polly”, “Vivian” and “Wiebke”, reaching a total cost of ca. EUR 5500 million indexed to 2012 (Aon Benfield, 2013). The cumulative damages associated with the windstorm series in December 1999 and January 2007 rank among the highest of the recent decades, with total costs reaching EUR 1500 million and about EUR 3000 million in terms of insured losses, respectively (Aon Benfield, 2013). Also the winter of 2013/14 has been characterised by multiple storms

¹Storm names as given by the *Freie Universität Berlin* as used by the German Weather Service (DWD). Source: <http://www.meteo-fu-berlin.de/adopt-a-vortex/historie/>.

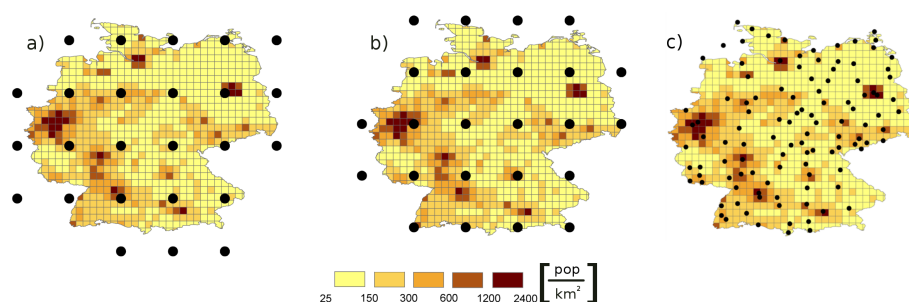


Figure 1. (a) Location of reanalysis grid points (black) over and near Germany and population density (POP, colours) in number of inhabitants km^{-2} per 0.25° grid cell; (b) same as (a) but for ECHAM5 GCM grid points; (c) same as (a) but for DWD stations. Only stations providing 80 % of the wind gust records for the period 1981/82 to 2010/11 are considered (112 stations). For each 0.25° grid cell, the wind/gust is associated using the nearest neighbour method.

leading to large socio-economic impacts (“Christian” 28 October 2013, “Xaver” 7 December 2013, “Dirk” 23 December 2013, “Anne” 3 January 2014, and “Christina” 5 January 2014), which have affected primarily the British Isles.

The estimation of return periods of single storms (event based losses) and storm series (cumulative losses) is needed to determine the “occurrence loss exceeding probability” (OEP; event loss) and the “aggregate loss exceeding probability” (AEP; accumulated loss per calendar year) for risk assessment and the fulfilment of the Solvency II (Solvency Capital Requirements, QIS5) requirements. As top annual aggregated market losses (like 1990 for Germany) are associated with multiple storms, the importance of clustering has long been discussed within the insurance industry. However, little to no attention has been paid to the clustering of wind-storm related losses in peer-review literature. In this study, the clustering of estimated potential losses associated with extratropical windstorms is analysed in detail for Germany and for recent decades. In particular, the probability of occurrence of multiple storm events per winter over Germany exceeding a certain return level is evaluated with help of reanalysis and general circulation model (GCM) data.

2 Data

In statistical terms, it is possible to build a simple storm loss model using both wind gusts and daily maximum 10 m wind speeds. For example, Pinto et al. (2007) gave evidence that loss estimations following the Klawns and Ulbrich (2003) approach based on both variables provide equivalent results. For this study, wind gusts are available and considered for German weather service (“Deutscher Wetterdienst”, hereafter DWD) observation data. As no gust data are available for reanalysis and GCM, a daily maximum of 10 m wind speed is used for those data sets.

Reanalysis data from the National Centre for Environmental Prediction/National Centre for Atmospheric Research (hereafter NCEP) as well as from the European Centre

for Medium Range Weather Forecast (ERA-Interim project, hereafter ERAI) are used in this study. The NCEP data are available on a Gaussian grid with a resolution of T62 (1.875° , roughly 200 km; Kistler et al., 2001), while the ERAI data are available on a reduced Gaussian grid with a resolution of T255 (0.7° ; about 80 km over central Europe; Dee et al., 2011). For comparability, ERAI is interpolated to the NCEP grid performed with a bilinear interpolation method (Fig. 1a shows relevant grid points for Germany). For both data sets, the 6-hourly instantaneous 10 m wind speed (hereafter wind) is considered. The daily maxima (largest values for each calendar day between 00:00, 06:00, 12:00 and 18:00 UTC) are selected. Based on these daily maxima the 98th percentiles (see Sect. 3) are calculated for 30 winters (October–March, 1981/82 to 2010/11) respectively.

In order to obtain statistically robust estimates of the return periods of storm series based on potential losses, a large ensemble of 47 simulations performed with the coupled ECHAM5/MPI-OM1 (European Centre Hamburg Version 5/Max Planck Institute Version – Ocean Model version 1; Jungclaus et al., 2006; hereafter ECHAM5) GCM is analysed. These simulations have a wide variety of setups, but are all consistent with greenhouse gas forcing conditions between the year 1860 (pre-industrial) and near future (2030) climate conditions. All simulations were performed with T63 resolution (1.875° , roughly 200 km, see grid in Fig. 1b); 37 of them were conducted for the ESSENCE (Ensemble SimulationS of Extreme weather events under Non-linear Climate change) project (Sterl et al., 2008). Details of all simulations can be found in Supplement A. Again, the 6-hourly instantaneous 10 m wind speed is used to determine the daily maxima. The 98th percentile for GCM data is calculated based on the 37 ESSENCE simulations for the winter half year, as the length of this data set is long enough to derive statistically stable estimates.

As the physical cause for building losses can be primarily attributed to the peak wind gusts (Della-Marta et al., 2009) a data set of daily maxima of the 10 m wind gust observations from DWD is used for comparability and validation

purposes. The time series of these data sets differ in terms of the length of the available time period and data quality (e.g. Born et al., 2012). After an evaluation, 112 stations (Fig. 1c) are considered for further analyses. For these stations, wind gusts for at least 80 % of the days in winter are available for the period 1981/82 to 2010/11. The 98th percentile at each station is calculated for the winter half year. Then, a normalisation of the 10 m wind gust observations with the 98th percentile at each station is performed. The normalised values were interpolated to the 0.25° grid of the population density (Fig. 1c) using the inverse distance weighted interpolation of second order. This method assumes that the interpolated value for each grid box should be influenced more by nearby stations and less by more distant stations. The second-order fit permits a higher weighting for nearer stations.

The German Insurance Association (“Gesamtverband der Deutschen Versicherungswirtschaft”, hereafter GDV) provides a simulation of daily residential building losses for private buildings for the period of 1984–2008 for the 439 administrative districts of Germany. This data were collected from most of the insurance companies active in the German market, so are representative of the insured market loss in Germany and are used here as a reference. Loss ratios, i.e. the ratio between losses attributed to one event and the total insured value for that area are used. Inflation effects can be neglected as well as other socio-economic factors that may have changed slightly during this period. More information can be found in Donat et al. (2011) and Held et al. (2013).

As insurance data are not available for the whole analysed period, population of the year 2000 is used as proxy for the estimation of potential losses. This data set was provided by the Centre for International Earth Science Information Network (CIESIN) of Columbia University and the Centro Internacional de Agricultura Tropical (CIAT). The population density is given as inhabitants km^{-2} , with a spatial resolution of $0.25^\circ \times 0.25^\circ$ (Fig. 1, coloured boxes). For grid boxes which are only partially within German borders the percentage of each box is calculated with the geoinformation system (GIS).

3 Methodology

In this section, the potential loss indices based on the approach by Klawns and Ulbrich (2003) and Pinto et al. (2012) are presented. These indices are used to select events exceeding a certain return level. For the chosen events, histograms are analysed, and statistical distributions like the Poisson and the negative binomial distribution are used to estimate return periods of storm series. As the GCM data overestimate the frequency of zonal weather patterns, the approach to calibrate GCM data towards reanalysis using weather types is described.

3.1 Storm loss indices

The potential loss associated with a storm can be quantified using simple empirical models (Palutikof and Skellern, 1991; Klawns and Ulbrich, 2003; Pinto et al., 2007). Here, calendar-day-based potential damages for Germany are estimated by using a modified version of the loss model of Klawns and Ulbrich (2003) for stations and gridded data. The general assumptions of the loss model are as follows:

- Losses occur only if a critical wind speed is exceeded. This threshold corresponds to the local 98th percentile (v_{98}) of the daily maximum wind speed (e.g. Palutikof and Skellern, 1991; Klawns and Ulbrich, 2003).
- Above this threshold, the potential damage increases with the cube of the maximum wind speed, as the kinetic energy flux is proportional to the cube of wind speed. This implies a strong non-linearity in the wind–loss relation.
- Insured losses depend on the amount of insured property values within the affected area. As real insured property values are not available, the local population density (POP) is used as proxy.
- To each population density grid cell, the wind data (re-analyses, GCM) from the nearest location are allocated (nearest neighbour approach).

Following these assumptions, the potential loss (LI_{raw}) per calendar day is defined by the sum of all grid points ij with v_{ij} exceeding $v_{98,ij}$ weighted by the population density:

$$LI_{\text{raw}} = \sum_{ij} \left[\left(\frac{v_{ij}}{v_{98,ij}} - 1 \right)^3 \right] \cdot \text{POP}_{ij} \cdot I(v_{ij}, v_{98,ij}) \quad (1)$$

$$\text{with } I(v_{ij}, v_{98,ij}) = \begin{cases} 0 & \text{for } v_{ij} < v_{98,ij} \\ 1 & \text{for } v_{ij} > v_{98,ij} \end{cases}$$

POP_{ij} = population density for grid point ij , v_{ij} = wind speed at grid point ij and $v_{98,ij}$ = 98th percentile at grid point ij .

Following Pinto et al. (2012), a meteorological index (MI_{raw}) is also considered. MI_{raw} is defined as the sum of all grid points ij per calendar day, where v_{ij} is exceeding $v_{98,ij}$ without weighting with the population density:

$$MI_{\text{raw}} = \sum_{ij} \left[\left(\frac{v_{ij}}{v_{98,ij}} - 1 \right)^3 \right] \cdot I(v_{ij}, v_{98,ij}). \quad (2)$$

In this study, the method is modified to identify individual events of high LI_{raw} (or MI_{raw}). In a first step overlapping 3-day sliding time windows of LI_{raw} (MI_{raw}) time series are analysed, as this corresponds to the 72 h event definition

often used by insurance companies in reinsurance treaties (Klawns and Ulbrich, 2003). Moreover, given that Germany is a comparatively small area, 3 days are reasonable for separating events. For each 3-day time window, the middle day is defined as event if it is a local maximum of LI_{raw} (MI_{raw}). If no maximum is identified within the 3-day window, the first day after an event (for all $LI_{\text{raw}} \neq 0$; considering the last day of the 3-day time window) is defined as event. The outcome is a time series of events. With this approach, storms like “Vivian” and “Wiebke” (26 and 28 February 1990) can be identified as separate events (see Supplement E).

In a second step, the local details of the identified events are analysed in more detail. In analogy to the above, the temporal local maximum of the 3-day time window at each grid point ij (following $\max_{3-D} \left(\frac{v_{ij}}{v_{98,ij}} \right)$) is analysed for each event. If the determined maximum $\max_{3-D} \left(\frac{v_{ij}}{v_{98,ij}} \right)$ is not at the middle day, $\frac{v_{ij}}{v_{98,ij}}$ on the event day is replaced with the identified maximum value of the first or the last day of the 3-day time window in LI_{raw} (MI_{raw}). In rare cases, events are only separated by 1 day (e.g. Vivian and Wiebke, see Supplement E). If $\max_{3-D} \left(\frac{v_{ij}}{v_{98,ij}} \right)$ is identified between both events (here 27 February 1990), it is allocated to the event with higher $\frac{v_{ij}}{v_{98,ij}}$. This ensures that each local maximum only counts once. To guarantee spatially coherent wind fields, larger values occurring on the first or third day only substitute the values from the middle day if multiple (spatially contiguous) nearby grid points exceed the 98th percentile.

The method to estimate potential losses of single events can be described as

$$LI_{3-D} = \sum_{ij} \left[\max_{3-D} \left(\frac{v_{ij}}{v_{98,ij}} \right) - 1 \right]^3 \cdot \text{POP}_{ij} \cdot I(v_{ij}, v_{98,ij}), \quad (3)$$

$$MI_{3-D} = \sum_{ij} \left[\max_{3-D} \left(\frac{v_{ij}}{v_{98,ij}} \right) - 1 \right]^3 \cdot I(v_{ij}, v_{98,ij}). \quad (4)$$

This new definition has the advantage that single storm events can be well separated. Furthermore, strong potential losses occurring 1 day before or 1 day after an event, which are probably associated with the same event, are incorporated in LI_{raw} (MI_{raw}).

Hereafter LI_{3-D} (MI_{3-D}) is named LI (MI) for simplicity. These formulations are used for reanalysis, DWD and GCM data. Then, the resulting time series of LI (MI) are ranked and 1-, 2- and 5-year return levels are computed. The selected samples of events exceeding each corresponding threshold (e.g. 30, 15 and 6 events respectively for 30 years of reanalysis data) are then assigned to individual winters. The naming is given by the second year, e.g. winter 1989/90 is named 1990.

3.2 Statistics

The Poisson distribution is the simplest approach to describe independent events and is often used to model the number of events occurring within a defined time period. This procedure is useful to describe the temporal distribution of events at a certain region and is typically used by insurance companies to estimate losses of winter storms. This discrete distribution depends on one parameter and is a special case of the binomial distribution. For the Poisson distribution the rate parameter λ is equal to both the variance ($\text{Var}(x)$) and mean ($E(x)$). For a random variable x the probability distribution is defined as

$$P(x) = \frac{\lambda^x e^{-\lambda}}{x!}, x = 0, 1, 2, \dots; E(x) = \lambda = \text{Var}(x). \quad (5)$$

After Mailier et al. (2006), the dispersion statistics (a simple measure of clustering) is defined as

$$\psi = \frac{\text{Var}(X)}{E(X)} - 1. \quad (6)$$

If the $\text{Var}(x) > E(x)$ the distribution is overdispersive (clustering), for $E(x) > \text{Var}(x)$ the distribution is underdispersive (regular) and for $E(x) = \text{Var}(x)$ it is a random process. Beside the Poisson distribution the negative binomial distribution is one of the major statistics that is used to describe insurance risks. Following Wilks (2006), the probability of the negative binomial distribution is defined as

$$P(x) = \frac{\Gamma(x+k)}{\Gamma(k) \cdot x!} (1-q)^k \cdot q^x \quad (7)$$

with $\Gamma()$ = gamma function, k = auxiliary parameter > 0 (see below), and $0 < q < 1$, $q = 1 - p$, p = probability.

As in our study $E(x)$ is fixed as the return level of considered events, q is the only free parameter. The estimation of q is done by a nonlinear least-square estimate using the Gauss–Newton algorithm.

Considering $E(x) = \frac{kq}{1-q}$ and $\text{Var}(x) = \frac{kq}{(1-q)^2}$

$$\Rightarrow k = \frac{(1-q)}{q} E(x) \quad (\text{following Wilks, 2006}). \quad (8)$$

The dispersion statistics can also be described as

$$\psi = \frac{1}{1-q} - 1 \geq 0. \quad (9)$$

For $q = 0$, the negative binomial distribution is equal to the Poisson distribution. The higher q , the higher is the overdispersion and therefore the clustering of events.

The return period is defined as the inverse of the probability (Emanuel and Jagger, 2010). The estimation of return periods of storm series consisting of events with a certain return level is calculated by the probability P for x events of certain intensity within 1 year:

$$\text{WKP}(x) = \frac{1}{P(x)} \quad (10)$$

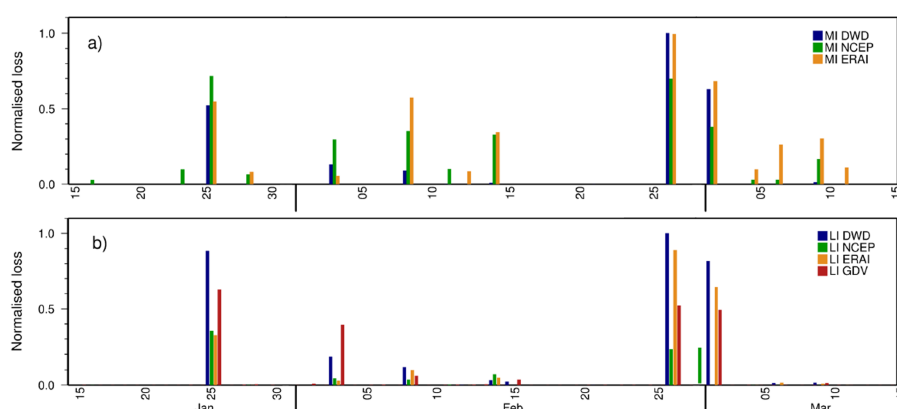


Figure 2. Time series of 3-day accumulated losses between 15 January and 15 March 1990. The values are normalised by the maximum accumulated loss of the period 1981/82 to 2010/11 for each data set. **(a)** Comparison between MI derived DWD gust observations (blue), MI estimates based on NCEP (green) as well as MI obtained from ERAI (orange); **(b)** same as **(a)** but for LI and additionally compared to simulated insurance data (GDV, red). Unlike MI, LI is population weighted.

3.3 Calibration of GCM data with circulation weather types

In order to obtain robust estimates of return periods for the historical storm series, the large ensemble of ECHAM5 simulations is considered to enhance the data sample. As the large-scale atmospheric circulation is too zonal over Europe in GCMs (e.g. Sillmann and Croci-Maspoli, 2009), a correction of the model bias towards the reanalysis climatology is necessary. This correction is performed based on weather types, so that the variability of weather patterns over Germany corresponds to the historical time period. The selected weather typing classification is the circulation weather type (CWT) following Lamb (1972) and Jones et al. (1993). The large-scale flow conditions over Germany are calculated from 00:00 UTC mean sea level pressure fields, using 10° E, 50° N (near Frankfurt/Main) as central grid point. Each day is classified into one of eight directional types defined as 45° sectors: northeast (NE), east (E), southeast (SE), south (S), southwest (SW), west (W), northwest (NW), and north (N). Two circulation types are considered: cyclonic (C) and anticyclonic (A). If neither rotational nor directional flow dominates, the day is attributed as hybrid CWT (e.g. anticyclonic-west). The correction is done by adapting the relative frequency of events per CWT in the GCM simulations to the number of events per CWT in the ERAI data (see Sect. 4.3). This is only a first-order correction of the model biases. In fact, differences in the probability density function of extreme losses per weather type may still be present (Pinto et al., 2010).

4 Results

In this section, the different loss indices (Sect. 4.1) and the events selection (Sect. 4.2) are first analysed for the

reanalysis period. Second, results of the calibration of GCM data based on CWTs are presented in Sect. 4.3. The estimation of return periods for storm series based on reanalysis (Sect. 4.4) and GCM data (Sect. 4.5) follow.

4.1 Comparison of loss indices for the reanalysis period

The loss indices described in Sect. 3.1 are now compared based on different data sets. First, the MIs based on both reanalysis data sets are compared to the MI derived from DWD data as an illustrating example (storm series of early 1990). Results for the period from 15 January to 15 March 1990 are displayed in Fig. 2a. The outcome shows that the timing of extreme events (“Daria” 25 January 1990, “Herta” 4 February 1990, “Judith” 7 February 1990, “Vivian” 26 February 1990 and “Wiebke” 1 March 1990) is generally well identified from all three data sets. In some cases, a 1-day shift is observed, e.g. for 12 and 15 February. Such modifications are associated with the methodology of the data assimilation within the data set (e.g. highest winds in NCEP may occur at 18:00 UTC of a certain day, for ERAI only 6 h later). In case of doubt the first day is taken (see Sect. 3.1). This means that the split-up of events and thus accurate event identification may depend on the data set. Though the timing of the events is well accessed, the relative intensity of the events sometimes differs from data set to data set (e.g. “Vivian”, 26 February 1990). The results for the LIs (Fig. 2b) are also compared to accumulated potential losses based on the GDV data. With this aim, the latter is also aggregated for time windows of 3 days. The timing of the identified events is predominantly correct. As expected, the findings are similar to those for the MIs, with a good assessment of the timing of the events and differences in terms of the relative intensity between data sets. A calibration of the intensity towards the GDV data is not performed, as a linear calibration (as implemented e.g. in Held et al., 2013) would not change the

Table 1. List of the identified top 30 events and corresponding return level for each event for NCEP, ERAI and DWD gust data. Dates are given as dd.mm.yyyy.

NCEP	Return level	ERAI	Return level	DWD	Return level
15.12.1982	1	24.11.1981	2	18.01.1983	1
01.02.1983	2	16.12.1982	1	01.02.1983	1
27.11.1983	1	04.01.1983	1	27.11.1983	1
14.01.1984	5	18.01.1983	1	14.01.1984	1
24.11.1984	2	01.02.1983	2	24.11.1984	5
19.01.1986	2	13.01.1984	1	01.01.1986	1
20.10.1986	2	15.01.1984	1	20.10.1986	1
19.12.1986	2	24.11.1984	5	19.12.1986	2
25.01.1990	5	06.12.1985	1	25.01.1990	5
14.02.1990	1	20.01.1986	2	03.02.1990	2
26.02.1990	5	19.12.1986	2	08.02.1990	2
28.02.1990	5	25.01.1990	2	14.02.1990	1
13.01.1993	2	08.02.1990	1	26.02.1990	5
24.01.1993	2	26.02.1990	5	01.03.1990	5
09.12.1993	1	01.03.1990	5	21.03.1992	1
28.01.1994	2	14.01.1993	1	11.11.1992	1
22.01.1995	5	24.01.1993	5	26.11.1992	2
02.12.1999	1	09.12.1993	1	13.01.1993	1
26.12.1999	1	28.01.1994	2	24.01.1993	2
31.01.2000	1	23.01.1995	1	09.12.1993	2
28.01.2002	1	28.10.1998	1	28.01.1994	2
27.10.2002	2	03.12.1999	2	23.01.1995	1
02.01.2003	1	26.12.1999	5	26.01.1995	1
31.01.2004	1	29.01.2002	1	28.03.1997	1
20.03.2004	1	26.02.2002	1	03.12.1999	1
12.02.2005	1	28.10.2002	2	26.12.1999	2
16.12.2005	1	21.03.2004	1	27.10.2002	2
18.01.2007	5	18.01.2007	5	18.01.2007	5
01.03.2008	1	01.03.2008	2	01.03.2008	2
28.02.2010	1	28.02.2010	1	28.10.2010	1

relative ranking of events within a certain data set. Nevertheless, storms on successive days cannot always be well separated with our methodology. For example, storms “Elvira” (4 March 1998) and “Farah” (5 March 1998) cannot be separated for either reanalysis or DWD data (not shown). However, this is also not possible based on insurance loss data. On the other hand, our method separates important storms like “Vivian” and “Wiebke” (26 February and 1 March 1990; Fig. 2).

The top 30 events for the two reanalysis data sets as well as the DWD observations are shown in Table 1. Per definition, these are the events exceeding the 1-year return level for each data set. The most prominent historical storms affecting Germany like “Kyrill” (18 January 2007), “Vivian” (26 February 1990) and “Daria” (25 January 1990) are identified in all three data sets as top events. However, some differences are found regarding the exceeded return level. For example, storm “Daria” is estimated as a 5-year return level event for NCEP and DWD data and as 2-year event for ERAI. These differences are partly attributed by the resolution of the data sets and to known caveats. For instance, the relatively weak values for “Lothar” (26 December 1999) in NCEP can be directly attributed to an insufficient representation of this storm

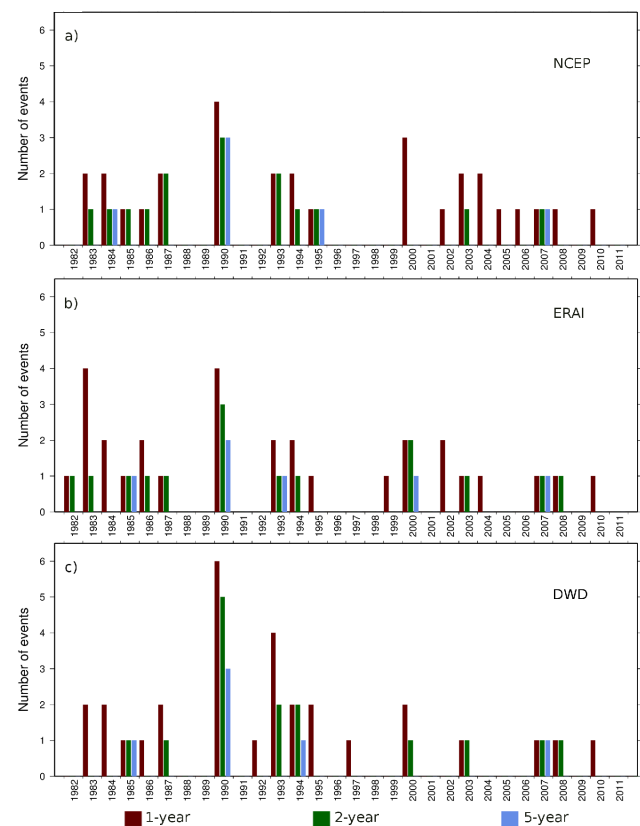


Figure 3. Time series of the number of events per winter exceeding the 1-year return level (red), 2-year return level (green) and 5-year return level (blue) between 1981/82 and 2010/11. (a) LI estimated based on NCEP; (b) same as (a) but for ERAI; (c) same as (a) but for DWD gust. The indicated year corresponds to the second year of a winter (2000 indicates 1999/00).

in the data set (Ulbrich et al., 2001; see their Fig. 1). Other differences may be associated with data availability or interpolation to the population density grid for DWD versus the lower resolution gridded data sets for NCEP and ERAI. In spite of these limitations, the method is able to identify consistent events, which constitutes a reliable basis to estimate the return period of storm series in the following. However, 70 % of the identified events in NCEP data are also found in ERAI and DWD data, and the same is valid for DWD and ERAI.

4.2 Comparison of identified events for the reanalysis period

Bar plots for different data sets and intensities (1-, 2-, 5-year return level events) are now analysed for the 30-year period. For each threshold, the selected LI samples (30, 15 and 6 events, respectively) are shown in Fig. 3. In some cases the number of events per winter differs from data set to data set. Nevertheless, in all three data sets a maximum of events is found in the winter 1989/90 (Fig. 3a, b denoted

1990). Differences in the identified number of events at the 1-year return level are determined for 11 winters. For example for ERAI, the winter 1983 features four 1-year events, while NCEP only features two events. For stronger events exceeding a 2- or 5-year return level, seven/six years with a difference in the number of events are identified. For instance at the 2-year return level for the storm series of 2000 (1999/00, see Fig. 3a, b) two events for ERAI, and no event for NCEP data are detected. This can be attributed to the limited representation of storms like “Lothar” (26 December 1999) in NCEP (c.f. Ulbrich et al., 2001). However, both data sets are generally in good agreement, identifying clearly the winters with well-known storm series like in 1990 or 2007. In comparison to the estimations based on the DWD observation data (Fig. 3c) some differences to the reanalysis data are apparent. For example the storm series of 2002 is not identified for DWD data. On the other hand, the storm series of 1990 includes six events for the DWD data (1-year return level). As mentioned in Sect. 4.1, this could be attributed both to known caveats of the data sets, station density vs. gridded data, and to the methodology used to assign the data to the population grid cells. In spite of these deviations, the historical storm series can be generally identified in all data sets. Furthermore, the resulting overall statistics over the 30 years are also similar (Supplement B) as the small permutations of the single events are in balance.

4.3 Calibration of GCM data based on CWTs

In order to enable the calibration of the GCM data, the distribution of the events for each CWT within the reanalysis period is analysed. Each loss event is assigned to the identified CWT for the corresponding date. Additionally to the 1-, 2- and 5-year return levels, a return level of 0.5 years is considered to help with the calibration. The resulting histograms are similar for both reanalysis data sets (Fig. 4a, b). Considering frequent events (0.5-year), most events are identified for W CWT. The focus on this class becomes more pronounced for higher return levels. For example for a return level of 5 years the maximum of all events are in the westerly CWT for both reanalyses. This predominance of windstorms in the westerly flow type is in line with previous results (e.g. Donat et al., 2010; Pinto et al., 2010). For the GCM data (Fig. 4c) the distribution of the events per CWT is different. Most frequent events (e.g. 0.5-year) are identified for A CWT. For higher return levels (e.g. 5-year) the events are more equally distributed over all CWTs than for the two reanalyses. This bias is corrected assuming the same relative frequency of events per CWT as in ERAI for GCM data. For example, two SW events are identified for the top 30 and ERAI, which corresponds to 6.7 % of all considered events. The corresponding number of events in GCM is 273 (6.7 % of 4092). Thus, the top 273 SW events are included in the event set of the 4092 top events. The resulting distribution is shown in Fig. 4d.

4.4 Estimation of return periods of storm series based on reanalysis

The identified frequency of events per year for the two reanalysis data sets as well as the DWD based data set is almost identical for the considered return levels (see Supplement B1). For succinctness, in the following only results based on ERAI data are discussed in detail. The return period of storm series with a certain return level is estimated based on the negative binomial and on the Poisson distribution (Supplement D, left). The related return periods are shown in Table 2 (left).

A return period about 65 years is estimated for a storm series with four 1-year return level events (like 1990) based on the Poisson distribution (Table 2). For the negative binomial distribution the assessed return period is ca. 49 years. On the other hand, for a return level of observed two 5-year events (like 1990), the estimated return periods are 61 years for Poisson and about 42 years for negative binomial distributions. A Ψ value of about 0.16 for 1-year return level and of 0.25 for 5-year return level are determined for the negative binomial distribution, both indicating serial clustering (see Table 3a). The Ψ values calculated with Eq. (6) are different, with more clustering for frequent events (0.24 for 1-year return level events) and less clustering for extreme events (0.17 at the 5-year return level, Table 3b). Nevertheless, both methods identify overdispersion for the events. The estimated return period of storm series with two events per year for 1-year level (like in 1984) with the negative binomial distribution and the Poisson distribution are closer to each other, with about 5.9 and 5.4 years (Table 2). In fact, for 1-year events large deviations between the two distributions are only found for four or more events per year. The same is true for 2-year (5-year) occurrences and three (two) or more events per year (Table 2). In these cases, the Poisson distribution clearly overestimates the return period of multiple events per winter.

In order to test the sensitivity to certain storm series like 1990, additional computations were performed based on NCEP and ERAI as above but single years (with three and four events) were removed respectively. Results show for all data little dependence on the selected years (not shown). For comparatively frequent storm series, a relatively small spread is identified, e.g. for 1-year return level and three events per year the estimated return period remains between 15 and 16 years. On the other hand, for 5-year return levels and three events the range is much larger, with estimates between 112 and 306 years (not shown). As the estimation of the return period is almost independent of the chosen years, the method is reliable for further application.

4.5 Estimation of return periods of storm series based on GCM data

The large ensemble of GCM runs is now considered to enhance the estimation of return periods of historical storm

Table 2. Estimated return periods for three different return levels (1-, 2-, 5-year) based on the Poisson distribution (Pois. RP), the empirical data for each data set (eRP), and the negative binomial distribution (Neg. Bin. RP; with uncertainty estimates* using the Gaussian error propagation) for NCEP, ERAI and independent selected GCM samples (GCM: all runs, GCM_{corr}, 37 ESSENCE runs: ESS_{corr}, 3 20C runs from MPI: 20C_{corr}, PRE_{corr} from MPI, 3 CSMT runs from MPI: CSMT_{corr}; all runs indexed with corr are bias corrected based on CWTs) considering only the number of years available for each data set respectively. The number of years is indicated below each data set. For further details see Table B1 in the Supplement.

		Events per year	ERAI	NCEP	GCM	ERAI	NCEP	GCM	GCM _{corr}	ESS _{corr}	20C _{corr}	PRE _{corr}
			30 years			30 years	30 years	4092 years	4092 years	2360 years	720 years	505 years
		Pois. RP	eRP			Neg. Bin. RP						
1-year Return Level	0	2.72	2.31	2.50	2.13	2.53 ± 1.54	2.49 ± 1.19	2.39 ± 0.11	2.35 ± 0.05	2.51 ± 0.09	2.4 ± 0.19	2.59 ± 0.26
	1	2.72	3.00	3.33	3.42	2.93 ± 1.54	2.98 ± 1.19	3.13 ± 0.11	3.2 ± 0.05	2.96 ± 0.09	3.11 ± 0.19	2.86 ± 0.26
	2	5.44	5.00	4.29	7.64	5.86 ± 3.6	5.96 ± 2.84	6.25 ± 0.29	6.39 ± 0.12	5.91 ± 0.2	6.21 ± 0.5	5.71 ± 0.58
	3	16	–	30	19	15 ± 19	15 ± 15	15 ± 1.4	15 ± 0.59	15 ± 1.05	15 ± 2.37	16 ± 3.20
	4	65	15	30	45	49 ± 89	46 ± 66	41 ± 6	40 ± 2	47 ± 5	42 ± 10	53 ± 16
	5	326	–	–	–	172 ± 419	155 ± 294	121 ± 23	110 ± 9	163 ± 22	124 ± 39	207 ± 85
2-year Return Level	0	1.65	1.58	1.58	1.54	1.62 ± 0.68	1.58 ± 0.09	1.57 ± 0.03	1.57 ± 0.02	1.60 ± 0.02	1.59 ± 0.02	1.62 ± 0.03
	1	3.3	3.00	3.75	4.07	3.5 ± 1.45	3.78 ± 0.22	3.81 ± 0.07	3.82 ± 0.05	3.62 ± 0.05	3.7 ± 0.05	3.47 ± 0.07
	2	13	30	15	13	13 ± 16	13 ± 2.25	13 ± 0.7	13 ± 0.51	13 ± 0.5	13 ± 0.5	13 ± 0.8
	3	79	30	30	51	65 ± 135	52 ± 15	51 ± 5	51 ± 3	58 ± 4	55 ± 3	65 ± 7
	4	633	–	–	–	388 ± 1132	229 ± 93	221 ± 28	218 ± 20	294 ± 28	254 ± 23	391 ± 56
5-year Return Level	0	1.22	1.15	1.15	1.21	1.2 ± 0.02	1.16 ± 0.03	1.21 ± 0.01	1.21 ± 0.01	1.22 ± 0.01	1.21 ± 0.01	1.22 ± 0.04
	1	6.11	7.50	10.00	6.60	7.45 ± 0.56	10.52 ± 1.06	6.74 ± 0.1	6.59 ± 0.05	6.38 ± 0.27	6.6 ± 0.23	6.24 ± 0.76
	2	61	30	–	53	42 ± 7	38 ± 9	48 ± 2	50 ± 1	54 ± 5	50 ± 4	57 ± 16
	3	916	–	30	334	225 ± 59	112 ± 40	369 ± 19	432 ± 11	567 ± 85	425 ± 51	707 ± 300

* As the propagation of uncertainty for one event per year and 1-year return level is not possible to identify, the error bars are set to be the same as for zero events per year.

Table 3. Ψ values for the different data sets: (a) calculated with Eq. (9) and with the information of the confidence interval (b) computed with $\psi = \frac{\text{Var}(X)}{\text{E}(X)} - 1$, RL: Return Level.

	RL	ERA-I	NCEP	GCM	GCM _{corr}	ESS _{corr}	20C _{corr}	CTRL _{corr}
(a)	1	0.1595 ± 0.1127	0.1972 ± 0.1123	0.3062 ± 0.0188	0.6383 ± 0.0055	0.1777 ± 0.0071	0.2919 ± 0.0294	0.1020 ± 0.0115
	2	0.0727 ± 0.0650	0.1962 ± 0.0271	0.2081 ± 0.0090	0.3168 ± 0.0039	0.1297 ± 0.0040	0.1661 ± 0.0049	0.0713 ± 0.0031
	5	0.2464 ± 0.0290	0.8186 ± 0.1881	0.1161 ± 0.0023	0.1095 ± 0.0025	0.0491 ± 0.0027	0.0908 ± 0.0043	0.0240 ± 0.0037
(b)	1	0.2414	0.1034	0.1756	0.2717	0.1863	0.1752	0.1604
	2	0.0690	0.2069	0.1442	0.1707	0.1210	0.0925	0.0513
	5	0.1724	0.8621	0.1033	0.1303	0.0741	0.0662	0.0004

series. The corresponding return periods are shown in Table 2 (right). The consideration of 4092 years leads to the identification of multiple years with four or more 1-year events. This enables more accurate estimates of the return period as well as lower uncertainties calculated with the Gaussian error propagation (Table 2). Following the above given examples, a return period of 41 years is assessed for a storm series with four events per year exceeding the 1-year return level (like 1990). This value is lower than for the negative binomial fit based on ERAI data and the Poisson distribution (49 and 65 years, respectively). The obtained return period for two events per year exceeding the 5-year level is about 48 years. Clear deviations between the Poisson distribution and the negative binomial distribution are also found for

four (three/two) or more events for 1- (2-/5-) year level (see Table 2, Supplement D).

The consideration of GCM data with bias correction (GCM_{corr}) leads only to a small difference for return periods, e.g. notable for less frequent events and higher return levels (Table 2). The Ψ for GCM attributions are in all cases clearly positive, also indicating clustering of the events (Table 3a). Clustering is also positive, but lower or similar when being calculated with Eq. (6) (Table 3b). However, unlike previous results obtained for extratropical cyclones (Pinto et al., 2013), the Ψ value does not increase for larger return levels. For more intense events (5-year return level) the derived Ψ becomes smaller (e.g. $\Psi = 0.11$ considering all GCM_{corr} runs), indicating less deviation from the Poisson distribution than for the 1-year events ($\Psi = 0.6$ considering all GCM_{corr}

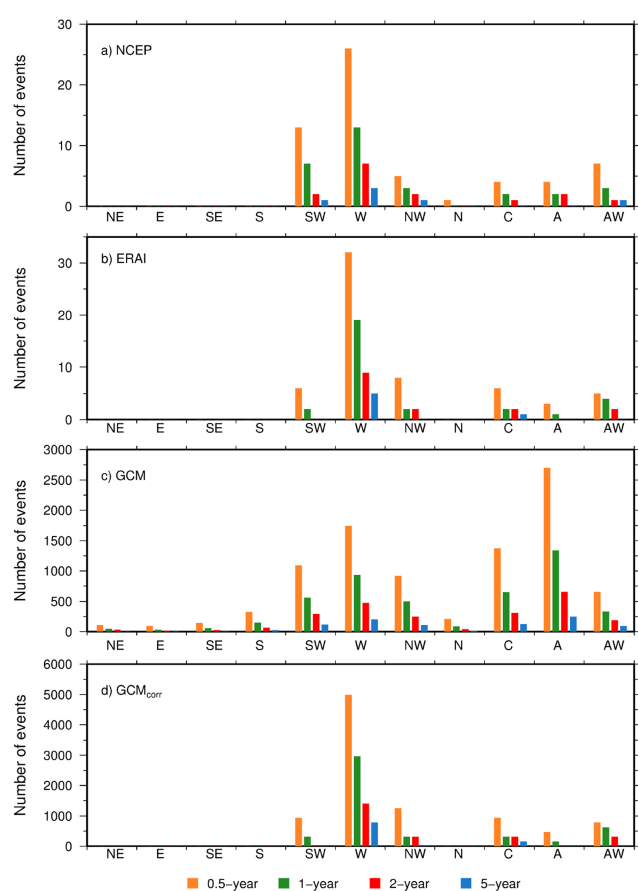


Figure 4. (a) Distribution of events exceeding a certain return level depending on the CWT for LI NCEP. Colours denotes the different return level (0.5-, 1-, 2- and 5-year events); (b) same as (a) but for ERAI; (c) same as (a) but for the GCM ensemble; (d) same as (c) but for the corrected frequency of events per weather type based on ERAI. For (a) and (b) the total number of years is 30, for (c) and (d) it is 4092 years.

runs). The decrease of Ψ values is contributed to the fact that the sample of lower intensity events includes also higher intensity events and therefore more clusters are expected. For higher return level the occurrence of cluster is more random and therefore closer to the Poisson distribution. The reason for the differences compared to Pinto et al. (2013) may be that they based their conclusions on lower percentiles (and thus a higher frequency of events). This suggests that clustering of windstorm and associated losses is quite complex, particularly in terms of intensity variations. Nevertheless, and in all cases, clear overestimation of the return period is identified for the GCM based on the Poisson distribution. This is an important result, as it indicates that return periods of storm series are better estimated with the negative binomial distribution than with the Poisson distribution, especially for winters with a considerable number of events.

Analogously to the historical data, a sensitivity analysis was performed regarding the GCM data. In this case, it was analysed how the estimates depend on the choice of GCM runs. With this aim, the computations were repeated for each of the 47 runs (see Supplement A) individually and combinations of them. As the length of the runs is different, this also provides some insight on how the results may be sensitive to the length of the time series. For example the estimated return periods of three events a winter above the 1-year return level are assessed to ca. 15 and 16 years depending on whether the whole data set, selected groups of runs or individual runs (see Table 2) are considered. The major difference is the uncertainty: while for all GCM_{corr} data, 15 ± 0.59 years is estimated, the value is for example 15 ± 1.05 years for all ESSENCE_{corr} runs, 16 ± 3.2 years for the PRE_{corr} run and for example 15 ± 8.24 years for the first Essence_{corr} run (length only 50 years; not included separately in Table 2). PRE_{corr} is different because it is expected to have more (multi) decadal variability (505 years of free running coupled GCM simulation) than shorter 50-year runs. These results demonstrate that the estimation of return periods by the negative binomial distribution is robust and depend only little on the length of data set. The more events per year are considered, the wider the uncertainty range. For a storm series as in 1990 (four events above the 1-year return level, three above the 2-year return level and two events above the 5-year return level) for all data sets and return levels the negative binomial based estimate for the return period is between 40 and 65 years. This is for all cases a more reliable estimate compared to the empirical data (see Supplement B2) than based on the Poisson distribution, which has an estimate of 65 years (1-year return level) and for more extreme events with a return level of 2-year (5-year) an assessment of 79 (61) years. The deviations between the Poisson and the negative binomial distribution are much larger if less frequent series are considered (Table 2).

For insurance applications, it is often desirable to consider not exactly a certain number of events, but rather a minimum value, e.g. three or more events per year above 2-year return level. With this aim, the estimations of Table 2 were computed for cumulative probabilities (Supplement C). Results are in line with the previous: for example, the estimated return periods for four or more events at the 1-year return level is between 26 and 40 years based on the negative binomial distribution, whereas by the Poisson distribution it is 53 years. For two or more events at the 5-year return level the range is between 42 and 53 years with the negative binomial distribution, while for the Poisson distribution it is 57 years. Also from this perspective, the results clearly indicate the importance of estimates with the negative binomial distribution, which considers explicitly the clustering of events.

5 Summary and conclusions

For insurance applications, it is important to use reliable methods to estimate “occurrence loss exceeding probability” (OEP) and the “aggregate loss exceeding probability” (AEP). With this aim, an adequate quantification of clustering is essential. In this study we analysed different methods to estimate the return period of series of windstorm related losses exceeding selected return levels. For the purpose of statistical robustness, a combination of two reanalysis data, observation DWD data and an ensemble of over 4000 years of GCM runs were considered. First, the potential loss for Germany was estimated using an approach of the storm loss model of Klawns and Ulbrich (2003) for all data sets and additionally a meteorological index (Pinto et al., 2012). These methods were adapted to separate consecutive potential losses associated with extreme events within 3 days. As Germany is a comparatively small area, this time frame is reasonable for separating events. Moreover, it accords to the 72 h event definition, which is often used by insurance companies in reinsurance treaties (Klawns and Ulbrich, 2003). The estimated events are ranked and only the top events representing a return level of 1-year, 2-year or 5-years are analysed. The distribution of the number of events per winter was analysed. This was followed by the estimation of the return period of storm series like in 1990 (with four storms in ERAI) with the Poisson distribution as well as with the negative binomial distribution. The main conclusion is that especially for storm series with many events per winter (e.g. four events exceeding the 1-year return level) the Poisson distribution clearly overestimates the return period for storm series, as overdispersion is evident. Deviations from the Poisson distribution are also identified when considering the long GCM data set (over 4000 years), but results show that mean estimates and uncertainties do vary between data sets (see Table 2). In general terms, the negative binomial distribution provides a good approximation of the empirical data. However, a constant overdispersion factor Ψ cannot be identified for storm losses, as Ψ changes both with intensities and between data sets. This suggests that clustering of windstorms and associated losses is a complex phenomenon and needs further discussion. The primary advantage of considering the extended GCM data set is a strong reduction in the uncertainties.

As qualitatively good insurance data or meteorological data (peak gusts) are mostly available only after 1970, it is difficult to classify the year 1990 based on the historical time period alone. According to our evaluation based on 30 years of observational data (NCEP, DWD, ERAI) there is a strong indication that the return period of this event combination (four events with a loss return level of ≥ 1 year) is longer than the existing data length (30 years). The used negative binomial distribution suggests return periods of about 49 years (ERAI). Nevertheless, the estimated uncertainty is large, as the data basis of only 30 years is clearly too short. By using the 4092 years of GCM data a strong reduction of the

uncertainty estimates was achieved. These results put the historical storm series into a much larger perspective: the estimates indicate that an occurrence of exactly four events like in 1990 takes place once in 40–53 years. If four or more events are considered, the estimation of the accumulated likelihood is between 26 and 40 years based on the negative binomial distribution.

Results of the present study are potentially helpful for insurance companies to parameterise loss frequency assumptions of severe winter storm events. In Germany, the possible number of significant storm events per year was intensively discussed after the storm series in 1990, which is the top annual aggregated loss for recent decades (e.g. for insurance of residential buildings in Germany, after inflation correction: GDV, 2012). Even over 20 years later, German companies use the 1990 storm series as an internal benchmark test for their reinsurance cover or capital requirements. A similar discussion took place in France after the events “Lothar” and “Martin” (Ulbrich et al., 2001) hit the country in late 1999.

The present results demonstrate that the negative binomial distribution provides good estimates of return periods for less frequent storm series. Future work should focus on a more detailed analysis of events with different return periods within one winter as this could improve results. Furthermore, an investigation of the clustering within single CWTs, especially for CWTs with a high frequency of events, could be helpful for a better understanding of the physical aspects of clustering. Another interesting investigation could be to perform a similar analysis of further European countries.

The Supplement related to this article is available online at doi:10.5194/nhess-14-2041-2014-supplement.

Acknowledgements. We acknowledge the provision of loss data by the German Association of Insurers (“Gesamtverband der Deutschen Versicherungswirtschaft”, GDV) within GDV-project “Climate change impacts on the loss situation in the German insurance sector” (2008–2011). We thank the European Centre for Medium-Range Weather Forecasts for the ERA-Interim reanalysis data sets, and the National Centres for Environmental Prediction/National Centre for Atmospheric Research for the NCEP reanalysis data. We thank the MPI for Meteorology (Hamburg, Germany) and Andreas Sterl from the KNMI (De Bilt, The Netherlands) for providing the GCM data. We also thank the Centre for International Earth Science Information Network (CIESIN), Columbia University; and Centro de Agricultura Tropical (CIAT) providing the Gridded population of the World Version3 (GPWv3): Population density grids. Palisades, NY: Socioeconomic Data and Applications Centre (SEDAC), Columbia University, available online under the following weblink: <http://sedac.ciesin.columbia.edu/gpw> (date of download: 5 April 2012). Furthermore we thank the CRAN-R-project for providing the open-source software package R: R Development Core Team (2011). R: A language and environment for statistical computing. R foundation for statistical computing, Vienna, Austria. ISBN

3-900051-07-0, <http://www.R-project.org/>. We thank the German Weather Service (DWD) for the wind gust data. Furthermore we thank the two referees, who helped to improve the manuscript. Finally, we are grateful to Julia Mömken for the CWT computations and Mark Meyers (both University of Cologne) for discussions.

Edited by: B. Merz

Reviewed by: R. Caballero and R. Vitolo

References

- Aon Benfield: Winterstürme in Europa – Historie von 1703 bis 2012. Veröffentlichung der Aon Benfield Analytics, Hamburg, available at: aonbenfield.de/sturmhistorie/sturmhistorie.pdf, last access: 6 June 2014, 43 pp., 2013 (in German).
- Bjerknes, J. and Solberg, H.: Life cycle of cyclones and the polar front theory of atmospheric circulation, *Geophysisks Publikationer*, 3, 3–18, 1922.
- Born, K., Ludwig, P., and Pinto, J. G.: Wind gust estimation for Mid-European winter storms: towards a probabilistic view, *Tellus A*, 64, 17471, doi:10.3402/tellusa.v64i0.17471, 2012.
- Dee, D. P., Uppala, S. M., Simmons, A. J., Berrisford, P., Poli, P., Kobayashi, S., Andrae, U., Balmaseda, M. A., Balsamo, G., Bauer, P., Bechtold, P., Beljaars, A. C. M., van de Berg, L., Bidlot, J., Bormann, N., Delsol, C., Dragani, R., Fuentes, M., Geer, A. J., Haimberger, L., Healy, S. B., Hersbach, H., Hólm, E. V., Isaksen, I., Kållberg, P., Köhler, M., Matricardi, M., McNally, A. P., Monge-Sanz, B. M., Morcrette, J.-J., Park, B.-K., Peubey, C., de Rosnay, P., Tavolato, C., Thépaut, J.-N., and Vitart, F.: The ERA-Interim reanalysis: configuration and performance of the data assimilation system, *Q. J. Roy. Meteor. Soc.*, 137, 553–597, doi:10.1002/qj.828, 2011.
- Della-Marta, P. M., Mathis, H., Frei, C., Liniger, M. A., Kleinn, J., and Appenzeller, C.: The return period of wind storms over Europe, *Int. J. Climatol.*, 29, 437–459, doi:10.1002/joc.1794, 2009.
- Donat, M. G., Leckebusch, G. C., Pinto, J. G., and Ulbrich, U.: Examination of wind storms over Central Europe with respect to Circulation Weather Types and NAO phases, *Int. J. Climatol.*, 30, 1289–1300, doi:10.1002/joc.1982, 2010.
- Donat, M. G., Pardowitz, T., Leckebusch, G. C., Ulbrich, U., and Burghoff, O.: High-resolution refinement of a storm loss model and estimation of return periods of loss-intensive storms over Germany, *Nat. Hazards Earth Syst.*, 11, 2821–2833, doi:10.5194/nhess-11-2821-2011, 2011.
- Emanuel, K. and Jagger, T.: On Estimating Hurricane Return Periods, *J. Appl. Meteorol. Clim.*, 49, 837–844, doi:10.1175/2009JAMC2236.1, 2010.
- Fink, A. H., Brücher, T., Ermert, V., Krüger, A., and Pinto, J. G.: The European storm Kyrill in January 2007: synoptic evolution, meteorological impacts and some considerations with respect to climate change, *Nat. Hazards Earth Syst. Sci.*, 9, 405–423, doi:10.5194/nhess-9-405-2009, 2009.
- GDV: Statistical Yearbook of German Insurance 2012, available at: <http://www.gdv.de/2012/10/statistical-yearbook-of-german-insurance-2012/>, last access: 8 January 2014, 2012.
- Gómara, I., Pinto, J. G., Woolings, T., Masato, G., Zurita-Gotor, P., and Rodriguez-Fonseca, B.: Rossby Wave-Breaking analysis of Explosive Cyclones in the Euro-Atlantic Sector, *Q. J. Roy. Meteor. Soc.*, 140, 738–753, doi:10.1002/qj.2190, 2014.
- Hanley, J. and Caballero, R.: The role of large-scale atmospheric flow and Rossby wave breaking in the evolution of extreme windstorms over Europe, *Geophys. Res. Lett.*, 39, L21708, doi:10.1029/2012GL053408, 2012.
- Held, H., Gerstengarbe, F. W., Pardowitz, T., Pinto, J. G., Ulbrich, U., Böhm, U., Born, K., Büchner, M., Donat, M. G., Karremann, M. K., Leckebusch, G. C., Ludwig, P., Nissen, K. M., Nocke, T., Osterle, H., Pahl, B. F., Werner, P. C., Befort, B. J., and Burghoff, O.: Projections of global warming-induced impacts on winter storm losses in the German private household sector, *Climatic Change*, 121, 195–207, doi:10.1007/s10584-013-0872-7, 2013.
- Jones, P. D., Hulme, M., and Briffa, K. R.: A comparison of lamb circulation types with an objective classification scheme, *Int. J. Climatol.*, 13, 655–663, doi:10.1002/joc.3370130606, 1993.
- Jungclaus, J. H., Keenlyside, N., Botzet, M., Haak, H., Luo, J. J., Latif, M., Marotzke, J., Mikolajewicz, U., and Roeckner, E.: Ocean Circulation and Tropical Variability in the Coupled Model ECHAM5/MPI-OM, *J. Climate*, 19, 3952–3972, doi:10.1175/JCL3827.1, 2006.
- Kistler, R., Collins, W., Saha, Suranjana, White, G., Woollen, J., Kalnay, E., Chelliah, M., Ebisuzaki, W., Kanamitsu, M., Kousky, V., van den Dool, H., Jenne, R., and Fiorino, M.: The NCEP/NCAR 50-year reanalysis: monthly-means CD-ROM and documentation, *B. Am. Meteorol. Soc.*, 82, 247–267, doi:10.1175/1520-0477(2001)082, 2001.
- Klawa, M. and Ulbrich, U.: A model for the estimation of storm losses and the identification of severe winter storms in Germany, *Nat. Hazards Earth Syst.*, 3, 725–732, doi:10.5194/nhess-3-725-2003, 2003.
- Lamb, H. H.: British Isles weather types and register of the daily sequence of circulation patterns 1861–1971 (Geophysical Memorial), HMSO, London, 85 pp., 1972.
- Maillet, P. J., Stephenson, D. B., Ferro, C. A. T., and Hodges, K. I.: Serial Clustering of Extratropical Cyclones, *Mon. Weather Rev.*, 134, 2224–2240, 2006.
- Marsland, S. J., Haak, H., Jungclaus, J. H., Latif, M., and Röske, F.: The Max-Planck-Institute global ocean-sea ice model with orthogonal curvilinear coordinates, *Ocean Model.*, 5, 91–127, doi:10.1016/S1463-5003(02)00015-X, 2003.
- MunichRe: Winter storms in Europe. II. Analysis of 1999 losses and loss potentials. Publication of Munich Re, available at: www.munichre.com (last access: 28 June 2012), 2001.
- Palutikof, J. P. and Skellern, A. R.: Storm severity over Britain: a report to Commercial Union General Insurance, Climatic Research Unit, School of Environmental Science, University of East Anglia, Norwich, UK, 1991.
- Pinto, J. G., Fröhlich, E. L., Leckebusch, G. C., and Ulbrich, U.: Changing European storm loss potentials under modified climate conditions according to ensemble simulations of the ECHAM5/MPI-OM1 GCM, *Nat. Hazards Earth Syst. Sci.*, 7, 165–175, doi:10.5194/nhess-7-165-2007, 2007.

- Pinto, J. G., Neuhaus, C. P., Leckebusch, G. C., Reyers, M., and Kerschgens, M.: Estimation of wind storm impacts over West Germany under future climate conditions using a statistical-dynamical downscaling approach, *Tellus A*, 62, 188–201, doi:10.1111/j.1600-0870.2009.00424.x, 2010.
- Pinto, J. G., Karremann, M. K., Born, K., Della-Marta, P. M., and Klawa, M.: Loss potentials associated with European windstorms under future climate conditions, *Clim. Res.*, 54, 1–20, doi:10.3354/cr01111, 2012.
- Pinto, J. G., Bellenbaum, N., Karremann, M. K., and Della-Marta, P. M.: Serial clustering of extratropical cyclones over the North Atlantic and Europe under recent and future climate conditions, *J. Geophys. Res.-Atmos.*, 118, 12476–12485, doi:10.1002/2013JD020564, 2013.
- Schwierz, C., Köllner-Heck, P., Zenklusen Mutter, E., Bresch, D. N., Vidale, P. L., Wild, M., and Schär, C.: Modelling European winter wind storm losses in current and future climate, *Climatic Change*, 101, 485–514, doi:10.1007/s10584-009-9712-1, 2010.
- Sillmann, J. and Croci-Maspoli, M.: Present and future atmospheric blocking and its impact on European mean and extreme climate, *Geophys. Res. Lett.*, 36, L10702, doi:10.1029/2009GL038259, 2009.
- Sterl, A., Severijns, C., Dijkstra, H., Hazeleger, W., van Oldenborgh, G. J., van den Broeke, M., Burgers, G., van den Hurk, B., van Leeuwen, P. J., and van Velthoven, P.: When can we expect extremely high surface temperatures?, *Geophys. Res. Lett.*, 35, L14703, doi:10.1029/2008GL034071, 2008.
- Ulbrich, U., Fink, A. H., Klawa, M., and Pinto, J. G.: Three extreme storms over Europe in December 1999, *Weather*, 56, 70–80, doi:10.1002/j.1477-8696.2001.tb06540.x, 2001.
- Vitolo, R., Stephenson, D. B., Cook, I. M., and Mitchell-Wallace, K.: Serial clustering of intense European storms, *Meteorol. Z.*, 18, 411–424, doi:10.1127/0941-2948/2009/0393, 2009.
- Wilks, D. S.: *Statistical Methods in the Atmospheric Science*, 2nd Edn., International Geophysics Series, Burlington, USA, 627 pp., 2006.

Supplement of Nat. Hazards Earth Syst. Sci., 14, 2041–2052, 2014
<http://www.nat-hazards-earth-syst-sci.net/14/2041/2014/>
doi:10.5194/nhess-14-2041-2014-supplement
© Author(s) 2014. CC Attribution 3.0 License.



Natural Hazards
and Earth System
Sciences

Open Access



Supplement of

On the clustering of winter storm loss events over Germany

M. K. Karremann et al.

Correspondence to: M. K. Karremann (mkarre@meteo.uni-koeln.de)

Supplementary A: Detailed information about the analysed data sets

The ECHAM5/MPI-OM1 model of the MAX-Planck-Institute in Hamburg (Germany) couples an atmospheric model and an ocean model (MPI-OM1). The ocean model interacts with a dynamically sea ice model (Marsland et al.; 2003) and has 23 vertical
5 levels. The atmospheric model has 31 vertical levels. The horizontal resolution is $1.875^\circ \times 1.875^\circ$ (T63). This model is performed well on a number of criteria, which were considered in the Fourth Assessment Report of the IPCC. In total we studied 47 different simulations from MPI. The References or DOIs for all experiments as well as the forcing are included in Table A1.

Table A1: Information of the used datasets. The indicated years correspond to the model forcing in terms of historical and/or projected greenhouse gas forcing.

Dataset (run)	Correspondent years (forcing)	Number of winters	Reference or DOI
PRE	well-mixed greenhouse gases CO ₂ , CH ₄ and N ₂ O constant for 1860	505	Roeckner, et al., 2006: IPCC-AR4 MPI-ECHAM5_T63L31 MPI-OM_GR1.5L40 Plcntrl (pre-industrial control experiment): atmosphere 6 HOUR values MPImet/MaD Germany. WDDC. DOI:10.1594/WDCC/EH5-T63L31_OM-GR1.5L40_CTL_6H.
ESSENCE (1-20)	1950-2000 (observed greenhouse gas concentrations)	1000	Sterl et al. (2008)
ESSENCE (21-37)	1950-2030 (until 2000: observed greenhouse gas concentrations 2001-2030: SRES A1B)	1360	Sterl et al. (2008)
ECHAM5/MPI-OM1 20C (1-3)	1860-2000: PRE initialised in year 2190 2001-2100: commitment experiment for 21 th century; constant 2000	720	Roeckner et al., 2006 IPCC-AR4 MPI-ECHAM5_T63L31 MPI-OM_GR1.5L40 20C3M runs no.1-3. WDDC. DOI:10.1594/WDCC/EH5-T63L31_OM-GR1.5L40_20C_1_6H. DOI:10.1594/WDCC/EH5-T63L31_OM-GR1.5L40_20C_2_6H. DOI:10.1594/WDCC/EH5-T63L31_OM-GR1.5L40_20C_3_6H.
C20SA (1-3)	2001-2030: ECHAM5/MPI-OM1 20C; anthropogenic aerosols = 0	87	Roeckner, 2004: EH5-T63L31_OM-GR1.5L40_C20SA_1, 6h values. WDDC. CERA-DB "EH5-T63L31_OM_C20SA_1_6H" "EH5-T63L31_OM_C20SA_2_6H" "EH5-T63L31_OM_C20SA_3_6H" http://cera-www.dkrz.de/WDCC/ui/Compact.jsp?acronym=EH5-T63L31_OM_C20SA_1_6H http://cera-www.dkrz.de/WDCC/ui/Compact.jsp?acronym=EH5-T63L31_OM_C20SA_2_6H http://cera-www.dkrz.de/WDCC/ui/Compact.jsp?acronym=EH5-T63L31_OM_C20SA_3_6H

			www.dkrz.de/WDCC/ui/Compact.jsp?acronym=EH5-T63L31_OM_C20SA_2_6H http://cera-www.dkrz.de/WDCC/ui/Compact.jsp?acronym=EH5-T63L31_OM_C20SA_3_6H
20C3M (1-3)	1860-2000: PRE plus solar constant and effects of volcanic aerosols	420	<p>Roeckner, 2005: IPCC MPI-ECHAM5_T63L31 MPI-OM_GR1.5L40 20C3M_all runs no.1-3: atmosphere 6 HOUR values MPImet/MaD Germany. WDDC. CERA-DB</p> <p>"EH5-T63L31_OM_20C3M_1_6H"</p> <p>"EH5-T63L31_OM_20C3M_2_6H"</p> <p>"EH5-T63L31_OM_20C3M_3_6H"</p> <p>http://cera-www.dkrz.de/WDCC/ui/Compact.jsp?acronym=EH5-T63L31_OM_20C3M_1_6H</p> <p>http://cera-www.dkrz.de/WDCC/ui/Compact.jsp?acronym=EH5-T63L31_OM_20C3M_2_6H</p> <p>http://cera-www.dkrz.de/WDCC/ui/Compact.jsp?acronym=EH5-T63L31_OM_20C3M_3_6H</p>

15 **Supplementary B:**

Table B1: As Table 2 but indicating the raw number of events per dataset. The different GCM datasets indexed by corr are results corrected by the CWT.

1-year Return Level		DWD	ERA-I	NCEP	GCM	GCM _{corr}	ESS _{corr}	20C _{corr}	PRE _{corr}
		30yrs	30yrs	30yrs	4092yrs	4092yrs	2360yrs	720yrs	505yr
Events per year	0	12	12	12	1705	1734	940	301	195
	1	10	10	9	1278	1258	790	242	180
	2	5	6	7	699	666	413	101	83
	3	2	0	1	289	286	153	42	33
	4	1	2	1	75	108	43	24	10
	5	0	0	0	33	30	14	7	4
	6	0	0	0	8	8	6	2	0
	7	0	0	0	4	2	1	1	0
	8	0	0	0	1	0	0	0	0
2-year Return Level									
Events per year	0	20	18	19	2591	2593	1473	454	311
	1	6	10	8	1068	1065	651	195	145
	2	3	1	2	342	341	190	53	40
	3	1	1	1	72	78	39	13	7
	4	0	0	0	17	10	4	5	2
	5	0	0	0	2	5	3	0	0
5-year Return Level									
Events per year	0	24	25	26	3388	3378	1943	595	414
	1	6	4	3	607	621	370	113	81
	2	0	1	0	82	84	40	13	10
	3	0	0	1	14	8	6	3	0
	4	0	0	0	0	0	1	0	0
	5	0	0	0	1	1	0	0	0

20

25

Table B2: As Table 2 but indicating the empirical return period based on the raw number of events per dataset. The different GCM datasets indexed by corr are results corrected by the CWT.

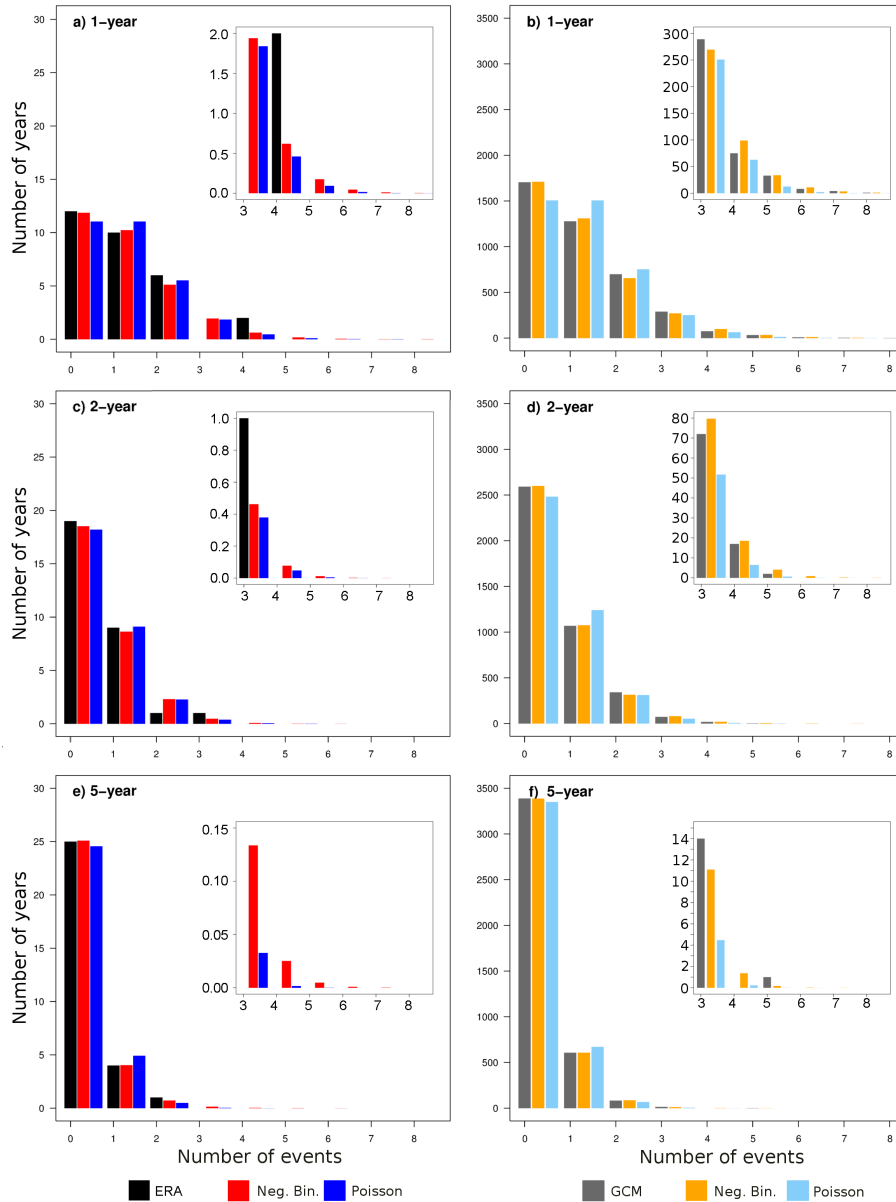
1-year Return Level		DWD 30yrs	ERA- 30yrs	NCEP 30yrs	GCM 4092yrs	GCM _{corr} 4092yrs	ESS _{corr} 2360yrs	20C _{corr} 720yrs	PRE _{corr} 505yrs
Events per year	0	2.50	2.50	2.50	2.4	2.36	2.51	2.39	2.59
	1	3.00	3.00	3.33	3.20	3.25	2.99	2.98	2.81
	2	6.00	5.00	4.29	5.85	6.14	5.71	7.13	6.08
	3	15	-	30	14	14	15	17	15
	4	30	15	30	55	38	55	30	51
	5	-	-	-	124	136	169	103	126
	6	-	-	-	512	512	393	360	-
	7	-	-	-	1023	2046	2360	720	-
	8	-	-	-	4092	-	-	-	-
2-year Return Level		Empirical return period							
Events per year	0	1.50	1.67	1.58	1.58	1.59	1.60	1.59	1.62
	1	5.00	3.00	3.75	3.83	3.84	3.63	3.69	3.48
	2	10	30	15	12	12	12	14	13
	3	30	30	30	57	52	61	55	72
	4	-	-	-	241	409	590	144	253
	5	-	-	-	2046	818	1364	-	-
5-year Return Level		Empirical return period							
Events per year	0	1.25	1.20	1.15	1.21	1.21	1.21	1.21	1.22
	1	5.00	7.50	10.00	6.74	6.60	6.38	6.61	6.23
	2	-	30	-	50	49	59	55	501
	3	-	-	30	292	511	393	240	-
	4	-	-	-	-	-	2360	-	-
	5	-	-	-	4092	4092	-	-	-

Supplementary C:

Accumulated return period estimated with negative Binomial distribution for x and
 35 more events. For example 3 or more events.

1-year Return Level	Pois	ERA1 30yrs	NCEP 30yrs	GCM 4092yrs	GCM _{corr} 4092yrs	ESS _{corr} 2360yrs	20C _{corr} 720yrs	PRE _{corr} 505yr
1	1.58	1.65	1.67	1.72	1.75	1.66	1.71	1.63
2	3.78	3.79	3.80	3.82	3.83	3.80	3.81	3.79
3	12.45	10.75	10.46	9.80	9.53	10.60	9.87	11.25
4	53	35	33	28	26	34	28	40
5	273	128	113	83	73	120	86	161
2-year Return Level								
1	2.54	2.61	2.73	2.74	2.74	2.67	2.70	2.61
2	11.09	10.50	9.83	9.78	9.76	10.15	9.97	10.51
3	70	54	40	40	39	47	43	55
4	571	332	181	172	170	242	204	335
5-year Return Level								
1	5.52	6.12	7.36	5.80	5.73	5.64	5.74	5.58
2	57	34	24	42	44	49	44	53
3	871	180	70	324	386	520	380	660

Supplementary D:



- 40 Histograms of the number of years with a certain number of events for the empirical data (black/grey), the Poisson distribution (dark/light blue) and the fitted negative Binomial distribution (red/yellow). (a) Number of events exceeding the 1-year return level of ERAI; (b) same as a) but for CGM data; (c) same as a) but for 2-year return level events; (d) same as b) for 2-year return level events; (e) same as a) but for 5-year return level events; (f) as b) but for 5-year return level events. For a), c) and e)
- 45 the total number of years is 30, for b), d) and f) it is 4092.

Supplementary E:

Date	LI_{raw}
20.02.90	0
21.02.90	0
22.02.90	0
23.02.90	0
24.02.90	0
25.02.90	0
26.02.90	270
27.02.90	31
28.02.90	281
01.03.90	158
02.03.90	0
03.03.90	0
04.03.90	0
05.03.90	0

Time series of LI_{raw} between 20 February 1990 and 05 March 1990 based on NCEP data. Identified events are marked in bold.

50

6 Return Periods of Losses associated with European Windstorm Series in a Changing Climate

Reference:

Karremann M.K., Pinto J.G., Reyers M. and Klawe M. (2014): Return periods of losses associated with European windstorm series in a changing climate, *Environ Res Lett* **9**: 124016, doi:10.10188/1748-9326/9/12/124016

©(2014) IOP Publishing Ltd

Permission to reprint:

This work is distributed under the Creative Commons Attribution 3.0 License. Page numbers are as published in Environmental Research Letters.

Return periods of losses associated with European windstorm series in a changing climate

Melanie K Karremann¹, Joaquim G Pinto^{1,2}, Mark Meyers¹ and Matthias Klawns³

¹Institute for Geophysics and Meteorology, University of Cologne, Germany

²Department of Meteorology, University of Reading, UK

³DeutscheRück AG, Düsseldorf, Germany

E-mail: mkarre@meteo.uni-koeln.de


Received 15 July 2014, revised 25 November 2014

Accepted for publication 26 November 2014

Published 15 December 2014

Abstract

Possible future changes of clustering and return periods (RPs) of European storm series with high potential losses are quantified. Historical storm series are identified using 40 winters of reanalysis. Time series of top events (1, 2 or 5 year return levels (RLs)) are used to assess RPs of storm series both empirically and theoretically. Additionally, 800 winters of general circulation model simulations for present (1960–2000) and future (2060–2100) climate conditions are investigated. Clustering is identified for most countries, and estimated RPs are similar for reanalysis and present day simulations. Future changes of RPs are estimated for fixed RLs and fixed loss index thresholds. For the former, shorter RPs are found for Western Europe, but changes are small and spatially heterogeneous. For the latter, which combines the effects of clustering and event ranking shifts, shorter RPs are found everywhere except for Mediterranean countries. These changes are generally not statistically significant between recent and future climate. However, the RPs for the fixed loss index approach are mostly beyond the range of pre-industrial natural climate variability. This is not true for fixed RLs. The quantification of losses associated with storm series permits a more adequate windstorm risk assessment in a changing climate.

 Online supplementary data available from stacks.iop.org/ERL/9/124016/mmedia

Keywords: European windstorms, storm series, climate change, storm losses, overdispersion, return periods, clustering

1. Introduction

Extreme windstorms are the most important natural hazards affecting Western Europe (Lamb 1991, Schwierz *et al* 2010). In situations when a recurrent extension of an intensified eddy driven jet towards Western Europe lasts for at least one week, multiple extreme cyclones may follow a similar path within a relatively short time period (e.g. early 1990). Such clustering

of cyclones over the North Atlantic and Western Europe has been identified in reanalysis data (Mailier *et al* 2006, Pinto *et al* 2013). In particular, extreme cyclones cluster more than non-extreme cyclones (Vitolo *et al* 2009, Pinto *et al* 2013). Windstorm clusters often have large socio-economic impacts and may cause high cumulative losses, like in 1990 with about 8.5bn € (DeutscheRück 2005). Another recent example is the windstorm series in winter 2013/2014, which mainly affected the British Isles. Due to the Solvency II requirements (Solvency Capital Requirements, QIS5), insurance companies need to improve the assessment of frequencies and return periods (RPs) of storm series and their ‘aggregate loss exceeding probability’ under present and future climate



Content from this work may be used under the terms of the Creative Commons Attribution 3.0 licence. Any further distribution of this work must maintain attribution to the author(s) and the title of the work, journal citation and DOI.

conditions. Karremann *et al* (2014) evaluated different methods to estimate RPs of windstorm series for Germany and identified the negative binominal distribution as the best approach.

Estimates of loss potentials for both recent climate and future climate projections are mostly restricted to annual losses (e.g. Pinto *et al* 2007, Donat *et al* 2011), and seldomly deal with single extreme events (e.g. Haylock 2011, Pinto *et al* 2012). Possible future changes of losses strongly depend on the model and the analysed periods (see Feser *et al* 2014 for a review on storminess affecting Europe). However, some studies identified shorter RPs for windstorms affecting Western/Central Europe in future decades (e.g. Della-Marta and Pinto 2009, Pinto *et al* 2012). With respect to storm series, results by Pinto *et al* (2013) point to a possible decrease of cyclone clustering over parts of Western Europe during the current century. In this study, RPs for multiple event losses associated with storm series under present and future climate conditions are analysed for several European regions. Following Karremann *et al* (2014), RPs from NCEP reanalysis and general circulation model (GCM) data are estimated theoretically and empirically. Methods and datasets are described in section 2, followed by results in section 3. A summary and discussion is given in sections 4 and 5.

2. Data and methods

Reanalysis data from the National Centre for Environmental Prediction/National Centre for Atmospheric Research (hereafter NCEP) with a horizontal resolution of 1.875° (about 140×210 km grid spacing at mid-latitudes; Kistler *et al* 2001) are analysed. For each calendar winter day (October–March) from 1973/1974 to 2012/2013, the largest of the four instantaneous 6 hourly 10 m wind speed is taken as the daily maximum. Twenty transient simulations performed with the coupled ECHAM5/MPI-OM1 GCM (Jungclauss *et al* 2006), also with a horizontal resolution of 1.875° , are considered: three realizations of MPI (Roeckner *et al* 2006) and 17 from the ESSENCE project (Sterl *et al* 2008). Maximum winds for 6 h periods (*wimax*) are used to determine the daily maximum wind. Pinto *et al* (2007) showed that results of the storm loss model (see below) are equivalent when using instantaneous wind speeds or *wimax* as input variables. For recent and future climate conditions, the periods of 1960–2000 and 2060–2100 are used, corresponding to the 20C and A1B scenarios. We assume that all ensemble-members are equally probable. The choice of a large ensemble for a single GCM model is motivated by the focus on statistical robustness of the results rather than on inter-model dependency or sensitivity (Taylor *et al* 2012). To quantify natural inter-decadal climate variability, a 505 year long pre-industrial run (PRE) of ECHAM5 with constant forcing (year 1860) is also analysed.

A modified version of the storm loss model by Klawe and Ulbrich (2003) is used to estimate cumulative losses of storm series. The potential damage is proportional to the cube of the daily maximum (gust) wind speed (Palutikof and

Skellern 1991, Klawe and Ulbrich 2003). Losses are primarily caused by wind gusts, when a certain local threshold is exceeded. For Western and Central Europe, the 98th percentile (supplementary H) is assumed to be a reasonable critical threshold, implying that buildings were constructed according to the local climatological wind conditions (Klawe and Ulbrich 2003). The 98th wind gust percentile over this area corresponds to about $20\text{--}21 \text{ m s}^{-1}$ (8 Bft). Such wind gust values imply wind speeds between 8 m s^{-1} and 11 m s^{-1} , depending on the given gust factor (relationship between wind gust and wind speed, e.g. Wieringa 1973, Born *et al* 2012). A careful analysis indicated that 9 m s^{-1} wind speed is an adequate minimum threshold for regions where the 98th percentile values are too low (parts of Scandinavia, the Mediterranean and South-Eastern Europe) and thus not reasonable for loss occurrence. The resulting potential damage is weighted with population density and aggregated to potential losses (LI). Further details can be found in Pinto *et al* (2012) and Karremann *et al* (2014). Population density of the year 2000 ($0.25^\circ \times 0.25^\circ$) is used as proxy for insurance data, possible population density changes in Europe are neglected. The dataset is provided by the Centre for International Earth Science Information Network of the Columbia University and the 'Centro Internacional de Agricultura Tropical'. LIs are estimated for single events for European countries/regions. Resulting event sets are ranked according to LI values, and 1, 2 and 5 year return levels (RLs) (abbreviated as 1yrl, 2yrl, and 5yrl) are generated (40, 20 and 8 events with highest LI in 40 winters, respectively). Time series are obtained by allocating the events corresponding to individual winters, enabling the estimation of empirical RPs for storm series with different RLs.

The probability for the incidence of multiple events per winter can be estimated theoretically with the negative binomial distribution, which is a standard distribution to analyse insurance risks. Estimated RPs using this theoretical distribution show the best agreement with empirically estimated RPs of windstorm series (see supplementary E, F, Karremann *et al* 2014). Theoretical RPs of multiple events per winter for given RLs are defined as the inverse of the probability of their occurrence. The clustering of events is determined by the dispersion statistics (ψ). More details can be found in supplementary B and in Karremann *et al* (2014) (see their section 3). The methodology is applied to 21 European countries/regions (supplementary A). Core Europe is defined as France, Belgium, Germany, The Netherlands, Denmark, Ireland and United Kingdom. Empirical RPs and theoretical RPs are estimated for both recent and future climate conditions.

3. Results

3.1. Clustering and related RPs for NCEP

Time series of windstorm related losses exceeding certain RLs are derived from NCEP data for 21 countries/regions of Europe (40 winters). For Core Europe, the most prominent

storm series occurred in winter 1989/1990 (hereafter 1990), with four 1yrl/2yrl events, and two 5yrl events (figure 1(a)). This windstorm series affected almost all individual countries within Core Europe (except Denmark), with at least four 1yrl events (figures 1(b)–(h)), and a maximum of seven 1yrl events for Belgium (figure 1(h)). Other prominent winters are 1984, which mainly affected Denmark and Belgium (figures 1(e), (h)), and 2007, when four storms (2yrl) hit Ireland (figure 1(f)). These and other windstorm series also affected regions outside of Core Europe, e.g. Sweden was hit by four 1yrl events in 2007 and three 2yrl events in 2000, Finland by three 2yrl events in 2002, and Portugal by two 5yrl events in 2010 (cf supplementary C).

Considering the five most prominent windstorm series (winters 1984, 1990, 2000, 2002, 2007), the maximum event numbers are typically four 1yrl events, three 2yrl events and two 5yrl events (cf figure 1; supplementary C). Further, several Core Europe countries were hit by three 1yrl events and two 2yrl events. Therefore, focus is given hereafter to such windstorm series (3 or more (3+) 1yrl events, 2+ 2yrl events, 2+ 5yrl events). Time series per winter (figure 1, supplementary C) provide the basis for the estimation of empirical RPs at different RLs and for the assessment of clustering. The empirical RPs are compared to theoretical estimated RPs. The coherence between the top 40 event lists (1yrl) for Core Europe and individual countries/regions are analysed to verify whether the same events hit multiple countries and whether results for different regions are correlated (supplementary D). Many of the top events for individual Core Europe countries are included in the top 40 for Core Europe (figure 2, colours). Best agreement is found for Germany, where 26 of the 40 1yrl events (65%) agree with Core Europe (figure 2(a)). Good accordance is also found for The Netherlands (57.5%) and United Kingdom (55%), while less coherence is found for Belgium (47.5%), France (37.5%), Denmark and Ireland (both 30%, figure 2(a)). For higher RLs results are less tight: Germany and The Netherlands feature more than 50% accordance with Core Europe for all three RLs. For the United Kingdom, a decreasing concurrence with increasing RL is found (figures 2(a)–(c)). These results reflect the typical tracks of strong cyclones affecting Core Europe, which often first hit the United Kingdom and then cross the North Sea either towards Germany or Scandinavia (e.g. Hanley and Caballero 2012).

The empirical RPs for Core Europe and individual countries based on NCEP are indicated as upper numbers in figure 2. Figures 2(a)–(c) includes the values for an exact number of events (e.g. 3 events per winter), and figures 2(d)–(f) values are for accumulated probabilities (e.g. 3+ events per winter). Differences of the estimates for the RPs between the two rows are as expected: RPs for accumulated events (e.g. 3+) are shorter than for an exact number of events, as the probability of the accumulated events is higher (cf also supplementary E for Core Europe).

A detailed overview for storm series affecting Core Europe as derived for NCEP is given in table 1 for accumulated likelihoods. For example, a storm series with 4+ 1yrl events occurred twice in 40 years (table 1; $\text{num}_N = 2$), while

four 2yrl events and two 5yrl events per winter appeared once (table 1; $\text{num}_N = 1$). Positive ψ -values (table 1, tRP_N column) of 0.19 (1yrl), 0.04 (2yrl), and 0.1 (5yrl) indicate statistically significant serial clustering at the 95% confidence level (Pearson's Chi-square test; cf details in supplementary I) for each RL. Independent from the RL, estimated RPs are similar for empirically (eRP_N) and theoretically (tRP_N) estimates when considering few events per winter (cp. eRP_N with tRP_N columns). If e.g. all years have either zero or one occurrence, no overdispersion is found, and thus theoretical RPs cannot be estimated ('-' in table 1). The uncertainty estimates for tRP_N are calculated with the Gaussian error propagation based on the standard error. Differences between eRP_N and tRP_N for a large number of events per winter can be explained by the length of the investigated time series: for eRP_N , the possible maximum estimate is 40 years, as the dataset consists only of 40 winters, while for tRP_N , the theoretical fit may estimate RPs which are nominally larger than the length of the dataset.

3.2. Clustering and related RPs for GCM data under recent climate conditions

GCM data is now considered to enhance the RP estimates for the storm series. With 20 ensemble members, more robust statistics can be obtained from these GCM simulations than from the NCEP data. As expected, the maximum number of events per winter is larger in the GCM dataset, with up to six events per winter for 1yrl (e.g. table 1). This was expected, as the GCM dataset consists of 800 winters and not only 40 winters, and thus may include rarer storm series. Moreover, GCMs tend to overestimate both the westerly flow over the North Atlantic (e.g. Sillmann and Croci-Maspoli 2009) and the clustering of cyclones over the Eastern North Atlantic (Pinto *et al* 2013). A correction of the GCM bias on clustering is possible and was attempted in Karremann *et al* (2014) using weather type frequencies, but only a small influence on the estimated RPs was found. Hence, biases are neglected and the uncorrected GCM data are used for further analysis.

Comparing the empirical results based on GCM data (eRP_{20C}) and NCEP data (eRP_N) for Core Europe, some discrepancies are found, particularly for higher numbers of events (see table 1, eRP_N versus eRP_{20C}). As for NCEP, significant overdispersion is identified for the GCM for all RLs. Both NCEP and GCM show similar ψ -values for 1yrl ($\psi = 0.19$ versus $\psi = 0.24$, respectively) and 2yrl events ($\psi = 0.04$ versus $\psi_{20C} = 0.09$, respectively), but less agreement for 5yrl ($\psi = 0.1$ versus $\psi = 0.02$; table 1). For accumulated probabilities (numbers in figures 2(d)–(f), differences in RPs between NCEP and GCM for individual countries are typically smaller than for exact number of events (figures 2(a)–(c)). As the accumulated probabilities are of higher interest for the insurance industry, in the following focus is given only to accumulated results. Although the input data slightly differs (wind and wimax, see section 2), the theoretical RPs for NCEP and GCM are also mostly similar (cf table 1, supplementary E). This result is in line with previous studies comparing results of the storm loss model (Pinto *et al* 2007), which found only small differences for NCEP and GCM. The empirical RPs outside Core Europe

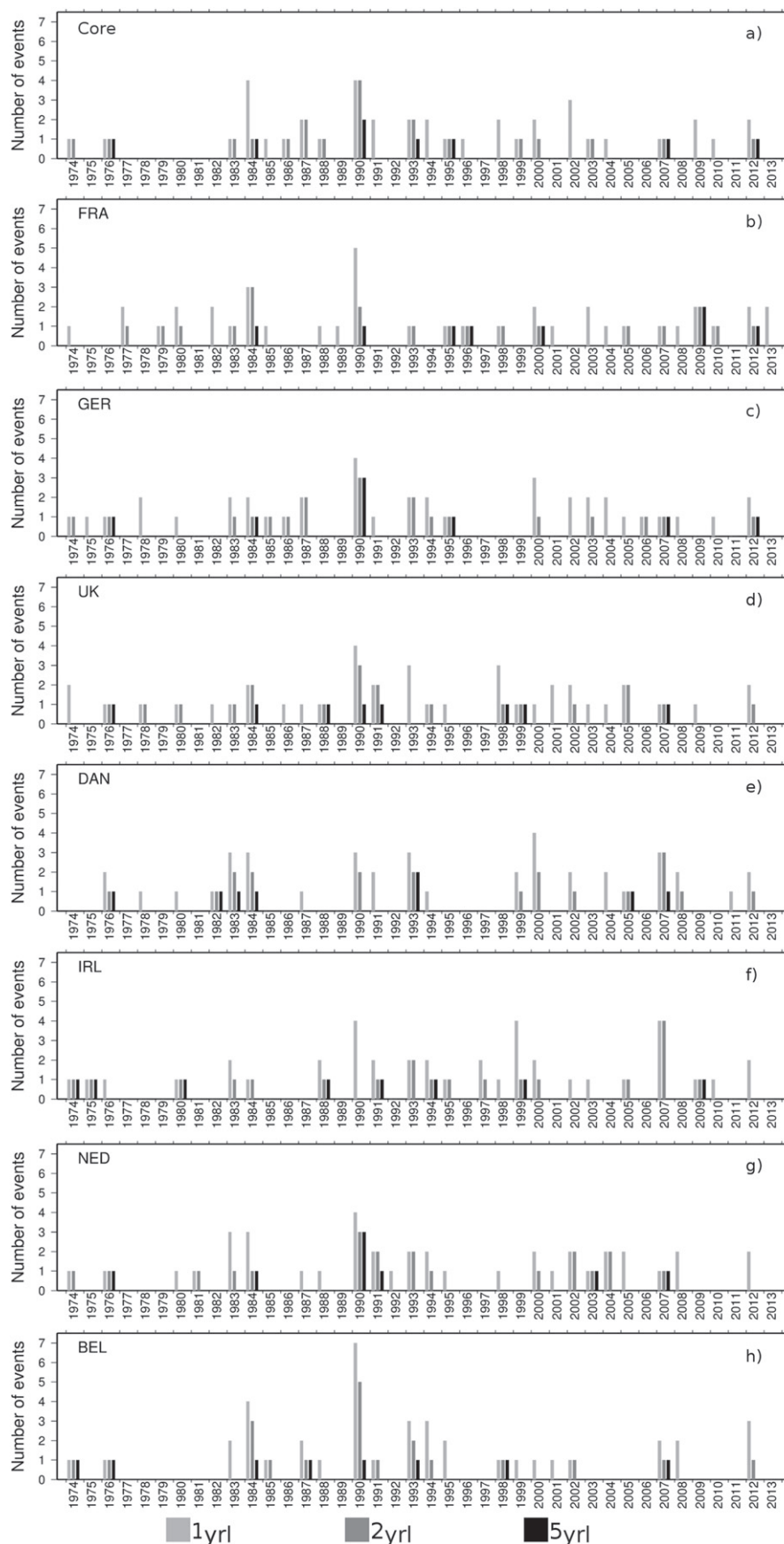


Figure 1. Identified number of events per winter for the NCEP data of the period 1973/1974–2012/2013. Colours denote the different return level: light grey 1yr, dark grey 2yr and black 5yr. The indicated years correspond to the second year, for example 1990 indicates the winter 1989/1990. The regions are (a) Core Europe (b) France (c) Germany (d) United Kingdom (e) Denmark (f) Ireland (g) The Netherlands and (h) Belgium.

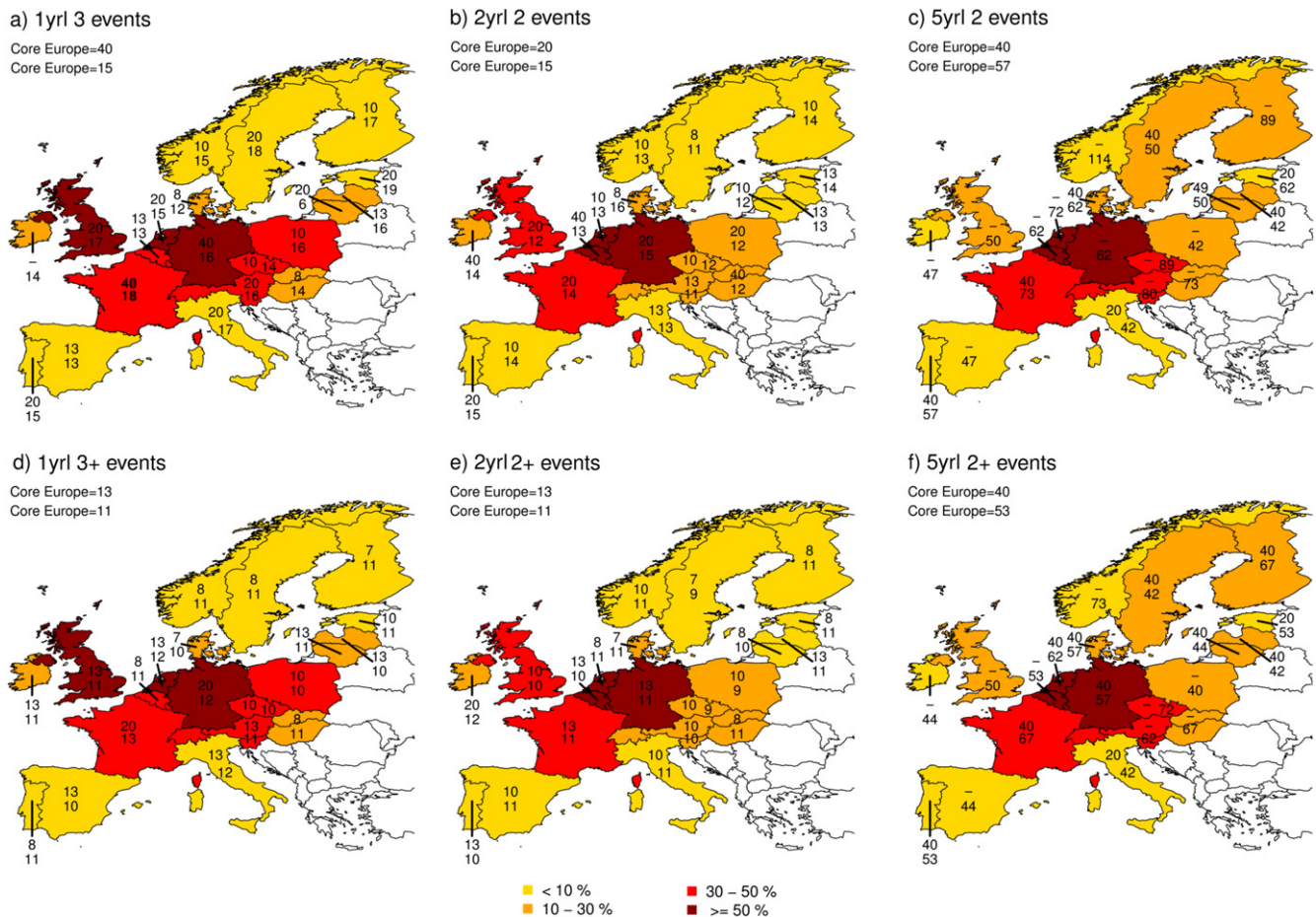


Figure 2. Analysed regions for different return levels and number of events. Colours denote the percentage of events with different return levels that hit Core Europe and the respective region (in %). Yellow: <10%; orange: 10–30%; red: 30–50%; dark red: >50%. Numbers denote the empirical RPs based on NCEP (upper number) and GCM (lower number). The return level and number of events are (a) for 1yrl with three events (b) for 2yrl considering two events (c) for 5yrl and two events (d) for 1yrl with three or more events (3+; accumulated) (e) 2yrl considering two or more events (2+; accumulated) (f) 5yrl considering two or more events (2+; accumulated).

show also good agreements between NCEP and GCM for almost all countries (figures 2(d)–(f)). The spread between both datasets increases for 2yrl with a rising number of events per winter (supplementary E).

The main advantage of considering the larger GCM data is in fact the reduction of the range of confidence intervals and the possibility to estimate longer RPs (table 1, right columns; Karremann *et al* 2014). As for NCEP data (section 3.1), substantial differences between the empirical and theoretical estimates are sometimes found for rarer storm series (e.g. 2yrl, 4+ events). This indicates that using the negative binominal distribution may not be in these cases the best fit to the empirical data. Nevertheless, possible future changes of RPs of storm series are analysed both theoretically and empirically in the next section. The advantage of estimations based on the empirical data is that all winters with multiple independent intense loss events are considered and not only winters with serial clustering events.

3.3. Future changes of clustering and related RPs

Possible changes of clustering and associated RPs in a changing climate are determined by comparing the two

periods 2060–2100 and 1960–2000. Results for Core Europe are presented in table 1. 1yrl, 2yrl, and 5yrl (800, 400 and 160 events in 800 winters GCM data, respectively) are compared theoretically (tRP_{20C} versus tRP_{RL} with a fixed RL in 2060–2100). While the ψ -values for 2yrl and 5yrl increase, a slight decrease is found for 1yrl events. This indicates an increase of clustering for strong events in a future climate, while weaker events may cluster less. Additionally to this perspective with a fixed RL (tRP_{RL}), future changes relative to a fixed 20C LI threshold (tRP_{LI}) are also considered. The former approach RP_{RL} enables the identification of shifts towards more/less clustering of the top 160, 400 or 800 events (i.e., top events more/less concentrated in single years, as total number is fixed). The latter approach tRP_{LI} detects the combined effect of clustering and possible shifts in rankings of intense losses under future climate conditions (see Pinto *et al* 2012). In fact, Pinto *et al* (2012) identified a significant positive change in the rankings of storms for most European countries in the A1B scenario (cf their figures 4, 7(b)). Such a perspective is quite important e.g. for insurance companies. For example, a 5yrl corresponds per definition to 160 events in 800 years in GCM data for 20C, while for a fixed 20C LI

Table 1. Estimates for accumulated probabilities for Core Europe for 1, 2 and 5 year return levels for NCEP (index N), GCM data considering a fixed return level (index RL) and a fixed 20C LI threshold (index LI). The RPs are assessed empirically (eRP) and theoretically (tRP) with uncertainty estimates using the Gaussian error propagation. Additionally the ψ -values are listed. For NCEP 40 winters are considered, for GCM 800 winters, respectively. tRPs estimates longer than 500 years are abbreviated as 500+. Bold and italic: significant shorter estimates compared to the natural climate variability.

	Number of events	num _N	num _{20C}	num _{RL}	num _{LI}	eRP _N	eRP _{20C}	eRP _{RL}	eRP _{LI}	tRP _N	tRP _{20C}	tRP _{RL}	tRP _{LI}
1yrl	—	—	—	—	—	—	—	—	—	$\psi = 0.19$	$\psi = 0.24$	$\psi = 0.20$	$\psi = 0.31$
Events per winter	1+	24	475	479	581	1.67	1.68	1.67	<i>1.38</i>	1.66 ± 0.12	1.69 ± 0.11	1.64 ± 0.10	<i>1.39 ± 0.62</i>
	2+	11	219	212	333	3.6	3.7	3.8	<i>2.4</i>	3.8 ± 0.7	3.8 ± 0.6	3.8 ± 0.5	<i>2.5 ± 1</i>
	3+	3	76	75	145	13	11	11	<i>6</i>	11 ± 3	10 ± 2	11 ± 3	<i>5 ± 5</i>
	4+	2	21	25	60	20	38	32	<i>13</i>	34 ± 15	31 ± 10	38 ± 12	<i>12 ± 12</i>
	5+	—	6	9	25	—	133	89	<i>32</i>	119 ± 69	100 ± 41	146 ± 61	<i>31 ± 31</i>
	6+	—	3	—	8	—	267	—	100	455 ± 322	346 ± 172	500+	<i>83 ± 83</i>
	7+	—	—	—	2	—	—	—	400	500+	500+	500+	236 ± 236
	8+	—	—	—	1	—	—	—	800	500+	500+	500+	500+
	9+	—	—	—	1	—	—	—	800	500+	500+	500+	500+
2yrl	—	—	—	—	—	—	—	—	—	$\psi = 0.04$	$\psi = 0.09$	$\psi = 0.21$	$\psi = 0.3$
Events per winter	1+	15	303	295	417	2.7	2.6	2.7	<i>1.9</i>	2.6 ± 0.7	2.9 ± 0.3	3.1 ± 0.2	<i>2.0 ± 0.2</i>
	2+	3	73	88	171	13	11	9	<i>5</i>	11 ± 7	9 ± 2	9 ± 1	<i>5 ± 3</i>
	3+	1	21	14	47	40	38	57	17	60 ± 60	29 ± 10	25 ± 5	<i>14 ± 14</i>
	4+	1	1	3	9	40	800	267	89	409 ± 409	95 ± 41	72 ± 17	<i>45 ± 45</i>
	5+	—	1	—	3	—	800	—	267	500+	310 ± 169	202 ± 60	149 ± 149
	6+	—	1	—	—	—	800	—	—	500+	500+	500+	500+
5yrl	—	—	—	—	—	—	—	—	—	$\psi = 0.10$	$\psi = 0.02$	$\psi = 0.04$	$\psi = -$
Events per winter	1+	7	144	143	250	5.7	5.6	5.6	3.2	5.8 ± 0.2	6 ± 0.9	6.1 ± 0.8	—
	2+	1	15	16	56	40	53	50	14	43 ± 3	37 ± 11	34 ± 9	—
	3+	—	1	1	8	—	800	800	100	353 ± 37	229 ± 105	187 ± 75	—
	4+	—	—	—	2	—	—	—	400	500+	500+	500+	—

threshold a total of 316 events in 2060–2010 exceed the present 20C RL for Core Europe.

For Core Europe, derived changes in tRP_{RL} are small if few events per winter are considered (table 1, tRP_{20C} versus tRP_{RL}). For more prominent storm series, differences between the two periods are larger (longer RPs for 1yrl, shorter RPs for 2yrl and 5yrl). For individual Core European countries, theoretical estimates of changes for fixed RLs (tRP_{RL}) are mostly coherent between RLs and number of events (figures 3(a)–(c)). For 1yrl and 3+ events, shorter RPs are estimated, except from Benelux and Ireland (figure 3(a)). Further, decreasing RPs are found for the Mediterranean area, Sweden, Lithuania, Latvia, AUTCHESVN and HUNSVK, while longer RPs are identified for Norway, Finland, Estonia, Poland and the Czech Republic. For 2yrl and 2+ events, results are similar: For Core Europe, reduced clustering (longer RPs) is found for Belgium, while for other countries shorter RPs are identified (figure 3(b)). Differences between the 1yrl and the 2yrl are identified only for Sweden and Italy (shorter 1yrl RPs and longer 2yrl RPs; see figures 3(a), (b)). At the 5yrl and 2+ events, theoretical estimations are not possible for most countries. Significances between the estimated RPs were computed with the Kolmogorov–Smirnov test for the whole distributions (supplementary I), but all RP changes are not statistically significant at the 95% confidence level. For the different RLs, ψ -value changes (supplementary F) are in line with RP changes.

The future changes of empirical RPs with a fixed RL (eRP_{RL} , figures 3(d)–(f)) are in most cases similar to those obtained theoretically (figures 3(a)–(c)). However, distinctions between empirical and theoretical RPs are found for some countries. Such differences may occur as the theoretical fit is performed for the whole spectrum of occurrences at a certain RL, while the empirical method only considers a certain number of events per winter. Moreover, estimates for eRP_{RL} are always possible, unlike tRP_{RL} (cf figures 3(c), (f)). Opposite tendencies at the 1yrl are found for Sweden, Finland, Estonia, AUTCHESVN, HUNSVK and The Netherlands (cf figures 3(a), (d)). For the 2yrl, differences only remain for Sweden, AUTCHESVN and France (cf figures 3(b), (e)). For 5yrl and 2+ events shorter RPs are found for most Core Europe countries except for Denmark and Ireland (figure 3(f)). Again, all RP changes are not significant at the 95% confidence level (Kolmogorov–Smirnov test). Generally, all regions with divergent tendencies between the two methods show in fact only marginal RP changes between present and future climate conditions (less than 1 year, supplementary F).

A much more homogeneous pattern of change is found for empirical RPs using fixed 20C LI as threshold (eRP_{LI} , figures 3(g)–(i)). For Core Europe and most individual European countries, the RPs now clearly decrease for the three shown RL. Only for Spain (1yrl and 2yrl), Portugal (2yrl), and Italy (1yrl, 2yrl, and 5yrl) longer RPs are found. Changes estimated theoretically (tRP_{LI}) are similar (supplementary G). These identified differences are significant for Denmark (2yrl), Estonia (1yrl), and Latvia (1yrl) at the 95%

significance level (Kolmogorov–Smirnov test). Detailed information on each country can be found in supplementary F.

In order to gain more insight on the possible changes of RPs due to climate change, the above results are also compared with RP estimates taken from the 505 year long pre-industrial run with constant forcing. This long run permits a quantification of natural inter-decadal climate variability (see, International ad hoc Detection and Attribution Group (IDAG) 2005 for a review), which we define as the range of RPs between the 5th and the 95th percentile for the whole run. These ranges are included in the tables of supplementary E and F (5% PRE, 95% PRE columns both for theoretical and empirical RPs). RP estimates outside of this range indicate significant differences to the pre-industrial climate variability and are marked in bold in these tables. A careful analysis of the data indicates that while estimates at the 1yrl for tRP_{20C} and tRP_{RL} are mostly within the 5th and 95th range of the control run, this is rarely the case for tRP_{LI} estimates. Moreover, while the deviations between PRE and tRP_{20C} as well as tRP_{RL} for high intense series (2yrl, 5yrl; figures 3(b), (c), underlined numbers) are predominantly towards longer RPs, the significant changes for tRP_{LI} are almost always towards shorter RPs (except some Southern European countries, supplementary E and F). Considering the empirical RPs, results are similar but differences between eRP_{RL} and eRP_{LI} are clearer: while for eRP_{20C} and eRP_{RL} almost all estimates are within the 5th and 95th range of the PRE run (figures 3(d)–(f) and supplementary E and F), the eRP_{LI} estimates are often outside this range, displaying shorter RPs for most countries except Southern Europe (figures 3(g)–(i) and supplementary E and F). Therefore, we conclude that the changes identified here for RP_{RL} are mostly probably also within the range of natural climate variability. On the other hand, results for RP_{LI} clearly show shorter RPs, which are mostly outside the range of natural climate variability, as a consequence of the combined effect of changes in clustering and shifts in ranking of top losses.

4. Summary

The main focus of this study is to estimate possible changes in clustering of potential losses associated with windstorms affecting Europe in a changing climate. In particular, possible alterations of RPs of storm series at different RLs are analysed. 40 winters of NCEP data are used as basis to identify historical storm series. Further, GCM ensembles for recent and future climate conditions (20C and A1B scenarios; each 800 years) are considered. Time series of top events (1yrl, 2yrl or 5yrl) are used to estimate RPs associated with multiple events per winter empirically or theoretically (negative binomial distribution). In line with previous results for Germany (Karremann *et al* 2014), overdispersion (clustering) is found for most European countries, and RPs based on NCEP and GCM data are similar for current climate conditions.

Future changes of RPs are estimated for fixed RLs and fixed 20C LI thresholds. The latter approach combines the

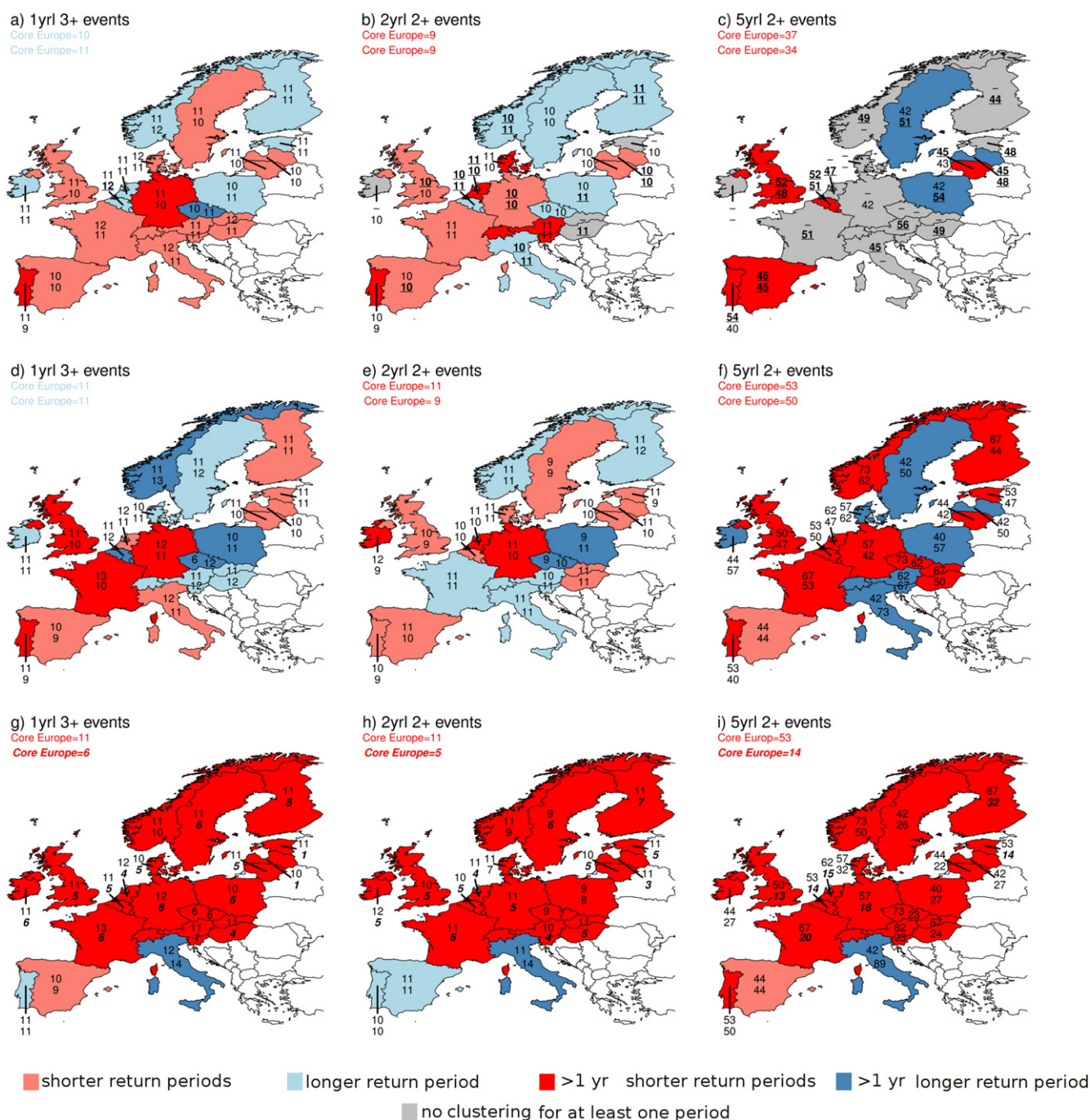


Figure 3. Future changes (2060–2100 minus 1960–2000) of RPs for storm series based on the accumulated events for single regions. Dark blue: increase of more than 1 year. Blue: increase of 0–1 year. Dark red: decrease of more than 1 year. Red: decrease of 0–1 year. Numbers denote the RP for 20C (upper number) and A1B (lower number). In italic and bold: changes, which are significant shorter compared to the natural climate variability. Bold and underlined: changes, which are significant longer compared to the natural climate variability. (a)–(c) RP changes estimated theoretically with a fixed RL (tRP_{RL}). (d)–(f) RP changes estimated empirically with a fixed RL (eRP_{RL}). (g)–(i) RP changes estimated empirically with a fixed 20C LI threshold (eRP_{LI}). For grey regions at least in one of the analysed periods no clustering is found. For more details see text.

effect of clustering and of possible shifts in event ranking in a changing climate, and is thus of particular interest for risk assessment. While changes are small and rather heterogeneous when considering fixed RLs, they are larger and homogeneous for fixed 20C LI thresholds, with clearly shorter RPs for almost all countries except Southern Europe.

However, only very few changes are statistical significant. RP estimates were also tested against the (pre-industrial) natural climate variability. In this case, RP estimates for future climate with fixed 20C LI thresholds typically show shorter RPs for most Central and Northern European countries. These RPs are mostly outside the 5th and 95th percentile range of

variability of a pre-industrial control run, and thus they are beyond the range of natural climate variability. This is not the case for most eRP_{20C} and eRP_{RL} .

5. Discussion and conclusions

Recent results by Pinto *et al* (2013) using the same GCM ensemble suggested that clustering of cyclones affecting Europe may change under future climate conditions, pointing to a decrease over the North Sea area (corresponding to longer RPs) and an increase for Scandinavia (shorter RPs). These results are sometimes partly in contrast with those obtained here for losses associated with extreme cyclones, particularly for 2yrl and 5yrl. These differences may be attributed to two main factors: first, the number of (cyclone) events considered in Pinto *et al* (2013) is much larger (typically about 10 events per year) than the number of loss events analysed here (one event per 1, 2, or 5 years). In fact, the conclusions of Pinto *et al* (2013) are rather in line with present results for lower RLs (1yrl) for Core Europe. Second, climate change signals between events regarding only the meteorological intensity (not considering the population density, MI) and loss events (additionally considering the population density, LI) may show a considerable spread (see discussion on MI and LI in Pinto *et al* 2012). Thus, at least a part of the identified differences may be attributed to the different thresholds concerning the extremes and the different target variables.

While the results for fixed RLs are quite heterogeneous, the changes of RPs are more pronounced for a fixed 20C LI threshold, showing clearly shorter RPs for all countries (except for Mediterranean region). This difference can be explained by the fact that the latter approach also considers the effect of changes of ranks for loss events. This result is in line e.g. with Della-Marta and Pinto (2009), who identified a shortening of return period for intense storms over the North Sea area during the 21st century, documenting a shift of the main storm track area towards the densely populated area of Central Europe. Furthermore, Pinto *et al* (2012) provided evidence that these changes in intense cyclones lead to an increase of top losses over Western Europe and shorter RPs of potential losses. As a consequence, more events exceeding a fixed LI are identified in the second half of the 21st century (e.g. 316 events in A1B instead of 160 in 20C, 5yrl), thus leading to increased clustering and shorter RPs for storm series.

In this study we have used a large ensemble of only one GCM, which is motivated by the focus on statistical robustness of the results rather than on inter-model sensitivity. Further, the changes of synoptic activity in this GCM are close to the CMIP3 ensemble average (Ulbrich *et al* 2008). Hence it can be expected that our results are probably representative for a CMIP3 multi-model ensemble. Future work should focus on earth system models (ESMs) of the CMIP5 ensemble. ESMs incorporate enhanced spatial resolution and additional components of the climate system, which may result in a better representation of mechanisms leading to the clustering of storms. This will also permit a

better estimate of the statistical significance of results based on such large multi-model ensembles, to provide more robust estimates of possible changes of cumulative risks associated with windstorm series affecting Europe.

Acknowledgments

We acknowledge the National Centres for Environmental Prediction/National Centre for Atmospheric Research for the NCEP reanalysis data. We thank the MPI for Meteorology (Hamburg, Germany) and Andreas Sterl from the KNMI (De Bilt, The Netherlands) for providing GCM data. We also thank the Centre for International Earth Science Information Network (CIESIN), Columbia University; and Centro de Agricultura Tropical (CIAT) providing the Gridded population of the World Version3 (GPWv3): Population density grids. Palisades, NY: Socioeconomic Data and Applications Centre (SEDAC), Columbia University. Available online under the following weblink: <http://sedac.ciesin.columbia.edu/gpw> (date of download: 5.4.2012). Furthermore we thank the CRAN-R-project for providing the open-source software package R: R Development Core Team (2011). R: A language and environment for statistical computing. R foundation for statistical computing, Vienna, Austria. ISBN 3-900051-07-0, URL <http://www.R-project.org/>.

References

- Born K, Ludwig P and Pinto J G 2012 Wind gust estimation for mid-European winter storms: towards a probabilistic view *Tellus A* **64** 17471
- Della-Marta P M and Pinto J G 2009 The statistical uncertainty of changes in winter storms over the North Atlantic and Europe in an ensemble of transient climate simulations *Geophys. Res. Lett.* **36** L14703
- Deutsche R 2005 *Sturmdokumentation 1997–2004* (Düsseldorf: Deutsche Rück Reinsurance Company) p 180 in German www.deutsche-rueck.de
- Donat M G, Leckebusch G C, Wild S and Ulbrich U 2011 Future changes of European winter storm losses and extreme wind speeds in multi-model GCM and RCM simulations *Nat. Hazards Earth Syst. Sci.* **11** 1351–70
- Feser F, Barcikowska M, Krueger O, Schank F, Weisse R and Xia L 2014 Storminess over the North Atlantic and Northwestern Europe-A review *Q. J. R. Meteorol. Soc.* doi:10.1002/qj.2364
- Hanley J and Caballero R 2012 Objective identification and tracking of multicentre cyclones in the ERA-interim reanalysis dataset *Q. J. R. Meteorol. Soc.* **138** 612–25
- Haylock M R 2011 European extra-tropical storm damage risk from a multimodel ensemble of dynamically-downscaled global climate models *Nat. Hazards Earth Syst.* **11** 2847–57
- International ad hoc Detection and Attribution Group (IDAG) 2005 Detecting and attributing external influences on the climate system: a review of recent advances *J. Clim.* **18** 1291–314
- Jungclaus J H, Keenlyside N, Botzet M, Haak H, Luo J J, Latif M, Marotzke J, Mikolajewicz U and Roeckner E 2006 Ocean circulation and tropical variability in the coupled model ECHAM5/MPI-OM *J. Clim.* **19** 3952–72
- Karremann M K, Pinto J G, v Bombard P J and Klawa M 2014 On the clustering of winter storm loss events over Germany *Nat. Hazards Earth Syst. Sci.* **14** 2041–52

- Kistler R *et al* 2001 The NCEP/NCAR 50 year reanalysis: monthly means CDROM and documentation *Bull. Am. Meteorol. Soc.* **82** 247–67
- Klawns M and Ulbrich U 2003 A model for the estimation of storm losses and the identification of severe winter storms in Germany *Nat. Hazards Earth Syst. Sci.* **3** 725–32
- Lamb H H 1991 *Historic Storms of the North Sea, British Isles, and Northwest Europe* (Cambridge: Cambridge University Press)
- Mailier P J, Stephenson D B, Ferro C A T and Hodges K I 2006 Serial clustering of extratropical cyclones *Mon. Weather Rev.* **134** 2224–40
- Palutikof J P and Skellern A R 1991 *Storm Severity Over Britain: a Report to Commercial Union General Insurance* (Norwich, UK: Climatic Research Unit, School of Environmental Science, University of East Anglia)
- Pinto J G, Bellenbaum N, Karremann M K and Della-Marta P M 2013 Serial clustering of extratropical cyclones over the North Atlantic and Europe under recent and future climate conditions *J. Geophys. Res.-Atmos.* **118** 12476–85
- Pinto J G, Fröhlich E L, Leckebusch G C and Ulbrich U 2007 Changes in storm loss potentials over Europe under modified climate conditions in an ensemble of simulations of ECHAM5/MPI-OM1 *Nat. Hazards Earth Syst. Sci.* **7** 165–75
- Pinto J G, Karremann M K, Born K, Della-Marta P M and Klawns M 2012 Loss potentials associated with European windstorms under future climate conditions *Clim. Res.* **54** 1–20
- Roeckner E *et al* 2006 Sensitivity of simulated climate to horizontal and vertical resolution in the ECHAM5 atmosphere model *J. Clim.* **19** 3771–91
- Schwierz C, Köllner-Heck P, Zenklusen Mutter E, Bresch D N, Vidale P L, Wild M and Schär C 2010 Modelling European winter wind storm losses in current and future climate *Clim. Change* **101** 485–514
- Sillmann J and Croci-Maspoli M 2009 Present and future atmospheric blocking and its impact on European mean and extreme climate *Geophys. Res. Lett.* **36** L10702
- Sterl A, Severijns C, Dijkstra H, Hazeleger W, van Oldenborgh G J, van den Broeke M, Burgers G, van den Hurk B, van Leeuwen P J and van Velthoven P 2008 When can we expect extremely high surface temperatures? *Geophys. Res. Lett.* **35** L14703
- Taylor K E, Stouffer R J and Meehl G A 2012 An overview of CMIP5 and the experiment design *Bull. Am. Meteorol. Soc.* **93** 485–98
- Ulbrich U, Pinto J G, Kupfer H, Leckebusch G C, Spangehl T and Meyers M 2008 Changing Northern hemisphere storm tracks in an ensemble of IPCC climate change simulations *J. Clim.* **21** 1669–79
- Vitolo R, Stephenson D B, Cook I M and Mitchell-Wallace K 2009 Serial clustering of intense European storms *Meteorol. Z.* **18** 411–24
- Wieringa J 1973 Gust factors over open water and built-up country *Bound.-Layer Meteorol.* **3** 424–41

Supplementary A:

Table S1. List of analysed regions. Names (and their abbreviations) of the regions are given in the 1st column. The numbers in the 2nd column denote the number of grid points of each region in NCEP/GCM. Threshold criteria for the determination of LI are given in the 3rd column.

Analysed region	Number of grid points	Threshold
Core Europe: France, Germany, Ireland, United Kingdom, Denmark, Netherlands, Belgium (Core)	99/95	98 th percentile
Austria, Switzerland, Slovenia (AUTCHESVN)	12/16	9 m/s
Belgium (BEL)	3/5	98 th percentile
Czech Republic (CZE)	8/7	98 th percentile
Denmark (DAN)	11/10	98 th percentile
Estonia (EST)	7/6	98 th percentile
Finland (FIN)	34/35	9 m/s
France (FRA)	33/31	98 th percentile
Germany (GER)	25/22	98 th percentile
Hungary, Slovakia (HUNSVK)	8/12	9 m/s
Ireland (IRL)	7/9	98 th percentile
Italy (ITA)	26/27	9 m/s
Lithuania (LVA)	6/9	98 th percentile
Latvia (LTU)	9/9	98 th percentile
Netherlands (NED)	6/6	98 th percentile
Norway (NOR)	41/44	9 m/s
Poland (POL)	20/23	98 th percentile
Portugal (POR)	8/9	98 th percentile
Spain (ESP)	28/31	9 m/s
Sweden (SWE)	37/39	9 m/s
United Kingdom (UK)	25/27	98 th percentile

Supplementary B:

The methods to estimate LIs presented in Karremann et al. (2014) and general assumptions are described:

A modified version of the loss model by Klawns and Ulbrich (2003) for stations is used to identify individual events of high LI. The occurrence of losses is only possible if a certain threshold is exceeded; here it is the local 98th percentile of the daily maximum wind speed or 9m/s (both named v_{th}). The potential loss rises with the cube of the maximum wind speed, as the kinetic energy flux is proportional to the cube of wind speed. So a strong non-linearity in the wind – loss relation is implied. Insured losses correlate to the sum of insured property values inside the considered region. As real insured property values are not available, the local population density (*POP*) is used as proxy. Gridded wind data is assigned to population density boxes with the nearest neighbor approach. First, calendar day based LIs are estimated by aggregating all grid points exceeding v_{th} weighted with the population density of the considered area. Corresponding to the 72-hour event definition used by insurance companies in reinsurance treaties, overlapping three-day sliding time windows of time series of LI are investigated. The second day of each time window is defined as event when it is a local maximum of LI. For all $LI \neq 0$ two days after an event date is defined as event when no maximum is identified within the three-day window. With this method we preselect the dates we are interested in and storms like “Vivian” and “Wiebke” (26. and 28.02.1990) can be separated. Afterwards more details of the local conditions of the defined dates are investigated. Analogous to the above at each grid point ij the temporal local maximum of a three-day sliding time window (named $max_{3D} \left(\frac{v_{ij}}{v_{thij}} \right)$) is investigated for each event. If $max_{3D} \left(\frac{v_{ij}}{v_{thij}} \right)$ is not at the second day, $\frac{v_{ij}}{v_{thij}}$ of the date is substituted in LI with $max_{3D} \left(\frac{v_{ij}}{v_{thij}} \right)$ of the first or the last day of the three-days. Sometimes event days are only separated by one day (e.g. Vivian and Wiebke). In the case of an identified $max_{3D} \left(\frac{v_{ij}}{v_{thij}} \right)$ between both events (here 27.02.1990), it is assigned to the day with higher $\frac{v_{ij}}{v_{thij}}$. With this method we guarantee that each local maximum only counts ones. Considering only spatial coherent wind fields, larger values occurring not at the second day only replace values of the second day, when multiple spatial contiguous nearby grid points exceed the threshold.

The method to estimate potential losses of single events can be described as:

$$LI = \sum_{ij} \left[max_{3D} \left(\frac{v_{ij}}{v_{thij}} \right) - 1 \right]^3 \cdot POP_{ij} \cdot I(v_{ij}, v_{thij})$$

The advantage of the new definition is that individual storm events can be well separated. Additionally, strong LIs occurring one day before or one day after a defined event, are incorporated in LI as it is probably associated with the same cyclone.

A simple theory describing independent events is the Poisson distribution, which is frequently used by insurance companies to describe the temporal distribution of events at a certain region, and to assess losses of windstorms. This special case of the Binomial distribution is discrete and depending on one parameter. The

rate parameter λ is equal to the variance ($\text{Var}(x)$) and mean ($E(x)$) at once. The probability distribution for a variable x is defined as:

$$P(x) = \frac{\lambda^x e^{-\lambda}}{x!}, \quad x=0,1,2,\dots; E(x) = \lambda = \text{Var}(x)$$

Following Mailier et al. (2006), a simple measure of clustering is the dispersion statistics defined as:

$$\psi = \frac{\text{Var}(X)}{E(X)} - 1$$

If the $\text{Var}(x) > E(x)$ the distribution clusters serial (overdispersion), for $E(x) > \text{Var}(x)$ the distribution is regular (underdispersive) and for $E(x) = \text{Var}(x)$ it is random. Another statistics describing insurance risks is the NBD. The probability of the NBD is defined as (Wilks, 2006):

$$P(x) = \frac{\Gamma(x+k)}{\Gamma(k) \cdot x!} (1-q)^k \cdot q^x$$

with $\Gamma()$ = gamma function, k =auxiliary parameter > 0 (see below), and $0 < q < 1$. $q = 1$ - probability.

Here, $E(x)$ ed as the return level of considered events, therefore q is the only free parameter. The estimation of q is done by a nonlinear least-square estimate using the Gauss-Newton algorithm.

$$\text{Considering } E(x) = \frac{kq}{1-q} \text{ and } \text{Var}(x) = \frac{kq}{(1-q)^2} \Rightarrow k = \frac{(1-q)}{q} \cdot E(x) \text{ (Wilks, 2006)}$$

The dispersion statistics can also be defined as:

$$\psi = \frac{1}{1-q} - 1 \geq 0.$$

The NBD is equal to the Poisson distribution if $q=0$. The higher q , the higher is the clustering of events.

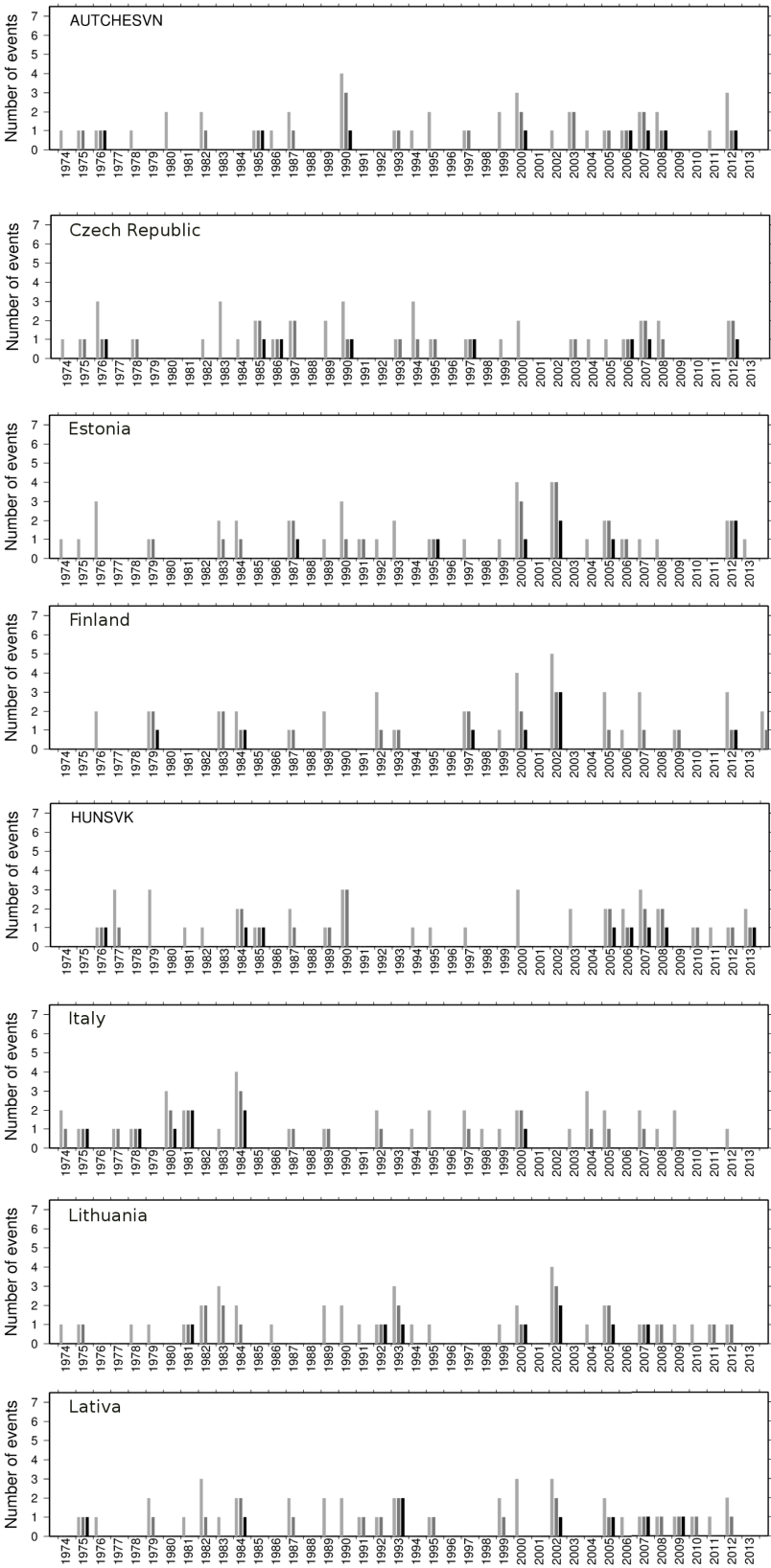
The inverse of the probability is defined as return period (Emanuel and Jagger, 2010). Return periods of storm series consisting of events with a certain return level are estimated by the probability P for x events of certain intensity within one winter.

$$WKP(x) = \frac{1}{P(x)}$$

References:

- Emanuel K and Jagger T 2010 On Estimating Hurricane Return Periods *J. appl. Meteorol. Clim.* **49** 837-844,
- Karremann M K, Pinto J G, v. Bomhard P J and Klawe M 2014 On the Clustering of winter storm loss events over Germany *Nat. Hazards Earth Syst. Sci.* **14** 2041-2052
- Mailier P J, Stephenson D B, Ferro C A T and Hodges K I 2006 Serial Clustering of Extratropical Cyclones *Mon. Weather Rev.* **134** 2224-40
- Wilks D S 2006 *Statistical Methods in the Atmospheric Science* (Second Edition International Geophysics Series Burlington USA) pp 627

Supplementary C:



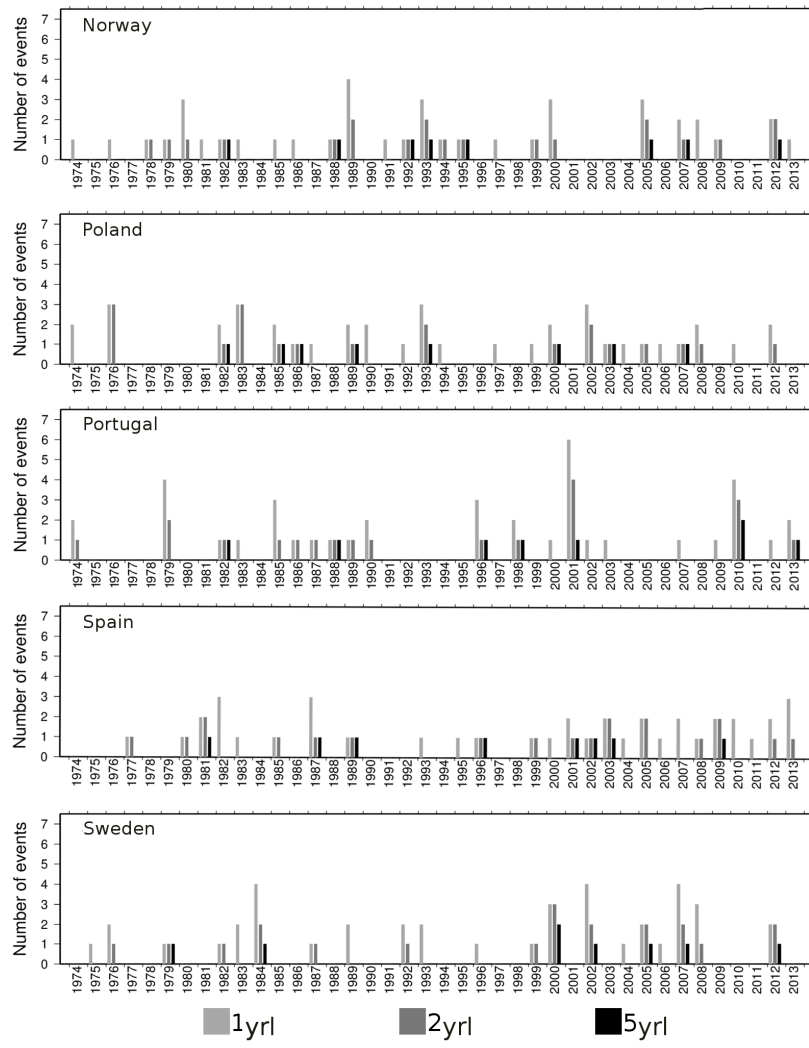


Figure S1. As Figure 1 but for the individual regions outside Core Europe.

Supplementary D:

Table S2. List of identified top 40 events and their return levels for Core Europe. Date is in format yyyyymmdd. The crosses mark events that are also within the top 40 events respective single countries. In the last line, the total number of events, which are common in Core Europe and the respective region, are presented.

Date	Return level	AUTCHESVN	BEL	CZE	DAN	EST	ESP	FIN	FRA	GER	HUNSVK	IRL	ITA	LVA	LTU	NED	NOR	POL	POR	SWE	UK
19740117	2	X	X	X						X						X					X
19760103	5	X	X	X	X					X	X	X				X		X		X	X
19830201	2		X							X			X			X					X
19831127	1		X							X											
19840114	5		X	X	X				X	X						X					X
19840116	1		X													X					X
19840208	1								X		X		X								
19841123	1		X						X	X			X					X			
19860119	2	X		X						X								X			
19861020	2		X	X						X								X			
19861219	2	X	X	X						X	X										
19880209	2											X									X
19900125	5		X		X				X	X						X					X
19900207	2		X		X									X	X	X					X
19900226	5	X	X	X	X	X			X	X	X	X				X		X			X
19900228	2	X	X	X						X	X	X				X		X			
19910105	1									X						X					X
19910108	1		X		X											X					X
19930113	5		X		X				X	X				X	X	X		X			
19930124	2	X	X	X	X					X		X				X		X			X
19931209	1			X						X		X				X					X
19940128	1	X		X						X						X					
19950122	5	X		X		X			X	X				X	X						X
19960207	1						X		X												
19971224	1											X									X
19980104	1								X							X					X
19981226	2				X							X									X
19991203	1				X					X				X	X	X		X			
19991227	2								X	X			X								
20011228	1															X					X
20020128	1			X	X					X	X			X	X			X			X
20020226	1		X													X					
20021027	2	X								X						X		X			X
20040131	1									X			X			X					X
20070118	5	X	X	X					X	X	X	X				X		X			X
20090124	1						X		X												
20090209	1								X												
20100228	1								X	X									X		
20111216	5	X		X					X	X	X		X					X			
20120103	1		X		X							X				X					X
Number of common events		12	19	16	12	2	2	0	15	26	8	10	6	5	5	23	0	15	1	1	23

Supplementary E

Table S3. As Table 1 but with additional information on the estimates based on the Poisson distribution (pRP) as well as the estimates for non-accumulated probabilities (upper numbers; index nac). Furthermore, the information on the 95% significance level of the natural climate variability is included (columns 5% ePRE, 5% tPRE, 95% ePRE and 95% tPRE). In columns eRP_{20C}, eRP_{RL} and eRP_{Ll} events which are significant shorter from natural climate variability are marked in bold. Bold and underlined numbers are significant longer than 95% PRE.

Core Europe

	Number of events	num _N ^{nac} num _N	num _{20C} ^{nac} num _{20C}	num _{RL} ^{nac} num _{RL}	num _{Ll} ^{nac} num _{Ll}	pRP _{nac} pRP	eRP _N ^{nac} eRP _N	eRP _{20C} ^{nac} eRP _{20C}	eRP _{RL} ^{nac} eRP _{RL}	eRP _{Ll} ^{nac} eRP _{Ll}	5% ePRE _{nac} 5% ePRE	95% ePRE _{nac} 95% ePRE	tRP _N ^{nac} tRP _N	tRP _{20C} ^{nac} tRP _{20C}	tRP _{RL} ^{nac} tRP _{RL}	tRP _{Ll} ^{nac} tRP _{Ll}	5% tPRE _{nac} 5% tPRE	95% tPRE _{nac} 95% tPRE
1yrl													ψ=0.19	ψ=0.24	ψ=0.20	ψ=0.31		
Events per winter	1	13	256	267	248	2.72	3.08	3.13	3.00	3.23	2.00	3.64	2.96±0.67	3.04±0.15	2.89±0.17	3.19±0.48	2.77	3.76
	1+	24	475	479	581	1.58	1.67	1.68	1.67	1.376	1.379	1.82	1.66±0.12	1.69±0.11	1.64±0.10	1.39±0.62	1.60	1.93
	2	8	143	137	188	5.4	5.0	5.6	5.9	4.3	4.0	10	5.92±1.59	6.1±1.9	5.8±0.4	4.8±1.1	5.6	7.5
	2+	11	219	212	333	3.8	3.6	3.7	3.8	2.4	3.3	5.0	3.8±0.7	3.8±0.6	3.8±0.4	2.5±1.0	3.8	4.0
	3	1	55	50	85	16	40	15	16	9	8	40	15±8	15.3±2	15.6±2	9±6	15	16.14
	3+	3	76	75	145	12	13	11	11	6	8	20	11±3	10±2	11±3	5±5	8	12
	4	2	15	16	35	65	20	53	50	23	20	-	47±38	44±8	51±10	20±20	33	59
	4+	2	21	25	60	53	20	38	32	13	20	-	34±15	31±10	38±12	12±12	18	47
	5	-	3	9	17	326	-	267	89	47	40	-	162±174	140±35	190±49	49±49	70	266
	5+	-	6	9	25	273	-	133	89	32	40	-	119±69	100±41	146±61	31±31	39	216
	6	-	3	-	6	500+	-	267	-	133	-	-	500+	475±147	500+	128±128	152	500+
	6+	-	3	-	8	500+	-	267	-	100	-	-	455±322	346±172	500+	83±83	86	500+
	7	-	-	-	1	500+	-	-	-	800	-	-	500+	500+	500+	356±356	329	500+
	7+	-	-	-	2	500+	-	-	-	400	-	-	500+	500+	500+	236±236	197	500+
	8	-	-	-	0	500+	-	-	-	-	-	-	500+	500+	500+	500+	716	500+
	8+	-	-	-	1	500+	-	-	-	800	-	-	500+	500+	500+	500+	491	500+
	9	-	-	-	1	500+	-	-	-	800	-	-	500+	500+	500+	500+	500+	500+
	9+	-	-	-	1	500+	-	-	-	800	-	-	500+	500+	500+	500+	500+	500+
2yrl													ψ=0.04	ψ=0.09	ψ=0.21	ψ=0.3		
Events per winter	1	12	230	207	246	3.3	3.3	3.5	3.7	3.3	2.2	4.4	3.4±1.4	4.3±0.2	4.7±0.1	3.3±0.2	3.5	5.1
	1+	15	303	295	417	2.5	2.7	2.6	2.7	1.9	2.1	3.1	2.6±0.7	2.9±0.3	3.1±0.2	2.0±0.2	2.6	3.2
	2	2	52	74	124	13	20	15	11	6	8	40	13±16	13±1	14±1	8±3	13.97	14.2
	2+	3	73	88	171	11	13	11	9	5	8	40	11±7	9±2	9±1	5±3	8.7	10.6
	3	0	20	11	38	79	-	40	73	21	13	-	70±140	42±8	39±4	21±18	37	67
	3+	1	21	14	47	70	40	38	57	17	13	-	60±60	29±10	25±5	14±14	23	56
	4	1	0	3	6	500+	40	-	267	133	-	-	468±1310	137±35	111±15	65±65	96	414
	4+	1	1	3	9	500+	40	800	267	89	40	-	409±409	95±41	72±17	45±45	58	357
	5	-	-	-	3	500+	-	-	-	267	-	-	500+	444±146	312±54	211±211	240	500+
	5+	-	1	-	3	500+	-	800	-	267	-	-	500+	310±169	202±60	149±149	145	500+
	6	-	1	-	-	500+	-	800	-	-	-	-	500+	500+	500+	500+	597	500+
	6+	-	1	-	-	500+	40	800	-	-	-	-	500+	500+	500+	500+	364	500+

5yrl											$\psi=0.10$	$\psi=0.02$	$\psi=0.24$	$\psi=-$				
Events per winter	1	6	129	127	194	6.11	6.7	6.2	6.3	4.1	5.0	8.0	6.7±0.4	7.1±0.6	7.4±0.02	-	6.7	8.2
	1+	7	144	143	250	5.52	5.7	5.6	5.6	3.2	5.0	6.7	5.8±0.2	6.0±0.9	6.1±0.8	-	5.8	6.4
	2	1	14	15	48	61	40	62	53	17	40	-	49±6	44±8	42±7	-	39	49
	2+	1	15	16	56	57	40	53	50	14	40	-	43±3	37±11	34±9	-	30	43
	3	-	1	1	6	500+	-	800	800	133	-	-	399±81	273±77	230±56	-	166	399
	3+	-	1	1	8	500+	-	800	800	100	-	-	353±37	229±105	187±75	-	125	353
	4	-	-	-	2	500+	-	-	-	400	-	-	500+	500+	500+	-	674	500+
4+	-	-	-	2	500+	-	-	-	400	-	-	500+	500+	500+	-	503	500+	

Supplementary F

Tables S4. As Table S3 but only for accumulated probabilities and without uncertainty estimates for tRP.

AUTCHESVN																		
	Number	num _N	num _{2HC}	num _{RL}	num _{LI}	pRP	eRP _N	eRP _{2HC}	eRP _{RL}	eRP _{LI}	5% PRE	95% PRE	tRP _N	tRP _{2HC}	tRP _{RL}	tRP _{LI}	5% PRE	95% PRE
1yrl																		
	1+	25	490	490	793	1.58	1.60	1.63	1.63	1.01	1.43	1.82	ψ=0.04	ψ=0.11	ψ=0.12	ψ=3.5	1.60	1.90
	2+	11	210	220	784	3.8	3.6	3.8	3.6	1.02	3.3	4.4	3.8	3.79	3.78	1.2	3.79	3.9
	3+	3	72	67	751	12	13	11	12	1.07	7	20	12	11	11	1.4	8	12
	4+	1	23	16	707	53	40	35	50	1.1	13	-	47	39	39	1.6	18	46
	5+	-		5	618	273	-	200	160	1.3	40	-	216	155	152	1.8	40	207
Events per winter	6+	-	1	2	524	500+	-	800	400	1.5	40	-	500+	500+	500+	2.2	91	500+
	1+	15	309	306	473	2.5	2.67	2.6	2.6	1.7	2.4	3.1	ψ=0.14	ψ=0.06	ψ=0.07	ψ=0.11	2.6	3.2
	2+	4	78	76	200	11	10	10	11	4	8	20	10	10.6	10.5	4	9	10.7
	3+	1	10	14	61	70	40	80	57	13	20	-	46	57	54	13	23	60
	4+	-	3	3	12	500+	-	267	467	67	40	-	231	361	500+	46	58	409
5yrl	5+	-	-	1	5	500+	-	-	160	160	-	-	500+	500+	500+	187	145	500+
	1+	8	143	147	214	5.5	5.0	5.6	5.4	3.7	5.0	8.0	ψ=-	ψ=0.01	ψ=-	ψ=-	5.8	8.8
	2+	-	13	12	35	57	-	62	67	23	13	-	-	56	-	-	23	43
	3+	-	3	1	4	500+	-	267	800	200	-	-	-	500+	-	-	50	353
	4+	-	1	-	-	500+	-	800	-	-	-	-	-	500+	-	-	102	500+
BEL																		
	Number	num _N	num _{2HC}	num _{RL}	num _{LI}	pRP	eRP _N	eRP _{2HC}	eRP _{RL}	eRP _{LI}	5% PRE	95% PRE	tRP _N	tRP _{2HC}	tRP _{RL}	tRP _{LI}	5% PRE	95% PRE
1yrl																		
	1+	20	490	497	580	1.58	2.00	1.63	1.61	1.38	1.38	1.74	ψ=0.99	ψ=0.12	ψ=0.05	ψ=0.34	1.60	1.84
	2+	10	216	205	325	3.8	4.0	3.7	3.9	2.5	3.1	5.0	4	3.79	3.78	2.5	3.79	3.88
	3+	5	73	66	160	12	8	11	12	5	10	40	8	11.09	11.86	5	9	11.82
	4+	2	13	21	60	53	20	62	38	13	20	-	16	38	46	29	20	47
	5+	1	7	8	27	273	40	114	100	30	40	-	33	150	211	77	47	207
	6+	1	1	3	9	500+	40	800	267	89	-	-	69	500+	500+	212	113	500+
	7+	1	-	-	4	500+	40	-	-	200	-	-	149	500+	500+	500+	283	500+
Events per winter	8+	-	-	-	1	500+	-	-	-	800	-	-	348	500+	500+	500+	500+	500+
	1+	13	305	307	461	2.5	3.1	2.6	2.6	1.7	2.2	2.9	ψ=0.43	ψ=0.09	ψ=0.08	ψ=0.02	2.7	2.9
	2+	3	78	78	172	11	13	10	10	5	8	20	9	10.4	10.5	5	9	10.1
	3+	2	14	15	48	70	20	57	53	17	40	-	29	52	54	16	24	46
	4+	1	3		13	500+	40	267	-	62	-	-	94	301	323	74	64	231
	5+	1	-	-	4	500+	40	-	-	200	-	-	307	500+	500+	405	168	500+
	6+	-	-	-	1	500+	-	-	-	800	-	-	500+	500+	500+	500+	446	500+

Events per winter	5yrl																	
	1+	8	143	143	253	5.5	5	5.6	5.6	3.2	5.0	5.7	$\psi=-$ -	$\psi=0.03$ 5.6	$\psi=0.04$ 5.6	$\psi=-$ -	5.76	5.77
	2+	-	15	16	57	57	-	53	50	14	40	-	-	52	51	-	42	43
	3+	-	2	1	11	500+	-	400	800	73	-	-	-	500+	500+	-	353	354

CZE																		
	Number	num _N	num _{20C}	num _{RL}	num _{LI}	pRP	eRP _N	eRP _{20C}	eRP _{RL}	eRP _{LI}	5% PRE	95% PRE	tRP _N	tRP _{20C}	tRP _{RL}	tRP _{LI}	5% PRE	95% PRE
Events per winter	1yrl												$\psi=0.08$	$\psi=0.29$	$\psi=0.12$	$\psi=0.26$		
	1+	25	470	490	560	1.58	1.6	1.7	1.63	1.43	1.48	2.11	1.62	1.71	1.64	1.45	1.60	2.33
	2+	11	218	222	297	3.8	3.6	3.7	3.6	2.7	3.3	5	3.8	3.81	3.79	2.7	3.79	4.4
	3+	4	82	68	140	12	10	5.71	12	5.71	5.71	20	12	10	11	6	8	12
	4+	-	23	15	43	53	-	35	53	19	20	-	43	28	38	16	13	47
	5+	-	6	4	12	273	-	133	200	67	40	-	182	87	149	43	22	216
	6+	-	1	1	3	500+	-	800	800	267	40	-	500+	283	500+	128	37	500+
Events per winter	2yrl												$\psi=-$	$\psi=0.25$	$\psi=0.09$	$\psi=0.4$		
	1+	16	291	305	366	2.5	2.5	2.8	2.6	2.19	2.22	3.1	-	2.8	2.6	2.4	2.58	3.2
	2+	4	88	78	118	11	10	9	10	6.8	6.7	20	-	10	10	7	9	11
	3+	-	19	15	28	70	-	42	53	29	20	-	-	37	52	20	22	60
	4+	-	1	1	2	500+	-	800	800	400	40	-	-	151	299	60	53	400
	5+	-	1	1	1	500+	-	800	800	800	40	-	-	500+	500+	189	128	500+
Event s per winter	5yrl												$\psi=-$	$\psi=-$	$\psi=-$	$\psi=-$		
	1+	8	147	144	209	5.5	5	5.4	5.6	3.8	5.0	6.7	-	-	-	-	5.8	8.2
	2+	-	11	13	35	57	-	73	62	23	20	-	-	-	-	-	23	43
	3+	-	2	3	6	500+	-	400	267	133	40	-	-	-	-	-	50	353

DAN																		
	Number	num _N	num _{20C}	num _{RL}	num _{LI}	pRP	eRP _N	eRP _{20C}	eRP _{RL}	eRP _{LI}	5% PRE	95% PRE	tRP _N	tRP _{20C}	tRP _{RL}	tRP _{LI}	5% PRE	95% PRE
Events per winter	1yrl												$\psi=1.19$	$\psi=0.06$	$\psi=0.14$	$\psi=-$		
	1+	20	498	486	611	1.58	2.00	1.61	1.65	1.31	1.43	1.91	2.08	1.61	1.65	-	1.60	1.96
	2+	13	202	214	356	3.8	3.1	4.0	3.7	2.3	3.1	5.0	4.0	3.79	3.79	-	3.79	3.9
	3+	6	80	73	164	12	7	10	11	5	7	20	8	11.7	11	-	8	11.8
	4+	1	16	15	67	53	40	50	53	12	13	-	15	44	36	-	17	46
	5+	-	3	5	26	273	-	267	160	31	40	-	29	193	136	-	36	207
	6+	-	1	1	5	500+	-	800	800	160	-	-	60	500+	500+	-	77	500+
	7+	-	-	-	-	500+	-	-	800	800	-	-	-	500+	500+	-	171	500+
	8+	-	-	-	-	500+	-	-	800	800	-	-	-	500+	500+	-	414	500+
	9+	-	-	-	-	500+	-	-	800	800	-	-	-	500+	500+	-	500+	500+
	10+	-	-	-	-	500+	-	-	800	800	-	-	-	500+	500+	-	500+	500+
	11+	-	-	-	-	500+	-	-	800	800	-	-	-	500+	500+	-	500+	500+
	12+	-	-	-	-	500+	-	-	800	800	-	-	-	500+	500+	-	500+	500+

2yrl														ψ=0.74	ψ=0.07	ψ=0.09	ψ=-		
Events per winter	1+	13	305	301	378	2.5	3.1	2.6	2.7	2.1	2.4	3.1	3.2	2.61	2.63	-	2.60	3.2	
	2+	6	72	72	117	11	7	11	11	6.8	6.7	20	9	10.5	10	-	9	10.6	
	3+	1	21	16	24	70	40	38	50	33	20	-	3	55	51	-	23	56	
	4+	-	2	3	7	500+	-	400	267	114	40	-	58	43	295	-	58	357	
	5+	-	-	1	1	500+	-	-	800	800	-	-	145	500+	500+	-	145	500+	
	6+	-	-	-	1	500+	-	-	-	800	-	-	-	500+	500+	-	364	500+	
	7+	-	-	-	1	500+	-	-	-	800	-	-	-	500+	500+	-	500+	500+	
	8+	-	-	-	1	500+	-	-	-	800	-	-	-	500+	500+	-	500+	500+	
	9+	-	-	-	1	500+	-	-	-	800	-	-	-	500+	500+	-	500+	500+	
	10+	-	-	-	1	500+	-	-	-	800	-	-	-	500+	500+	-	500+	500+	
	11	-	-	-	1	500+	-	-	-	800	-	-	-	500+	500+	-	500+	500+	
5yrl													ψ=0.10	ψ=-	ψ=-	ψ=-			
Events per winter	1+	7	145	144	206	6	6	5.5	5.6	4.0	5.0	7.0	5.8	-	-	-	5.8	7	
	2+	1	14	13	25	57	40	57	62	32	20	-	43	-	-	-	26	43	
	3+	-	1	3	5	500+	-	800	267	160	-	-	353	-	-	-	85	353	
ESP																			
	Number	num _N	num _{20C}	num _{RL}	num _{LI}	pRP	eRP _N	eRP _{20C}	eRP _{RL}	eRP _{LI}	5% PRE	95% PRE	tRP _N	tRP _{20C}	tRP _{RL}	tRP _{LI}	5% PRE	95% PRE	
Events per winter	1yrl																		
	1+	26	479	466	453	1.58	1.54	1.67	1.72	1.77	1.43	1.81	ψ=-	ψ=0.22	ψ=0.32	ψ=0.38	1.60	1.87	
	2+	11	219	211	204	3.8	3.6	3.7	3.8	3.9	3.1	5.0	-	3.80	3.82	3.90	3.79	3.91	
	3+	3	82	93	92	12	13	10	9	9	7	40	-	10	10	10	9	12	
	4+	-	18	26	20	53	-	44	31	40	20	-	-	31	27	27	19	46	
	5+	-	2	4	4	273	-	400	200	200	40	-	-	105	79	75	45	207	
6+	-	-	-	-	500+	-	-	-	-	-	-	-	373	243	221	107	500+		
Events per winter	2yrl																		
	1+	16	304	293	275	2.5	2.5	2.6	2.7	2.9	2.1	3.1	ψ=-	ψ=0.09	ψ=0.21	ψ=-	2.7	3.3	
	2+	4	76	84	72	11	10	11	10	11	7	40	-	9.8	10.4	-	9	10.1	
	3+	-	18	22	18	70	-	44	36	44	20	-	-	52	39	-	22	46	
4+	-	2	1	-	500+	-	400	800	-	40	-	-	299	169	-	53	231		
Events per winter	5yrl																		
	1+	8	141	140	137	5.5	5.0	5.67	5.7	5.8	5.0	5.7	ψ=-	ψ=0.08	ψ=0.08	ψ=-	5.76	7.0	
	2+	-	18	18	18	57	-	44	44	44	40	-	-	46	45	-	26	43	
	3+	-	1	2	2	500+	-	800	400	400	-	-	-	431	403	-	85	500+	
4+	-	-	-	-	500+	-	-	-	-	-	-	-	-	500+	500+	-	261	500+	

EST

	Number	num _N	num _{20C}	num _{RL}	num _{LI}	pRP	eRP _N	eRP _{20C}	eRP _{RL}	eRP _{LI}	5% PRE	95% PRE	tRP _N	tRP _{20C}	tRP _{RL}	tRP _{LI}	5% PRE	95% PRE
1yrl													$\psi=0.19$	$\psi=0.19$	$\psi=0.17$	$\psi=2.6$		
Events per winter	1+	24	475	483	786	1.58	1.67	1.68	1.66	1.02	1.43	1.91	1.67	1.67	1.66	1.09	1.59	1.96
	2+	10	194	213	753	3.78	4.0	4.1	3.8	1.06	3.1	5.0	3.8	3.80	3.79	1.2	3.79	4.0
	3+	4	72	75	693	12	10	11	11	1.2	8	20	11	11	11	1.5	8	12
	4+	2	29	20	585	53	20	28	40	1.4	20	-	34	33	35	1.7	17	49
	5+	-	11	5	469	273	-	73	160	1.7	20	-	117	117	125	2.1	36	239
	6+	-	4	2	346	500+	-	200	400	2.3	-	-	443	439	485	2.7	78	500+
	7+	-	3	1	253	500+	-	267	800	3	-	-	500+	500+	500+	3.3	174	500+
	8+	-	3	1	170	500+	-	267	800	5	-	-	500+	500+	500+	4.2	422	500+
	9+	-	3	-	109	500+	-	267	-	7	-	-	500+	500+	500+	5.5	500+	500+
	10+	-	2	-	70	500+	-	400	-	11	-	-	500+	500+	500+	7	500+	500+
	11+	-	2	-	37	500+	-	400	-	22	-	-	500+	500+	500+	9	500+	500+
	12+	-	2	-	22	500+	-	400	-	36	-	-	500+	500+	500+	12	500+	500+
	13+	-	-	-	8	500+	-	-	-	100	-	-	500+	500+	500+	16	500+	500+
	14+	-	-	-	3	500+	-	-	-	267	-	-	500+	500+	500+	22	500+	500+
	15+	-	-	-	1	500+	-	-	-	800	-	-	500+	500+	500+	31	500+	500+
2yrl													$\psi=0.96$	$\psi=-$	$\psi=0.19$	$\psi=0.33$		
Events per winter	1+	12	313	296	402	2.54	3.33	2.56	2.7	2.0	2.2	3.6	3.38	-	2.7	2.1	2.6	3.9
	2+	5	70	85	151	11	8	11	9	5	6	20	8	-	10	5	9	11
	3+	2	14	18	49	70	20	57	44	16	20	-	21	-	41	15	18	56
	4+	1	2	1	11	500+	40	400	800	73	40	-	47	-	185	47	34	357
	5+	-	1	-	3	500+	-	800	-	267	-	-	107	-	500+	151	65	500+
5yrl													$\psi=0.63$	$\psi=-$	$\psi=0.05$	$\psi=-$		
Events per winter	1+	6	142	142	240	5.5	6.7	5.6	5.6	3.3	5.0	6.7	7.0	-	5.7	-	5.8	7.0
	2+	2	15	17	57	57	20	53	47	14	20	-	26	-	48	-	26	43
	3+	-	2	1	11	500+	-	400	800	73	-	-	84	-	500+	-	85	353
	4+	-	1	-	-	500+	-	800	-	-	-	-	261	-	500+	-	261	500+

FIN

	Number	num _N	num _{20C}	num _{RL}	num _{LI}	pRP	eRP _N	eRP _{20C}	eRP _{RL}	eRP _{LI}	5% PRE	95% PRE	tRP _N	tRP _{20C}	tRP _{RL}	tRP _{LI}	5% PRE	95% PRE
1yrl													ψ=1.86	ψ=0.12	ψ=0.11	ψ=0.12		
Events per winter	1+	18	483	490	548	1.58	2.22	1.66	1.63	1.46	1.43	1.74	2.34	1.64	1.63	1.47	1.60	1.85
	2+	13	190	212	259	3.8	3.1	4.2	3.8	3.1	3.1	4.4	4.4	3.79	3.78	3.0	3.79	3.9
	3+	6	71	71	101	12	7	11	11	8	10	40	8	11	11	8	9	12
	4+	2	24	19	33	53	20	33	42	24	40	-	13	38	39	23	20	47
	5+	1	12	6	15	273	40	67	133	53	40	-	23	149	155	81	47	216
	6+	-	4	2	4	500+	-	200	400	200	-	-	41	500+	500+	310	114	500+
	7+	-	4	-	1	500+	-	200	-	800	-	-	74	500+	500+	500+	286	500+
	8+	-	3	-	-	500+	-	267	-	-	-	-	149	500+	500+	500+	776	500+
	9+	-	3	-	-	500+	-	267	-	-	-	-	390	500+	500+	500+	500+	500+
	10+	-	2	-	-	500+	-	400	-	-	-	-	500+	500+	500+	500+	500+	500+
	11+	-	2	-	-	500+	-	400	-	-	-	-	500+	500+	500+	500+	500+	500+
	12+	-	2	-	-	500+	-	400	-	-	-	-	500+	500+	500+	500+	500+	500+
2yrl					-								ψ=0.41	ψ=0.05	ψ=0.05	ψ=0.29		
Events per winter	1+	14	308	305	368	2.5	2.9	2.6	2.6	2.18	2.2	2.9	2.9	2.59	2.56	2.3	2.6	3.1
	2+	5	74	69	110	11	8	11	12	7	8	20	9	10.64	10.67	7	9	10.58
	3+	1	17	15	24	70	40	47	53	33	40	-	30	58	59	22	24	56
	4+	-	1	8	10	500+	-	800	100	80	-	-	98	375	389	76	54	357
	5+	-	-	2	2	500+	-	-	400	400	-	-	325	500+	500+	277	168	500+
	6+	-	-	1	1	500+	-	-	800	800	-	-	500+	500+	500+	500+	446	500+
5yrl													ψ=0.39	ψ=-	ψ=0.09	ψ=-		
Events per winter	1+	6	145	139	170	5.52	6.67	5.5	5.76	4.7	5.0	5.7	6.4	-	5.70	-	5.76	5.77
	2+	1	12	18	25	57	40	67	44	32	40	-	30	-	44	-	42	43
	3+	1	3	3	5	500+	40	267	267	160	-	-	125	-	376	-	353	353
	4+	-	-	-	1	500+	-	-	-	1	-	-	500+	-	500+	-	500+	500+

FRA

	Number	num _N	num _{20C}	num _{RL}	num _{LI}	pRP	eRP _N	eRP _{20C}	eRP _{RL}	eRP _{LI}	5% PRE	95% PRE	tRP _N	tRP _{20C}	tRP _{RL}	tRP _{LI}	5% PRE	95% PRE
1yrl													ψ=-	ψ=0.06	ψ=0.10	ψ=0.17		
Events per winter	1+	26	496	490	569	1.58	1.54	1.61	1.63	1.41	1.38	1.90	-	1.61	1.63	1.43	1.59	1.92
	2+	10	210	194	287	3.8	4.0	3.8	4.1	3.0	3.1	5	-	3.79	3.78	2.8	3.79	3.95
	3+	2	64	80	124	12	20	13	10	6	7	20	-	11.7	11	7	8	12.1
	4+	1	21	25	40	53	40	38	32	20	13	-	-	45	40	18	18	49
	5+	1	6	4	12	273	40	133	200	67	40	-	-	200	161	55	39	239
	6+	-	3	3	4	500+	-	267	267	200	-	-	-	500+	500+	187	87	500+
	7+	-	-	-	2	500+	-	-	-	400	-	-	-	500+	500+	500+	200	500+
	8+	-	-	-	2	500+	-	-	-	400	-	-	-	500+	500+	500+	500	500+
	9+	-	-	-	1	500+	-	-	-	800	-	-	-	500+	500+	500+	500+	500+

2yrl Events per winter	1+	16	308	307	397	2.5	2.5	2.6	2.6	2.0	2.2	3.1	$\psi=-$ -	$\psi=0.04$ 2.60	$\psi=0.05$ 2.58	$\psi=0.23$ 2.2	2.58	3.4
	2+	3	72	71	135	11	13	11	11	6	8	20	-	10.72	10.70	6	8.6	10.73
	3+	1	16	14	37	70	40	50	57	22	20	-	-	59	59	19	21	60
	4+	-	4	4	8	500+	-	200	200	100	40	-	-	403	400	67	47	409
	5+	-	-	2	3	2.54	-	-	400	267	-	-	-	500+	500+	254	107	500+
	6+	-	-	2	2	11	-	-	400	400	-	-	-	500+	500+	500+	241	500+
5yrl Events per winter	1+	7	147	142	227	5.5	5.7	5.4	5.6	3.5	5.0	6.7	$\psi=0.10$ 5.8	$\psi=-$ -	$\psi=0.03$ 5.6	$\psi=-$ -	5.8	6.4
	2+	1	12	15	41	57	40	67	53	20	40	-	43	-	51	-	30	43
	3+	-	1	3	9	500+	-	800	267	89	40	-	353	-	500+	-	125	353
	4+	-	-	-	1	500+	-	-	-	800	-	-	500+	-	500+	-	503	500+
GER																		
1yrl Events per winter	Number	num _N	num _{20C}	num _{RL}	num _{LI}	pRP	eRP _N	eRP _{20C}	eRP _{RL}	eRP _{LI}	5% PRE	95% PRE	tRP _N	tRP _{20C}	tRP _{RL}	tRP _{LI}	5% PRE	95% PRE
	1+	25	493	474	559	1.58	1.6	1.62	1.69	1.43	1.38	1.90	$\psi=-$ -	$\psi=0.09$ 1.62	$\psi=0.24$ 1.69	$\psi=0.33$ 1.44	1.61	1.96
	2+	12	214	219	305	3.8	3.3	3.7	3.7	2.6	2.9	4.4	-	3.79	3.81	2.6	3.78	4.0
	3+	2	68	76	143	12	20	12	11	6	7	40	-	11	10	6	8	12
	4+	1	17	18	52	53	40	47	44	15	20	-	-	41	30	13	17	45
	5+	-	5	9	17	273	-	160	89	47	40	-	-	171	98	34	36	205
	6+	-	2	1	7	500+	-	400	800	114	40	-	-	500+	337	93	76	500+
	7+	-	1	1	3	500+	-	800	800	267	40	-	-	500+	500+	261	169	500+
	8+	-	-	1	1	500+	-	-	800	800	-	-	-	500+	500+	500+	406	500+
	9+	-	-	1	1	500+	-	-	800	800	-	-	-	500+	500+	500+	500+	500+
	10+	-	-	-	1	500+	-	-	-	800	-	-	-	500+	500+	500+	500+	500+
	11+	-	-	-	1	500+	-	-	-	800	-	-	-	500+	500+	500+	500+	500+
	12+	-	-	-	1	500+	-	-	-	800	-	-	-	500+	500+	500+	500+	500+
2yrl Events per winter	1+	16	299	301	397	2.5	2.5	2.7	2.7	2.0	2.2	3.3	$\psi=-$ -	$\psi=0.12$ 2.65	$\psi=0.12$ 2.66	$\psi=0.34$ 2.1	2.68	3.72
	2+	3	74	79	152	11	13	11	10	5	7	20	-	10.23	10.18	6	8.6	10.10
	3+	1	19	18	39	70	40	42	44	21	20	-	-	48	47	16	18	46
	4+	-	6	2	8	500+	-	133	400	100	40	-	-	259	248	50	37	231
	5+	-	1	-	2	500+	-	800	-	400	-	-	-	500+	500+	161	73	500+
	6+	-	1	-	1	500+	-	800	-	800	-	-	-	500+	500+	500+	144	500+
5yrl Events per winter	1+	6	145	138	226	5.5	7	5.5	5.8	3.5	5.0	6.7	$\psi=0.39$ 6.4	$\psi=-$ -	$\psi=0.11$ 5.0	$\psi=-$ -	5.76	6.95
	2+	1	14	19	44	57	40	57	42	18	40	-	30	-	42	-	23	43
	3+	1	1	2	5	500+	40	800	400	160	40	-	125	-	330	-	54	353
	4+	-	-	1	1	500+	-	-	800	800	-	-	500+	-	500+	-	121	500+

HUNSVK																		
	Number	num _N	num _{20C}	num _{RL}	num _{LI}	pRP	eRP _N	eRP _{20C}	eRP _{RL}	eRP _{LI}	5% PRE	95% PRE	tRP _N	tRP _{20C}	tRP _{RL}	tRP _{LI}	5% PRE	95% PRE
1yrl Events per winter	1+	23	499	496	621	1.58	1.74	1.60	1.61	1.29	1.38	1.81	ψ=0.44	ψ=0.06	ψ=0.08	ψ=0.34	1.59	1.95
	2+	12	209	222	396	3.8	3.3	3.8	3.6	2.0	3.1	5.0	3.8	3.79	3.78	2.2	3.79	3.96
	3+	5	74	68	184	12	8	11	12	4	8	40	9	11.7	11	4	8	11.9
	4+	-	16	11	75	53	-	50	73	11	20	-	24	45	42	9	17	47
	5+	-	2	3	31	273	-	400	267	26	40	-	63	200	176	21	37	216
	6+	-	-	-	12	500+	-	-	-	67	-	-	176	500+	500+	53	80	500+
	7+	-	-	-	3	500+	-	-	-	267	-	-	500+	500+	500+	139	181	500+
2yrl Events per winter													ψ=0.41	ψ=-	ψ=0.05	ψ=0.11		
	1+	15	320	309	423	2.5	2.9	2.5	2.6	1.9	2.2	3.1	3.0	-	2.6	1.9	2.7	3.2
	2+	5	70	75	153	11	8	11	11	5	8	40	9	-	11	5	9	10
	3+	1	9	14	38	70	40	89	57	21	20	-	30	-	58	19	23	46
	4+	-	1	2	7	500+	-	800	400	114	-	-	325	-	387	80	58	231
	5+	-	-	-	1	500+	-	-	-	800	-	-	500+	-	500+	380	145	500+
5yrl Event s per winter													ψ=-	ψ=-	ψ=0.04	ψ=-		
	1+	8	147	142	201	5.5	5	5.4	5.6	4.0	5.0	6.7	-	-	5.6	-	5.8	7.0
	2+	-	12	16	34	57	-	67	50	24	20	-	-	-	49	-	26	43
	3+	-	1	2	6	500+	-	800	400	133	40	-	-	-	500+	-	85	353
IRL																		
	Number	num _N	num _{20C}	num _{RL}	num _{LI}	pRP	eRP _N	eRP _{20C}	eRP _{RL}	eRP _{LI}	5% PRE	95% PRE	tRP _N	tRP _{20C}	tRP _{RL}	tRP _{LI}	5% PRE	95% PRE
1yrl Events per winter	1+	23	486	486	573	1.58	1.74	1.65	1.65	1.40	1.43	1.82	ψ=0.35	ψ=0.16	ψ=0.16	ψ=0.23	1.60	1.87
	2+	11	222	224	308	3.8	3.6	3.6	3.6	2.6	3.1	5	3.8	3.79	3.79	2.7	3.79	3.9
	3+	3	73	70	141	12	13	11	11	6	8	40	10	11	11	6	9	12
	4+	3	15	18	46	53	13	53	44	17	13	-	26	35	35	15	20	47
	5+	-	4	2	7	273	-	200	400	114	40	-	76	129	130	42	45	216
	6+	-	-	-	3	500+	-	-	-	267	-	-	234	500+	500+	128	108	500+
2yrl Events per winter													ψ=-	ψ=-	ψ=0.16	ψ=0.35		
	1+	16	319	300	392	2.5	2.5	2.5	2.7	2.0	2.2	3.1	-	-	2.69	2.2	2.6	3.72
	2+	2	67	85	148	11	20	12	9	5	8	40	-	-	10	6	9	11
	3+	1	11	14	36	70	40	73	57	22	13	-	-	-	44	17	18	56
	4+	2	3	1	8	500+	40	267	800	100	40	-	-	-	213	51	37	357
	5+	-	-	-	-	500+	-	-	-	-	-	-	-	-	500+	162	73	500+
5yrl Event s per winter Event s per													ψ=-	ψ=-	ψ=-	ψ=-		
	1+	8	141	146	189	5.52	5	5.7	5.5	4.2	5.0	6.7	-	-	-	-	5.8	8.2
	2+	-	18	14	30	57	-	44	57	27	20	-	-	-	-	-	23	43
	3+	-	1	-	1	500+	-	800	-	800	40	-	-	-	-	-	54	353

ITA

	Number	num _N	num _{20C}	num _{RL}	num _{LI}	pRP	eRP _N	eRP _{20C}	eRP _{RL}	eRP _{LI}	5% PRE	95% PRE	tRP _N	tRP _{20C}	tRP _{RL}	tRP _{LI}	5% PRE	95% PRE
1yrl Events per winter	1+	24	496	491	464	1.58	1.67	1.61	1.63	1.72	1.43	1.82	ψ=0.21	ψ=0.05	ψ=0.11	ψ=-	1.60	1.93
	2+	12	202	214	177	3.8	3.3	4.0	3.8	4.5	3.1	5	3.8	3.79	3.78	-	3.79	3.95
	3+	3	68	71	56	12	13	12	11	14	8	20	11	11.8	11	-	8	11.9
	5+	1	22	22	17	53	40	36	36	47	20	-	32	45	39	-	18	47
	5+	-	9	2	1	273	-	89	400	800	40	-	109	205	156	-	39	216
	6+	-	3	-	-	500+	-	267	-	-	40	-	396	500+	500+	-	86	500+
2yrl Events per winter	1+	15	302	311	285	2.5	2.7	2.7	2.6	2.8	2.4	2.9	ψ=0.14	ψ=0.09	ψ=0.02	ψ=-	2.68	2.99
	2+	4	75	71	59	11	10	11	11	14	7	20	10	10.36	11	-	9	10.1
	3+	1	12	17	13	70	40	67	47	62	40	-	46	51	64	-	24	46
	5+	-	6	1	1	500+	-	133	800	800	40	-	231	292	476	-	66	231
	5+	-	3	-	-	500+	-	267	-	-	-	-	500+	500+	500+	-	179	500+
	6+	-	2	-	-	500+	-	400	-	-	-	-	-	500+	500+	-	485	500+
5yrl Events per winter	1+	6	141	149	137	5.5	6.7	5.7	5.4	5.8	5.0	8.0	ψ=0.63	ψ=0.08	ψ=-	ψ=-	5.76	8.2
	2+	2	19	11	9	57	20	42	73	89	20	-	26	45	-	-	23	43
	3+	-	-	-	-	500+	-	-	-	-	40	-	85	402	-	-	54	353
	5+	-	-	-	-	500+	-	-	-	-	-	-	261	500+	-	-	121	500+

LTU

	Number	num _N	num _{20C}	num _{RL}	num _{LI}	pRP	eRP _N	eRP _{20C}	eRP _{RL}	eRP _{LI}	5% PRE	95% PRE	tRP _N	tRP _{20C}	tRP _{RL}	tRP _{LI}	5% PRE	95% PRE
1yrl Events per winter	1+	27	488	473	582	1.58	1.48	1.64	1.69	1.37	1.48	1.82	ψ=-	ψ=0.13	ψ=0.26	ψ=0.34	1.60	1.85
	2+	9	206	216	339	3.8	4.4	3.9	3.7	2.4	3.3	5	-	3.79	3.80	2.5	3.79	3.9
	3+	3	76	83	159	12	13	11	10	5	7	20	-	11	10	5	9	12
	4+	1	24	23	64	53	40	33	35	13	20	-	-	38	29	11	20	47
	5+	-	5	4	19	273	-	160	200	42	40	-	-	146	93	28	47	216
	6+	-	1	1	7	500+	-	800	800	114	-	-	-	500+	311	73	114	500+
	7+	-	-	-	2	500+	-	-	-	400	-	-	-	500+	500+	197	286	500+
2yrl Events per winter	1+	14	301	300	432	2.5	2.9	2.7	2.7	1.9	2.2	2.9	ψ=0.4	ψ=0.14	ψ=0.15	ψ=0.23	2.60	3.2
	2+	5	82	82	167	11	8	10	10	5	7	20	9	10	10	5	9	11
	3+	1	15	17	59	70	40	53	47	14	20	-	30	46	45	14	23	56
	4+	-	2	1	18	500+	-	400	800	44	-	-	98	234	224	47	58	357
	5+	-	-	-	2	500+	-	-	-	400	-	-	327	500+	500+	166	145	500+
5yrl Events per winter	1+	7	140	139	206	5.5	5.7	5.7	5.8	3.9	5.0	6.7	ψ=0.1	ψ=0.08	ψ=0.10	ψ=-	5.76	6.95
	2+	1	18	19	36	57	40	44	42	22	20	-	43	45	42.75	-	26	42.77
	3+	-	2	2	4	500+	-	400	400	200	-	-	353	403	352.7	-	85	353.1
	4+	-	-	-	-	500+	-	-	-	-	-	-	500+	500+	500+	-	261	500+

LVA

	Number	num _N	num _{20C}	num _{RL}	num _{LI}	pRP	eRP _N	eRP _{20C}	eRP _{RL}	eRP _{LI}	5% PRE	95% PRE	tRP _N	tRP _{20C}	tRP _{RL}	tRP _{LI}	5% PRE	95% PRE
1yrl													ψ=0.07	ψ=0.20	ψ=0.27	ψ=3.57		
Events per winter	1+	25	478	469	793	1.58	1.6	1.67	1.71	1.01	1.43	1.91	1.61	1.67	1.70	1.09	1.60	1.95
	2+	12	205	206	779	3.8	3.3	3.9	3.9	1.03	3.3	5.0	3.3	3.80	3.81	1.2	3.79	4.0
	3+	3	77	81	738	12	13	10	10	1.08	7	20	12	10	10	1.4	8	12
	4+	-	28	31	685	53	-	29	26	1.17	13	-	43	33	29	1.6	17	47
	5+	-	9	10	605	273	-	89	80	1.3	40	-	189	114	90	1.8	37	216
	6+	-	3	3	509	500+	-	267	267	1.6	40	-	500+	421	298	2.2	79	500+
	7+	-	-	-	411	500+	-	-	-	2	-	-	500+	500+	500+	2.6	178	500+
	8+	-	-	-	295	500+	-	-	-	3	-	-	500+	500+	500+	3.1	435	500+
	9+	-	-	-	209	500+	-	-	-	4	-	-	500+	500+	500+	4	500+	500+
	10+	-	-	-	152	500+	-	-	-	5	-	-	500+	500+	500+	5	500+	500+
	11+	-	-	-	80	500+	-	-	-	10	-	-	500+	500+	500+	6	500+	500+
	12+	-	-	-	52	500+	-	-	-	15	-	-	500+	500+	500+	7	500+	500+
	13+	-	-	-	37	500+	-	-	-	22	-	-	500+	500+	500+	9	500+	500+
	14+	-	-	-	20	500+	-	-	-	40	-	-	500+	500+	500+	12	500+	500+
	15+	-	-	-	8	500+	-	-	-	100	-	-	500+	500+	500+	15	500+	500+
2yrl													ψ=-	ψ=0.07	ψ=0.25	ψ=0.24		
Events per winter	1+	17	306	288	511	2.5	2.4	2.6	2.8	1.6	2.2	3.3	-	2.6	2.8	1.6	2.68	2.69
	2+	3	76	83	241	11	13	11	10	3	8	20	-	10	10	3.3	8.63	8.65
	3+	-	15	25	100	70	-	53	32	8	20	-	-	54	37	8	19.6	19.7
	4+	-	3	3	38	500+	-	267	267	21	40	-	-	329	147	23	43	45
	5+	-	-	1	13	500+	-	-	800	62	40	-	-	500+	500+	68	92	95
	6+	-	-	-	3	500+	-	-	-	267	-	-	-	500+	500+	223	201	500+
5yrl													ψ=0.10	ψ=0.08	ψ=0.05	ψ=-		
Events per winter	1+	7	141	141	178	5.5	5.7	5.7	5.7	4.5	5.0	6.7	5.8	5.7	5.7	-	5.8	8.2
	2+	1	19	16	30	57	40	42	50	27	20	-	43	45	48	-	23	43
	3+	-	-	3	6	500+	-	-	267	133	40	-	353	402	500+	-	54	353
	4+	-	-	-	-	500+	-	-	-	-	-	-	500+	500+	500+	-	121	500+

NED

	Number	num _N	num _{20C}	num _{RL}	num _{LI}	pRP	eRP _N	eRP _{20C}	eRP _{RL}	eRP _{LI}	5% PRE	95% PRE	tRP _N	tRP _{20C}	tRP _{RL}	tRP _{LI}	5% PRE	95% PRE
1yrl													ψ=0.21	ψ=0.14	ψ=0.13	ψ=0.34		
Events per winter	1+	24	488	487	603	1.58	1.67	1.64	1.64	1.33	1.43	1.74	1.68	1.64	1.64	1.36	1.60	1.77
	2+	12	221	212	338	3.8	3.3	3.6	3.8	2.4	3.4	5.7	3.8	3.79	3.79	2.3	3.79	3.84
	3+	3	69	71	178	12	13	12	11	4	7	20	10	11	11	5	9	12
	4+	1	17	18	69	53	40	47	44	12	20	-	32	37	37	10	24	47
	5+	-	4	6	27	273	-	200	133	30	40	-	109	141	144	25	64	216
	6+	-	1	5	10	500+	-	800	160	80	-	-	396	500+	500+	63	176	500+
	7+	-	-	1	4	500+	-	-	800	200	-	-	500+	500+	500+	169	511	500+
	8+	-	-	-	3	500+	-	-	-	267	-	-	500+	500+	500+	467	500+	500+
	9+	-	-	-	1	500+	-	-	-	800	-	-	500+	500+	500+	500+	500+	500+

Events per winter	2yrl												$\psi=0.41$	$\psi=0.05$	$\psi=0.08$	$\psi=0.15$		
	1+	14	309	306	448	2.5	2.9	2.6	2.6	1.8	2.2	2.9	2.9	2.6	2.6	1.8	2.7	3.1
	2+	5	76	78	178	11	8	11	10	4	7	20	9	<u>11</u>	<u>10.4</u>	5	9	10.1
	3+	1	13	15	53	70	40	62	53	15	40	-	30	<u>58</u>	<u>53</u>	14	25	45
	4+	-	2	1	15	500+	-	400	800	53	-	-	100	<u>377</u>	<u>311</u>	51	72	231
	5+	-	-	-	6	500+	-	-	-	133	-	-	325	500+	500+	205	202	500+
	6+	-	-	-	4	500+	-	-	-	200	-	-	-	500+	500+	500+	570	500+
Events per winter	5yrl												$\psi=0.39$	$\psi=-$	$\psi=0.06$	$\psi=-$		
	1+	6	145	141	253	5.5	6.7	5.5	5.7	3.2	5.0	7.0	6.4	-	5.7	-	5.8	7.0
	2+	1	13	17	54	57	40	62	47	15	20	-	30	-	47	-	26	43
	3+	-	2	2	9	500+	40	400	400	89	-	-	125	-	<u>465</u>	-	85	353
	4+	-	-	-	-	500+	-	-	-	-	-	-	500+	-	500+	-	261	500+

NOR

	Number	num _N	num _{20C}	num _{RL}	num _{LI}	pRP	eRP _N	eRP _{20C}	eRP _{RL}	eRP _{LI}	5% PRE	95% PRE	tRP _N	tRP _{20C}	tRP _{RL}	tRP _{LI}	5% PRE	95% PRE
Events per winter	1yrl												$\psi=-$	$\psi=0.09$	$\psi=0.06$	$\psi=0.1$		
	1+	26	492	495	530	1.58	1.54	1.63	1.62	1.51	1.38	1.90	-	1.63	1.61	1.51	1.60	1.94
	2+	8	210	215	263	3.8	5.0	3.8	3.7	3.0	2.9	5	-	3.79	3.78	3.2	3.79	3.96
	3+	5	71	62	77	12	8	11	13	10	7	20	-	11	11.6	9	8	11.8
	4+	1	19	18	29	53	40	42	44	28	20	-	-	41	44	28	17	46
	5+	-	5	7	9	273	-	160	114	89	40	-	-	166	191	105	36	207
	6+	-	3	3	3	500+	-	267	267	267	40	-	-	500+	500+	437	79	500+
	7+	-	-	-	1	500+	-	-	-	800	-	-	-	500+	500+	500+	177	500+
Events per winter	2yrl												$\psi=-$	$\psi=0.12$	$\psi=0.03$	$\psi=0.6$		
	1+	16	299	309	341	2.5	2.5	2.7	2.6	2.4	2.1	3.1	-	2.66	2.6	2.70	2.68	3.5
	2+	4	76	70	93	11	10	11	11	9	7	40	-	<u>10.2</u>	<u>11</u>	7	9	10.1
	3+	-	16	17	23	70	-	50	47	35	40	-	-	47	62	20	20	46
	4+	-	4	3	5	500+	-	200	267	160	40	-	-	249	448	53	44	231
	5+	-	3	1	2	500+	-	267	800	400	-	-	-	500+	500+	143	210	500+
	6+	-	2	-	1	500+	-	400	-	800	-	-	-	500+	500+	382	470	500+
Events per winter	5yrl												$\psi=-$	$\psi=0.05$	$\psi=-$	$\psi=-$		
	1+	8	137	144	168	5.5	5	5.9	5.6	4.8	5.0	7.0	-	5.6	-	-	5.8	7.0
	2+	-	11	13	16	57	-	73	62	50	20	-	-	49	-	-	26	43
	3+	-	4	2	3	500+	-	200	400	267	-	-	-	500+	-	-	85	353
	4+	-	-	1	1	500+	-	-	800	800	-	-	-	500+	-	-	261	500+

POL

	Number	num _N	num _{20C}	num _{RL}	num _{LI}	pRP	eRP _N	eRP _{20C}	eRP _{RL}	eRP _{LI}	5% PRE	95% PRE	tRP _N	tRP _{20C}	tRP _{RL}	tRP _{LI}	5% PRE	95% PRE
1yrl													ψ=0.23	ψ=0.20	ψ=0.12	ψ=0.24		
Events per winter	1+	24	478	489	548	1.58	1.67	1.67	1.64	1.46	1.38	1.90	1.69	1.67	1.64	1.47	1.59	1.95
	2+	12	205	216	290	3.8	3.0	3.9	3.7	2.8	3.3	5.0	3.8	3.8	3.8	2.9	3.79	3.96
	3+	4	79	70	125	12	10	10	11	6	7	40	10	10	11	7	8	12
	4+	-	29	17	37	53	-	28	47	22	20	-	3	33	38	17	17	48
	5+	-	5	6	9	273	-	160	133	89	40	-	100	11	148	50	37	227
	6+	-	3	2	3	500+	-	267	400	267	-	-	343	411	500+	155	80	500+
	1+	-	1	-	-	1.58	-	800	-	-	-	-	500+	500+	500+	500+	181	500+
2yrl													ψ=0.33	ψ=0.21	ψ=0.04	ψ=0.28		
Events per winter	1+	14	293	310	366	2.5	2.9	2.7	2.6	2.2	2.2	3.1	2.9	2.8	2.6	2.3	2.7	3.48
	2+	4	85	75	106	11	10	9	11	8	7	20	9	10	11	7	9	10.1
	3+	2	19	15	27	70	20	42	53	30	20	-	33	39	59	23	18	46
	4+	-	2	-	6	500+	-	400	-	133	40	-	118	168	401	79	5	231
	5+	-	1	-	2	500+	-	800	-	400	-	-	435	500+	500+	292	67	500+
	6+	-	-	-	1	500+	-	-	-	800	-	-	500+	500+	500+	500+	128	500+
	1+	-	-	-	-	500+	-	-	-	-	-	-	-	-	-	-	-	-
5yrl													ψ=-	ψ=0.11	ψ=0.02	ψ=-		
Events per winter	1+	8	139	143	183	5.5	5.0	5.8	5.6	4.4	5.0	8.0	-	5.79	5.6	-	5.76	8.2
	2+	-	20	14	30	57	-	40	57	27	20	-	-	42	54	-	23	43
	3+	-	1	3	7	500+	-	800	267	114	40	-	-	332	500+	-	54	353
	4+	-	-	-	-	500+	-	-	-	-	-	-	-	500+	500+	-	121	500+

POR

	Number	num _N	num _{20C}	num _{RL}	num _{LI}	pRP	eRP _N	eRP _{20C}	eRP _{RL}	eRP _{LI}	5% PRE	95% PRE	tRP _N	tRP _{20C}	tRP _{RL}	tRP _{LI}	5% PRE	95% PRE
1yrl													ψ=0.71	ψ=0.004	ψ=0.49	ψ=0.54		
Events per winter	1+	21	486	448	424	1.58	1.9	1.65	1.79	1.89	1.33	1.82	1.89	1.65	1.80	1.93	1.60	2.02
	2+	9	211	218	202	3.8	4.4	3.8	3.7	4.0	3.6	5.7	3.9	3.79	6.9	4.3	3.79	4.0
	3+	5	76	88	72	12	8	11	9	11	6	40	8	11	9	10	8	12
	4+	3	21	31	24	53	13	38	26	33	20	-	19	36	22	25	16	47
	5+	1	4	11	10	273	40	200	73	80	40	-	42	134	58	64	32	216
	6+	1	2	4	2	500+	40	400	200	400	-	-	97	500+	154	164	66	500+
	1+	-	-	-	-	500+	-	-	-	-	-	-	-	-	-	-	-	-
2yrl													ψ=0.22	ψ=0.006	ψ=0.34	ψ=-		
Events per winter	1+	14	302	283	256	2.5	2.9	2.7	2.8	3.13	2.1	3.07	2.8	2.7	2.9	-	2.6	3.5
	2+	3	82	91	80	11	13	10	9	10	8	40	8	10	9.4	-	8.6	11
	3+	2	15	23	18	70	20	53	35	44	20	-	39	47	32	-	20	56
	4+	1	1	3	3	500+	40	800	267	267	-	-	165	243	116	-	43	357
5yrl													ψ=0.10	ψ=0.0004	ψ=0.13	ψ=-		
Events per winter	1+	7	144	137	124	5.5	5.7	5.6	5.8	6.5	5.0	6.7	5.8	5.6	5.80	-	5.76	8.2
	2+	1	15	20	16	57	40	53	40	50	20	-	43	54	40	-	23	43
	3+	-	1	3	1	500+	-	800	267	800	40	-	353	500+	294	-	54	353
	4+	-	-	-	-	500+	-	-	-	-	-	-	500+	500+	500+	-	121	500+

SWE

	Number	num _N	num _{20C}	num _{RL}	num _{LI}	pRP	eRP _N	eRP _{20C}	eRP _{RL}	eRP _{LI}	5% PRE	95% PRE	tRP _N	tRP _{20C}	tRP _{RL}	tRP _{LI}	5% PRE	95% PRE
1yrl Events per winter	1+	20	486	478	559	1.58	2.0	1.65	1.67	1.43	1.38	1.82	ψ=1.12	ψ=0.13	ψ=0.2	ψ=0.27		
	2+	12	205	217	295	3.8	3.3	3.9	3.7	3.0	3.1	4.4	4.1	3.79	3.79	1.44	1.60	1.90
	3+	5	71	69	127	12	8	11	12	6	8	40	8	11	10	6	8	12
	4+	3	26	25	53	53	13	31	32	15	20	-	16	38	33	15	18	47
	5+	-	10	8	22	273	-	80	100	36	40	-	31	145	112	41	38	216
	6+	-	2	3	7	500+	-	400	267	114	-	-	61	500+	413	120	84	500+
	7+	-	-	-	1	500+	-	-	-	800	-	-	126	500+	500+	367	191	500+
2yrl Events per winter	1+	13	295	298	369	2.5	3.1	2.7	2.68	2.16	2.22	2.9	ψ=0.74	ψ=0.20	ψ=0.17	ψ=0.42		
	2+	6	85	85	124	11	7	9	9	6	7	40	3.2	2.72	2.71	2.4	2.68	3.1
	3+	1	12	15	27	70	40	67	53	30	20	-	9	9.9	9.9	6	9	10.0
	4+	-	4	2	9	500+	-	200	400	89	-	-	23	41	43	19	24	46
	5+	-	2	-	1	500+	-	400	-	800	-	-	58	184	199	56	64	231
	6+	-	2	-	1	500+	-	400	-	800	-	-	145	500+	500+	170	168	500+
	7+	-	2	-	1	500+	-	400	-	800	-	-	364	500+	500+	500+	446	500+
5yrl Events per winter	1+	7	138	143	181	5.5	5.7	5.8	5.6	4.4	5.0	6.7	ψ=0.10	ψ=0.11	ψ=0.04	ψ=-	5.8	7.0
	2+	1	19	16	31	57	40	42	50	26	20	-	5.8	5.6	5.6	-	-	43
	3+	-	3	1	5	500+	-	267	800	160	-	-	43	42	51	-	26	353
	4+	-	-	-	-	500+	-	-	-	-	-	-	353	331	500+	-	85	500+
	5+	-	-	-	-	500+	-	-	-	-	-	-	500+	500+	500+	-	261	500+

UK

	Number	num _N	num _{20C}	num _{RL}	num _{LI}	pRP	eRP _N	eRP _{20C}	eRP _{RL}	eRP _{LI}	5% PRE	95% PRE	tRP _N	tRP _{20C}	tRP _{RL}	tRP _{LI}	5% PRE	95% PRE
1yrl Events per winter	1+	26	487	481	579	1.58	1.54	1.64	1.66	1.38	1.43	1.90	ψ=-	ψ=0.14	ψ=0.20	ψ=0.32		
	2+	10	215	215	341	3.78	4.0	3.7	3.7	2.4	3.3	5.0	-	1.64	1.67	1.40	1.59	2.06
	3+	3	71	81	151	12	13	11	10	5	6	40	-	3.79	3.79	2.5	3.79	4.1
	4+	1	23	21	60	53	40	35	38	13	20	-	11	10	10	5	8	12
	5+	-	4	2	25	273	-	200	400	32	-	-	-	37	33	12	16	49
	6+	-	-	-	3	500+	-	-	-	267	-	-	-	139	112	30	30	239
	7+	-	-	-	-	500+	-	-	-	-	-	-	-	500+	414	79	61	500+
2yrl Events per winter	1+	15	303	292	416	2.5	2.7	2.6	2.7	1.9	2.2	3.6	ψ=0.14	ψ=0.12	ψ=0.23	ψ=0.33		
	2+	4	82	87	170	11	10	10	9	5	7	20	2.7	2.66	2.8	2.0	2.68	4.2
	3+	1	13	18	51	70	40	62	44	16	13	-	10	10.2	9.6	5	8.7	10.1
	4+	-	2	3	11	500+	-	400	267	73	40	-	46	48	38	14	17	46
	5+	-	-	-	1	500+	-	-	-	800	-	-	231	254	159	42	30	231
	6+	-	-	-	-	500+	-	-	-	-	-	-	500+	500+	500+	134	53	500+
	7+	-	-	-	-	500+	-	-	-	-	-	-	500+	500+	500+	441	95	500+
5yrl Events per winter	1+	8	144	142	245	5.5	5	5.6	5.6	3.3	5.0	6.7	ψ=-	ψ=0.03	ψ=0.05	ψ=-	5.8	8.2
	2+	-	16	17	62	57	-	50	47	13	20	-	-	5.6	5.7	-	-	43
	3+	-	-	1	8	500+	-	-	800	100	40	-	-	52	48	-	23	353
	4+	-	-	-	2	500+	-	-	-	400	-	-	-	500+	500+	-	54	500+
	5+	-	-	-	-	500+	-	-	-	-	-	-	-	500+	500+	-	121	500+

Supplementary G:

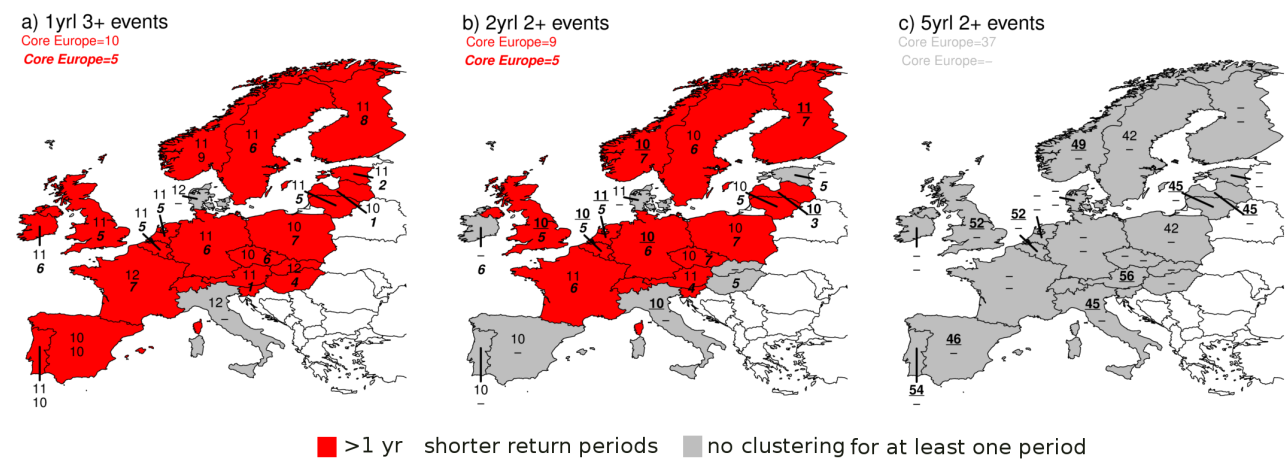


Figure S2. As Figures 3g-i but based on the negative Binomial distribution (tRP_{LL}).

Supplementary H:

In this paper, 10m instantaneous wind data is used for NCEP, while wimax (maximum wind of the last six hours) is considered for GCM data. The 98th percentiles over Europe for GCM wimax and NCEP wind are shown in Figure S3. For more details on the differences and its implications for the results of the wind storm loss model see main text.

In this study, the 98th percentile of present day conditions is used for the computation of LI for both present and future climate conditions. A sensitivity study using the 98th percentile for 2060-2100 as threshold reveals similar results to those presented in the main text where the 98th percentile for 1960-2000 is used.

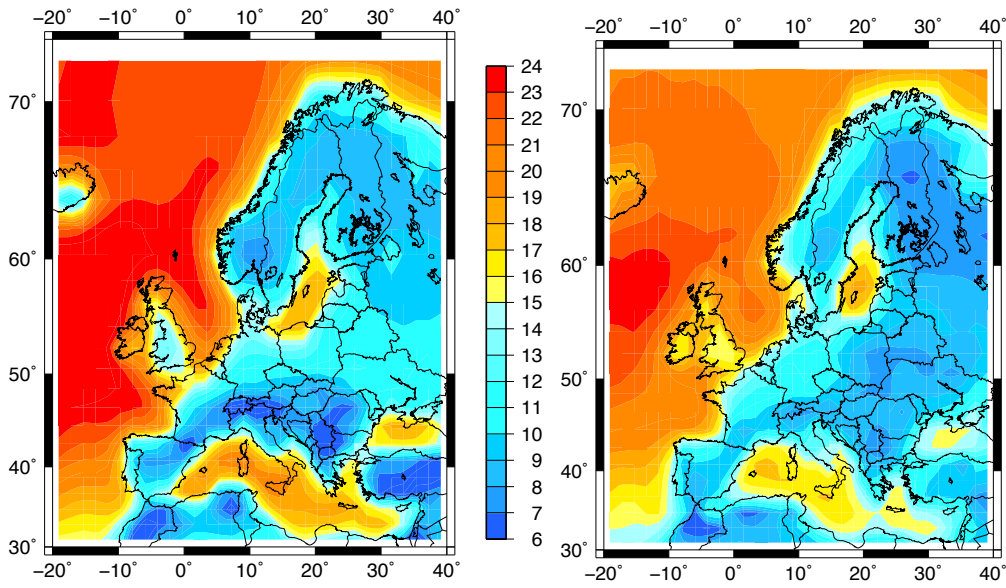


Figure S3. 98th percentiles for GCM wimax data (left) and NCEP wind (right).

Supplementary I - Significance tests:

a) Pearson's Chi-square test:

The significance of the clustering of events can be estimated with Pearson's Chi-squared test for the goodness of fit. Here, data is compared to values based on the Poisson distribution. The test statistic is defined as:

$\chi^2 = \sum_{i=1}^n \frac{(O_i - E_i)^2}{E_i}$, where $O_i = \text{frequency}$, $E_i = \text{expected (theoretically) frequency}$, $n = \text{number of classes}$.

For each significance level α , the critical value c depends on the k degrees of freedom, and can be found in the published tables in the literature. If $\chi^2 > c$, results are significant different from a Poisson distribution, and thus clustering is significant.

Reference: Plackett, R.L., 1983: Karl Pearson and the Chi-Squared Test, *International Statistical Review*, **51**, 59-72, DOI:10.2307/1402731

b) Kolmogorov-Smirnov test:

The two-sample Kolmogorov-Smirnov test is a statistical test to compare similarities between two probability distributions and is a general nonparametric method. This test quantifies the maximum distance between empirical distribution functions of two samples. The null hypothesis is that both samples are from the same distribution. The test can be applied for continuous distributions and tends to be more sensitive near the center of the distribution than at the tails.

For increasing ordered data X_1, X_2, \dots, X_N , the empirical distribution functions is defined as: $EDF = n(i)/N$
 $n(i) = \text{number of points less than } X_i$.

The Kolmogorov-Smirnov test is defined as:

$$D = \max_{1 \leq i \leq N} (F(X_i) - i/N, i/N - F(X_i))$$

$F = \text{theoretical cumulative distribution of the distribution being tested, which must be a continuous distribution.}$

The null hypothesis is rejected if the test statistic D exceeds a critical value (published Tables). The correspondent R-routine was used for the computations.

References:

Chakravart, Laha, and Roy, 1967: *Handbook of Methods of Applied Statistics*, Vol. 1, John Wiles and Sons, pp 392-394

Wilks D S 2006 *Statistical Methods in the Atmospheric Science* (Second Edition International Geophysics Series Burlington USA) pp 627

c) Natural climate variability:

An alternative way to test the significance of possible changes of RPs in a changing climate is to compare the estimated RPs for selected periods with a benchmark for (unperturbed) natural climate variability. With this aim, a 505-year long pre-industrial run with constant forcing (year 1860) is used as benchmark. This long run permits an adequate quantification of the range of natural inter-decadal climate variability (see discussion in the review paper IDAG, 2005, section 3b). RPs for 40 year time slices were computed for the whole 505 years simulation, resulting in a total of 466 periods (1-year shift per 40 year period). In the present case, we define the range of RPs between the 5th and the 95th percentiles from these 466 periods as natural climate variability. These ranges are included in the tables of Supplementary F (5% PRE, 95% PRE). If RP estimates for RP_{20C} , RP_{RL} and RP_{LI} are outside of this range, this is an indication for significant differences to the pre-industrial climate variability (marked in bold in these tables and Figure 3). Given this definition, please note that RP_{20C} may already be outside the range of natural climate variability, and not only RP_{RL} and RP_{LI} .

Reference: International ad hoc Detection and Attribution Group (IDAG), 2005: Detecting and attributing external influences on the climate system: a review of recent advances. J. Climate, 18, 1291-1314.

7 Summary and Discussion

This study analyses potential losses linked to windstorms for present and future climate conditions. The aim is to identify and improve reliable models to estimate potential loss events caused by individual cyclones, and to quantify clustering and return periods of high potential loss storm series. The analysed region is Europe, with focus on Core Europe, which is defined as France, Germany, Denmark, the Netherlands, Belgium, Ireland and Great Britain. Empirical storm loss models are applied for the estimation of potential losses associated with individual windstorms considering both purely meteorological parameters (MI) as well as on considering socio-economic aspects (LI), like a proxy for insured values within a region. The models are driven with reanalysis datasets and GCM data for present and future climate conditions. Following, a ranking of the identified storm losses is performed. The results for MI and LI are compared to identify in how far changes in LI can directly be related to changes in cyclone activity. For individual events, return periods of losses as well as a possible shift in intensity is investigated for the end of the 21st century (Chapter 3). Since in the past highest costs were associated with storm series it is of high importance to find reliable methods for the estimation of clustering of high potential losses. Therefore two theoretical distributions (Poisson and negative Binomial distribution) are tested to quantify, which is the best to estimate clustering and return periods of loss based on storm series for Germany (Chapter 5). Finally, a possible change in clustering of high potential loss events and return periods of storm series are analysed. The methods of Chapter 5 are applied to 21 regions of Europe. In the end, the assessment of changes in clustering of storm series is performed empirically and with the negative Binomial distribution (Chapter 6). In the following, the main results of the papers are presented, followed by a conclusion and an outlook.

7.1 Summary Paper I (Chapter 3)

Simple empirical models are used to estimate potential losses associated with individual windstorms focusing on both a purely meteorological severity (MI) and a socio-economic severity (LI). In addition to MI, LI also considers the population density as a proxy for insured values within an area and includes the effect that windstorms hit populous areas more often by chance. A novel approach of the storm loss model of Klawns and Ulbrich (2003) is considered to identify time series of LI based on reanalysis data (ERA40 and NCEP). Afterwards, the time series are calibrated with daily based real loss data aggregated for Germany provided by the German Association of Insurers for the period 1997-2007. This method is reliable to de-cluster almost all historical events. The assessed top 10 loss events based on reanalysis data are comparable to the top 10 ranking statistics of MunichRe (2010), although the positions for single storms differs. The intensity and frequency of events for reanalysis and present day climate conditions for GCM are similar. Therefore, the method can be applied to ECHAM5/MPI-OM1 GCM data for present (20C: 1960-2000) and future climate conditions (IPCC scenario B2, A1B, A2: 2060-2100) for countries of Europe. The most important outcomes are:

- Robust relationships between MI and LI are found. For most cases MI and LI are in accordance, with a correlation of about 99% e.g. for Germany. The relation between LI and MI decreases, when the investigated area increases, especially when non-continental regions are considered in MI. Nevertheless, LI is largely dependant on MI. For larger areas other factors, e.g. if a cyclone hits high populous areas by chance, get more important for LI. This indicates that parameters, which may be partially related with chance play also an important role for the signal in LI.
- Particularly for parts of Western and Central Europe for both LI and MI more intense losses linked to extreme windstorms are identified in all analysed GCM simulations for the end of the 21st century. An increase of about 65% of the maximum loss according to the A1B and A2 scenarios are estimated.

Nevertheless, changes in intensity are not always significant and are highly dependant on the considered country and scenario. With exception of Norway, all countries show a trend towards higher intensities of loss events for at least one IPCC future scenario.

- Return periods for a given return level show shorter return periods for MI and LI at the end of the 21st century for most countries in Core Europe. Findings are significant for MI, while for LI results are not statistically significant except for the A2 scenario. Three different tendencies are identified considering both rank statistics and return periods for LI outcomes.
 1. More intense losses and shorter return periods for all three climate scenarios in Germany, Belgium, Netherlands, Poland, Estonia, Croatia, Austria, Bosnia and Hungary
 2. Lower losses and longer return periods for Norway in all three climate scenarios
 3. Higher losses and sometimes shorter return periods in some scenarios for all other countries

7.2 Summary Paper II (Chapter 5):

In Paper II clustering of storm series associated with high potential loss events are investigated. Therefore a modified approach of the storm loss model of Klawns and Ulbrich (2003) is used to generate LI and MI for Germany. The model introduced in Paper I is further adapted to separate damages associated with extreme events within three days. Three days is a reasonable time-frame for separating events as it is according to the 72-hour event definition, often used by insurance companies in reinsurance treaties (c.f. Klawns and Ulbrich, 2003). It is also reliable, as cyclones normally cross areas with an expansion of single countries in this period. Outcomes of the model are ranked and the top events representing a certain return level (1-, 2-, 5-year) are distributed over the winters. This distribution provides the basis for the analysis with theoretical distributions. A validation of the identified extreme events is done with daily aggregated simulations of building losses in Germany provided by the German Association of Insurers for the period 1984-2008. The estimation

of clustering and return periods of series of windstorm related losses are assessed empirically and with the Poisson and negative Binomial distribution. The model is applied to 30 winters of two reanalysis data sets (ERA-Interim and NCEP) interpolated to the same resolution, observation from German weather station data and an ensemble of over 4000 years GCM runs for present day climate conditions (20C). The main results are:

- The best theoretical distribution to estimate clustering of historical losses associated with windstorms in Europe is the negative Binomial distribution. Especially for storm series with many events per winter the Poisson distribution clearly overestimates the empirical estimations considering both reanalysis data and the GCM data ensemble.
- Return periods for GCM data and reanalysis data are similar, but with much lower uncertainties for GCM.

7.3 Summary Paper III (Chapter 6):

Paper III aims to estimate possible future changes in clustering and return periods of losses associated with cyclone series affecting Europe. Therefore, the methods presented in Paper II are applied to 40 winters of NCEP data and a GCM data ensemble of 800 years each for recent and future climate conditions (20C: 1960-2000; A1B: 2060-2100) in 21 regions/countries of Europe. The most important results are:

- Results for Germany (Chapter 5) are confirmed for other European regions.
- The clustering changes with the considered return level, the number of storms within a storm series and between datasets. In general, only small changes of clustering and return periods are identified for the end of the 21st century when considering changes based on fixed return levels:
 1. shorter return periods for 2-year and 5-year return level for Core Europe
 2. at the 1-year return level longer return periods for Core Europe
 3. for most countries in Western Europe and Iberia shorter return periods
 4. longer return periods for Scandinavia, Poland and Czech Republic

- Considering fixed loss intensities (LI 20C, as in Chapter 3) changes indicate more distinct results with shorter return periods for all regions and return levels with exception of the Mediterranean area.
- Nevertheless, all detected changes are probably within the range of natural climate variability.

7.4 Discussion and Outlook

The identified results of possible higher intensities and shorter return periods of storms in Western and Central Europe in a future climate (Chapter 3) are in agreement with previous studies. For example Schwierz et al. (2010) found based on ECHAM5 and HadCM3 for countries of Central Europe an increase in intensity and frequency of storms.

The identified changes can be grouped in a purely meteorological severity of events (MI) and a socio-economical (LI), which considers the effect hitting more densely populated areas more often by chance or not. Comparing assessed changes in LI or MI with changes in cyclone activity (e.g. Della-Marta and Pinto, 2009), the spatial scale has to be taken into account. For example, changes in cyclone intensity lead to changes in surface winds several 100s of km south or south-west of the cyclone centre (e.g. Pinto et al., 2007; Pfahl, 2014) as here the strongest wind speeds linked to cyclones typically occur (e.g. Fink et al., 2009). So an increase of cyclone intensity over Great Britain induce a change of strong winds over the Benelux, Germany, and France. Therefore, changes in MI and LI are expected in this region. This fact may explain that MI and LI over Great Britain only found small shifts in intensity despite an estimated shortening of return periods of extreme cyclones in that area (e.g. Della-Marta and Pinto (2009)). On the other hand larger changes in intensity of windstorms are detected for the Benelux, France and Germany.

An application of the presented methods to CMIP5 datasets, which consider more complex models, with a broader set of experiments (Taylor et al., 2012) would be desirable. CMIP5 data includes a more complete ocean field as well as other aspects of the climate system like aerosol, biogeochemical and cryospheric fields. This

may give an insight of the interactions between atmosphere and for example the biosphere. Another advantage of CMIP5 is that in general the spatial resolution is higher than in CMIP3 and many more output fields are archived. Moreover, it could be interesting to use a multi-model ensemble of CMIP5 or CMIP3 to identify the inter-model variance of the results.

Due to a lack of available insurance data the validation of the storm loss model with real loss data provided by insurers is only done for Germany and a time period of ten years (Chapter 3) or with a simulation of daily residential building losses for private buildings between 1984 and 2008 (Chapter 5), respectively. Nevertheless, to improve the storm loss model it is important to calibrate the model for a longer time period and all regions with available insured data. This might be historical loss ratio data or actually insured values within a certain area. For future work, a calibration for a longer period and all regions of Europe would be desirable. However, this might remain a problem as availability of such datasets is rare. Moreover, changes in insurance data are not only given by changes in losses. Over the years insurance fraud has been increased to. Furthermore, it has to be taken into account, that the insurance data are not homogeneous in time and particularity per countries is given. Additionally, the individual storm events themselves are regulated individually. Another parameter, which could be regarded in the storm loss model is the input data, considering gust wind data of observation stations in whole Europe, if available.

Outcomes for the quantification of clustering and return periods of losses linked to extreme cyclones show that the negative Binomial distribution is the best method for less frequent storm series (Chapter 5). This distribution is often used to describe insurance risks considering over-dispersion (e.g. Ismail and Jemain, 2007). As only sparse peer-reviewed literature is available on the topic of clustering, particularly with focus on climate change, the present work is an important contribution to extend the current knowledge about clustering. Nevertheless, particularly for 2yrl and 5yrl, the changes in potential losses linked to storm series as identified in this study are not always coherent with changes of clustering of cyclones itself (Mailier, 2007; Pinto et al., 2013). Analysing the same database as in the present work, Pinto et al. (2013) found a decrease in clustering of cyclones over most of Europe. Several factors may be responsible for differences between clustering of cyclones and the estimated losses. The maximum surface wind speeds associated with extreme cyclones are ex-

pected several 100s km south of the cyclone centre. Therefore the maximum losses linked to clustering cyclones are also expected to occur south of the cyclone centre. Furthermore, the considered number of events in this study is much lower than in Pinto et al. (2013), who considered about 10 events per year. This explains that results considering the 1yrl are rather in line with the ones of Pinto et al. (2013) for Core Europe. A further factor is the difference between results considering cyclones, MI and LI. MI is highly correlated to the cyclone activity pattern. In this study LI, also considering a proxy for insured values, is analysed, and therefore slight differences are expected (see Chapter 5). Additionally, the analysed month differs: the present study analyses October till March, while Pinto et al. (2013) considered December till February, which could lead to some differences between results. Finally, the methods to calculate the dispersion are not similar. Pinto et al. (2013) used the variance-to-mean ratio method (ratio between variance and mean) of the numbers of cyclones crossing a certain grid point, while in this study the clustering is estimated by the negative Binomial distribution on country base. Nevertheless, identified characteristics of the results based on the two methods are similar for the same region (see Chapter 5, Table 3). Results for the change in clustering including changes in intensity of single event losses are in line with the ones presented in Chapter 3. The expected increase in intensity and shorter return periods of single storms as well as a possible change in clustering and return periods of storm series for future climate conditions may have a high impact on the re-insurance market for natural hazards in Europe (e.g. Changnon et al., 1997). Insurers are highly interested in the distribution of annual extremes, the return periods of rare events, the frequency of extreme events, the mean excess above a critical value, the distribution of these excesses and the time development of these records (Embrechts et al., 2003). Therefore, this work presents an important progress in the understanding of high potential loss events associated with winter storms. As for insurance companies, the yearly accumulated loss is of high interest, and thus the consideration of storm series with potential high loss storms is important. A challenge may be the covering of claims for winters with several high impact storms, without risking the solvency of the company. Therefore the financial authorities, like the Committee of European Insurance and Occupational Pensions Supervisors, proposed standards to measure the financial strength of insurance companies. Nevertheless, insurers are more inter-

ested in the near future, especially for the next decade. So future work may focus on the next decades, similar to the decadal predictions of the MIKLIP project (BMBF supported) or IMPETUS (NERC funded). Beyond that, a continuously adaptation on the technical approaches of measuring windstorm risk would be interesting. In the present work, a change in population density is not considered, as in Central Europe past changes can almost be neglected. Nevertheless, in order to include a possible change in living standards and insured values the storm loss model could use future projections of population density, which is used as proxy of the insured values within a region. Certainly, the best input data would be the insured values themselves.

Further investigations could focus on clustering of cyclones/losses depending on certain large-scale weather circulations. Due to the physically factors contributing to clustering of cyclones it is expected that clustering of losses is e.g. higher in the westerly than in the easterly or southerly weather types (e.g. Pinto et al., 2014). Such an analysis could help to better understand the physical aspects of clustering of losses, which should be supported by a more detailed investigation of the atmospheric conditions leading to clustering. However, the analysed dataset for each weather type has to be large enough to get statistical stable results. The present results are expected to be near the ensemble mean behaviour of the IPCC GCM simulations. Nevertheless, future work should consider a larger sample of GCM data, to analyse inter-model variations, which are found for example in Woollings et al. (2012), who analysed synoptic patterns for 22 models of CMIP 3. As for paper 1 it would be also interesting to analyse the CMIP5 data, as they consider other subsystems of the climate system than CMIP3 and newer forcing (see discussion above).

Although the demand on information of changes in clustering of cyclones and the associated impact on economy and social life is high, almost no articles are available. Therefore, the findings of this thesis are a valuable contribution to the current knowledge about the impact of cyclones on loss values and clustering of storm events providing a basic information on how to estimate clustering of events theoretically.

8 References

- Adamson, D. S., Belcher, S. E., Hoskins, B. J., and Plant, R. S. (2006). Boundary layer friction in mid-latitude cyclones. *Q. J. R. Meteorol. Soc.*, 132:101–124.
- Alexandersson, H., Tuomenvirta, H., Schmith, T., and Iden, K. (2000). Trends of storms in NW Europe derived from an updated pressure data set. *Clim. Res.*, 14:71–73. doi:10.3354/cr014071.
- Allan, R., Tett, S., and Alexander, L. (2009). Fluctuations in autumn-winter severe storms over the British Isles: 1920 to present. *Int. J. Climatol.*, 29:357–371. doi:10.1002/joc.1765.
- Amtmann, R. (1986). Dynamische Windbelastung von Nadelbäumen. *Forstliche Forschungsberichte, Schriftenreihe der Forstwirtschaftlichen Fakultät der Universität München und der Bayer. Forstlichen Versuchs- und Forschungsanstalt*, 74.
- Angermann, A. (1993). *Sturmszenarien und Schadenhäufigkeit von Stürmen über Deutschland*. PhD thesis, Diplomarbeit am Institut für Meteorologie und Geophysik der Universität zu Köln.
- Anstey, J. A., Davini, P., Gray, L. J., Woollings, T. J., Butchart, N., Cagnazzo, C., Christiansen, B., Hardiman, S. C., Osprey, S. M., and Yang, S. (2013). Multimodel analysis of Northern Hemisphere winter blocking: Model biases and the role of resolution. *J. Geophys. Res. Atmos.*, 118:3956–3971. doi:10.1002/jgrd.50231.
- AON Benfield (2013). Winterstürme in Europa - Historie von 1703 bis 2012. *Aon Benfield Analytics*, 125:pp.43. <http://www.aonbenfield.de/sturmhistorie/sturmhistorie.pdf> [cited 06.06.2014].

-
- Bader, J., Mesquita, M. D. S., Hodges, K. I., Keenlyside, N., Østerhus, S., and Miles, M. (2011). A review on Northern Hemisphere sea-ice, storminess and the North Atlantic Oscillation: 500 observations and projected changes. *Atmos. Res.*, 101:809–834. doi:10.1016/j.atmosres.2011.04.007.
- Baehr, C., Pouponneau, B., Ayrault, F., and Joly, A. (1999). Dynamical characterization of the FASTEX cyclogenesis cases. *Q. J. R. Meteorol. Soc.*, 125:3469–3494. doi:10.1002/qj.49712556117.
- Bärring, L. and von Storch, H. (2004). Scandinavian storminess since about 1800. *Geophys. Res. Lett.*, 31:L20202. doi:10.1029/2004GL020441.
- Bengtsson, L., Hodges, K. I., and Keenlyside, N. (2009). Will Extratropical Storms Intensify in a Warmer Climate? *J. Climate*, 22:2276–2301. doi:10.1175/2008JCLI2678.1.
- Bengtsson, L., Hodges, K. I., and Roeckner, E. (2006). Storm Tracks and Climate Change. *J. Clim.*, 19:3518–3543. doi:10.1175/JCLI3815.1.
- Bishop, C. H. and Thorpe, A. J. (1994). Frontal wave stability during moist deformation frontogenesis. Part I: Linear wave dynamics. *J. Atmos. Sci.*, 51:852–873.
- Bjerknes, J. and Solberg, H. (1922). Life cycles of cyclones and the polar front theory of atmospheric circulation. *Geofys. Publ.*, 3:1–18.
- Blackmon, M. L. (1976). A climatological spectral study of the 500 mb geopotential height of the Northern Hemisphere. *J. Atmos. Sci.*, 33:1607–1623. doi:10.1175/1520-0469(1976)033<1607:ACSSOT>2.0.CO;2.
- Blender, R., Fraedrich, K., and Lunkeit, F. (1997). Identification of cyclonetrack regimes in the North Atlantic. *Q. J. R. Meteorol. Soc.*, 123:727–741. doi:10.1002/qj.49712353910.
- Born, K., Ludwig, P., and Pinto, J. G. (2012). Wind Gust Estimation for Mid-European Winter Storms: Towards a Probabilistic View. *Tellus A*, 64:17471. doi:10.3402/tellusa.v64i0.17471.

-
- Brönnimann, S., Martius, O., von Waldow, H., Welker, C., Luterbacher, J., Compo, G. P., Sardeshmukh, P. D., and Usbeck, T. (2012). Extreme winds at northern mid-latitudes since 1871. *Meteorol. Z.*, 21:13–27. doi:10.1127/0941-2948/2012/0337.
- Browning, K. A. and Reynolds, R. (1994). Diagnostic study of a narrow cold-frontal rainband and severe winds associated with a stratospheric intrusion. *Quart. J. Roy. Meteor. Soc.*, 120:235–257.
- Businger, S. and Businger, J. A. (2001). Viscous dissipation of turbulence kinetic energy in storms. *J. Atmos. Sci.*, 58:3793–3796.
- Carlson, T. N. (1980). Airflow through midlatitude cyclones and the comma cloud pattern. *Mon. Wea. Rev.*, 108:1498–1509. doi:10.1175/1520-0493(1980)108<1498:ATMCAT>2.0.CO;2.
- Chaboureaud, J. P. and Thorpe, A. J. (1999). Frontogenesis and the development of secondary wave cyclones in FASTEX. *Q. J. R. Meteorol. Soc.*, 125:925–940.
- Chandler, A. M., Jones, E. J. W., and Patel, M. H. (2001). Property loss estimation for wind and earthquake perils. *Risk Analysis*, 21.
- Chang, E. K. (1993). Downstream development of baroclinic waves as inferred from regression analysis. *J. Atmos. Sci.*, 50:2038–2053.
- Changnon, S. A., Changnon, D., Fosse, E. R., Hoganson, D. C., Roth, R. J., and Totsch, J. M. (1997). Effects of Recent Weather Extremes on the Insurance Industry: Major Implications for the Atmospheric Sciences. *B. Am. Meteorol. Soc.*, 78:425–435. doi:10.1175/1520-0477(1997)078<0425:EORWEO>2.0.CO;2.
- Charney, J. G. (1947). The dynamics of long waves in a baroclinic westerly current. *J. Meteor.*, 4:135–162.
- Ciavola, P., Ferreira, O., Haerens, P., Koningsveld, M. V., Armaroli, C., and Lequeux, Q. (2011). Storm impacts along European coastlines. *Environmental Science Policy Part 1: The joint effort of the MICORE and ConHaz Projects*, 14:912–923. doi:10.1016/j.envsci.2011.05.011.

-
- Dacre, H. F. and Gray, S. L. (2006). Life-cycle simulations of low-level frontal waves and the impact of deformation strain. *Q. J. R. Meteorol. Soc.*, 132:2171–2190. doi:10.1256/qj.05.238.
- Danard, M. B. (1964). On the influence of released latent heat on cyclone development. *J. Appl. Meteorol.*, 3:27–37. doi:/10.1175/1520-0450(1964)003<0027:OTIORL>2.0.CO;2.
- Delcambre, S. C., Lorenz, D. J., Vimont, D. J., and Martin, J. E. (2013). Diagnosing Northern Hemisphere jet portrayal in 17 CMIP3 global climate models: Twentieth-century intermodel variability. *J. Clim.*, 26:4910–4929. doi:10.1175/JCLI-D-12-00359.1.
- Della-Marta, P. M. and Pinto, J. G. (2009). The statistical uncertainty of changes in winter storms over the North Atlantic and Europe in an ensemble of transient climate simulations. *Geophys. Res. Lett.*, 36:L14703. doi:10.1029/2009GL038557.
- Deroche, M.-S., Choux, M., Codron, F., and Yiou, P. (2014). Three variables are better than one: detection of european winter windstorms causing important damages. *Nat. Hazards Earth Syst. Sci.*, pages 981–993. doi:10.5194/nhess-14-981-2014.
- Deutsche Rück (2014). Sturmdokumentation 2013 Deutschland. *Deutsche Rück Reinsurance Company Düsseldorf*, page 52.
- Donat, M., Leckebusch, G. C., Pinto, J. G., and Ulbrich, U. (2010a). Examination of wind storms over Central Europe with respect to circulation weather types and NAO phases. *Int. J. Climatol.*, 30:1289–1300. doi:10.1002/joc.1982.
- Donat, M. G., Leckebusch, G. C., Wild, S., and Ulbrich, U. (2010b). Benefits and limitations of regional multi.model ensembmles for storm loss estimations. *Clim. Res.*, 44:211–225. doi:10.3354/cr00891.
- Donat, M. G., Renggli, D., Wild, S., Alexander, L. V., Leckebusch, G. C., and Ulbrich, U. (2011). Reanalysis suggests long-term upward trends in Ezropean storminess since 1871. *Geophys. Res. Lett.*, 38:L14703–L14703. doi:10.1029/2011GL047995.

-
- Dorland (1999). Vulnerability of the Netherlands and Northwest Europe to storm damage under climate change. *Clim. Change*, 43(513-45). doi:10.1023/A:1005492126814.
- Dritschel, D. G., Haynes, P. H., and Jukes, M. N. (1991). The stability of a two-dimensional vorticity filament under uniform strain. *J. Fluid Mech.*, 230:647–665.
- Embrechts, P., Klüppelberg, C., and Mikosch, T. (2003). *Modelling Extremeal Events for Insurance and Finance*. Springer.
- Feser, F., Barcikowska, M., Krueger, O., Schenk, F., Weisse, R., and Xia, L. (2014). Storminess over the North Atlantic and Northwestern Europe - A Review. *Q. J. R. Meteorol. Soc.* doi:10.1002/qj.2364.
- Fink, A. H., Brücher, T., Ermert, V., Krüger, A., and Pinto, J. G. (2009). The European storm Kyrill in January 2007: Synoptic evolution, meteorological impacts and some considerations with respect to climate change. *Nat. Hazards Earth Syst. Sci.*, 9:405–423.
- Fink, A. H., Pohle, S., Pinto, J. G., and Knippertz, P. (2012). Diagnosing the influence of diabatic processes on the explosive deepening of extratropical cyclones. *Geophys. Res. Lett.*, 93(7). doi:10.1029/2012GL051025.
- Gómara, I., Pinto, J. G., Woollings, T., Masato, G., Zurita-Gotor, P., and Rodríguez-Fonseca, B. (2014). Rossby Wave-Breaking analysis of Explosive Cyclones in the Euro-Atlantic sector. *Q. J. R. Meteorol. Soc.*, 140:738–753. doi:10.1002/qj.49702511003.
- Grams, C. M., Binder, H., Pfahl, S., Piaget, N., and Wernli, H. (2014). Atmospheric processes triggering the Central European floods in June 2013. *Nat. Hazards Earth Syst. Sci. Discuss.*, 2:427–458. doi:10.5194/nhess-14-1691-2014.
- Gulev, S. K., Zolina, O., and Grigoriev, S. (2001). Extratropical cyclone variability in the Northern Hemisphere winter from the NCEP/NCAR reanalysis data. *Clim. Dynam.*, 17:795–809. doi:10.1007/s003820000145.

-
- Harrold, T. W. (1973). Mechanisms influencing the distribution of precipitation within baroclinic disturbances. *Q. J. R. Meteorol. Soc.*, 99:232–251. doi:10.1002/qj.49709942003.
- Harvey, B., Shaffrey, L. C., Woollings, T. J., Zappa, G., and Hodges, K. I. (2012). How large are projected 21st century storm track changes? *Geophys. Res. Lett.*, 39. doi:10.1029/2012GL052873.
- Hegerl, G. C., Zwiers, F. W., Braconnot, P., Gillett, N. P., Luo, Y., Orsini, J. A. M., Nicholls, J., Penner, J. E., and Stott, P. A. (2007). Understanding and Attributing Climate Change. *Climate Change 2007: The Physical Science Basis. Contribution of Working Group I to the Fourth Assessment Report of the Intergovernmental Panel on Climate Change*, edited by: Solomon, S., Qin, D., Manning, M., Chen, Z., Marquis, M., Averyt, K. B., Tignor, M., and Miller, H. L.
- Held, H., Gerstengarbe, F. W., Pardowitz, T., Pinto, J. G., Ulbrich, U., Born, K., Donat, M. G., Karremann, M. K., Leckebusch, G. C., Ludwig, P., Nissen, K. M., Österle, H., Prah, B. F., Werner, P. C., Befort, D. J., and Burghoff, O. (2013). Projections of global warming-induced impacts on winter storm losses in the German private: household sector. *Clim. Change.*, 121:195–207. doi:10.1007/s10584-013-0872-7.
- Henry, J. A. (1922). J. Bjerknes and H. Solberg On the life cycles of cyclones and the polar front theory of atmospheric circulation. *Mon. Wea. Rev.*, 50:468–473.
- Hewson, T., Magnusson, L., Breivik, O., Prates, F., Tsonevsky, I., and de Vries, H. J. W. (2014). Windstorms in northwest Europe in late 2013. *ECMWF Newsletter*, 139:22–28. www.ecmwf.int/sites/default/files/Newsletter_139_smaller.pdf.
- Hodges, K. I., Hoskins, B. D. Y., Boyle, J., and Thorncroft, C. (2003). A comparison of recent reanalysis datasets using objective feature tracking: Storm tracks and tropical easterly waves. *Mon. Weather Rev.*, 131:2012–2036. doi:10.1175/1520-0493(2003)131<2012:ACORRD>2.0.CO;2.
- Hurrell, J. W. and Deser, C. (2009). North Atlantic climate variability: the role of the

-
- North Atlantic Oscillation. *J. Mar. Syst.*, 78:28–41. doi:10.1016/j.jmarsys.2008.11.026.
- Ismail, N. and Jemain, A. A. (2007). Handling Overdispersion with Negative Binomial and Generalized Poisson Regression Models. *Casualty Actuarial Society Forum*, pages 103–185.
- Joly, A. and Thorpe, A. J. (1991). The stability of time-dependent flows: An application to fronts in developing baroclinic waves. *J. Atmos. Sci.*, 42:163–182. doi:10.1175/1520-0469(1991)048<0163:TSOTDF>2.0.CO;2.
- Klawa, M. and Ulbrich, U. (2003). A model for the estimation of storm losses and the identification of severe winter storms in Germany. *Nat. Hazards Earth. Syst. Sci.*, 3:725–732. doi:10.5194/nhess-3-725-2003.
- Köppen, W. (1881). Die Zugbahnen der barometrischen Minima in Europa und auf dem nordatlantischen Ocean und ihr Einfluss auf Wind und Wetter bei uns (in German). *Mitt. Geogr. Ges. Hamb.*, 1:76–97.
- Lamb, H. H. (1991). *Historic storms of the North Sea, British Isles, and Northwest Europe*. Cambridge University Press, Cambridge.
- Lambert, S. J. and Fyfe, J. C. (2006). Changes in winter cyclone frequencies and strengths simulated in enhanced greenhouse warming experiments: results from the models participating in the IPCC diagnostic exercise. *Clim. Dyn.*, 26:713–728. doi:10.1007/s00382-006-0110-3.
- Leckebusch, G. C., Renggli, D., and Ulbrich, U. (2008). Development and application of an objective storm severity measure for the Northeast Atlantic region. *Meteorol. Z.*, 17:575–587. doi:10.1127/0941-2948/2008/0323.
- Leckebusch, G. C., Ulbrich, U., Fröhlich, L., and Pinto, J. G. (2007). Property loss potentials for European midlatitudes sztorm in a changing climate. *Geophys. Res. Lett.*, 34(5). doi:10.1029/2006GL027663.
- Ludwig, P., Pinto, J. G., Meyers, M., and Gray, L. (2014). The role of anomalous SST and surface fluxes over the southeastern North Atlantic in the explosive

-
- development of windstorm Xynthia. *Q. J. R. Meteorol. Soc.* doi:10.1002/qj.2253.
- Mailier, P. J. (2007). *Serial clustering of extratropical cyclones*. PhD thesis, Univ. of Reading, United Kingdom (available at ethos.bl.uk).
- Mailier, P. J., Stephenson, D. B., Ferro, C. A. T., and Hodges, K. I. (2006). Serial Clustering of Extratropical Cyclones. *Mon. Weather Rev.*, 134:2224–2240.
- Matulla, C., Schöner, Alexandersson, H., von Storch, H., and Wang, X. (2008). European storminess: late nineteenth century to present. *Clim. Dyn.*, 31:125–130.
- McCabe, G. J., Clark, M. P., and Serreze, M. C. (2001). Trends in Northern Hemisphere surface cyclone frequency and intensity. *J. Clim.*, 14:2763–2768. doi:10.1175/1520-0442(2001)014<2763%3ATINHSC>2.0.CO;3B2.
- MunichRe (1993). Winterstürme in Europa. *Publication of the Munich Re*.
- MunichRe (2001). Winter storms in Europe II. Analysis of 1999 losses and loss potentials. www.munichre.com [cited 23.01.2012].
- MunichRe NatCatSERVICE (2014). Loss events in Europe 1980-2013. http://www.munichre.com/site/corporate/get/documents_E-168371002/mr/assetpool.shared/Documents/5_Touch/_NatCatService/Significant-Natural-Catastrophes/2013/10-costliest-winter-storms-ordered-by-insured-losses-Europe.pdf [cited 06.08.2014].
- Orlanski, I. (1998). Poleward deflection of storm tracks. *J. Atmos. Sci.*, 55:2577–2602.
- Palutikof, J. P. and Skellern, A. R. (1991). *Storm severity over Britain: a report to Commercial Union General Insurance*. Climatic Research Unit, School of Environmental Science, University of East Anglia, Norwich (UK).
- Parker, D. J. (1998). Secondary frontal waves in the North Atlantic region: A dynamical perspective of current ideas. *Q. J. R. Meteorol. Soc.*, 124:829–856. doi:10.1002/qj.49712454709.

-
- Pfahl, S. (2014). Characterising the relationship between weather extremes in Europe and synoptic circulation features. *Nat. Hazards Earth Syst. Sci.*, 14:1461–1475. doi:10.519/nhess-14-1461-2014.
- Pinto, J. G., Bellenbaum, N., Karremann, M. K., and Della-Marta, P. M. (2013). Serial clustering of extratropical cyclones over the North Atlantic and Europe under recent and future climate conditions. *J. Geophys. Res. Atmos.*, 118:12,476–12,485. doi:10.1002/2013JD020564.
- Pinto, J. G., Gómar, I., Masato, G., Dacre, H. F., Woollings, T., and Caballero, R. (2014). Large-scale dynamics associated with clustering of extra tropical cyclones affecting Western Europe. *J. Geophys. Res. Atmos.* doi:10.1002/2014JD022305.
- Pinto, J. G., Ulbrich, U., Leckebusch, C. G., Spangehl, T., Reyers, M., and Zacharias, S. (2007). Changes in storm track and cyclone activity in three SRES ensemble experiments with the ECHAM5/MPI-OM1 GCM. *Clim. Dyn.*, 29:195–210. doi:10.1007/s00382-007-0230-4.
- Pinto, J. G., Zacharias, S., Fink, A. H., Leckebusch, G. C., and Ulbrich, U. (2009). Factors contributing to the development of extreme North Atlantic cyclones and their relationship with the NAO. *Clim. Dyn.*, 32:711–737. doi:10.1007/s00382-008-0396-4.
- Plant, R. S., Craig, G. C., and Gray, S. L. (2003). On a threefold classification of extratropical cyclogenesis. *Q. J. R. Meteorol. Soc.*, 129:2989–3012.
- Raible, C. C. (2007). On the relation between extremes of midlatitude cyclones and the atmospheric circulation using ERA40. *Geophys. Res. Lett.*, 34:L07703. doi:10.1029/2006GL029084.
- Renfrew, I. A., Thorpe, A. J., and Bishop, C. H. (1997). The role of the environmental flow in the development of secondary frontal cyclones. *Q. J. R. Meteorol. Soc.*, 123:1653–1675.
- Riemer, M., Jones, S. C., and Davis, C. A. (2008). The impact of extratropical transition on the downstream flow: An idealized modelling study with a straight jet. *Q. J. R. Meteorol. Soc.*, 134:69–91. doi:10.1002/qj.180.

-
- Rivals, H., Cammas, J.-P., and Renfrew, I. A. (1998). Secondary cyclogenesis: The initiation phase of a frontal wave observed over the eastern Atlantic. *Q. J. R. Meteorol. Soc.*, 124:243–267. doi:10.1002/qj.49712454511.
- Roberts, J. F., Champion, A. J., Dawkins, L. C., Hodges, K. I., Shaffrey, L. C., Stephenson, D. B., Stringer, M. A., Thornton, H. E., and Youngman, B. D. (2014). The XWS open access catalogue of extreme European windstorms from 1979-2012. *Nat. Hazards Earth Syst. Sci. Discuss.*, 2:2011–2048. doi:10.5194/nhessd-2-2011-2014.
- Rockel, B. and Woth, K. (2007). Extremes of near-surface wind speed over Europe and their future changes as estimated from an ensemble of RCM simulations. *Clim. Change*, 81:267–280. doi:10.1007/s10584-006-9227-y.
- Schär, C. and Davies, H. C. (1990). An instability of mature cold fronts. *J. Atmos. Sci.*, 47:929–950. doi:10.1175/1520-0469(1990)047<0929:AIOMCF>2.0.CO;2.
- Schraft, A., Durand, E., and Hausmann, P. (1993). Stürme über Europa - Schäden und Szenarien. Publikation der Schweizer Rückversicherungs-Gesellschaft.
- Schultz, D. M. and Vaughan, G. (2011). Occluded fronts and the occlusion process: A fresh look at conventional wisdom. *Bull. Amer. Meteor. Soc.*, 92:443–466.
- Schwierz, C., Köllner-Heck, P., Mutter, E. Z., Bresch, D. N., Vidale, P. L., Wild, M., and Schär, C. (2010). Modelling European winter wind storm losses in current and future climate. *Clim. Change*, 101:485–514. doi:10.1007/s10584-009-9712-1.
- Semple, A. T. (2003). A review and unification of conceptual models of cyclogenesis. *Met. Apps.*, 10:39–59. doi:10.1017/S135048270300505X.
- Simmonds, I. and Keay, K. (2002). Surface fluxes of momentum and mechanical energy over the North Pacific and North Atlantic Oceans. *Meteorol. Atmos. Phys.*, 80:1–18.
- Simmonds, I., Keay, K., and Lim, E.-P. (2003). Synoptic activity in the seas around Antarctica. *Mon. Weather Rev.*, 131:272–288.

-
- Simmons, A. J. and Hoskins, B. J. (1979). The downstream and upstream development of unstable baroclinic waves. *J. Atmos. Sci.*, 36:1239–1254.
- Storch, H. and Weisse, R. (2007). *Regional storm climate and related marine hazards in the North Atlantic*. in Diaz, H. E., and Murnane, R. J. (eds.), *Climate Extremes and Society*, Cambridge University Press, Cambridge.
- Taylor, K. E., Stouffer, R. J., and Meehl, G. A. (2012). An overview of CMIP5 and the experiment design. *Bull. Amer. Meteor. Soc.*, 4:485–498. doi:10.1175/BAMS-D-11-00094.1.
- Trenberth, K. E., Jones, P. D., Ambenje, O., Bojariu, R., Easterling, D., Tank, A. K., Parker, D., Rahimzadeh, F., Renwick, J. A., Rusticucci, M., Soden, B., and Zhai, P. (2007). *Observations: Surface and Atmospheric Climate Change Climate Change 2007: The Physical Science Basis*. Contribution of Working Group I to the Fourth Assessment Report of the Intergovernmental Panel on Climate Change, edited by: Solomon, S., Qin, D., Manning, M., Chen, Z., Marquis, M., Averyt, K. B., Tignor, M., and Miller, H. L., Cambridge University Press, Cambridge, UK, 235–336,.
- Trigo, I. (2006). Climatology and interannual variability of storm-tracks in the Euro-Atlantic sector: a comparison between ERA-40 and NCEP/NCAR reanalyses. *Clim. Dyn.*, 26:127–143.
- Uccellini, L. W. (1990). Process contributing to the rapid development of extratropical cyclones: The Eric Palmen Memorial Volume, ed. Newton, C. and Holopainen, E. *Am. Meteorol. Soc.*, pages 81–107.
- Ulbrich, U., Klawns, A. H. F. M., and Pinto, J. G. (2001). Three extreme storms over Europe in December 1999. *Weather*, 56:70–80. doi:10.1002/j.1477-8696.2001.tb06540.x.
- Ulbrich, U., Leckebusch, G. C., and Pinto, J. G. (2009). Extra-tropical cyclones in the present and future climate: a review. *Theor. Appl. Climatol.*, 96:117–131.
- Wang, X. L., Swail, V. R., and Zwiers, F. W. (2006). Climatology and changes of extratropical cyclone activity: Comparison of ERA-40 with NCEP-NCAR reanalysis for 1958–2001. *J. Clim.*, 19:3145–3166. doi:10.1175/JCLI3781.1.

-
- Wanner, H., Bronnimann, S., Casty, C., Gyalistras, D., Luterbacher, J., Schmutz, C., Stephenson, D. B., and Xoplaki, E. (2001). North Atlantic oscillation. Concepts and studies. *Surv. Geophys.*, 22:321–382.
- Weisse, R., von Storch, H., and Feser, F. (2005). Northeast Atlantic and North Sea Storminess as Simulated by a Regional Climate Model during 1958–2001 and Comparison with Observations. *J. Climate*, 18:465–479.
- Welker, C. and Martius, O. (2013). Decadal-scale variability in hazardous winds in northern Switzerland since end of the 19th century. *Atmos. Sci. Lett.*, 15(2):86–91. doi:10.1002/as12.467.
- Wernli, H., Sirren, S., Lininger, M. A., and Zillig, M. (2002). Dynamical aspects of the life-cycle of the winter storm "Lothar" (24-26 December 1999). *Q. J. R. Meteorol. Soc.*, 128:405–429. doi:10.1256/003590002321042036.
- Wieringa, J. (1973). Gust factors over open water and built up country. *Bound. Layer Meteor.*, 3.
- Woollings, T., Gregory, J. M., Pinto, J. G., Reyers, M., and Brayshaw, D. J. (2012). Responses of the North Atlantic storm track to climate change shaped by ocean-atmosphere coupling. *Nature Geoscience*, 5:313–317. doi:10.1038/ngeo1438.
- Zappa, G., Shaffrey, L. C., Hodges, K. I., Sansom, P. G., and Stephenson, D. B. (2013). A multimodel assessment of future projections of North Atlantic and European extratropical cyclones in the CMIP5 climate models. *J. Climate*. doi:10.1175/JCLI-D-12-00573.1.

9 List of Abbreviations

BCM	<u>B</u> ergen <u>C</u> limate <u>M</u> odel, University of Bergen
BMBF	Federal Ministry of Education and Research (<u>B</u> undes <u>m</u> inisterium für <u>B</u> ildung und <u>F</u> orschung)
CMIP3	<u>C</u> oupled <u>M</u> odel <u>I</u> ntercomparison <u>P</u> roject Phase <u>3</u>
CMIP5	<u>C</u> oupled <u>M</u> odel <u>I</u> ntercomparison <u>P</u> roject Phase <u>5</u>
DWD	German weather service (<u>D</u> eutscher <u>W</u> etter <u>D</u> ienst)
ECHAM	<u>E</u> uropean <u>C</u> entre <u>H</u> amburg <u>M</u> odel
ECHAM5	<u>E</u> uropean <u>C</u> entre <u>H</u> amburg <u>M</u> odel Version <u>5</u>
ECMWF	<u>E</u> uropean <u>C</u> entre for <u>M</u> edium <u>W</u> eather <u>F</u> orecast
ERA	<u>E</u> CMWF <u>R</u> eanalysen
GCM	<u>G</u> eneral <u>C</u> irculation <u>M</u> odel
GDV	German Association of Insurance Companies ("Gesamtverband der <u>D</u> eutschen <u>V</u> ersicherungsgesellschaften")
HadCM3	<u>H</u> adley <u>C</u> entre Coupled <u>M</u> odel Version <u>3</u>
HadGEM1	<u>H</u> adley Centre <u>G</u> lobal <u>E</u> nvironmental <u>M</u> odel version <u>1</u> , Met Office
IMPETUS	<u>I</u> mproving <u>P</u> redictions of Drought for <u>U</u> se Decision-Making
IPCC	<u>I</u> ntergovernmental <u>P</u> anel on <u>C</u> limate <u>C</u> hange
LI	potential socio-economic loss index
MI	potential meteorological loss index
MIKLIP	Decadal Predictions (<u>M</u> ittelfristige <u>K</u> limap <u>ro</u> gnosen)
MPI	<u>M</u> ax- <u>P</u> lanck- <u>I</u> nstitut
NAO	<u>N</u> orth <u>A</u> tlantic <u>O</u> scillation
NCEP	<u>N</u> ational <u>C</u> enter for <u>E</u> nvironmental <u>P</u> rediction
NERC	<u>N</u> ational <u>E</u> nvironmental <u>R</u> esearch <u>C</u> ouncil
OM	<u>O</u> cean <u>M</u> odel
PNA	<u>P</u> acific <u>N</u> orth <u>A</u> merica

10 Appendix

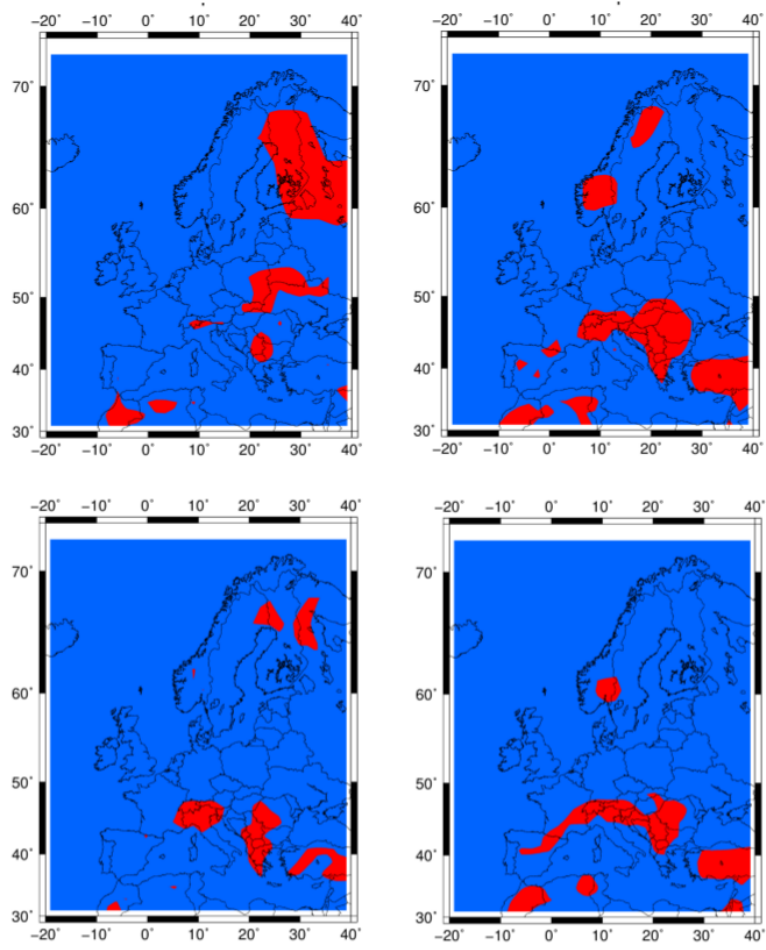


Fig. 10.1: 98th percentile for NCEP (upper left), ERA40 (upper right), ERA-Interim (lower left) and GCM (lower right). Blue: 98th percentile $> 8\text{m/s}$ red: 98th percentile $< 8\text{m/s}$.

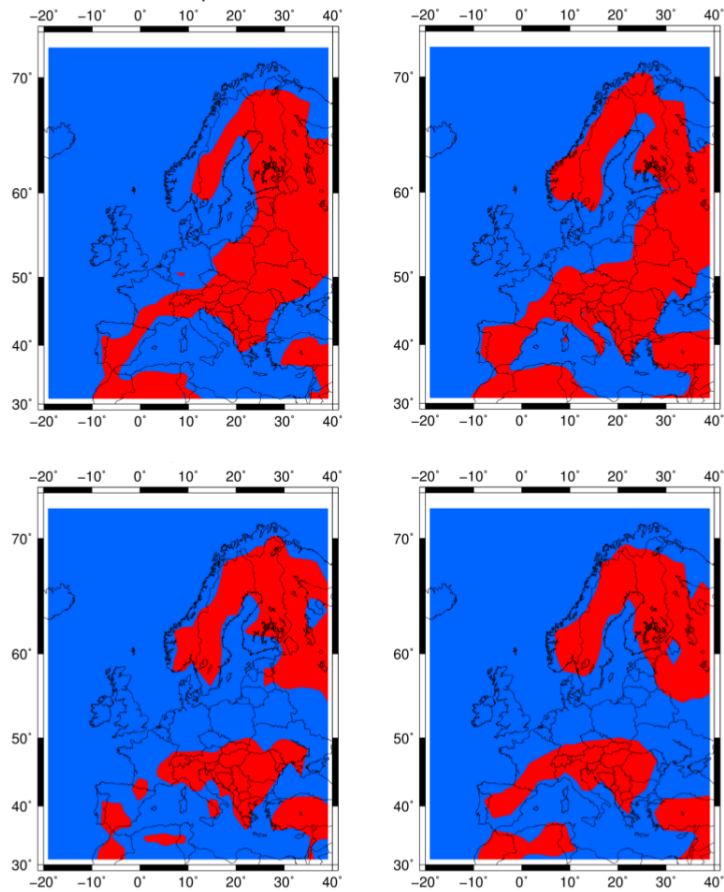


Fig. 10.2: 98th percentile for NCEP (upper left), ERA40 (upper right), ERA-Interim (lower left) and GCM (lower right). Blue: 98th percentile $> 10\text{m/s}$ red: 98th percentile $< 10\text{m/s}$.

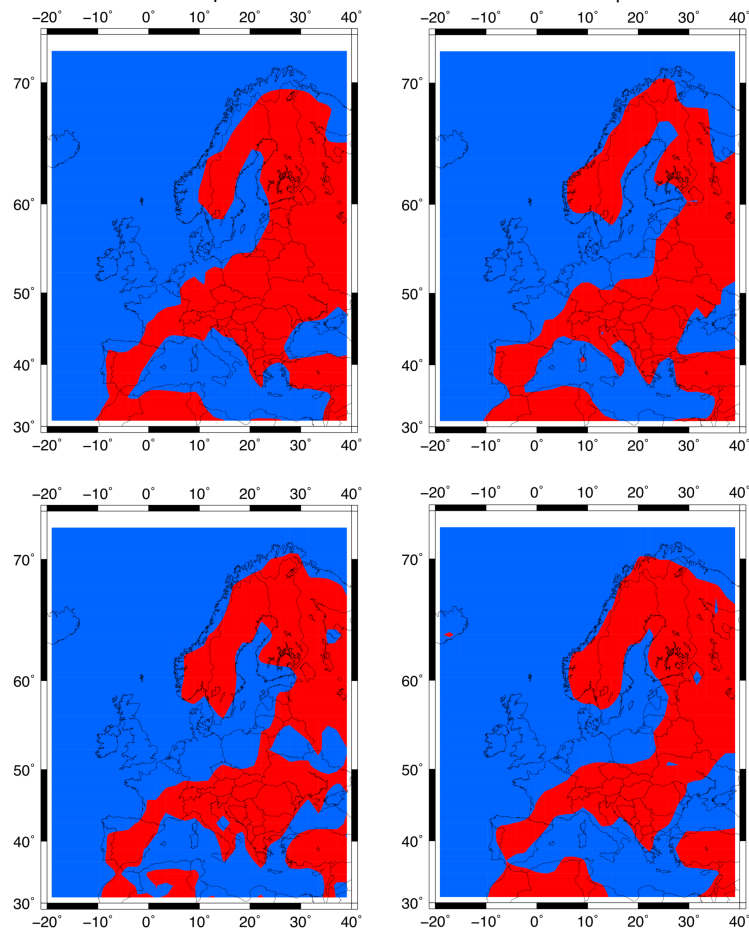


Fig. 10.3: 98th percentile for NCEP (upper left), ERA40 (upper right), ERA-Interim (lower left) and GCM (lower right). Blue: 98th percentile $> 11\text{m/s}$ red: 98th percentile $< 11\text{m/s}$.

11 Danksagung

Zuletzt möchte ich mich bei allen bedanken, die mich in den letzten Jahren unterstützt haben. An erster Stelle danke ich Herrn Prof. Dr. Michael Kerschgens dafür, dass er die Rolle des Doktorvaters übernommen hat. Darüber hinaus danke ich Prof. Dr. Roel Neggers für die Begutachtung dieser Arbeit und Herrn Prof. Dr. Martin Melles für die Übernahme des Prüfungsvorsitz. Weiterhin gilt mein Dank Herrn PD Dr. Joaquim G. Pinto für die Mitbetreuung, eine sehr gute Zusammenarbeit mit hilfreichen Diskussionen und für das Korrekturlesen der Arbeit.

Ich möchte mich zudem bei allen Kollegen am Institut für Geophysik und Meteorologie für die tolle Arbeitsatmosphäre bedanken, insbesondere bei allen Mitarbeitern der AG RegClim, die mich mit Rat und Tat unterstützt haben.

Mein besonderer Dank gilt Rabea Haas, mit der ich die vielen Stunden im gemeinsamen Büro verbringen durfte und die immer eine Idee hatte, wenn ich nicht weiter wusste. Außerdem danke ich Julia Mömken für das Korrekturlesen der Arbeit und für gute Tipps. Zusätzlich möchte ich Sven Ulbrich für zahlreiche anregende Diskussionen danken.

Ein großes Dankeschön an meine Koautoren, ohne deren Hilfe die Publikationen nie die Form angenommen hätten, in der sie zum Schluß erschienen sind.

Zuletzt gilt mein Dank meiner Familie und meinen Freunden, die mich immer unterstützt haben und sehr viel Geduld und Verständnis aufgebracht haben, insbesondere, dass ich in den letzten Monaten kaum Zeit für sie hatte.

12 Beiträge

Beiträge zu den jeweiligen Artikeln

1. Pinto J.G., Karremann M.K., Born K., Della-Marta P.M. and Klawe M. (2012): Loss potentials associated with European windstorms under future climate conditions, *Clim Res*, 54:1-20 (Chap. 3):

Das Konzept für die vorliegende Veröffentlichung wurde in Zusammenarbeit mit Dr. JG Pinto. entwickelt. Die Bearbeitung der Daten, sämtliche Berechnungen, sowie die Auswertungen und Analysen wurden von mir durchgeführt. Des Weiteren wurden alle Grafiken und Bilder von mir erstellt. Dr. K Born hat die Erstellung einiger Programmteile unterstützt. Der erste Textentwurf wurde von mir verfasst. Die Ausarbeitung des Textes fand in enger Zusammenarbeit mit Herr Dr. JG Pinto statt. Dr. M Klawe und Dr. PM Della-Marta haben zusätzlich zu den Teilen mit Bezug zur Versicherungswirtschaft beigetragen.

2. Karremann M.K., Pinto J.G., von Bomhard P.J. and Klawe M. (2014): On the clustering of winter storm loss events over Germany, *Nat Hazards Earth Sys* 14:2041-2052 (Chap. 5):

Das Konzept für diesen Artikel wurde zusammen mit Dr. JG Pinto und Dr. M Klawe entwickelt. Eine erste Machbarkeitsstudie erfolgte zu Teilen durch PJ v. Bomhard im Rahmen seiner Bachelorarbeit, die ich mit betreut habe. Die Aufbereitung der Daten, alle weiteren Entwicklungen, Berechnungen und Analysen sowie die Erstellung der Grafiken wurden von mir durchgeführt. Der erste Textentwurf wurde ebenfalls von mir verfasst. Das Manuskript wurde zusammen mit Dr. JG Pinto und Dr. M Klawe zu einer finalen Version gebracht.

3. Karremann M.K., Pinto J.G., Reyers M. and Klawe M. (2014): Return periods of losses associated with European windstorm series in a changing climate, *Environ Res Lett* 9:124016 (Chap. 6):

Dieses Konzept wurde ebenfalls in Zusammenarbeit mit Dr. JG Pinto entwickelt. Die Durchführung sämtlicher Analysen, die Berechnungen und Erstellung der Grafiken wurden von mir erstellt. Der erste Textentwurf wurde von mir angefertigt. Der Inhalt und die Struktur ist mit den Koautoren Dr. M Reyers, Dr. JG Pinto und Dr. M Klawe abgestimmt. Eine finale Ausarbeitung zur Verbesserung der Lesbarkeit fand in Zusammenarbeit mit den Koautoren statt.

13 Erklärung

Ich versichere, dass ich die von mir vorgelegte Dissertation selbständig angefertigt, die benutzten Quellen und Hilfsmittel vollständig angegeben und die Stellen der Arbeit - einschließlich Tabellen, Karten und Abbildungen -, die anderen Werken im Wortlaut oder dem Sinn nach entnommen sind, in jedem Einzelfall als Entlehnung kenntlich gemacht habe; dass diese Dissertation noch keiner anderen Fakultät oder Universität zur Prüfung vorgelegen hat; dass sie - abgesehen von unten angegebenen Teilpublikationen - noch nicht veröffentlicht worden ist, sowie, dass ich eine solche Veröffentlichung vor Abschluss des Promotionsverfahrens nicht vornehmen werde. Die Bestimmungen der Promotionsordnung sind mir bekannt. Die von mir vorgelegte Dissertation ist von Prof. Dr. Michael Kerschgens betreut worden.

Folgende Teilpublikationen liegen vor:

1. Pinto J.G., Karremann M.K., Born K., Della-Marta P.M. and Klawe M. (2012): Loss potentials associated with European windstorms under future climate conditions, *Clim Res*, **54**:1-20, doi:10.3354/cr01111
2. Karremann M.K. , Pinto J.G., von Bomhard P.J. and Klawe M. (2014): On the clustering of winter storm loss events over Germany, *Nat Hazards Earth Sys* **14**:2041-2052, doi:10.5194/nhess-14-2041-2014
3. Karremann M.K., Pinto J.G., Meyers M. and Klawe M. (2014): Return periods of losses associated with European windstorm series in a changing climate, *Environ Res Lett* **9**:124016, doi:10.10188/1748-9326/9/12/124016

Köln, den 15.08.2014